Cenozoic Structural and Stratigraphic Development of the Faroe-Shetland Basin and Faroe Graben

Fríðbjørg Biskopstø

Thesis submitted as partial fulfilment of the requirements for the degree of Doctor of Philosophy (Ph. D) in Geology

University of Edinburgh

2004

To my daughter Caitlyn.

ACKNOWLEDGEMENTS

I would like to acknowledge everyone that has helped, encouraged and supported me during the research and writing up of this thesis, including:

My supervisor Professor John Underhill, thanks for the enthusiasm and support, during my PhD study.

Statoil, for their logistic and financial support and Total, BP Exploration and DGS Veritas for allowing access to their respective seismic datasets. Tony Doré, David Ellis, Ragnar Poulsen, Gareth Allinson, Michelle O'Callaghan and Lois of Statoil are thanked for their support of the research.

David Mudge is thanked for the support and help with the biostratigraphic and chronostratigraphic calibration of the wells.

Staff at the University of Edinburgh, thanks to, Helena Jack, Gordon, Ian McNab, Lisa Thorburn, Gerard White, Justin, Shane, James Jarvis and Chris Pace.

Chris Jackson, David Ellis, Douglas Paton and Mike Young thanks for proof reading and comments on earlier drafts of the thesis.

Thanks to my family and friends abroad and in Edinburgh. Solveigh, thank you for your friendship, encouragement and support. Olga and Abraham, thank you for the initial guidance into studying geoscience. Thanks to my parents and Caitlyn's grandparents for believing in me, for your tireless support and for looking after Caitlyn.

Mike, thank you for the love and patience that you have shown throughout this challenging time.

ABSTRACT

Seismic stratigraphic analyses of the late Palaeocene-Present transitional to post-rift succession in the Faroe-Shetland Basin and Faroe Graben (FSC) on the NE Atlantic volcanic passive continental margin have revealed the occurrence of an Early Eocene dendritic palaeo-drainage system and Middle Eocene-Miocene contractional inversion structures.

The palaeo-drainage system consists of a significant NNW-SSE trending distributary channel (40km long, 5km wide and up to 400m deep), fed by numerous tributaries (100m deep). The drainage system incised into a major delta system (Colsay Sandstone Member) and was subsequently infilled and draped by estuarine deposits (Hildasay Sandstone Member and Balder Formation). The excellent preservation of the palaeo-valleys indicates that uplift, incision and subsequent infilling of the drainage system occurred relatively rapid (biostratigraphically constrained to ca. 1 My). The uplifting responsible for the incision event (at c. 54.7 Ma, earliest Ypresian) was widespread and extends as far as the North Sea (Bressay area) and SE England (London Basin). Furthermore, coeval volcanic activity is consistent with the drainage system having resulted from transient uplift driven by a mantle-plume. This transient uplift event (incision and infill) in the FSC provides important new evidence for the evolution of the ancestral Iceland mantle plume and its influence on stratigraphic development.

The inversion structures, developed in Middle Eocene, Oligocene and Middle Miocene, are marked by folding with the syn/post inversion stratigraphy onlapping and thinning over the structures. The location and orientation of the inversion structures suggest that the underlying Mesozoic structural configuration, especially the NW-SE transfer zones, influenced their development. Temporal and spatial relationships between the inversion structures in the FSC and similar structures identified along the length of the NW Atlantic margin suggest that a complex interaction of different forces (related to plate-reorganizations and plume activity)

acted in concert and are responsible for their generic development. The timing and nature of the movement of the inversion structures in the FSC provide new temporal constraints which help to understand better the controlling mechanism of passive continental margins.

LIST OF CONTENT

LIST OF FIGURES

LIST OF ABBREVIATION

The abbreviation list is in alphabetic order.

BTIP	British Tertiary Large Igneous Provinces
FPLG	Faroe Plateau Lave Group
FSC	Faroe-Shetland Channel
LCB	lower crustal body
LIP	Large Igneous Provinces
NAIP	North Atlantic Large Igneous Provinces
NNSB	Northern North Sea basin
PCM	passive continental margins
SDRS	seaward dipping reflector sequences
VPCM	volcanic passive continental margins

SECTION ONE:

INTRODUCTION AND BACKGROUND

CHAPTER ONE

1.0. INTRODUCTION

1.1. RATIONALE

There is increasing evidence that passive continental margins are not as structurally inactive as indicated by the classic post-rift subsidence model of McKenzie (1978). Rather, passive continental margins can go through multiple stages of post-rift/post break-up deformation and are hence, dynamic (e.g. Ziegler, 1988; Roberts, 1989; Boldreel and Andersen, 1993, 1994; Nadin et al., 1997; Doré and Lundin, 1996; White and Lovell, 1997; Japsen, 1997; Eldholm et al., 2000). For example, passive continental margins that are situated in the vicinity of a mantle plume may experience uplift that punctuates subsidence, and extensive volcanism, according to the plume theory by Campbell and Griffiths (1990). The surface expressions associated with mantle plume dynamics, the regional uplift (both transient and permanent) and the age and duration of the associated igneous activity, has major implications for the stratigraphic evolution of adjacent sedimentary basins on the passive margin. Given that the presence of mantle plumes can be recognised at many times throughout geological history, primarily by the occurrence of distinctive igneous geochemical signatures (e.g. Saunders et al., 1997), it is surprising that few unequivocal ancient examples of the dynamic behaviour of the lithosphere above plumes have been documented through the analysis of the stratigraphic and sedimentary record. Relatively few studies (e.g. Underhill and Partington, 1993 and 1994; Dam et al., 1998) have linked surface uplift, incision and sediment distribution with mantle upwelling. Thus, the relationship between mantle plume dynamics and associated topography and basin evolution, especially in a passive margin, are relatively poorly understood.

Furthermore, some passive continental margins (e.g. the NE Atlantic margin) have in addition to plume related uplift, experienced uplift/inversion as a result of compressional tectonics, forming dome structures (e.g. off mid Norway; Blystad et

al., 1995; Doré and Lundin, 1996; Vågnes et al., 1998). This also has major implication for the structural and stratigraphic evolution. The inversion structures on passive continental margins, and specifically the NE Atlantic margin, have generally been related to, 1) changes in plate boundary mechanics, such as ridge push and far-field orogenic compressional forces (Boldreel and Andersen, 1993, 1994; Doré and Lundin, 1996) and, 2) other mechanisms, including plume flux enhanced by changes in mid-Atlantic-ridge interaction (Lundin and Doré, 2002). Despite several mechanisms being proposed, the genesis of these structures remains unclear and furthermore, the timing of their development needs to be better constrained in order to fully understand their evolution and influence on structural and stratigraphic development.

This study aims to investigate the stratigraphic evolution of a passive continental margin in the vicinity of a mantle plume(s), in order to better understand the stratigraphic evolution and the surface expressions related to thermal uplift associated with a mantle plume. In addition, this study aims to investigate the location (with respect to underlying structure), timing, nature and growth of inversion structures in order to precisely constrain their evolution, determine their influence on the stratigraphy, and to better understand their potential genesis.

In contrast to many other studies, excellent 2D and 3D seismic data integrated with well and biostratigraphic data allow tight age constraints to be placed on the stratigraphy. Thus, enabling temporal constraints to be placed on seismic and sequence stratigraphic evolution and on the key events that controlled these.

1.2. AIMS AND OBJECTIVES

The volcanic passive continental margin of the North Atlantic has experienced uplift associated with a mantle plume (e.g. Nadin and Kusznir, 1997) and also uplift related to compressional stresses (structural inversion) (e.g. Roberts, 1989; Boldreel and Andersen, 1993, 1994; Doré and Lundin, 1996; Lundin and Doré, 1997). The study area, the Faroe-Shetland Basin and the Faroe Graben (FSC), located on the NE Atlantic continental margin (west of Shetland) is thus, an ideal location in which to investigate the nature, products and controls of both plume and inversion related

uplifts. The main aim of this study, therefore, is to integrate structural and stratigraphic data from the FSC in order to determine the tectonic and stratigraphic development during the final stage of rifting (transition stage) and the post-rift stage and to consider the influence of plume(s) and inversion of this development. More specifically this thesis aims to:

1) Examine the post-rift stratigraphy from seismic and well data in the FSC, in order to define the main depositional packages within the basin and the depositional environments within.

2) Examine in more detail the nature and geometry of deposits under- and over-lying volcaniclastics and lavas that belong to (or are age equivalent to) the Faroe Plateau Lava Group of the Faroe Islands, in order to determine the sedimentary history and volcanic stratigraphy of the late Palaeocene-earliest Eocene in the FSC.

3) Integrate detailed stratigraphic information (i.e. the defined depositional packages) from the Late Palaeocene/earliest Eocene section, especially that above and below a major erosion surface, with the timing and history of the North Atlantic Large Igneous Province. This is in order to consider the interplay of sedimentation, erosion and igneous activity. Furthermore, to examine whether the nature and geometry of the sedimentary successions (seismic stratigraphy and stratal thickness relationships) enables the evolution of the mantle plume and specifically changes in mantle plume flux to be constrained.

4) Determine whether the late Palaeocene/earliest Eocene prominent erosion surface in the FSC can be correlated into the North Sea and southern England. This is in order to see if the Late Palaeocene/earliest Eocene uplift/erosion in the FSC occurred on a more regional scale.

5) Analyse how the post-rift burial of a volcanic passive continental margin (NE Atlantic) on data from the FSC compares with the predicted post-rift subsidence curve for volcanic passive continental margins.

6) To examine the seismic sequence stratigraphy (geometries and thickness of depositional packages), the sedimentology and facies of a post-rift deformed (updomed) section to determine whether it has undergone structural inversion. To determine the number, the timing and the nature of inversion movements and consider the structural and other main controls on their evolution. This including examining the Mesozoic basement structural (rift) configuration in order to investigate whether the underlying basement structuration influenced the orientation and position of later inversion features.

7) To integrate the spreading history of the North Atlantic ridge system (including, plate reorganisation events, changes in spreading rate) with the evolution of the inversion structures in the FSC, in order to determine possible causes that have influenced the post-rift tectono-stratigraphy and the development of the inversion structures.

8) To integrate the detailed stratigraphic information from the post-rift, Early Eocene to Present section, with the evolution of inversion features on passive continental margin elsewhere (e.g. the inversion features along the Norwegian continental margin and the Rockall area) in order to investigate whether these structures have any common mechanisms for their generation.

9) To synthesise observations from the study area and discuss their general implications for volcanic passive continental margins and post-rift stratigraphy.

1.3. DATASET AND METHODOLOGY

This study utilises seven 3D seismic surveys (sf9697, Q204_v2, west_of_clair, rns_white_zone, tr7-p1, tr8_95b and mc3D_wz_96_97_98) and one 2D survey (of-94). In total, the 3D surveys cover a total area of 11230 km^2, whilst the 2D survey has a line spacing of 12-24 km and covers 25300 km^2 (Fig. 1.1). In total 54 wells have been examined and tied with the seismic interpretation.

Seismic sequence stratigraphic analysis and interpretation has been carried out, based on the sequence stratigraphic principles initially developed by Vail et al. (1977) and subsequently extended by other workers (e.g. Van Wagoner et al., 1990; Vail et al., 1991). In particular, the interpretation has been based on the identification and mapping of key seismic surfaces, defined by seismic reflector terminations.

The Paleogene and Neogene succession can be divided into several major depositional packages, separated by key stratal surfaces, which record major breaks in sedimentation. These depositional packages can further be subdivided into genetically related depositional units based on internal seismic reflector terminations, which reflect fluctuations in relative sea level. Seismic isochron (i.e. time thickness) maps have enabled the sediment thickness distribution for each depositional package to be determined.

1.4. THESIS LAYOUT

This thesis contains eight chapters arranged into three sections that deal with specific aspect of the research.

Section One: Introduction and Background

Following this introductory chapter (Chapter One), Chapter Two and Chapter Three provide the background information on which this thesis is based.

Chapter Two summarises previous research concerning passive continental margins, with emphasis on volcanic passive continental margins (VPCM). The key issues being 1) the thermal dynamics associated with the igneous products on VPCM, both in relation to mantle-plume and underplating, and how the resultant surface topographic expressions may effect the stratigraphy in the overlying basins,

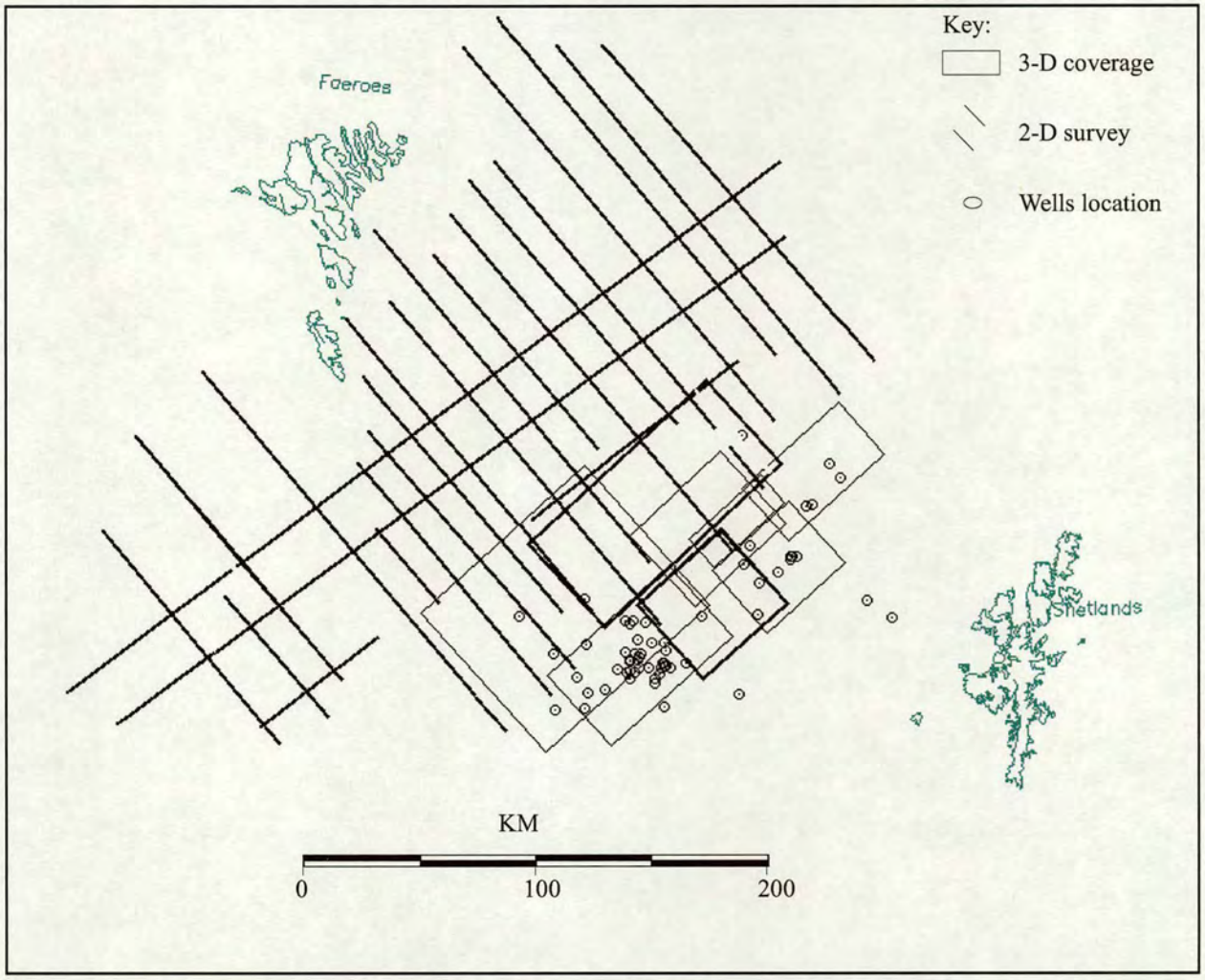

Figure 1.1. Figure. Location map showing the data-set of seismic and well coverage in study area (see text).

2) stresses (ridge push, drag) and tectonic lineaments associated with mid-ocean ridge and how theses may influence volcanic passive continental margins and hence inversion features on such margins, 3) far-field stresses, for example linked to orogenic activity, and how these effect passive continental margins and, 4) the tectonic and stratigraphic evolution of the North Atlantic VPCM is presented as a case study, with emphasis on the above key issues and especially the timing of major events.

Chapter Three summarises previous research concerning the West of Shetland area. The extensional rift phases and the mega-stratigraphy of the FSC are summarized, with emphasis on the stratigraphy of the Paleogene interval. The timing of stratigraphic events, including the bio-, chrono- and igneous stratigraphy is summarised.

Section Two: Paleogene-Recent Post-rift Succession; The Faroe-Shetland Basin and Faroe Graben (FSC)

Section two contains three chapters (Chapters Four to Six).

Chapter Four describes the structural basement configuration of the FSC that have been interpreted from seismic profiles. The orientation and evolution of the main structures are interpreted.

Chapter Five describes the sedimentary evolution of the late Palaeocene to Early Eocene (early Paleogene) interval of the FSC , including development of an incision surface associated with uplift immediately prior to the initial opening of the North Atlantic. The nature and timing of events is analysed and interpreted, including the controlling mechanisms.

Chapter Six describes the structural and sedimentary evolution of the Eocene to Present interval, including the inversion features identified (i.e. the Foinaven Monocline, the Foinaven Anticline and the Corona Anticline). The timing and nature of these features is analysed and interpreted, including the controlling mechanisms.

Section Three: Discussion and Conclusions

Section three contains two chapters (Chapter Seven to Eight). Chapter Seven

discusses the results from the previous data chapters (Chapter Four to Six) and is divided into two main sections. Section one discusses the results from Chapter Four and Five and section two discussed the results from Chapter Four and Six. The main observations are considered in relation to the regional tectonic, volcanic and stratigraphic events that were outlined in Chapters Two and Three. Furthermore, the results from this study, relating to the causal mechanisms for uplift and inversion, are put into context with more generic theories. Chapter Eight presents the main conclusions obtained from Chapters Four to Seven.

CHAPTER TWO

2.0. VOLCANIC PASSIVE CONTINENTAL MARGINS

2.1. INTRODUCTION

This chapter summarises the main characteristics of passive continental margins, with particular emphasis made on volcanic passive continental margins. Furthermore, those characteristics that are most likely to influence the transitional- to post-rift evolution of passive continental margins are considered.

This chapter is divided into three main sections. Firstly, the various types of passive continental margins that have been identified to date are defined and described, together with the processes involved and the controls on these. This is in order to differentiate between the different types of margins and also to enable other margins to be compared with the study area. Secondly, a more detailed description is made of volcanic passive continental margin and, in particular the volcanic activity that occurs and the associated surface expressions during the transition to the post rift phase and also during the post-rift thermal subsidence phase, when uplift and inversion can occur. Finally, the evolution of the North Atlantic volcanic passive continental margin is summarised. The intention is to put into context the main tectonic and magmatic events and directly correlate with the structural and sedimentary transitional- to post-rift evolution in the study area.

2.2. PASSIVE CONTINENTAL MARGINS

Passive continental margins (PCM) are formed when continental rifting leads to continental break up and the formation of oceanic crust (e.g. Salveson, 1976, 1978; McKenzie, 1978 (Fig. 2.1). Passive continental margins are generally characterised by a continental zone (Zone I), a transition zone (Zone II) and an oceanic zone (Zone III) (e.g. Eldholm, 2000) (Fig. 2.2). The continental zone, represents a thinned and rifted crust of tilted fault blocks, overlain by a seaward thickening sedimentary

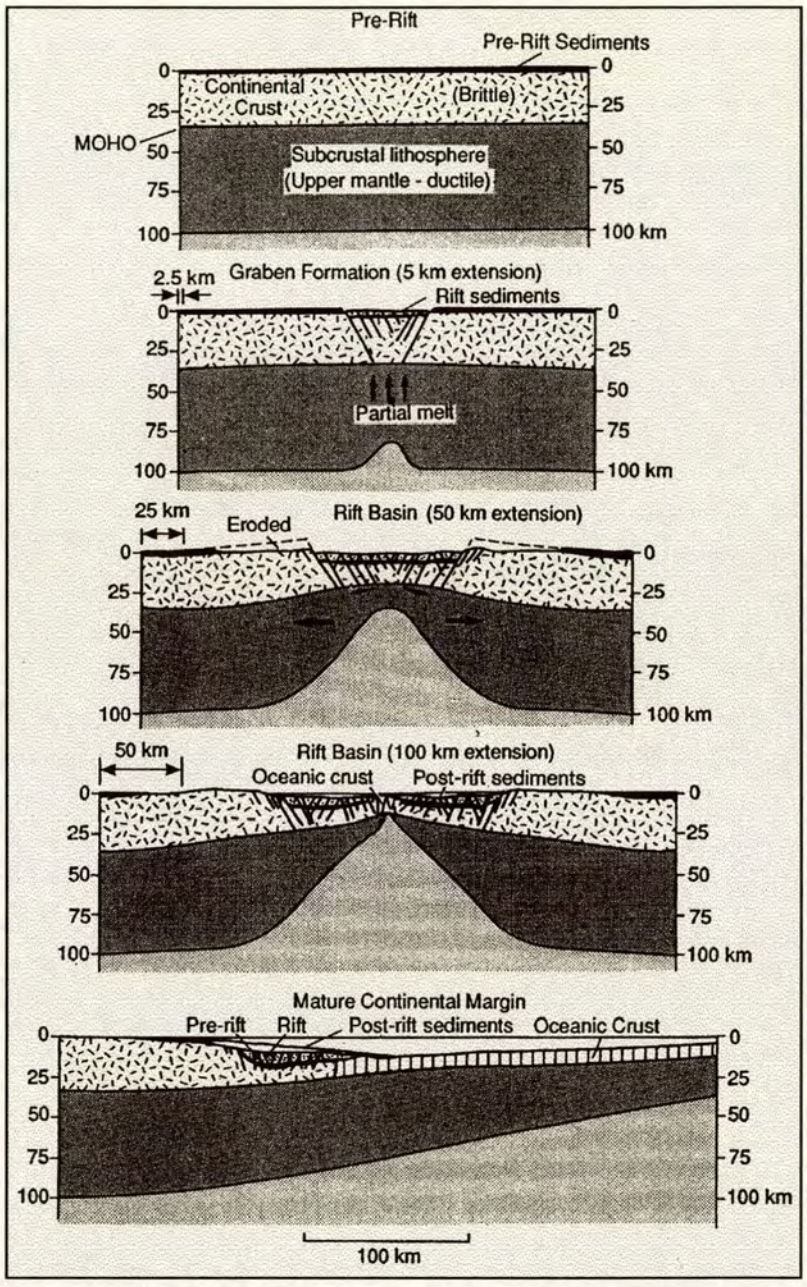

Figure 2.1. A schematic model, showing progressive stages of rift basin evolution and the eventual formation of passive continental margins (see text) (after Allen and Allen, 1990).

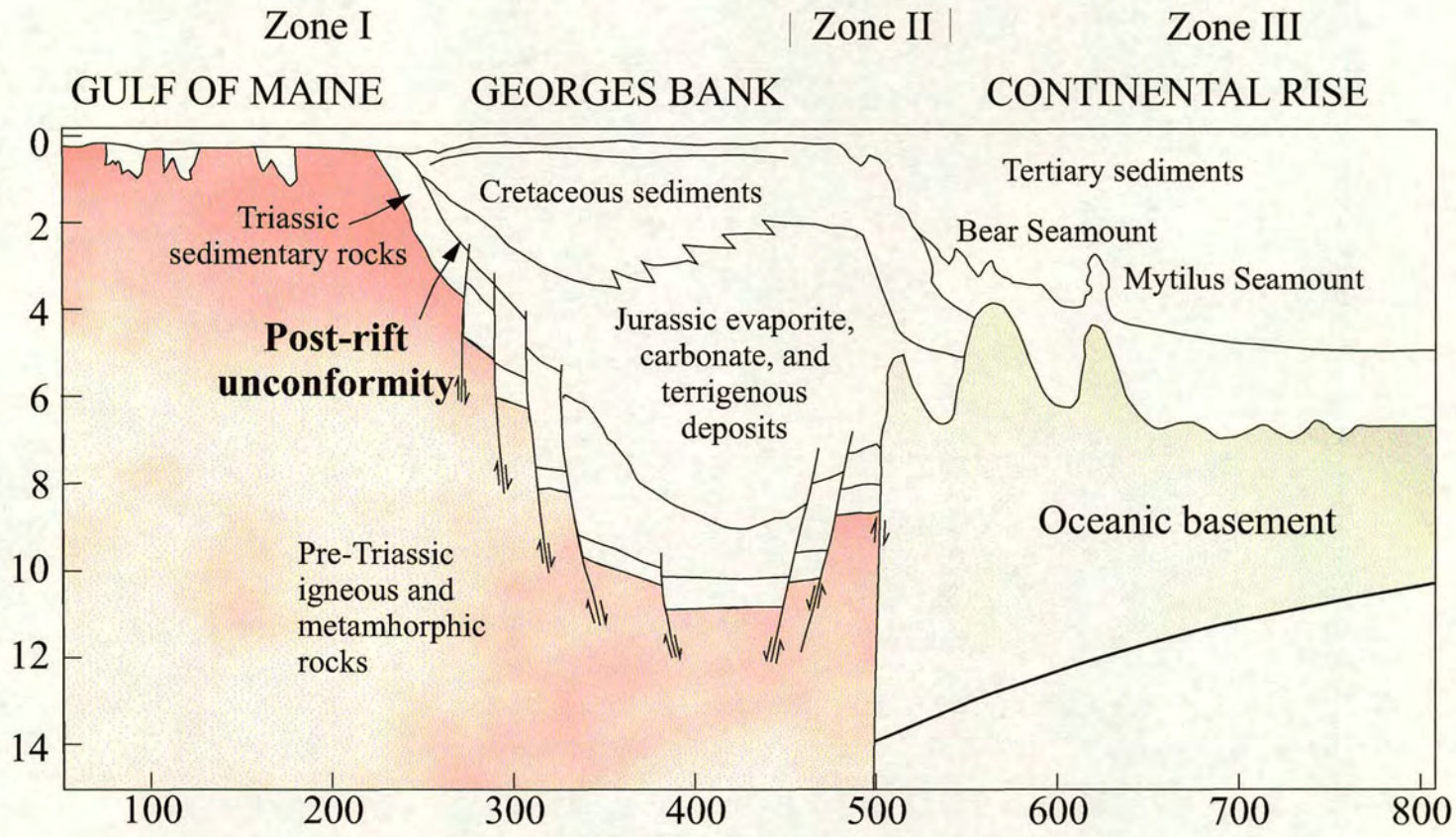

Figure 2.2 Structural cross-section, showing the continental zone (Zone I), transition zone (Zone II) and oceanic zone (Zone III) (see text for definition) of a passive continental margin across the Gulf of Maine and the Georges Bank (after Sheridan, 1974).

wedge, which consist of two mega sequences: a syn-rift sequence and a post-rift sequence, which are separated by a break-up unconformity (Falvey, 1974). Oceanwards, the extensional basins give way at the continent-ocean crust boundary, which represents the transition zone to oceanic crust and the mid ocean ridge system. The main processes that influence the evolution of passive continental margins can be divided into two stages; 1) a rifting stage and, 2) a post rift stage (Fig. 2.1).

Rifting Stage

The early stage of rifting is characterised by an initial thinning and thermal uplift of both the continental crust and subcrustal lithosphere, resulting in the development of significant deviatoric stresses (Ziegler, 1992). The thinning depends on the original thickness of the lithosphere and the stretching factor (β), whilst the uplift is an isostatic response to upwelling of the asthenosphere underneath the stretched crust and lithosphere, controlled by convectional forces in the asthenosphere. The amount of uplift depends mainly on the temperature of the upwelling asthenosphere and the volume of melt generated, which further depends on the lithospheric stretching factor, strain rates, the thermal state of the asthenosphere and of the availability of volatiles (McKenzie and Bickle, 1988; White and McKenzie, 1989; Wilson 1989; Campbell and Griffiths, 1990; Latin et al., 1990; Latin and Waters, 1991, 1992). Thus decompression (pressure and temperature) of partial melting of upwelled asthenosphere can lead to volcanism associated with the rifting (e.g. White, 1988).

In the upper crust the rifting leads to brittle fracture and fault controlled subsidence, resulting in the formation of extensional rift basins. These basins are typically in the form of grabens and half-grabens that in-fill with syn rift sediments, derived from the uplifted regions at the rift margins. Marked stratigraphic thickness changes in the syn-rift from the footwalls to hanging walls of the normal faults are indicative of growth faulting associated with the extension (Williams et al., 1989).

When the crust has been thinned to crustal level (ca. β=5), continental break-up and generation of an oceanic spreading centre occurs. Thus the rift evolves into two continental margins separated by a mid ocean ridge (White and McKenzie, 1989).

Post-rift Stage

The rifting stage ceases when continental break-up occurs, and subsequently the post-rift stage begins (Fig. 2.1). When rifting has ceased, the elevation of the surface of the crust changes immediately to maintain isostatic equilibrium (McKenzie, 1978). This is due to progressive cooling and thermal contraction of the asthenosphere that leads to subsidence (White and McKenzie, 1989). The thermal contraction is the main mechanism of post-rift subsidence when the flexural rigidity of the lithosphere is low, but with time as the continents cool as they drift away from the spreading centre the flexural rigidity increases (Watts, 1982). It is the stretching factor (β) and also the magnitude of the thermal anomaly at the end of rifting that controls the amount of post rift subsidence (e.g. Ziegler, 1988).

After the cessation of the extensional faulting in the upper crust, a postrift mega-sequence is deposited. The postrift mega-sequence may be deposited after a period of non-deposition and/or erosion marked by a break-up unconformity, which may remove part of the synrift mega-sequence (e.g. Williams et al., 1989) (Fig. 2.2). The way in which the lithosphere distributes the sedimentary loads is by flexure. Variations in flexural strength across the margin are large when it is young but decreases with time as the margin cools and becomes more rigid (e.g. Watts et al., 1982) (Fig. 2.3). The stretching event and the type of margin determines the first order depth and size of the post-rift basin, but the flexural (elastic or visco-elastic) response of the crust has also a substantial influence on the sedimentary depositional sequences during the post-rift stage. It is the interplay of sediment supply with subsidence and sea level change that determines the post rift stratigraphic patterns (e.g. Vail et al., 1977; Watts, 1982; Watts et al., 1982; White and McKenzie, 1988) (Fig. 2.4).

Post-rift stratigraphic evolution and subsidence history

The stratigraphic evolution of PCM is controlled by the type of margin and whether the margin is sediment nourished or starved. Passive continental margins can be divided up into three different main types; these are 1) non-volcanic, 2) intermediate

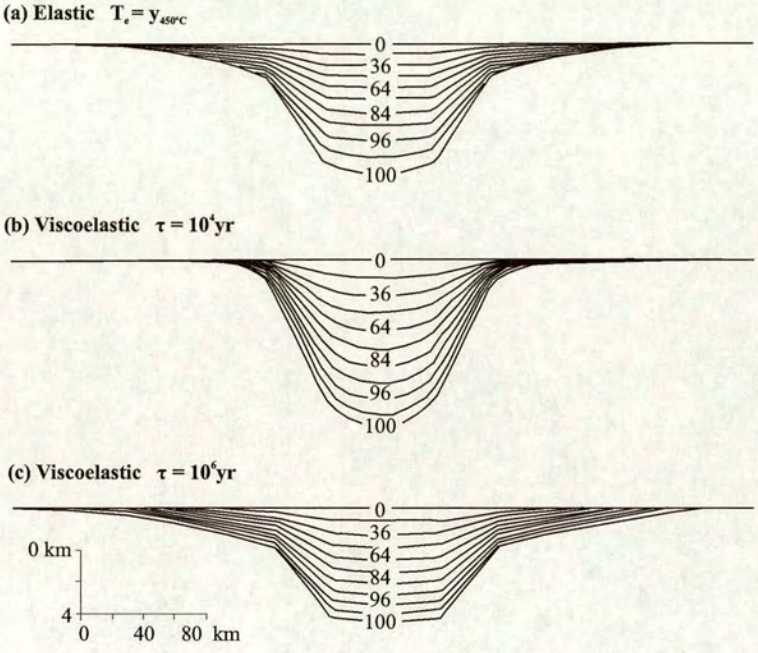

Fig 2.3. A model of calculated post-rift stratigraphy within rifted basins (stretching factor β=2) that overly lithosphere of contrasting rheology; a) *elastic lithosphere*, produces stratigraphic onlap and steers-head geometry, b) viscoelastic lithosphere, produces stratigraphic offlap and a gradually narrowing basin geometry and c) viscoelastic lithosphere, produces similar geometries to a) but differs in being characterised by stratigraphic offlap (after Watts et al., 1982).

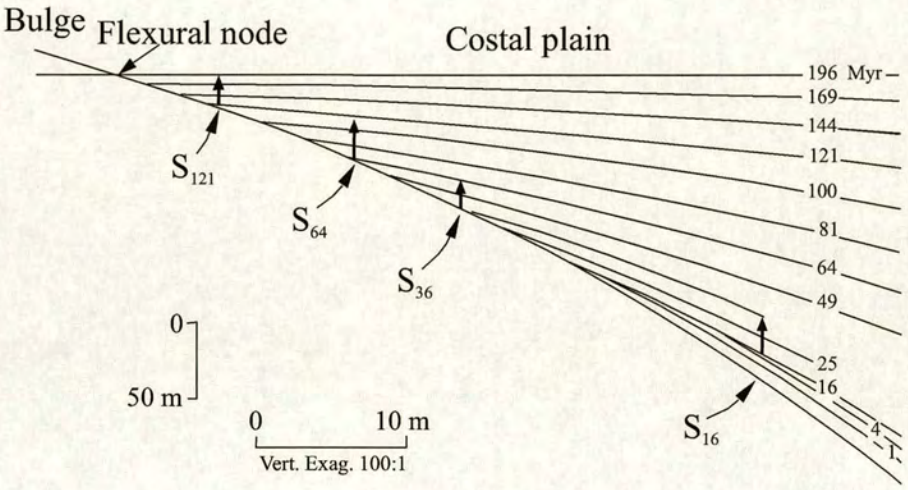

Figure 2.4. A model showing the amount of stratigraphic coastal plain and shelf infill with time, after thermal post-rift subsidence (S). Sediments rapidly infill the continental shelf, keeping a constant bathymetry with time. The sedimentary load flexes a cooling plate that increases in rigidity with time since heating. Solid lines are the boundaries of stratigraphic units with ages indicated in My since the end of rifting (after Watts, 1982).

and 3) volcanic. Figure 2.5 shows an example of the two end-members.

Non-volcanic passive continental margins represent deep sedimentary basins, having a stretching factor of greater than four ($\beta>4$); and an expected subsidence of more than 2.7 km (McKenzie, 1978). In addition they are devoid of volcanic material (White, 1988). World-wide examples of non-volcanic margins are the passive continental margins of the Bay of Biscay, the Western Approaches and the Newfoundland margin (e.g. White and McKenzie, 1989 (Figure 2.6 a and b).

Intermediate passive continental margins, which represent the majority of the worldwide passive continental margins, are without excessive volcanism and have only weakly developed volcanic seaward dipping reflector sequences (SDRS) (White, 1988). Examples of intermediate passive continental margins are the Baltimore canyon trough and the Carolina trough (Fig 2.6a and c).

Volcanic passive continental margins (VCPM) are defined by off-lapping (Fig. 2.8) lava piles of sub aerially deposited SDRS, a characteristic high-velocity lower crustal body (LCB), and also by voluminous and extensive flood basalts (Eldholm et al., 1995). Seaward dipping reflector sequences (SDRS) have been discovered along the Mesozoic rifted margins of the Central and South Atlantic Ocean, and sections of the margins of Antarctica, Northwest India and Northwest Australia (Coffin and Eldholm, 1992) (Fig. 2.6b). Examples of VPCM are the Rockall margin and the Vøring margin of the NE Atlantic (Fig. 2.5 and Fig. 2.6a and d).

A post rift subsidence model by McKenzie (1978), for a normal crustal thickness (ca. 30 km thick) and asthenosphere temperatures of a non-volcanic to intermediate passive continental margin (e.g. that has not experienced major volcanism) predicts an initial rapid subsidence followed by decreasing rates of subsidence as isostatic equilibrium is regained (Fig. 2.7). In volcanic passive continental margins where the underlying asthenosphere is hotter than non-volcanic and intermediate margins, due to the presence of a nearby thermal mantle plume, the post-rift subsidence curve shows an initial uplift during the first 2-3 My after break-up and the plateau becoming submerged 15-25 My after opening and sea-floor spreading (e.g. Skogseid and Eldholm, 1988; Skogseid, 1994) (Fig. 2.7).

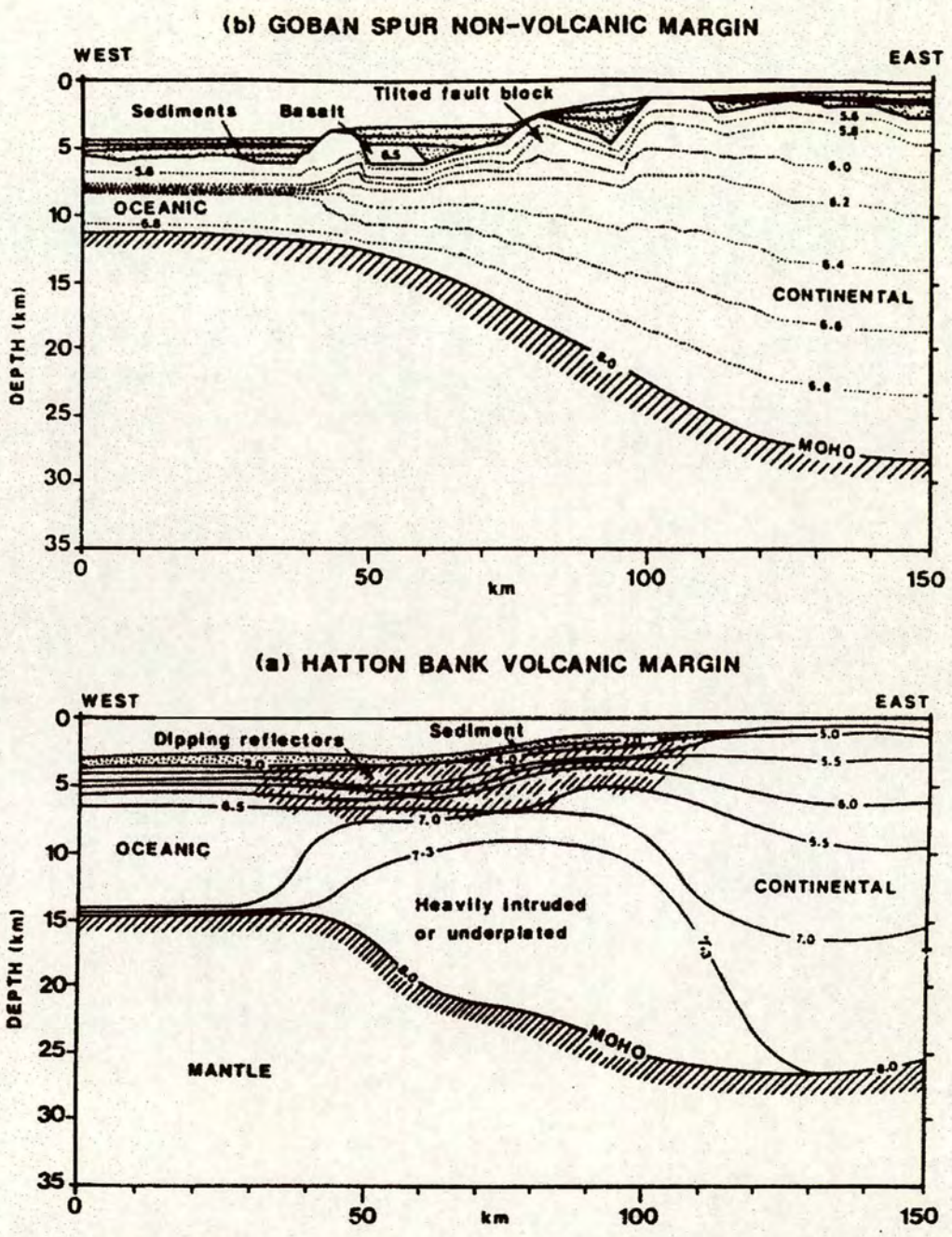

Figure 2.5. Two Cross-sections showing, a) a typical volcanic continental margin west of Hatton Bank (after white et al., 1987; Morgan et al., 1989), and b) a typical non-volcanic margin on the Goban Spur (after Horsefield et al., 1992) (from White, 1992).

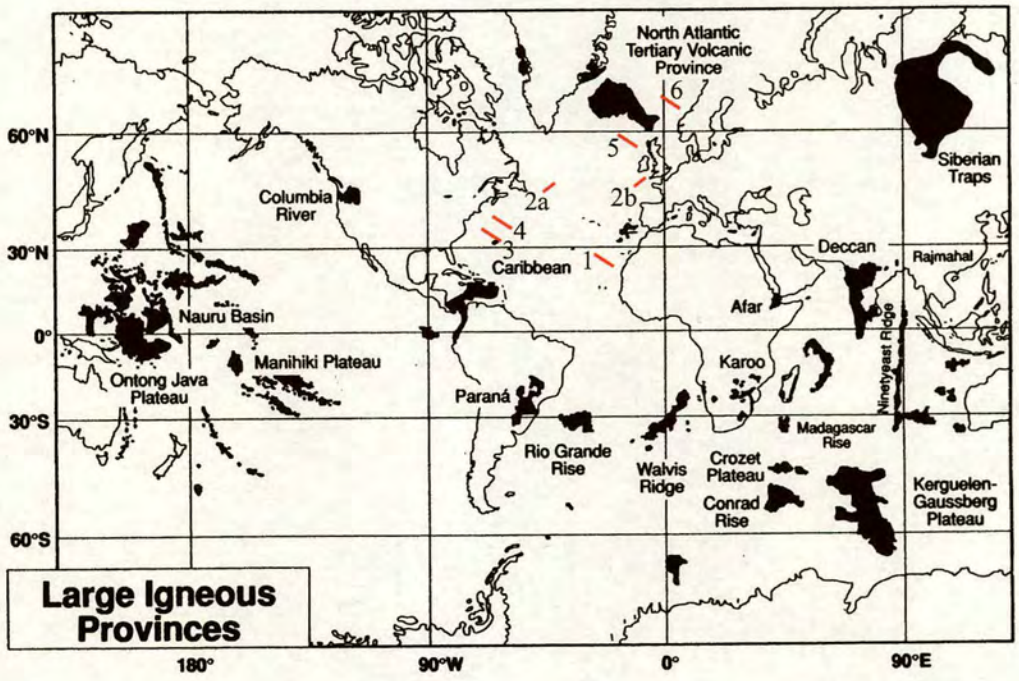

Figure 2.6a. World map, showing the locations (in red colour) of profiles illustrated in 2.6.b-d. Also, the present-day locations of known Large Igneous Provinces (see text in the following section) are shown. Seaward-dipping reflector sequences (SDRS), which represent a substantial volcanic contribution to some continental margins, are not shown (see for example Fig. 2.12a). (from: Saunders et al., 1992).

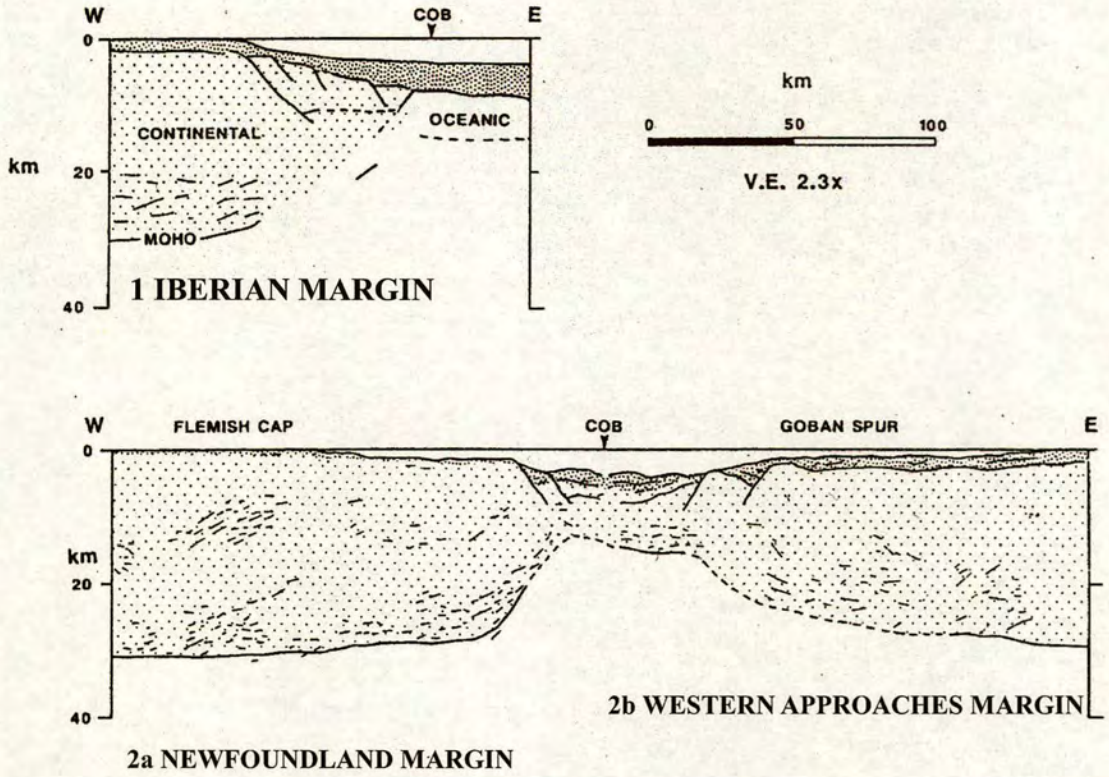

Figure 2.6 b. Cross-sections showing the deep crustal structure of the Iberian (profile 1), the Newfoundland (profile 2a) and the Western Approaches (profile 2b) non-volcanic passive continental margins (see text). For locations see Figure 2.6a. The cross-sections show the presence of tilted fault blocks (open stipple) across the rifted continental crust (zone I) with normal-depth oceanic crust. Triangles along the top of the profile indicate the location of velocity control points (from: White and McKenzie, 1989).

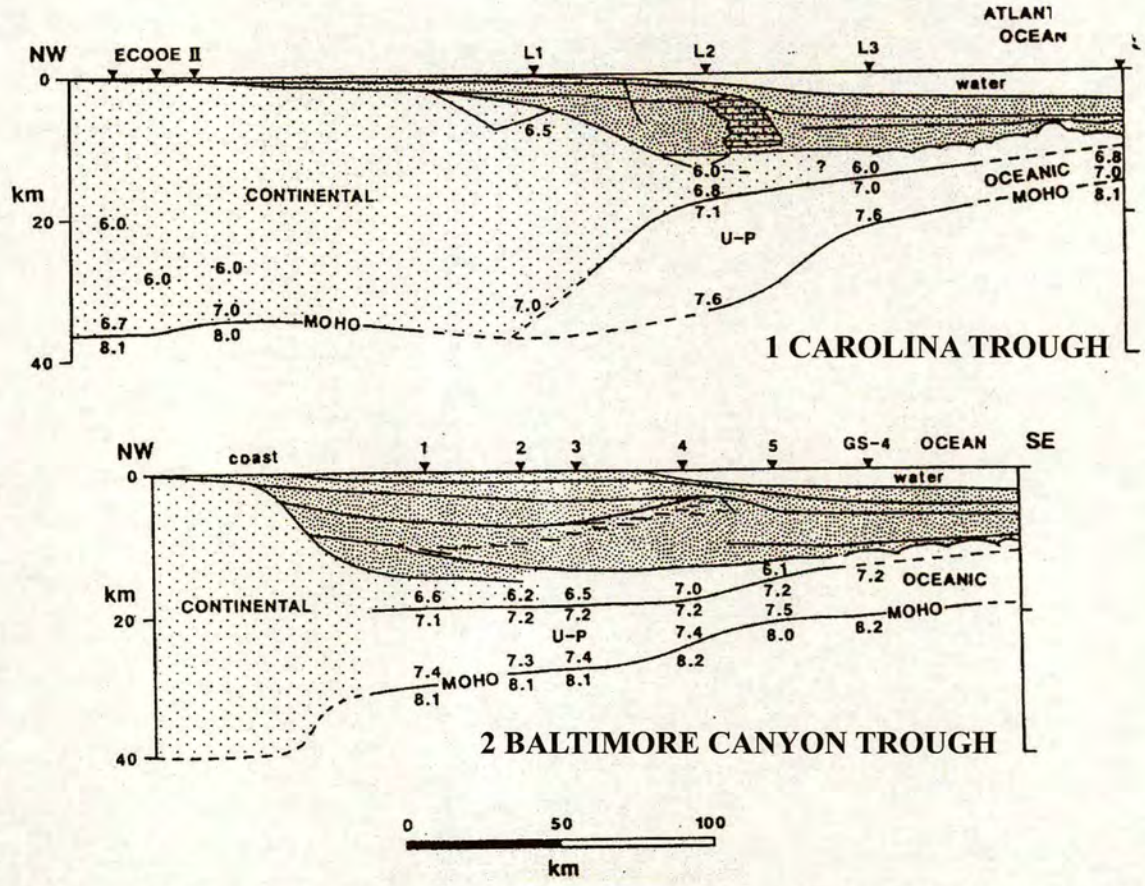

Figure 2.6c. Cross-sections showing the deep crustal structure of the east coast U.S. margin across the Carolina trough (profile 3) and the Baltimore Canyon trough (profile 4). The cross-sections show the presence of tilted fault blocks (zone I) and also extrusive basalts generating limited seaward-dipping reflector sequences (SDRS; diagonal shading) in zone II. Key to symbols and scale is the same as for Figure 2.6b. (from White and McKenzie, 1989).

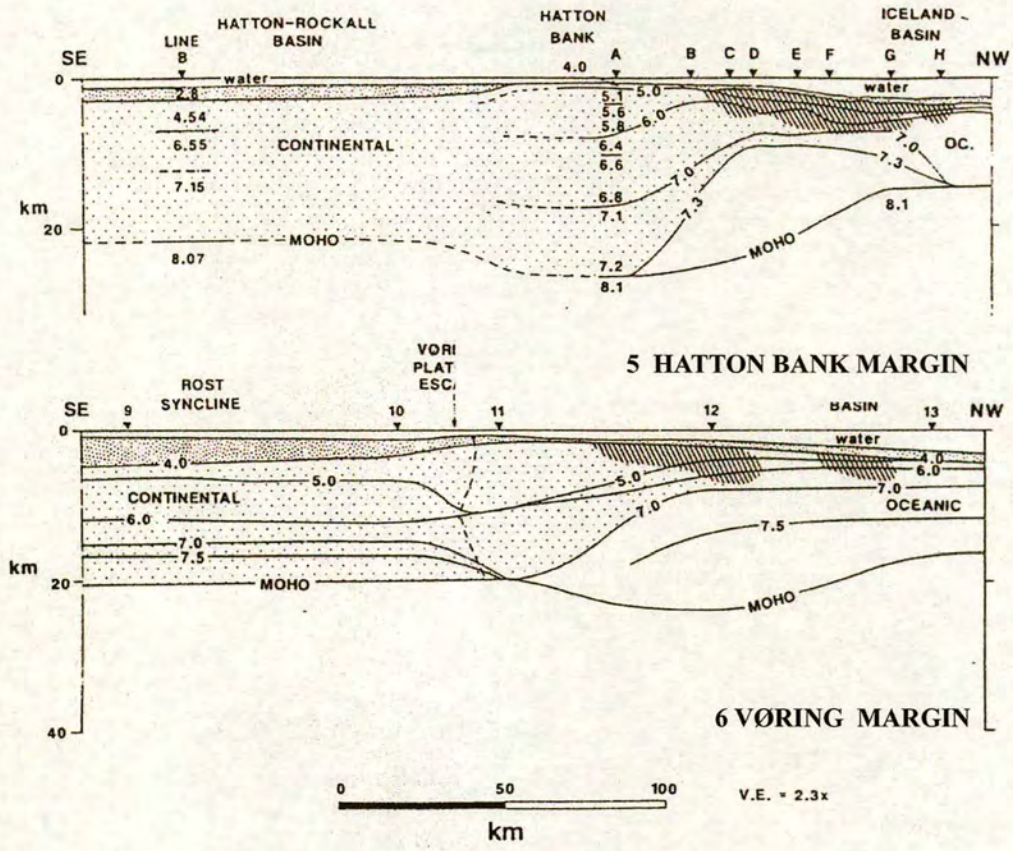

Figure 2.6d. Cross sections showing deep crustal structure across two sections of the volcanic continental margins in the northern North Atlantic; the Hatton Bank margin (profile 5) and the Vøring Plateau (profile 6) (fig. 2.6a). Key to symbols is the same as for Fig. 2.6b and c. See text and more details about volcanic passive continental margins in section 2.3, including Figure 2.8. (From White and McKenzie, 1989).

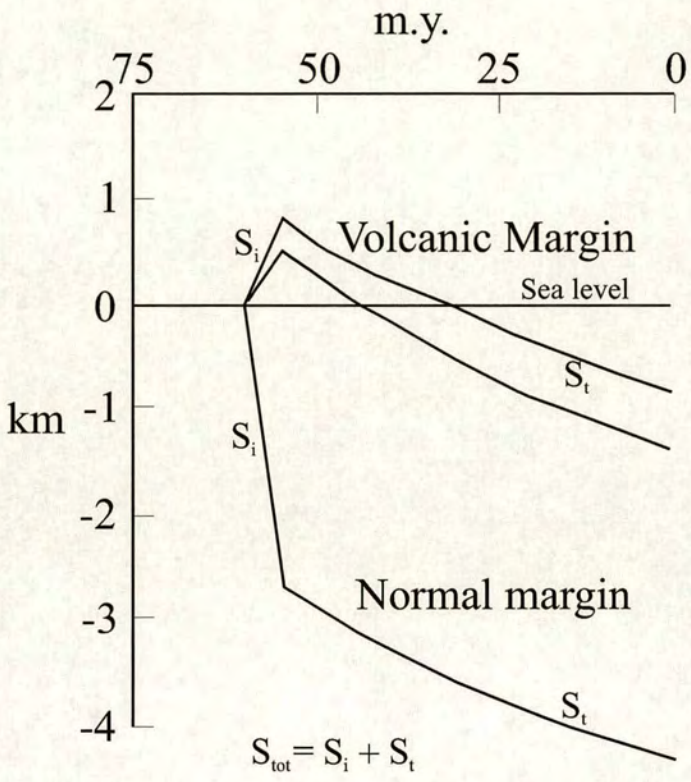

Figure 2.7. Models showing subsidence curves representing the post-rift thermal subsidence history assuming continental break-up at 56 Ma, for 1) non-volcanic to intermediate (normal) passive continental margins and 2) volcanic passive continental margins (see text). The total subsidence (S_{tot}) is the sum of the initial (S_i) and thermal (S_t) subsidence (from Skogseid and Eldholm, 1988).

2.3. VOLCANIC PASSIVE CONTINENTAL MARGINS

The igneous products of volcanic passive continental margins are generally referred to as Large Igneous Provinces (LIP) (e.g. Saunders et al., 1997) (Fig. 2.6a). The geochemical composition of LIP, suggest that they were emplaced before normal sea floor spreading developed, during the rifting stage (Eldholm et al., 2000). Magmatic activity on VPCM can be categorised into three different environments within zones I to III. The products that characterises each environment are described below (Fig. 2.8).

Zone I: continental zone; Lava is intruded into the extended continental crust and the syn-rift sediments, forming sill- and dyke-complexes and intrusive centres. The sill complexes and the dykes are mainly thought to have intruded at weak fracture zones both during extension and after continental break-up (Eldholm et al., 1987). The intrusive centres are typically located in horst/ridges on the extended margin, which can be seen on gravity maps and corresponding seismic profiles (Fig. 2.8). The intrusive centres are termed strato-shield volcano complexes (Ritchie et al., 1999). The dynamics of these are not fully understood, but they are believed to have a local thermal uplift effect at the time of intrusion (e.g. Coffin and Eldholm, 1992; Larsen et al., 1994)(Fig. 2.8).

Lavas are also locally extruded onto the continental crust forming flood basalts. Continental flood basalts are subaerially extruded and overlie the syn-rift mega-sequence. The flood basalts are erupted during a short period, contemporaneous with the main rifting (White and Mckenzie, 1989) and generally develop stacked horizontal flows, but also progradational clinoforms if they extend beyond the coastline. The igneous products within zone I are formed during the transition stage from rifting to ocean floor spreading (Fig. 2.8). This is evidenced by the cessation of volcanic activity on the volcanic margin after the start of ocean floor spreading, recorded by radiometric (Ar-Ar) age dating.

Zone II : Transition zone; The seaward dipping reflectors sequences (SDRS) consist of sub-aerially extruded volcanics along the continental margin. On seismic multichannel profiles they form seaward-dipping clinoform reflectors in the form of progradation of volcanic flows (Hinz and Weber, 1976; Hinz and Schluter, 1978;

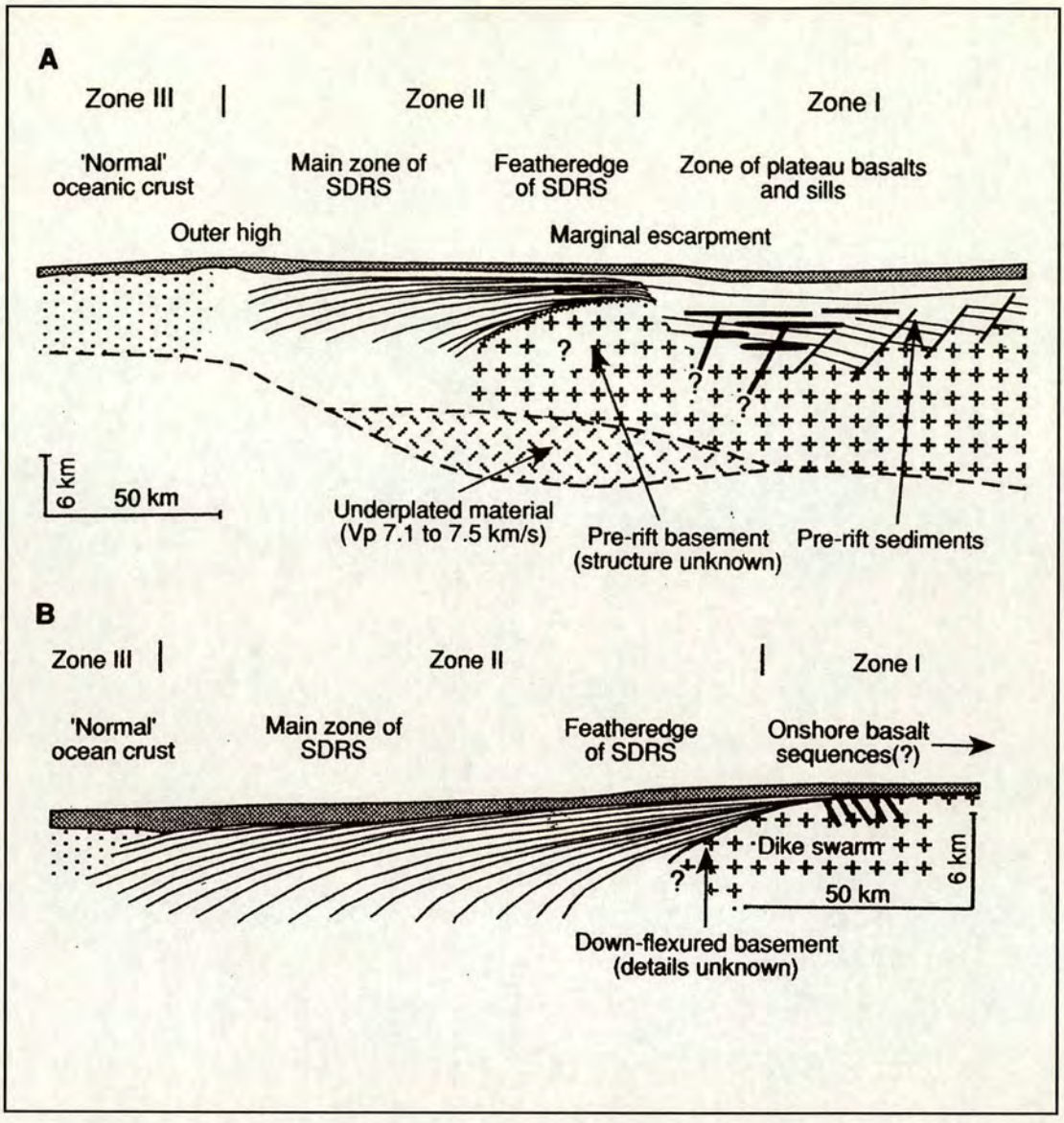

Figure 2.8. Schematic diagrams illustrating the general structure of volcanic passive continental margins (see text and characteristics for zone I-III). A) In this example, break-up takes place within an older continental rift zone that is partly reactivated and intruded by sills. This type of margin is typified by the Vøring Plateau (Eldholm, Thiede, Taylor, et al., 1987). B) A volcanic passive continental margin developed in a cratonic area such as the Southeast Greenland Margin. The basement has been strongly deformed flexurally below the featheredge of the SRDS; as in example A, continental flood basalts may build up in Zone I and on the adjacent land, with sills being restricted to sedimentary basins, should any be present. High seismic-velocity lower crust, possibly representing underplated igneous crust, is present below the central part of the margin (cf. Holbrook and Keleman, 1993). (from Larsen et al., 1994).

Talwani and Eldholm, 1977; Eldholm et al., 1979) (Fig. 2.8). The SDRS consist of igneous material and are interbedded with terrestrial and marine sediments, indicating that at times the crust has been thermally uplifted above sea level (Fig. 2.7). The break-up unconformity may be obscured underneath the SDRS. Furthermore, the SDRS form as spreading initiates (Cox, 1989; White and McKenzie, 1989; Coffin and Eldholm, 1992).

Another characteristic of zone II is the less dense lower crustal body (LCB) material added to the continental crust (White et al., 1987; Larsen and Jakupsdottir, 1988; Mutter et al., 1988; Coffin and Eldholm, 1992, 1994). The LCB has been detected on deep angle seismic profiles as a sequence (up to ca. 30 km thick) of high velocity (7.1-7.5 km/s) (White et al., 1987, 1992; Holbrook and Keleman, 1993) and is interpreted/identified as igneous material (White et al., 1987) that accretes at the base of the lithosphere (underplating) at the time of continental separation (Barton and White, 1997) (Fig. 2.8). The LCB is produced by adiabatic decompression and is one of the main factors that produced uplift of VPCM above sea level (White and McKenzie, 1989) (Fig.2.7). Furthermore, this underplating has a permanent uplift effect along the margins (Brooks, 1973; White and McKenzie, 1989; Cox, 1989) and may thus interrupt and can even reverse the lithospheric cooling process (Ziegler, 1988) (Figs. 2.8 and 2.9).

Zone III: Oceanic zone; at the ocean-spreading centre volcanic material feeds directly to the surface forming massive ridges (15-30 km thick) that characterise the topography (Talwani and Eldholm, 1977) (more on mid-ocean ridge systems in section 2.4.2) (Fig. 2.8).

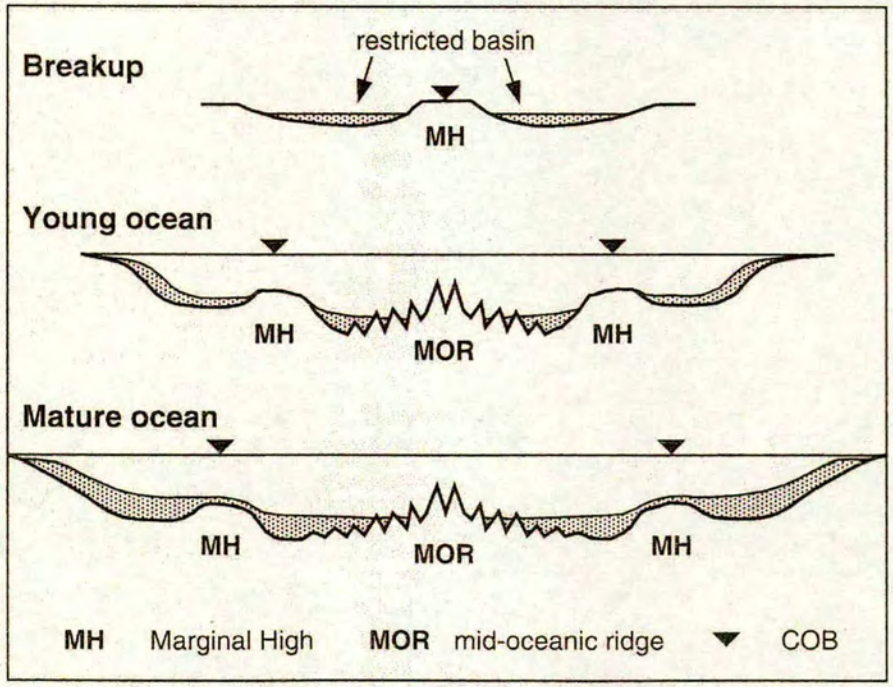

Figure 2.9. Schematic illustration of volcanic continental margin showing basin segmentation creating across-margin barriers for water mass circulation and sediment deposition caused by late rift uplift construction of extrusive edifices along the continent-ocean boundary (COB) (from Eldholm, 2002).

2.4. VOLCANIC PASSIVE CONTINENTAL MARGINS AND MANTLE PLUMES

Large Igneous Provinces (LIP) that characterise VPCM, are thought to be associated with mantle plumes (e.g. Morgan, 1971; White and McKenzie, 1989; Duncan and Richards, 1991; Larsen et al., 1991; Eldholm et al., 2000). A mantle plume is a body of rock that is buoyantly ascending from a boundary layer deep within the mantle (e.g. Morgan, 1971, 1972 and 1981). The temperatures within a plume are much greater than normal asthenospheric temperatures underlying an extended continental crust and lithosphere (McKenzie, 1984; McKenzie and Brickle, 1988). There are three main layers within the mantle where it is thought that plumes ascend from. These are: 1) the 650 km discontinuity between the upper and lower mantle (White and Mckenzie, 1989) (Fig. 2.10, model 1), 2) the core-mantle boundary (the "D" layer) (Griffiths and Canbell, 1990; Richards et al., 1989) (Fig. 2.10, model 2) or, 3) the "D" layer but stall at the 650 km discontinuity and eventually trigger convective instability in the thermal boundary layer at this layer (Trackley et al., 1993) (Fig. 2.10, model 3). Plumes have a large size, bulbous head and rise either, 1) diapirically through the ambient mantle (e.g. Griffiths and Campbell, 1990), 2) as steady-state systems, whereby material is fed through thin feeder conduit to a flattened mushroom-shaped head (e.g. White and McKenzie, 1989; Kent, 1991) or, 3) episodic systems, whereby material rises as a series of blobs from a boundary layer (e.g. Schilling and Noe-Nygaard, 1974; Schilling, 1975) (Fig. 2.10).

Two models have been put forward to explain what happens when plume heads reach the base of the lithosphere, leading to the production of LIP. These are, 1) the incubation model (Kent, 1991) and 2) the impact model (Richards et. al., 1989; Campbell and Griffiths, 1990). The incubation model suggests that the plume heads accumulate gradually beneath thick (150km) lithosphere for up to 150 My. before the lithosphere can thin enough to allow the voluminous extrusion of lavas (Fig. 2.11, A), or alternatively, there is an incubation, but with the thermal anomaly channelled by pre-existing topography at the base of the lithosphere, or by contemporaneous extension, resulting in extensive decompression melting (White and McKenzie, 1989; Thompson and Gibson, 1991) (Fig. 2.11, B). In contrast to the

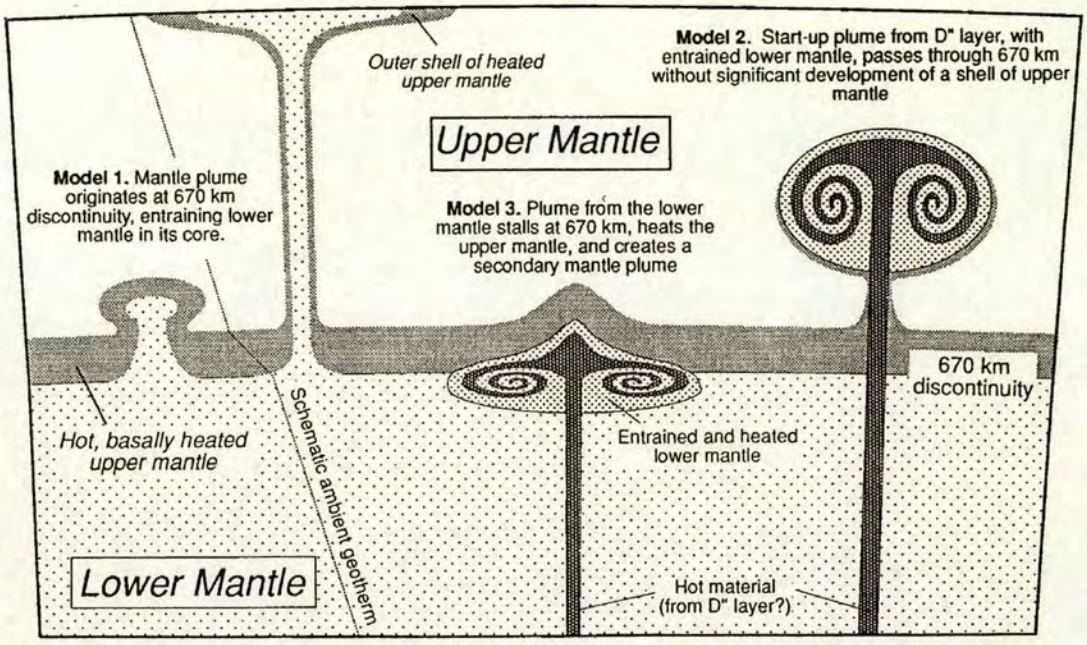

Figure 2.10. Schematic representation of three plume models, 1) a plume originating by instability in the boundary layer at the base of the upper mantle (Model 1) will be composed of upper mantle with entrained lower-mantle material in its centre, 2) by contrast, a plume originating at the core-mantle boundary and penetrating the 670 km discontinuity (Model 2) will be composed mostly of lower mantle and 3) a lower-mantle plume, which stalls at the 670 km discontinuity (Model 3) will produce a layer of hot lower mantle, which may ultimately trigger instability in the upper mantle and produce a plume, or plumes, similar to Model 1 (from Fitton et al., 1997).

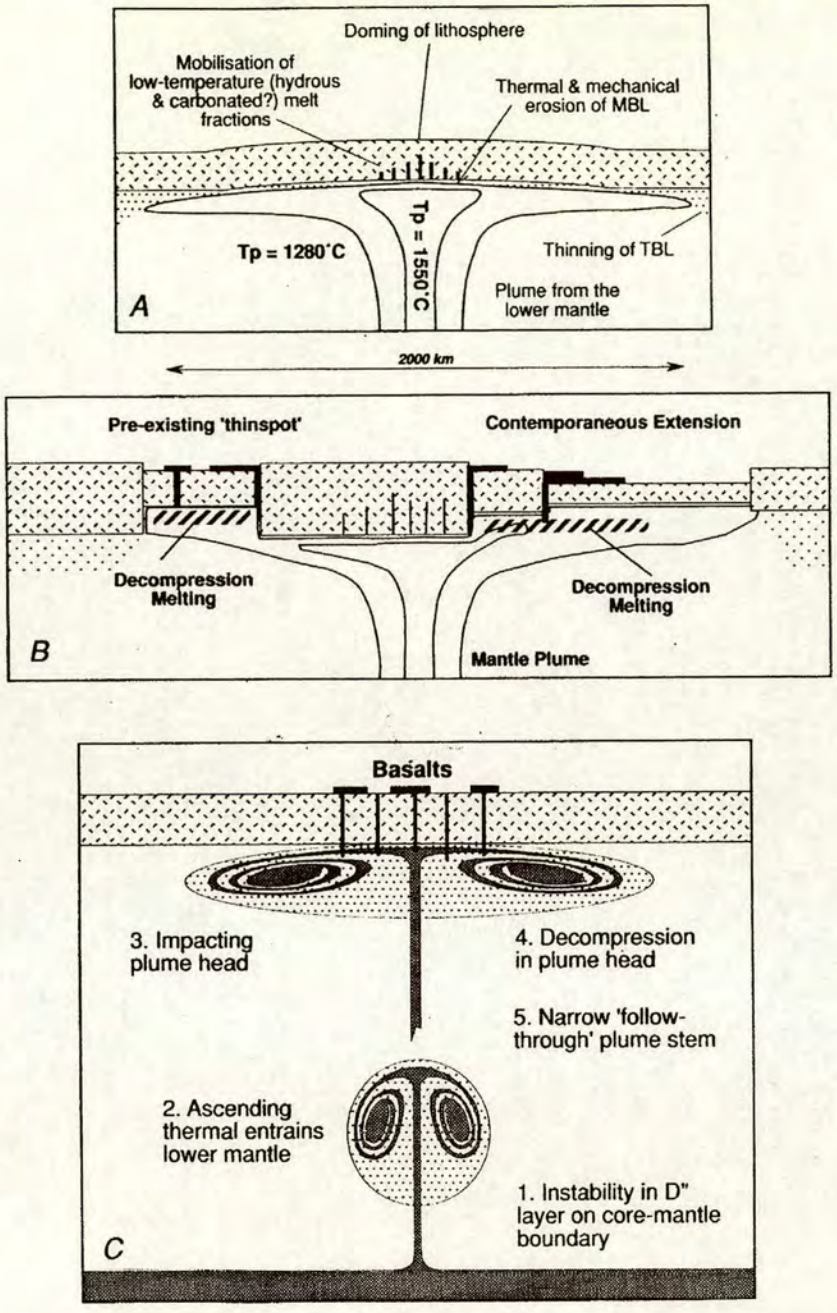

Figure 2.11. Schematic diagrams of plume-lithosphere interactions. a) Incubation of a plume head (potential temperature (T_p) of the plume core is shown to be 270°C greater than ambient mantle) beneath thick mechanical boundary layer (> 100 km). Extensive melting will result only if the lithosphere is extended and thinned (McKenzie & Brickle, 1988; White and Mckenzie, 1989); (b) As for (a) but with the thermal anomaly channelled by pre-existing topography at the base of the lithosphere, or by contemporaneous extension, resulting in extensive decompression melting (White & McKenzie, 1989; Thompson & Gibson, 1991); (c) Impacting plume-head 'start-up' model of Campbell & Griffiths (1990), Griffiths & Campbell (1990) and Richards et al., (1989). According to this model, if the plume temperature is sufficiently high (ΔT_p) > 300°C?) melting may precede lithosphere extension; picrites are erupted above the hottest part of the plume (from Larsen et al., 1994).

incubation model, the plume-impaction model predicts that plumes ascend relatively quickly (about 10 My.) and impact with the base of the lithosphere (Fig. 2.11, C).

Surface expression as a result of dynamic magmatic activity on VPCM

The addition of new material to the crust (underplating) and the thermal support produced by a mantle plume, affects the basin dynamics (e.g. White and McKenzie, 1989) and hence the stratigraphic evolution of VPCM's.

However, in contrast to the permanent uplift effect caused by underplating, a plume impacting the lithosphere causes only a transient surface uplift of the lithosphere of about 1 km elevation above the centre of the plume (White and Mckenzie, 1989; Griffiths and Campbell, 1990). This uplift can be more if extensive lithospheric stretching occurred prior to the ascent of the plume.

The surface uplift generated by a rising plume is commonly followed by subsidence and volcanism (e.g. White and Mckenzie, 1989; Griffiths and Campbell, 1990). There are thought to be two periods of plume related subsidence (Campbell and Griffiths, 1990). These are, 1) when the plume reaches the base of the lithosphere, but before the onset of the main period of volcanism, the plume head deflects which results in a period of subsidence and, 2) there is a second period of subsidence when the magma escapes from the mantle during volcanic extrusion and subsequently loads the earth's surface with volcanic material. Volcanism is thought to start suddenly and extend over a large and roughly equidimentional area of ca. 2000-2500 km in diameter (White, 1988; White and Mckenzie, 1989; Griffiths and Campbell, 1990). Following volcanism, a rapid thermal contraction of plume occurs leading to the creation of a narrow linear volcanic chain, 100-300 km in width, and thus the later surface expression of the plume is more linear (Campbell and Griffiths, 1990), such as the Greenland-Iceland-Faroes Ridge in the North Atlantic (Talwani and Eldholm, 1977). This change in expression of the plume is a result of decay of the mantle thermal anomaly by conductive heat loss to the surface, which causes extremely gradual, regional subsidence over a period of order 10^9 years (e.g. White, 1988).

Subsidence creates accommodation space/depocentres for the accumulation of sediments, particularly if the basin sinks below sea level. Thus the surface expressions of plumes on VPCM, in addition to the LIP, are doming (Courtney and White, 1986; Sleep, 1990) and magmatic underplating (Cox, 1989). In the stratigraphic record, the main effects of initial thermal uplift are shoaling of the shelfal strata accompanied by stratal thinning/erosion over the uplift area. A continued uplift (less than 10 My) leads to erosion and the development of unconformities (e.g. Rainbird and Erns, 2001). Evidence for plume-related uplift is found in the stratigraphic record in East Greenland for example. The plateau basalts in East Greenland erupted contemporaneously with the initiation of sea-floor spreading flowed onshore, where they became intercalated with fluvial and lacustrine sediments (Larsen, 1984). In west Greenland, subaerial lavas were erupted in the Nuussuaq embayment, with the northern region being overlain subsequently by non-marine sediments (Rolle, 1985). Clarke and Pederson (1976) report that after initial subaqueous volcanic breccias were produced in west Greenland, the basalt flows became subaerial. Across the present Baffin bay, at Cape Dyer, on the conjugate margin of the North Atlantic VPCM, the basalts were extruded over terrestrial sediments and flowed seaward (Clarke and Upton, 1971). In west and east Greenland Palaeocene magmatism and contemporaneous shallowing and incision and subsequent valley infill have been associated with transient plume uplift and subsidence (Dam et al., 1998).

In summary, VPCM in the vicinity of a plume experience uplift followed by subsidence and extensive volcanism associated with LIP. Underplating has a permanent uplift effect in contrast to the transient plume related uplift. The plume dynamics in addition to the volcanic productivity and underplating has great implication for the stratigraphic evolution of sedimentary basins.

Plate boundary forces acting on PCM

The main focus in this section is to describe the plate-interactions and plate motion that occur at mid-ocean ridges, especially at the initial continental break-up and sea-floor spreading in order to understand the nature of the motion of the underlying and

adjacent lithospheric plates. The structural lineaments and stresses generated during plate movements during mid-ocean ridge spreading may influence the generation of subsequence structures on passive continental margins (e.g. Bott, 1992, 1993). Long distance plate boundary forces, for example linked to plate collision/orogenic activity, are also considered.

During the early stages of sea-floor spreading, modifications in stress patterns controlling the divergence of the respective plates can result in a rearrangement of the sea-floor spreading axis (e.g. Arctic-North Atlantic, Indian Ocean). During the early phases of oceanic basins at divergent plate margins, ridge-jumps occur frequently, due to the abandonment of earlier spreading axes and the development of new ones (e.g. Palaeocene Labrador Sea, Oligocene Norwegian-Greenland Sea; Cande et. al., 1989). Furthermore, activity along sea-floor spreading axes can terminate abruptly if far-field stresses, resulting from plate interaction, impede further plate divergence. Examples are the early Oligocene abandonment of the Labrador-Baffin Bay sea-floor spreading and in the Bay of Biscay and Rockall Trough (Ziegler, 1993). These, nearly contemporaneous and rapid termination of activity along, distant sea-floor spreading axes could be explained by changes in plate interaction and resulting plate boundary reorganization (e.g. Ziegler, 1993).

During orogenic cycles compressional stresses are often transmitted over large distances into continental cratons giving rise to broad-scale lithospheric deflection (e.g. upwarping of arches, stress-induced subsidence of basins; Cloetingh, 1988) and the reactivation of crustal discontinuities (e.g. upthrusting of basement blocks, basin inversion (Ziegler, 1988, 1990). Examples are the Late Cretaceous-Palaeocene intra-plate deformation of Europe during the early phases of the Alpine orogeny, the late Cretaceous-early Palaeocene deformation of the US Rocky mountains and the Cenozoic deformation of the Argentinian Andean foreland (Petersen 1989; Ziegler 1990).

Driving mechanisms for lithospheric plate motions

The lithospheric plates represent the upper boundary layer of the earths convection system and thus their motion is thought to be linked to mantle convection (Zoback

and Magee, 1991). Convection occurs in the asthensophere and results from radioactivity and/or secular cooling of the mantle. All concentrated flow originates in the upper cold boundary layer, which stirs the interior as it sinks (Bird, 1998).

Mid-ocean ridge systems are driven mainly as a result of divergent stresses leading to the progressive opening of oceanic basins. This spreading is accompanied by edge forces or body forces contributing to the plate divergence. These forces are termed ridge push and underside frictional drag forces (Bott, 1992; Ziegler, 1992).

Ridge push force acts roughly perpendicular to the ridge axis (Zoback, 1992; Golke and Coblentoz, 1996) and has a strong effect on the stress distribution both locally near the ridge crest and within the adjacent passive continental margins (Bott, 1993). Ridge-push forces are thought to be amplified when plume activity is centered on a spreading axis (Lister, 1975; Dahlen, 1981; Bott, 1982, 1991; Bott and Kusznir, 1984; Dewey, 1988; Wortel et al., 1991) by causing a weakening of the lithosphere (Ziegler, 1992).

Basal shear friction (drag) may be considered as a passive force acting over the entire plate and may be either driving or resistive. The orientation of the shear stresses is assumed to be parallel to the direction of absolute plate motion (e.g. Meijer and Wortel, 1992), but this is unconstrained (Wilson, 1993). Drag forces may induce either compressional or extensional intra-plate stresses depending upon the absolute motion of the plate and other boundary conditions (Wilson, 1993). Drag beneath continents may be considerably greater than that beneath the oceans (e.g. Forsyth and Uyeda, 1975; Chapple and Tullis, 1977; Sabadini et al., 1992).

There is much controversy as to what effect the ridge-push and the drag forces have when coupled with deviatoric tensional stresses above upwelling convection cells (e.g. Wilson, 1992). Some workers think that these forces have no effect, but that the lithospheric plates drive themselves by convection alone and incidentally stir the rest of the mantle (e.g. Bird, 1998). However, as sea floor spreading axes can be offset at transform faults, it is hard to see how transform faults could be related to a major upwelling convection cells of the deep mantle (Ziegler, 1992). On the basis of finite element modelling, ridge push and subduction pull are in general, able to drive the plates without the need for basal drag exerted by the

convecting asthenosphere (Bott, 1993). Ridge push does not however contribute significantly to driving the plates (Bott, 1991), particularly during the break-up of a Pangea-type mega continent, shear traction forces in combination with deviatoric tensional stresses are the main plate moving mechanisms (Ziegler, 1992). On the other hand, during periods of dispersed continents, ridge push forces play a more dominant role driving the oceanic plates (Ziegler, 1992). With progressive widening of an oceanic basin, accompanied by cooling of the oceanic lithosphere away from the spreading axis, ridge push forces increase and may contribute to the movement of the diverging plates.

Bott (1993) demonstrates that basal drag may become an important plate moving force when a mid-ocean ridge is underlain by a mantle plume. For example, when a mid-ocean ridge is associated with a hotspot, as in the case of the North Atlantic and the Iceland plume, the main plate driving force comes from the greatly increased shear drag acting on the base of the lithosphere, resulting from buoyancy driven flow (Bott, 1991, 1993). As a result, the normal ridge push forces may increase by more than double, generating a large deviatoric compression extending into bordering continents (Bott, 1993). Thus, ridge push force related to the presence of the plume could considerably accelerate plate motion (Bott, 1993). This suggests that variation in plume flux may create variation in plate motion and hence change the quantity of intraplate stress and cause inversion deformation of the upper crust. Furthermore, along divergent margins, the forces are directed away from the plate interior and along transform zones, with the forces acting tangential to the boundary (Forsyth and Uyeda 1975; Zoback, 1992).

In summary; Plate interaction, driven largely by shear-traction of the mantle convection systems and their changes, together with ridge-push and slab forces may play an important role in the development of intra-continental rift systems, the opening of new oceanic basins and the inception (start) of and activity along subduction zones (Ziegler, 1992). The formation of structural inversion on continental margins, is not well understood tectonic processes but these boundary forces may play a role.

2.5. THE NORTH ATLANTIC VOLCANIC PASSIVE CONTINENTAL MARGIN

The North Atlantic passive continental margin is composed of numerous grabens and half grabens that developed as a result of repeated rifting phases since the end of the Caledonian orogeny (ca. 350 Ma) (Ziegler, 1988). These rifting phases led to thinning of the underlying continental crust and lithosphere until the eventual break-up in the early Eocene (Ziegler, 1988; Doré et al., 1999). The sedimentary basins have each differing and complex structural and stratigraphic histories and have played an important role in the evolution of the Paleogene passive margin basins.

The North Atlantic; A volcanic passive continental margin

The final rifting phase was associated with voluminous igneous material and represents the distribution of Tertiary igneous rocks that extends from Canada to the British Isles (e.g. Saunders et al., 1997) (Fig. 2.12, A). This Large Igneous Province of the North Atlantic (NAIP) is thought to have been produced in the vicinity of a proto-Icleandic plume (e.g. White and McKenzie, 1989; Skogseid et. al., 1992; Eldholm and Grue, 1994). The bulk of the activity occurred in two main phases. Phase 1 began about 62 My ago, and lasted for 2 to 4 My, whilst Phase 2 began at about 56 Ma and lasted 2-3 My (White et al., 1987; Saunders et al., 1997) (Fig. 2.13). Most of the magmas associated with Phase 1 were erupted through and onto continental crust (zone I and II; Fig.2.8). The magmatic activity of Phase 2 was followed by continent separation and ocean floor spreading between Greenland and Europe (Fig. 2.12). On both sides of the North Atlantic, SDRS have been recognised (White, 1988). The SDRS dated as 54.7+/- 1.8 Ma, offshore Greenland (Jolley, 1998; Holmes, 1998) are products of the initial sea floor spreading that started at Chron24r (Vogt and Avery, 1974 dated as ca. 56-53 Ma (Berggren et. al., 1995; Eldholm et al., 2000). ODP sites show that the SDRS are interbedded with terrestrial sediments (Larsen et al., 1994) indicating buoyant elevation at the spreading centre (Fig. 2.9). Accreted igneous material (LCB) underlies the SDRS (Fig. 2.8), which has been detected on deep angle seismic and assumed to have been emplaced coeval to the SDRS (e.g. White et al., 1987).

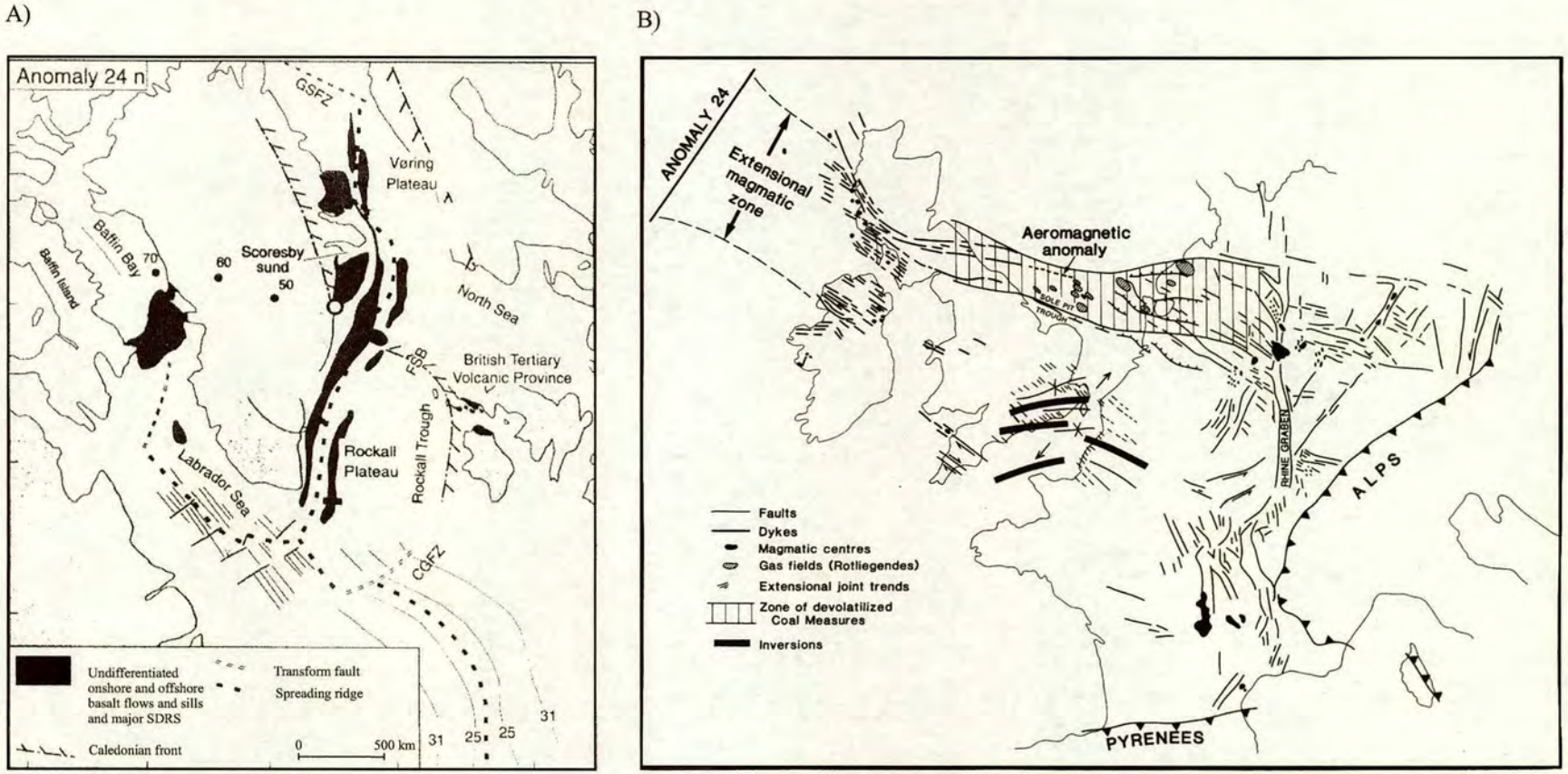

Figure 2.12. a) Plate reconstruction of the North Atlantic at magnetic Chron C24n time (53 Ma). Annotated circles mark the location of the Iceland plume (stem) at 70, 60, and 50 Ma according to Lawver and Müller (1994). GSFZ = Greenland Senja Fracture Zone. CGFZ = Charlie Gibbs Fracture Zone. FSB = Faroe-Shetland Basin. (from: Larsen and Saunders, 1998).b) Map of NW Europe showing the main tectonic features developed in the Palaeocene to Oligocene (from: Dewey and Windley 1988).

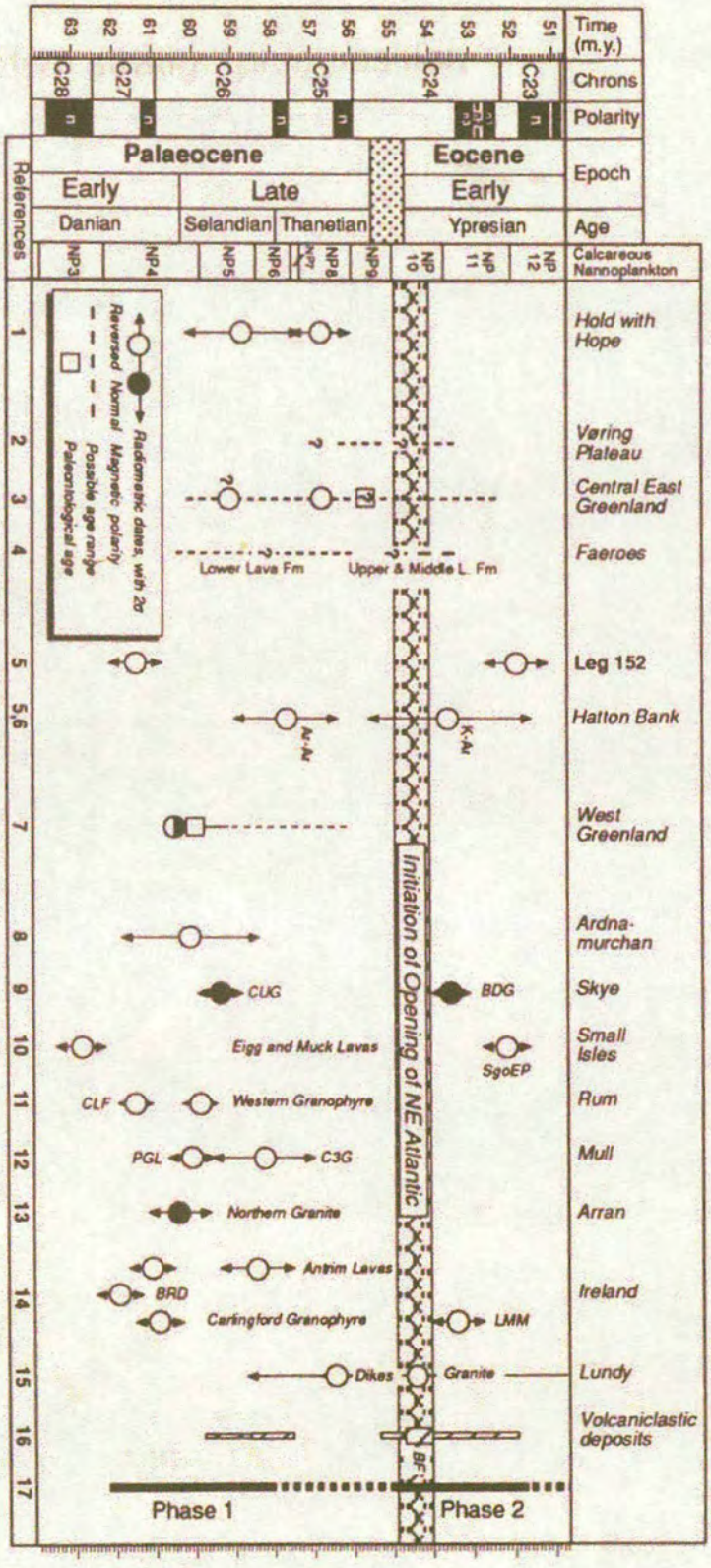

Figure 2.13. Time scale and event chart for the North Atlantic Igneous province showing two main phases of volcanic activity (see text) (from Saunders et al., 1998).

Sill complexes and dykes have been recorded both onshore and offshore, together with continental flood basalts within the NAIP (e.g. Ritchie and Hitchen, 1996). At present the entire North Atlantic is about 1 km anomalously shallow compared with other ocean basins of similar age, due to the thermal subsidence that commenced at the time of break-up, when the depositional surface was near or above sea level (White, 1988). There is no record of magmatic activity on the continental crust after continental break-up and the start of North Atlantic oceanic spreading. This is thought to be partly due to the mantle plume that was localised at the spreading axis after break-up and today the Iceland hotspot is located 240 km east of the Reykjanes and Kolbeinsey ridges (Lawver and Müller, 1994). All of the above suggests that the North Atlantic margin characterises a VPCM.

The North Atlantic mid-ocean ridge system

The ocean crust of the North Atlantic is made up of the present day North Atlantic mid-ocean ridge system, which is an epicentral belt that consists of five main segments 1) the Reykjanes Ridge, 2) Iceland, 3) the Kolbeinsey Ridge, 4) the Mohns Ridge and 5) the Knipovich (Fig. 2.14). Southeast of the Kolbeinsey Ridge is the proposed location of the extinct Aegir Ridge (e.g. Talwani and Eldholm, 1977). Each segment is separated by fracture zones (transform faults) that offsets the oceanic belt (Talwani and Eldholm, 1977). The evolution of oceanic basins is deduced from analysis of sea-floor magnetic anomalies. The five segments all have a unique history of spreading, and have tectonically influenced the surrounding region during major plate-reorganizations events and hence, have implications for the stratigraphic development in the surrounding basins on the adjacent shelf and onshore areas from Paleogene to present day. The following sub-section will go into more detail concerning the main steps in the evolution of the mid-Atlantic ocean ridge system, since the commencement of continental break-up. This is during the transitional and post-rift evolution of the adjacent passive continental margins.

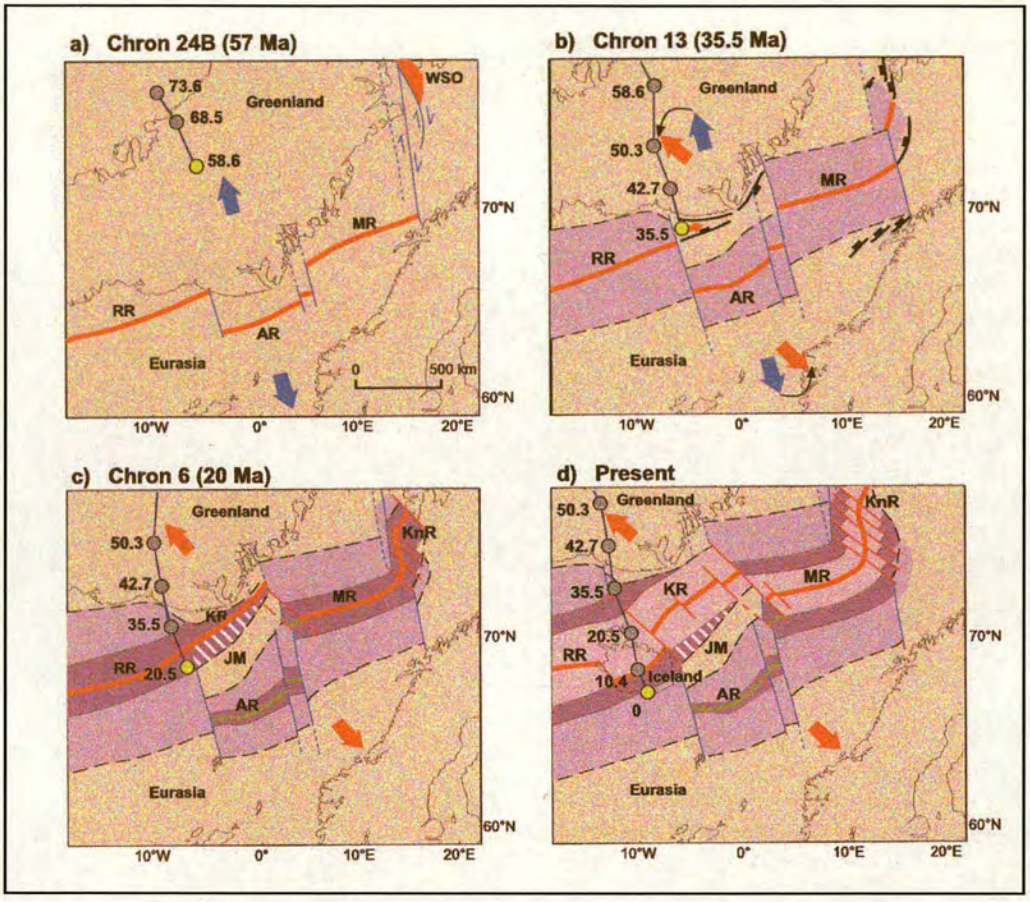

Figure 2.14. Plate tectonic evolution of the North Atlantic see text). RR, AR, KR, MR, KnR: Reykjanes, Aegir, Kolbeinsey, Mohns and Knipovich ridges. Annotated circles mark the location of the Iceland plume (stem) at 70, 60, and 50 Ma according to Lawver and Müller (1994) (from Lundin and Dore, 2002).

The North Atlantic spreading history

The initial opening of the North Atlantic resulted in extensive volcanism, regional ash falls and major plate reorganisations of the spreading pattern (e.g. Vogt and Avery, 1974; Egloff and Johnson, 1975; Srivastava, 1978; Eldholm et al., 2000) (Fig. 2.12). Rifting successively propagated northward, initially into the Labrador Sea and Rockall Trough, and then into the NE Atlantic (Srivastave and Tapscott, 1986) (Fig.2.15). In some instances the line of separation was guided by pre-existing anisotropy in the lithosphere, but the thermal swell associated with the ancestral Iceland mantle plume may also have exerted an important control during the Palaeogene (Hill, 1991).

In the North Atlantic area, increased tectonic activity was accompanied by the northward propagation of the Central Atlantic sea-floor spreading axis into the Labrador Sea during the Late Cretaceous (Ziegler, 1988) (Fig. 2.15). At the same time, the sea-floor spreading axis in the Bay of Biscay and the southern part of the Rockall Trough became extinct (Kristoffersen, 1978; Srivastava, 1978; Olivet et al., 1984). The Labrador Sea, which contains the remnants of a mid-ocean ridge, was spreading contemporaneously with the North Atlantic during the Paleogene, resulting in the northward movement of Greenland (e.g. Drake et al., 1963, Ziegler, 1992). The sea floor spreading in the Labrador Sea, was initially oriented northeast-southwest, but changed to a more northerly orientation when the North Atlantic spreading began to propagate northwards (e.g. Srivastava, 1978, Srivastava and Tapscott, 1986). A triple junction came into existence as Greenland separated from both North America and Europe (e.g. Roest and Srivastava, 1989) (Fig 2.15). The contemporous spreading in the Labrador Sea and in the North Atlantic was thought to be relatively short lived (e.g. Talwani and Eldholm, 1977). As a result of the major shift in plate motion at the opening of the Atlantic, sea floor spreading in the Labrador Sea became oblique and stopped after Chron 20, but prior to Chron 13 (Middle Eocene to earliest Early Oligocene) (Srivastava and Tapscott, 1986, Roest and Srivastava, 1989).

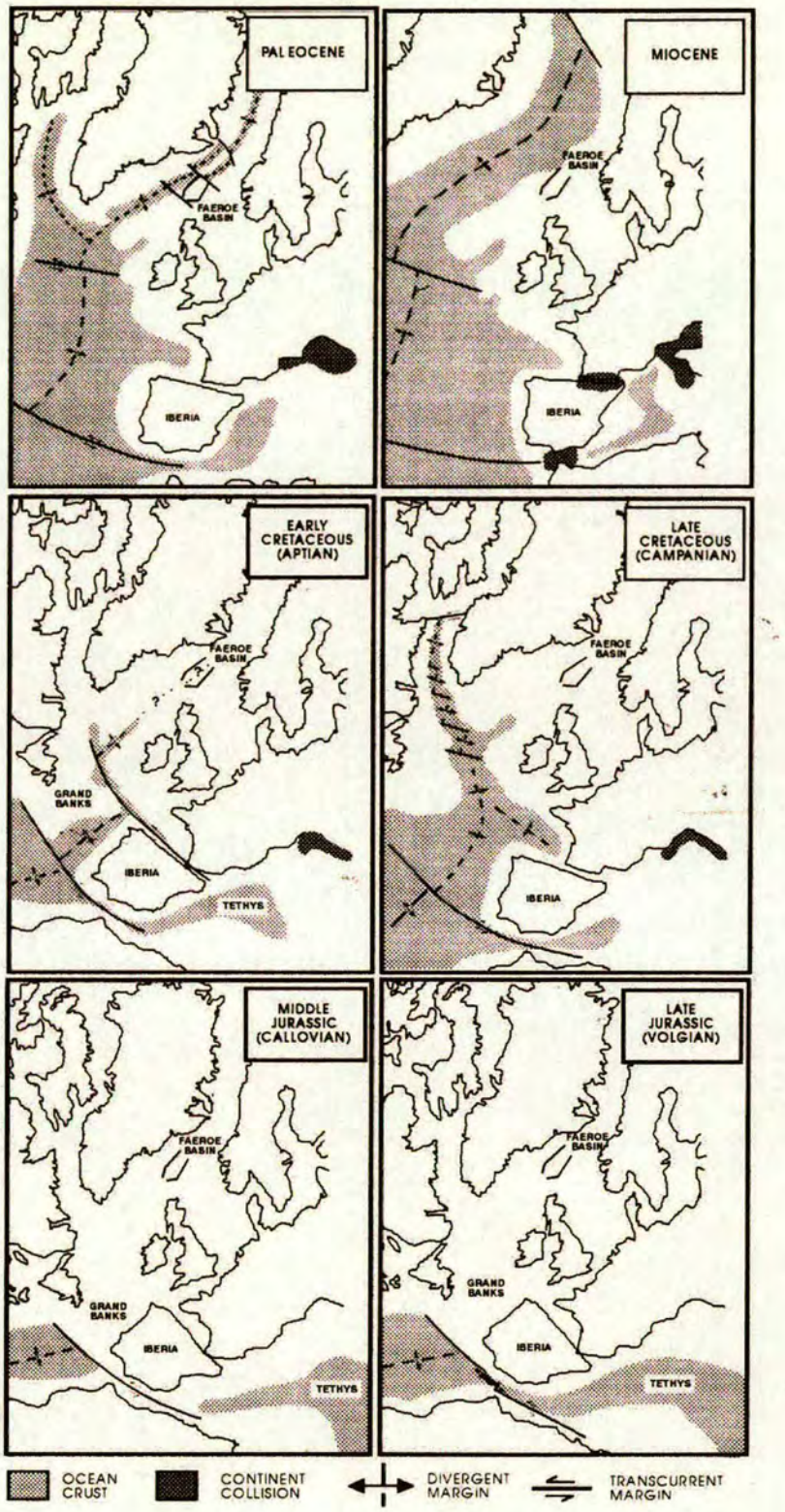

Figure 2.15. Maps showing the general plate configuration of the North Atlantic from Middle Jurassic to Miocene showing the position of the Faeroe Basin=FSC (after Rumph et al., 1993).

With the termination of spreading in the Labrador Sea, an important plate reorganisation occurred between magnetic anomaly 13 and 7 (the Oligocene) (Talwani and Eldholm, 1977) (Fig. 2.14). The change in spreading motion led to oblique spreading along both the Reykjanes and Mohns Ridges, and orthogonal spreading along the propagating Kolbeinsey Ridge (Srivastava and Tapscott, 1986; Vogt et al., 1980). During this period, seafloor spreading on the Aegir ridge stopped (north of Reykjanes ridge) as the locus of spreading shifted to the west on the Kolbeinsey ridge (Talwani and Eldholm, 1977). Therefore, the abandonment of the Aegir Ridge system was associated with a possible ridge jump from the Aegir Ridge to the Kolbeinsey Ridge (Gronlie et. al., 1979) (Fig. 2.14). The simultaneous northward propagation of the Reykjanes Ridge into the area west of the Jan Mayen microcontinent indicates that between magnetic anomaly 7 and 6 Jan Mayen was completely separated from Greenland (Larsen, 1988). The Reykjanes Ridge extended further north than it does at present. When Iceland came into existence, subsequent to anomaly 7 (Talwani and Eldholm, 1977), Iceland grew southward at the expense of the Reykjanes Ridge, and in addition an eastward shift in the ridge axis occurred in the vicinity of the Reykjanes Peninsula (Talwani and Eldholm, 1977). Prior to the existence of Iceland, the corresponding section of the mid-ocean ridge formed what are now the 15-30 km thick Iceland-Faroe and Iceland-Greenland Ridges that characterise the ocean bottom topography across this area, representing the plume track since opening (Talwani and Eldholm, 1977; Lawver and Müller, 1994). From magnetic anomaly 6 to present day, no major plate reorganisation events have been recorded (Fig. 2.14).

The addition of new crust and changes in spreading rates affects the subsidence and subsequent evolution of the adjacent rifted region (Mosar et al., 2000). During the Oligocene, the North Atlantic deep-water circulation became well established (Tucholke and Fry, 1985). Reconstruction of the subsidence history of the ridge system suggests that its eastern parts sank beneath sea level some time during the Middle Eocene, while between Iceland and Greenland the ridge sank during the Early to Middle Miocene (Thiede and Eldholm, 1983). However, the

distribution of shallow water benthic foraminifera indicates that the Nordic seas were effectively isolated from any "deep" Atlantic influence until about Middle Miocene time (Berggren and Schnither, 1983; Thiede, 1983).

Location of mantle plume(s)

The mantle plume in the North Atlantic is thought to have been situated beneath East Greenland during continental break-up. It has been postulated that the igneous province shows a younger age from Baffin Islands and west Greenland towards East Greenland, as a consequence of the plume track through this region (White, 1988) (Fig. 2.12a). Lawver and Müller (1994) have located the proto Icelandic mantle plume, at 61 Ma, in West Greenland a few hundred kilometre inland, by shifting the present plume location backwards in time within a fixed global frame of hotspots (Fig. 2.12a and 2.14). The proposed West Greenland plume location is consistent with the presence of flood basalt in this area that is dated at 61 Ma (e.g. Storey et al., 1998). However, the location of the plume in West Greenland falls short of explaining the near simultaneous flood volcanism in SE Greenland and the British isles, more than 1500 km to the east. Thus their model is uncertain.

Structural Inversion

Subsidence history of the North Atlantic

In the NE Atlantic, normal post-rift subsidence seems to have been outpaced by several uplift events (e.g. Joppen and White, 1990). In the NE Atlantic, Paleocene-Eocene uplift is superimposed onto the post-rift subsidence predicted by McKenzie (1978) (e.g. Turner and Scrutton, 1993; Clift and Turner, 1994; Joppen and White, 1990; Keen et al., 1987; Keen et al., 1990; White et al., 1992) and has been related to regional uplift generated by plume dynamics and also to some extent to underplating (e.g. Nadin et al., 1995, 1997).

In addition to the tectonic and magmatic events in the North Atlantic and Labrador Sea during the Paleogene, major orogenic events in the Alpine region occurred (Fig. 2.12b). At the same time, the NW European passive continental margin experienced structural inversion of sedimentary basins. External horizontal rather than isostatic vertical forces are required for inversion (Lowell, 1995). Structural inversion occurs when basin bounding/controlling extensional faults reverse their movement due to compressional tectonics. Extensional basins become positive structural features, which generally involves uplift of the basin floor and deformation of the basin fill (e.g. Williams et al., 1989; Roberts, 1989). The characteristic geometry of inversion structures include domes, anticlines, reverse faults and tectonic inversion structures, which are developed to a greater or lesser degree in an inverted basin (Bally, 1984; Williams et al., 1989; Doré et al., 1997) (Fig. 2.16). The formation of these structures implies that during basin inversion a commensurate amount of crustal shortening occurs, which is responsible for the deformation of the basin fill (Ziegler, 1988). The structural style of inverted basins is very variable and depends on the pre-inversion configuration of the respective basin, the lithologic composition of its sedimentary fill, the degree of inversion (amount of strain), and the orientation of the basin axis relative to the greatest principal stress that induced the inversion (Ziegler, 1988). Some pre-existing lows or sags can apparently be inverted in the absence of reactivated normal faults, as in the southern Altiplano of Bolivia and offshore Sabah, Borneo (Lowell, 1995). The most common horizontal driving force of inversion is transpression, or the combination of compression and strike-slip, which can enable substantial uplift to occur (Lowell, 1995).

Inverted basins can be seen from the Bristol Channel, the Weald and the English Channel to Holland; examples include, the Isles of Wight and Purbeck monoclines (Plint, 1982, Gale et al., 1999) and the west Netherland Basin (e.g. Ziegler, 1987) (Fig. 2.12b). Inversion features have also been identified along the length of the NE Atlantic margin (Roberts, 1989; Doré & Lundin, 1996; Boldreel and Andersen, 1993 and 1994; Doré et al., 1997 and 1999). For example the Ormen Lange dome and the Helland Hansen dome in the Norwegian Sea and the Wyville-

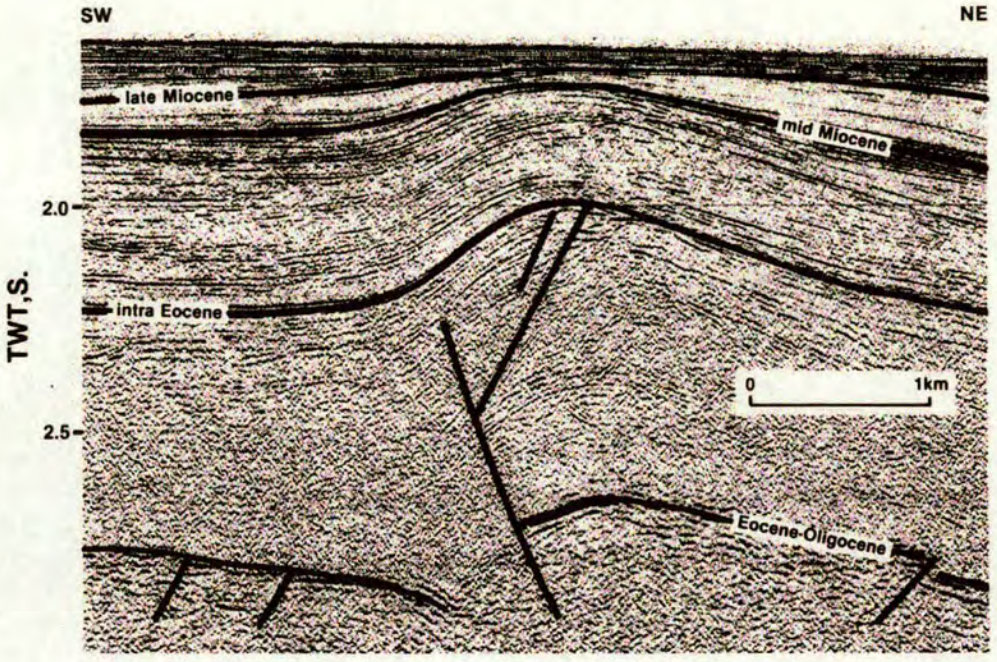

Figure 2.16. A seismic section, showing example of an anticline located southwest of Bill Bailey Bank on the NE Atlantic margin. From: Boldreel and Andersen (1993).

Thompson Ridge in the Rockall area (Boldreel and Andersen, 1993 and 1994) and also in the Faroe Shetland Basin (Lundin and Doré, 1996) (Fig. 2.16).

Basin inversion in and around the British Isles has taken place at different times and has been focused in different areas (Ziegler, 1987). During the early phase of the Alpine collision (Late Cretaceous-Eocene), transmission of compressional stress occurred through the European foreland and was most important in the southern North Sea region, apparently diminishing in importance westwards (Ziegler 1982, 1987). The next phase of inversion (Oligocene) occurred in response to subduction along the northern margin of Biscay and collision in the Pyrenees (Roberts, 1989). Compression was focused in the basins of the western British Isles and Bay of Biscay (Roberts, 1989). Along the NW Atlantic margin, inversion occurred in phases between the Eocene and Miocene (Lundin and Doré, 2002).

The cause of inversion and the growth history of these inversion features have been associated with the Alpine orogeny and/or plate reorganisation related to the North Atlantic oceanic spreading history. The general convergence of Africa and Europe from 95 Ma to Present adequately explains the in-plane compression and hence inversion of northwest European basins (Ziegler, 1987, 1998). On the NE Atlantic margin the timing and the location of the inversion features favors ridge push as the main source of the compression (Vågnes et al., 1998), although potential influence from plate reorganization (Lundin and Doré, 1996; Doré et al., 1997) and Alpine collision have also been suggested (Roberts, 1989; Boldeel and Andersen, 1993). Furthermore, and by contrast, differential loading has been proposed as the main mechanism for the growth of inversion domes (Stuevold et al., 1992).

The inversion structures (arches or domes) show a variety of different orientations with respect to the stress-strain field generated from ridge push, and many structures may follow the trends of the local basin-bounding tectonic structures especially if there has been oblique fault reactivation (Lundin and Doré, 1996). The Paleogene inversion structures have each undergone their own development, and although the timing is only loosely constrained, there seem to be two major 'pulses' of inversion; during the Early Tertiary and the Miocene.

To summarise, several mechanisms have been proposed for the inversion features that occur on the NE Atlantic margin. These are 1) the Alpine stress field, 2) rifting and subareal sea-floor spreading, 3) variation in the spreading rates on the oceanic ridge segments (Mosar et al., 2002), 4) underplating and the influence of the Iceland hotspot, 5) ridge push and mantle drag, 6) asymmetric spreading and mantle drag and 7) differential sediment loading, creating horizontal forces in the basin (Vågnes et al., 1998).

CHAPTER THREE

3.0 GEOLOGICAL SETTING FOR THE FAROE SHETLAND CHANNEL: STRUCTURE, STRATIGRAPHY AND VOLCANIC ACTIVITY

3.1. INTRODUCTION

The aim of this chapter is to give an overview of the structure and the stratigraphy of the FSC based on the previously documented literature. This knowledge is built upon in chapter four, five, six and seven, in order to achieve the main objectives (see chapter one). The first section of this chapter outlines the structural setting of the FSC, including the extensional rift history and deposition of mega-sequences. The second part focuses more on the younger post-rift interval and introduces the general stratigraphy, including the litho-, chrono- and igneous-stratigraphy that is relevant for this study. In this thesis the FSC refers to basins and sub-basins in the West of Shetland area. These include the East Faroe Graben and the Faroe Shetland Basin and associated Foinaven- Foula- and Flett- sub-basin (Fig. 3.1). The final section focuses on the Palaeogene igneous activity.

3.2. GEOLOGICAL SETTING; STRUCTURE AND MEGA-STRATIGRAPHY

Trending NE-SW, the FSC is bounded to the southeast by the Shetland Spine Fault (west of the British Isles), to the northwest by the Faroe Platform, to the northeast by the Erlend Platform and to the southwest by the Judd Platform (Fig. 3.1 and 3.2). The East Faroe Graben and the Faroe Shetland Basin are separated by the Sandøy Ridge, the South and North Westray Ridge, and in the northeast by the Corona Ridge (Fig. 3.1). In addition to the NE-SW trend the basins are thought to be further subdivided into sub-basins by cross-cutting transfer faults (e.g. Rump et al., 1993) although the

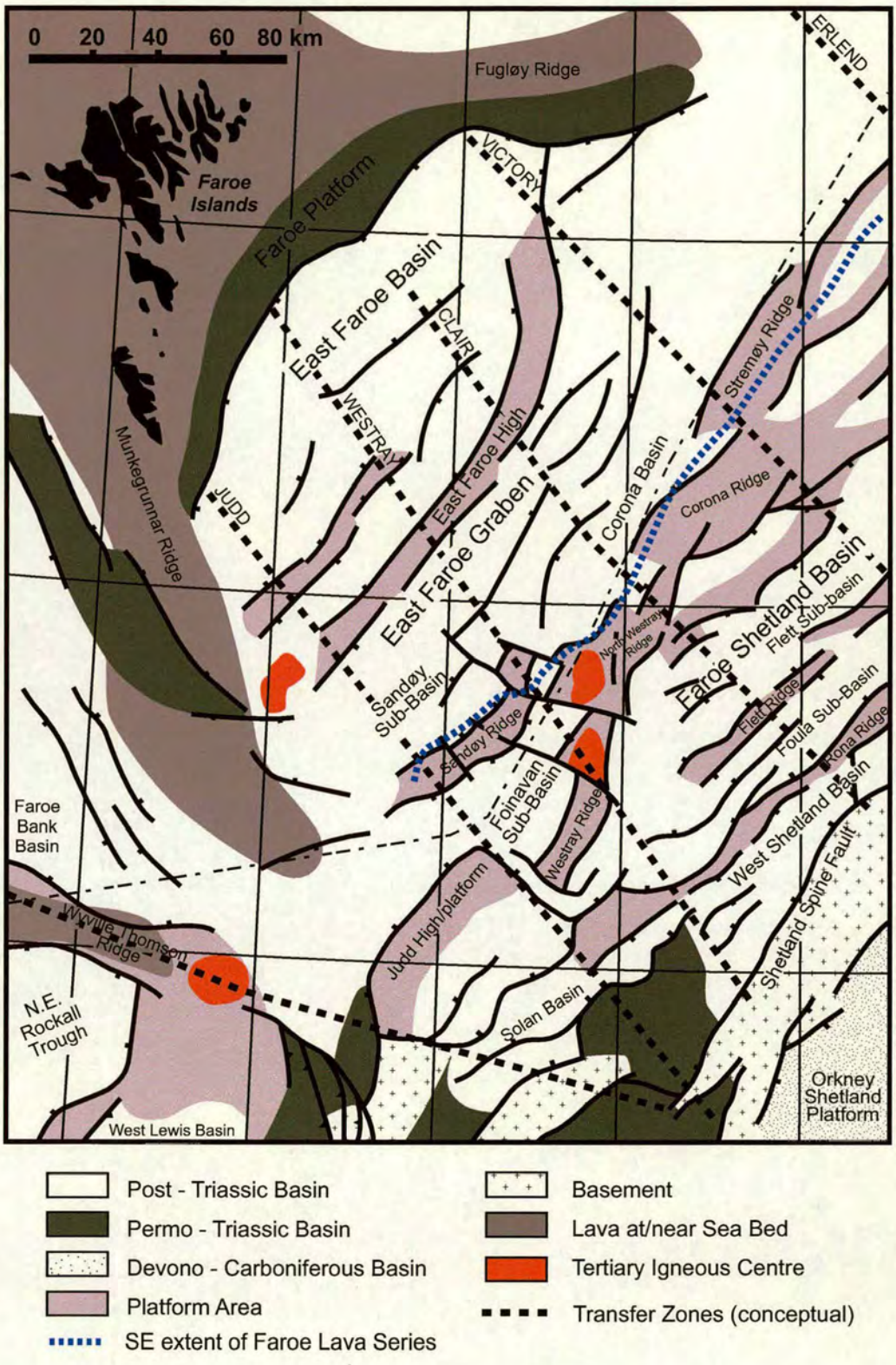

Figure 3.1. Offshore geological map indicating pre-Palaeogene structural basement configurations in the FSC: the Judd High, the East Faroe High, the Rona Ridge, the Sandøy Ridge, the South- and North Westray Ridge, the Corona Ridge and transfer zones (dashed line) separating the FSC into basins and sub-basins. (From Ellis et al., 2002).

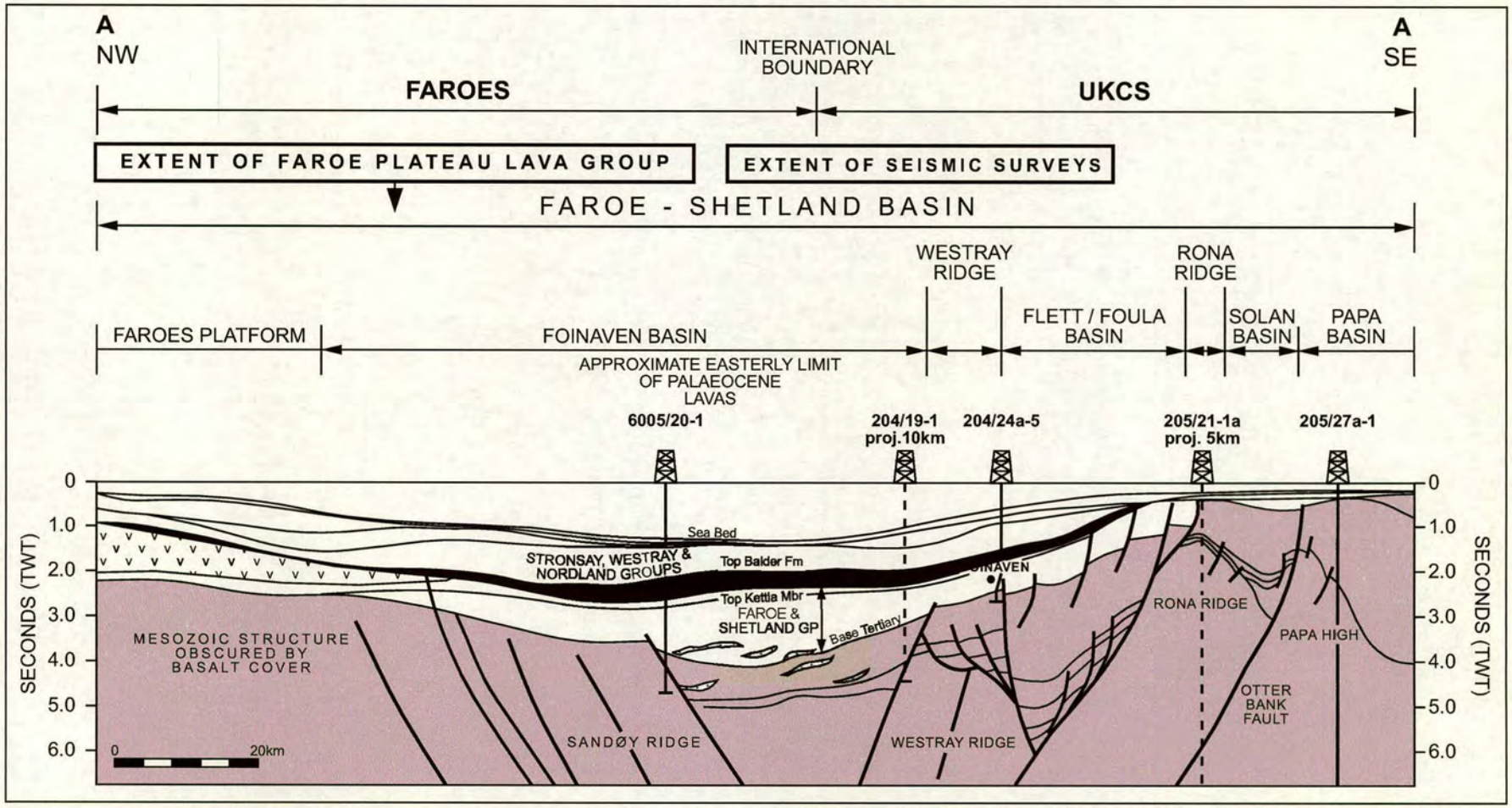

Figure 3.2. Regional NW-SE trending seismic section across the Foinaven Sub-basin showing the typical post-rift (steer's horn) geometry. Also, the easterly limit of the basalts that belong to the Faroe Plateau Lava Group is highlighted (modified after Carmichael et al., 1999). Location of the cross-section is shown on Fig.3.1.

exact number of these faults remains unclear (Fig. 3.3). The sub-basins represent from southwest to northeast the Sandøy-, Foinaven-, Foula-, Flett-, and Erlend sub-basins (Fig. 3.1). The transfer fault trend is an important influence on the basin geometry and stratigraphic evolution (Rumph et al., 1993), acting for example as fairways for sediment distribution (Naylor et al., 1999), and as bounding surfaces to lava flow distribution (Ellis et al., 2002).

Main structural events

The Caledonian Orogeny: The basins and sub-basins within the FSC developed as a result of a series of extensional rift episodes that occurred after crustal collapse of the Caledonian Orogeny (Ziegler, 1989; 1990). The major thrust sheets of the Caledonian Orogeny had been emplaced by the end of the Silurian period; however, episodic tectonic activity continued until the Carboniferous (Earle et al., 1985). How far northwest the thrust sheets developed is not known (Duindam and van Hoorn, 1987). There is an overall NE-SW, NNE-SSW trend, for example the Shetland Spine fault, that most likely reflects the old Precambrian grain of the basement, that were reactivated during subsequent extensional rift episodes (e.g. Duniam and van Hoorn, 1987; Roberts, 1989). Thus the location of the extension faults was controlled by the structure of the underlying Palaeozoic terrains (Roberts, 1989).

At least three major phases of extension and subsidence occurred during 1) the Devonian-Carboniferous, 2) the Permian-Triassic and 3) the Late Jurassic-Late Cretaceous.

Extensional Phase 1, Devonian-Carboniferous: The first phase of rifting occurred in the Devonian to the Carboniferous. Evidence from seismic and well data in the FSC shows that Precambrian crystalline rocks are capped by Devonian-Carboniferous red beds of fluvial origin (the Clair Group) recording this extensional phase (e.g. Duindam and van Hoorn, 1987).

Extensional Phase 2, Permian-Triassic: During the Permian-Triassic it is thought that extensional reactivation of the Caledonian thrust planes occurred (Brewer and Smythe, 1984) and peneplanation resulting in erosion and the creation of a major unconformity. The sedimentary succession comprises evaporitic and

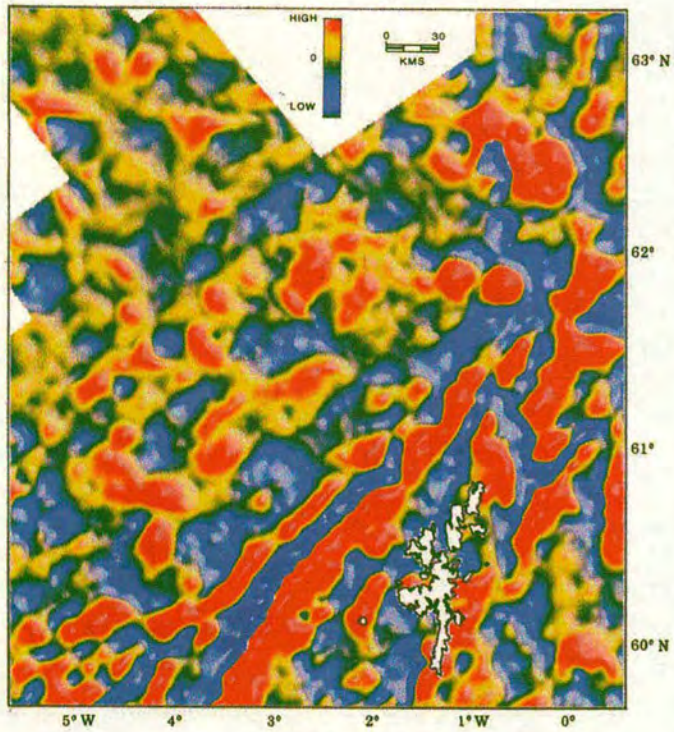

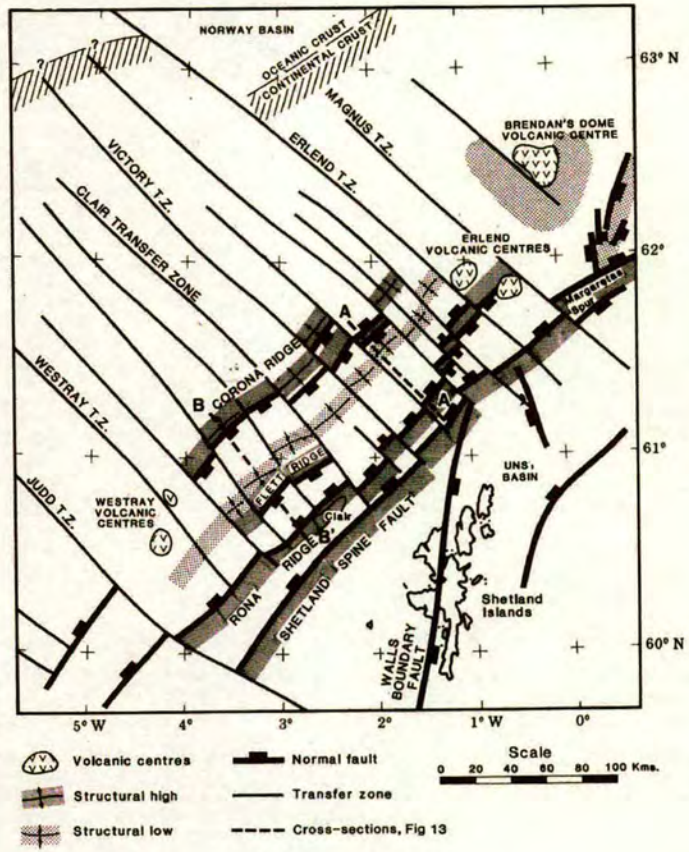

Figure 3.3. a) Gravity map of the FSC area, calculated by regional fields of wavelengths greater than 50 km from Bouguer gravity data. B) Map showing the interpreted structural configuration, including transfer zones and volcanic centres (from Rumph et al., 1993).

clastic red-bed sequences (Steel, 1974). The Permian-Triassic rift-geometry is obscured by subsequent rifting and also by major intra-Jurassic (Callovian) erosion. However, the bedding of the Permian-Triassic aged sedimentary remnants within the Solan and West Shetland basins dip/thicken predominantly southeast-ward and appears to have been controlled by northwest-dipping faults.

The early Jurassic to Bajocian (Middle Jurassic) extensional events have been documented from the Sea of Hebrides area (Morton, 1989). In the FSC Middle and Upper Jurassic (Bajocian-Bathonian and Oxfordian-Volgian) sandstones and conglomerates have been encountered in well 206/5-1 and interpreted to be deposited close to an active fault scarp (Hitchen and Ritchie, 1987). However, seismic and well evidence indicate that the orientation of this fault scarp is not clear and that the sediments are preserved in a slide block in the hanging wall, suggesting that these sediments were not influenced by Jurassic movements (Dean et al., 1999). In addition, N-S and NNE-SSW fault trends mapped in the FSC (e.g. over the Corona Ridge) are truncated by Late Cretaceous to Palaeocene faults, which trend NE-SW (Dean et al., 1999). N-S trending fault activity mainly during the Jurassic has been recorded in NW Europe (e.g. Doré et al., 1997), implying that this trend of fault in the FSC could also be of Jurassic age. However, it has been stated that the occurrence and orientation of Jurassic rifting in the FSC is still inconclusive (Dean et al., 1999).

Extensional Phase 3, Late Jurassic to Late Cretaceous: The onset of this rifting phase is marked by a major unconformity in the sedimentary succession near the top of the Middle Jurassic (Callovian). Progressive rifting during the Lower Cretaceous (the Valanginian-Barremian, which perhaps continued into the Apto-Albian) and the Upper Cretaceous (the Senomanian-Santonian and the Campanian-Maastrictian) is manifested in the sedimentary succession with the locus of fault activity and hence depocentres, changing through time (e.g. Dean et al., 1999). A progressive basin enlargement resulted with sediment derived from the West Shetland Platform locally spilling over and thus old basement highs are overlain by Cretaceous strata of different ages (Dean et al., 1999). The progressive rifting is evidenced in 1) *the Neocomanian*: as thick coarse clastic successions thickening into

the hanging wall of the Shetland Spine Fault and onlap and thin onto the Rona Ridge, where they represent calcareous sandstone facies (Dean et al., 1999), 2) *the Apto-Albian*: active faulting continued on the Shetland Spine Fault, and contemporaneous uplift and erosion occurred on the Rona Ridge (Dean et al., 1999), 3) *the Cenomanian-Santonian*: as rifting became focused along the Rona Fault which propagated south-westwards and down-throwing Lower Cretaceous basement highs into the basin and 4) *the Campanian-Maastrictian*: renewed extensional fault activity is reflected in the major displacements along the Shetland Spine Fault and the Westray Faults that downthrow the entire Rona Ridge into the basin (Duindam and van Hoorn, 1987; Hitchen and Ritchie, 1987; Dean et al., 1999). The active Shetland Spine Fault permitted the accumulation of 300-600m of early Palaeocene (Shetland Group) shales, which thickens to the northwest of the Rona Ridge (Dean et al., 1999). Furthermore, the Westray Ridge seems to have been an emergent high (or near sea-level) as indicated from the absence of Campanian-Maastrictian section in the south FSC (e.g. wells 204/19-1 and 204/23-1) (Dean et al., 1999).

In general, during the Lower Cretaceous the Rona Ridge, the Judd Platform and the Westray Ridge (Fig. 3.1) may have been connected forming a palaeo-high at this time. This is evidenced from the thin Lower Cretaceous successions recorded over these areas (e.g. Dean et al., 1999). Marked Lower Cretaceous thickness variations across the normal faults indicate that the fragmentation of the region into distinct depocentres commenced in the latest Jurassic-early Cretaceous. Middle Jurassic to Lower Cretaceous sequences one to two kilometres thick are downfaulted along the west side of the Rona Ridge to a depth of 6 km (Duindam and van Hoorn, 1987). Sands derived from the West Shetland Platform could have entered the FSC only near localised axial depressions (e.g. transfer faults/fault linkage points) of the Rona Ridge. The much more deeply buried Flett Ridge (within the centre of the Faroe Shetland Channel) is a westward-dipping fault-block bounded to the east by a prominent east-dipping normal fault. Lower Cretaceous strata blanket the underlying Jurassic sequence and show thickening towards this fault. The Flett Ridge was therefore active mostly during the Early Cretaceous (Duindam and van Hoorn, 1987).

During the Upper Cretaceous most of the basin-margin highs and platforms were submerged, and very thick mudstone was deposited, which blanketed these highs. Thus by Campanian times, most palaeohighs were inactive (e.g. Judd Platform) and had been drowned (e.g. Rona Ridge) and the Shetland Platform was probably also submerged as indicated by the widespread deposition of fine-grained clastics (shales and carbonates) (Dean et al., 1999). In addition to rifting a eustatic sea-level rise resulted in drowning of the rift margins and fault blocks within the rift such that erosion became negligible by Late Cretaceous times (Dean et al., 1999). The lack of rift shoulder uplift is taken as an indication that rifting was not accompanied by a significant thermal anomaly or an increase in heat flow. This is regarded as a consequence of the long rift duration (ca. 70 Ma) (Dean et al., 1999). Most faults die out in the youngest part of the Upper Cretaceous, but locally the activity seems to have extended well into the Palaeocene (see below).

Early Tertiary (Palaeocene-Eocene): Extension was succeeded by passive thermal subsidence (Roberts, 1989). Regional cross-sections across the FSC demonstrate that the stratigraphic configuration of the Palaeocene basin-fill is that of a well-defined post-rift ('steer's horn') geometry (e.g. Lamers & Carmichael, 1999) (Fig. 3.2). This is largely consistent with a phase of post-rift thermal subsidence following Cretaceous rift activity However, the Palaeocene has also been interpreted to represent a period of rifting accompanied by significant uplift and erosion as indicated by the basinward shift in the main depocentres between the Cretaceous rifting episode and the Palaeocene (e.g. Ridd, 1983; Dean et al., 1999) (Fig. 3.4). In addition to the uplift recognized from anomalous Palaeocene and Eocene subsidence patterns (Turner and Scrutton, 1993; Clift and Turner, 1994; Joppen and White, 1990; Keen et al., 1987; Keen et al., 1990; White et al., 1992) active rifting occurred along the length of the North Atlantic during the early and mid Palaeocene, evidenced by folding and faulting (e.g. Ebdon et. al., 1995). In the FSC, the early-mid Palaeocene interval represents mainly deep marine clastic sedimentation and deposition of mounded facies typical of basin floor fans (e.g. Ebdon et al., 1995; Lamers and Carmichael, 1999; Naylor et al., 1999). Evidence for the deposition of coeval lavas (early-mid Palaeocene) can be found in NW Scotland, for example

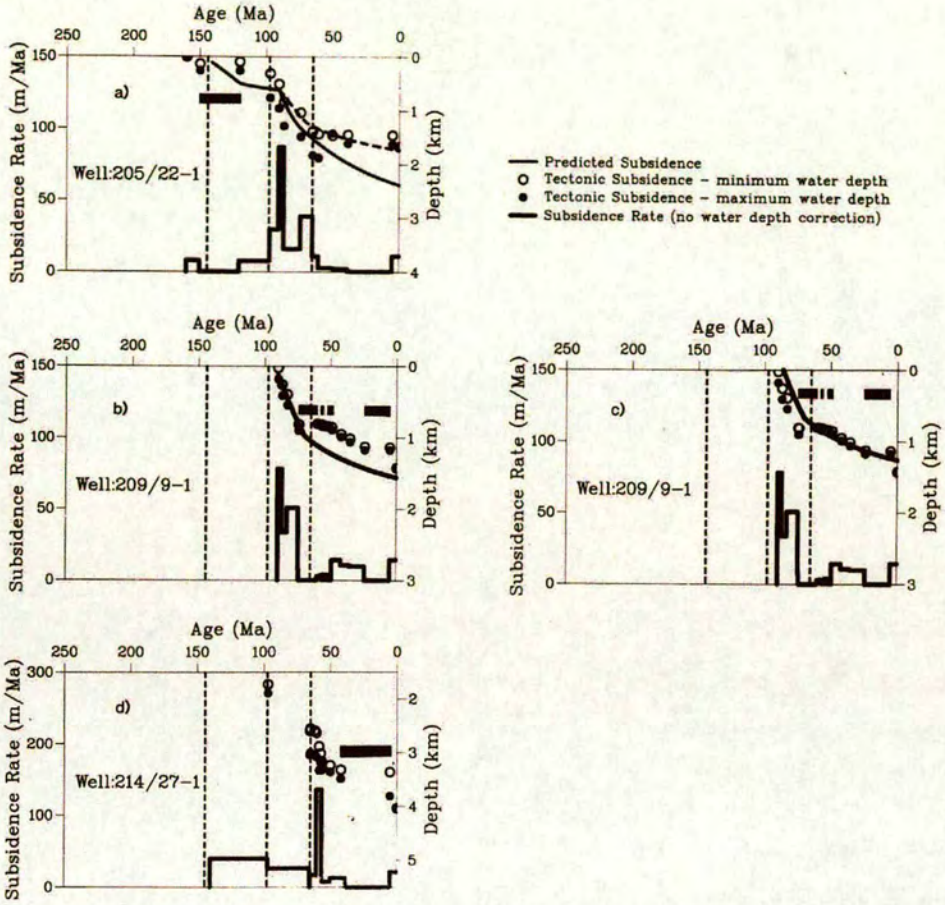

Figure 3.4. Subsidence curves, showing the post-rift subsidence history of the Faroe Shetland Channel (dashed line) compared with predicted subsidence curve (solid line) by theoretical models. Note the low and decreasing rates of Early Tertiary subsidence. These rates are much lower than those predicted by theoretical models fitted to the high rates of Late Cretaceous subsidence (solid line) (from Turner and Scrutton, 1993).

Antrim and Muck/Eigg (e.g. Bell and Jolley, 1997; Naylor et al. 1999) and in the Faroe Islands (The Faroe Plateau Lavas Group) (e.g. Waagstein, 1988). Deposition of sub-marine fan systems has been associated with uplift related to the igneous activity (e.g. White and Lovell, 1997; Lamers and Carmichael, 1999; Naylor et. al., 1999). Plume-related magmatic underplating has previously been invoked to explain the Palaeocene uplift (White and Lovell, 1997). The thermal impact associated with the volcanic activity enhanced uplift and erosion of the British Isles at the beginning of the Tertiary (e.g. Ziegler, 1982; Roberts, 1989), estimated by Joppen and White (1990) from apatite fission track studies to have been in the order of 1.5 km. Alternative explanations are based on analysis of the post-rift subsidence history of the FSC and the NNSB (Nadin and Kusznir, 1997) and show a transient phase of uplift in the Palaeocene. The uplift in the FSC (ca. 900m, deduced from stratigraphy) is transient and on that basis is thought to be associated with mantle plume, although a permanent uplift component may also have occurred (Nadin et al., 1997).

The general tectonic development since the beginning of extensional rifting comprises a long period of extension and rifting that ended in Early Eocene time forming what subsequently became the NE Atlantic margin (Roberts, 1975; Ziegler, 1982; Ridd, 1983; Duindam & Van Hoorn, 1987; Mudge & Rashid, 1987; Stoker, Hitchen & Graham, 1993). Early Tertiary igneous rocks are present in the centre of the rift system. Thus, rifting considerably thinned the underlying continental crust and allowing igneous intrusions to be emplaced (Megson, 1987; Mudge, 1987; Mudge and Rashid, 1987; Roberts et al., 1988). Flexural modelling using gravity and magnetic data suggests that the continental lithosphere has been relatively weak during much of the Mesozoic-Cenozoic evolution (Kimbell et al., 2004). Synchronous and subsequently to the opening of the North Atlantic Ocean the FSC was affected by compression and development of inversion features (e.g. Andersen and Boldreel, 1993, 1994).

3.3. CENOZOIC STRATIGRAPHY

Analysis of exploration wells throughout the Faroe-Shetland Channel has led to the development of robust lithostratigraphic and sequence stratigraphic schemes to describe and sub-divide the Cenozoic (Palaeocene-Present) section in the UK Continental Shelf (UKCS). The Palaeocene-Eocene section, which forms the focus of Chapter Five, is divided into four component lithostratigraphic units; the Shetland, Faroe, Moray and Stronsay Groups (Knox et al., 1997) (Fig. 3.5). The Eocene-Present section, which forms the focus of Chapter Six, is divided into three component lithostratigraphic units; the Stronsay, the Westray and the Nordland groups (Knox et al., 1997) (Fig. 3.6). In Chapter Five the main focus is on the Paleocene-Eocene section, whilst in Chapter Six the main focus is on the Eocene-Miocene section.

The transition between the Palaeocene and the Eocene (60-50 Ma) was marked by important changes in global climate, plate tectonics and in the global carbon cycle (e.g. Berggren et al., 1997; Beerling and Jolly, 1998). Several key stratigraphic events are recognised, including, 1) a major change in land mammal assemblages (e.g. Hooker, 1991; Koch et al., 1992; Aubry et al., 1996; Wing, 1998; Berggren et al., 1995), 2) major (35-50%) extinction of benthic foraminifera (Thomas, 1998; Thomas & Shackeleton, 1996), 3) the apparance of three short-ranging planktic foraminifera (Kelly et al., 1996), 4) weakening of atmospheric circulation (Rea et al., 1990), 5) increased precipitation and/or temperature, reflected in widespread increased rates of weathering and the production of kaolinite (Gibson, et al., 1993), 6) increased warming of high-latitude surface water and deep water, by ca. 5-7°C (Kennett & Scott, 1991), and an associated decrease in the carbon isotope values of benthic and planktonic foraminifera and bulk carbonates (Shackleton, 1986; Zachos et al., 1993).

Unlike the hot and humid Palaeocene-Eocene interval (e.g. Gibson et al., 1993), the transition between the Oligocene and the Miocene (ca. 22.5-26.7 Ma) was marked by several episodes of high-latitude cooling and continental glaciations. This is evidenced from the oxygen isotope record obtained in ODP sites (Zachos et al., 1997). The presence of Upper Oligocene and Lower Miocene glacial

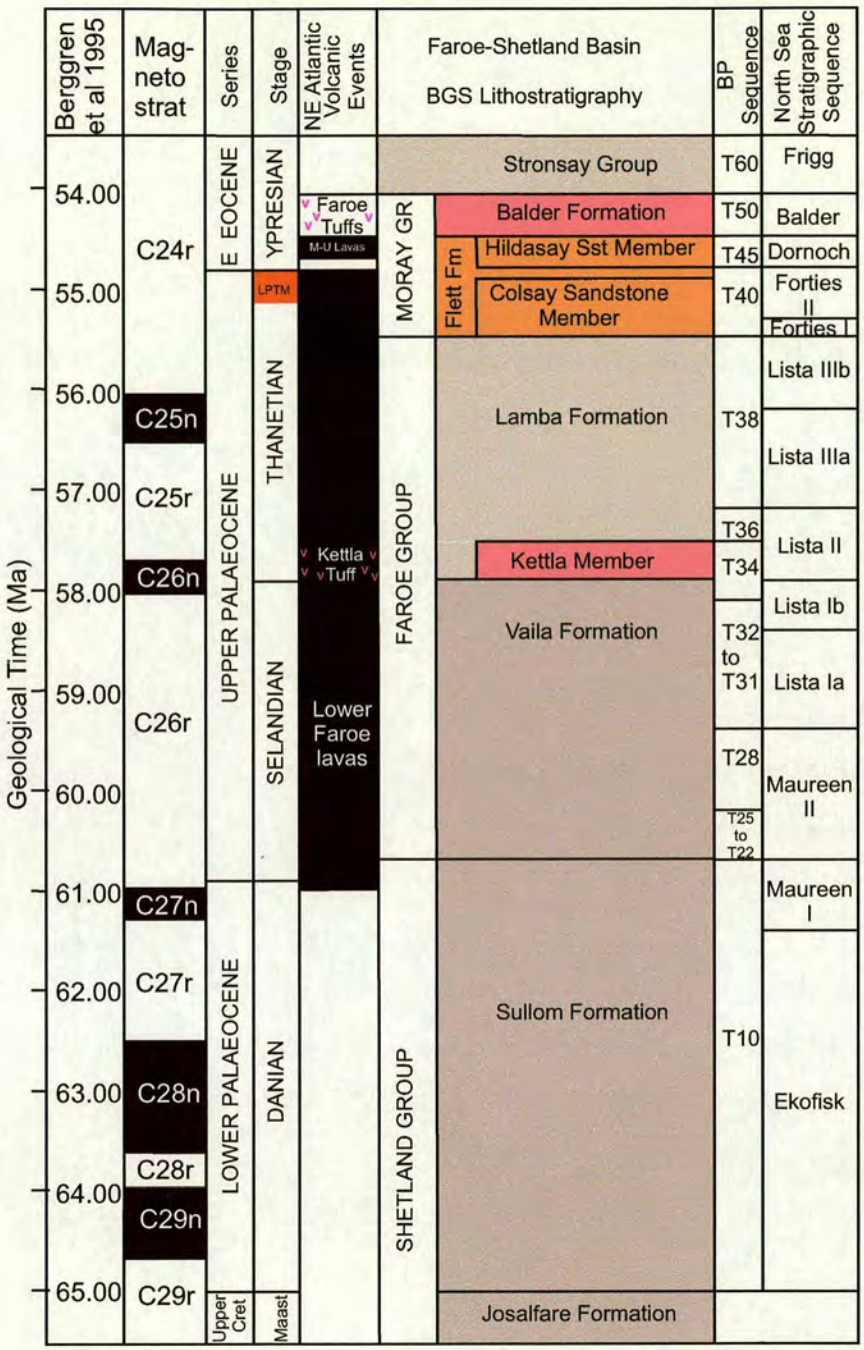

Figure 3.5. General Cenozoic Stratigraphy of the United Kingdom Continental Shelf (UKCS) in the West Shetland area. Time scale and magnetostratigraphy (from Berggren et al., 1995). Volcanic events: Lower Series 61-56 (from Waagstein, 1995). Basaltic lavas in well 205/9-1 age equivalent to the T40 are age equivalent to the Lower Series (e.g. Ellis et al., 2002). Note that these dates differ from the age dates from Jolley et al., 2002 (see text). Middle and Upper Series (modified from Waagstein, 1988; Riisager, 2002). The BGS lithostratigraphy of the FSC, the NNSB and the BP 'T-sequence' scheme (from Mudge and Bujak, 2001). The late Palaeocene thermal maximum (LPTM) (from Norris and Rohl, 1999; Rohl et al. 2000).

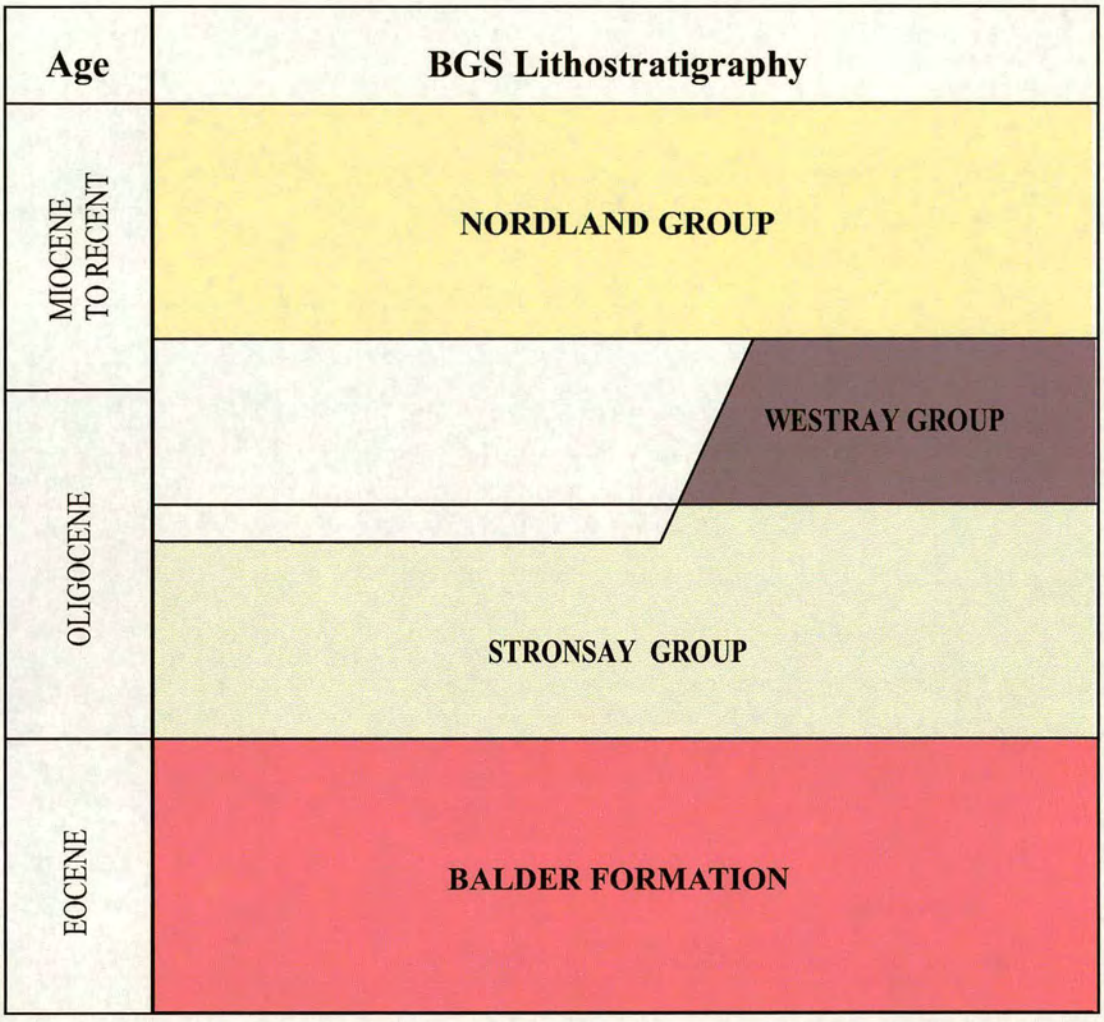

Figure 3.6. Lithostratigraphic nomenclature for the late Paleogene to Neogene of the UK west of Shetland area. From: Knox et al. (1997).

marine sediments (in the western equatorial Atlantic Ocean), as well as a prominent eustatic lowering (Haq et al., 1987) at the Oligocene/Miocene boundary (ca. 23.7 Ma) (Miller et al., 1996), suggests that part of the $\delta^{18}O$ increase was due to ice sheet expansion (Zachos et al., 1997).

During the Pliocene-Pleistocene glaciations and intergalciation periods occurred in the Northern Hemisphere (e.g. Stoker, 1999).

Lithostratigraphy

The early Tertiary stratigraphy in the FSC is generally described as a regressive sequence (Duindam and van Hoorn, 1987). It is composed of 1) an aggradational sequence of deep-marine mudstones and basin-floor fan sandstones of Danian to Selandian age (ascribed to the Shetland- and the Faroe Group), 2) a progradational sequence of a relatively less open-marine environment of Thanetian age (ascribed to the Lamba Formation, the Faroe Group) and finally 3) a progradational sequence of more restricted marine and non-marine deltaic to coastal plain lignitic sandstones of late Thanetian to early Ypresian age (ascribed to the Moray Group), reflected in the evolution of microfossil assemblages within the FSC (e.g. Mudge and Bujak, 2001). A widespread blanket of terrestrial extruded flood-basalts of Late Palaeocene age is present on the platforms to the northwest and north of the FSC (e.g. Duindam and van Hoorn, 1987; Ellis, et al., 2002) (Fig. 3.1 and 3.2).

The *Shetland Group* consists primarily of calcareous mudstones with subordinate sandstones, which are largely ascribed to the Sullom Formation (Knox et al., 1997). Biostratigraphic studies have shown that sediments belonging to the Shetland Group range from Late Cretaceous to earliest late Palaeocene in age, indicating that it is broadly equivalent to the Chalk Group in the North Sea (Knox et al., 1997).

The *Faroe Group* consists of a succession of mudstones and sandstones that lie between the Shetland and Moray Groups (Knox et al., 1997). They are late Palaeocene in age and have been shown to be equivalent to the Lista Formation and upper part of the Maureen Formation in the North Sea (Knox & Holloway, 1992). Internally, the Faroe Group is subdivided into the Vaila and Lamba Formations. The

Vaila Formation is Selandian in age and consists of medium-grey, variably silty mudstones with thick sandstone interbeds present in sub-basinal depocentres (Knox et al., 1997). The overlying Lamba Formation ranges from Selandian to Thanetian in age. It also consists of mudstones, which locally contain major sandstones some of which are ascribed to the Westerhouse Member (Knox et al., 1997). The lowermost unit in the Lamba Formation forms an important regional seismic marker, and consists of volcaniclastics, primarily composed of tuffaceous siltstones, ascribed to the Kettla Member. The Kettla Member has been shown to be age equivalent to the tuffs of the Glamis Member (also known as the Balmoral Tuffite or Andrew Tuff) in the Central North Sea (Knox and Holloway, 1992).

The *Moray Group* consists of late Palaeocene (Thanetian) to early Eocene (Ypresian) aged paralic and shallow marine sandstone-dominated sediments that occur in the UK Central and Northern North Sea (Deegan and Scull, 1977, Knox & Holloway, 1992) and deeper water mudstone-dominated sediments in the UK southern North Sea (Mudge and Copestake, 1992; Knox and Holloway, 1992; Lott and Knox, 1993). Similarity in the sedimentary successions has led to the use of the same term (i.e. Moray Group) in the West Shetlands area, where it is subdivided into the Flett and Balder Formations (Knox et al., 1997). The Flett Formation consists of shallow marine sandstones and subsidiary mudstones. Whilst it has been difficult to differentiate component lithostratigraphic units throughout the basin, it has proved possible for two sandstones units, the Hildasay and Colsay Sandstone Members, to be identified and correlated in depocentres in more distal, north-eastern parts of the basin (Knox et al., 1997; Ritchie et al., 1999). The Balder Formation overlies the Flett Formation and marks the top of the Moray Group. In the West Shetlands area, it consists of grey, variably silty and carbonaceous clastic sediments, which are interbedded with numerous tuffs derived from short-lived explosive eruptions. The Balder Formation is sometimes informally divided into two component parts: a lower tuff-rich unit and an upper relatively tuff-poor unit (Knox et al., 1997). Similar to the Kettla Member, the Balder Formation may be traced even further afield and has been recorded in the Southern North Sea and onshore areas of continental Europe (e.g.

Belgium and Denmark; Knox & Holloway, 1992), over 1000 km from its presumed source (Table 1a and 1b).

Younger sediments have been ascribed to three main lithostraigraphic units (Fig. 3.6). The oldest, the *Stronsay Group* directly overlies the Moray Group and consists of Eocene-aged sandstones, siltstones and mudstones. It is succeeded by Oligocene to early mid-Miocene-aged calcareous mudstones, siltstones and sandstones ascribed to the *Westray Group* and late mid-Miocene to recent glauconitic and shelly clastic sediments ascribed to the *Nordland* Group (Knox et al., 1997).

Sequence Stratigraphy

A regional stratigraphic framework for the Palaeocene sequences in the FSC has been defined by extensive mapping of seismic reflectors and analysis of wells that have been constrained by the regional biostratigraphic scheme (e.g. Ebdon et al., 1995). At least three different stratigraphic schemes for the FSC are available, including the sequence scheme (numbered 10-90) by Mitchell et al. (1993), the 'T-sequence' scheme (termed T10-T50) adopted by BP and Shell, and the 'AMG-sequence' scheme (termed 10-90) that have evolved from the work by Mitchell et al. (1993) and the Atlantic Margin group (an alliance of Mobil, Statoil and Enterprise). The scheme by Mitchell et al. (1993) is based on sequence boundaries, whereas the sequences used by BP and Shell are based on maximum flooding surfaces. Comparison with earlier studies undertaken in the North Sea has demonstrated that the majority of bioevents that Mudge & Bujak (2001) recognize in the West Shetlands area also characterize the Paleogene succession in areas east of the Shetland Islands (Mudge & Copestake, 1992; Mudge & Bujak, 1994, 1996). Also, Ebdon et al. (1995) utilized the North Sea regional stratigraphic framework identified by BP and Shell and compared and correlated the general North Sea sequence stratigraphy to the lithostratigraphic units to the sequences identified in the southern FSC. Significantly, the similarity between the stratigraphic successions has enabled Mudge & Bujak (2001) to calibrate the succession in the FSC, to the BGS lithostratigraphy (Knox et al., 1997), BP and Shell's sequence stratigraphic scheme, to the standard planktonic foraminiferal (P) and nannoplanktonic (NP) biozones and,

to the magnetostratigraphic and absolute timescales of Berggren et al. (1995) (Fig. 3.5). The time scale by Berggren et al. (1995) is used throughout this thesis.

Chronostratigraphy

The absolute age of the Palaeocene and Eocene stratigraphic interval has been established by Cande and Kent (1995). Correlations using planktonic foraminifera obtained from the Ocean Drilling Program (ODP) sites has enabled the Cande and Kent (1995) scheme to be extended to the sedimentary record in general (Berggren et al., 1995) and the North Sea and West of Shetlands, including the FSC (Berggren and Aubry, 1996). The time scale by Cande and Kent (1995) allows an improved correlation between the biostratigraphically dated sedimentary successions and the radiometrically dated lava successions of the North Atlantic borderlands (Knox, 1996).

Correlation between the litho- and sequence stratigraphic (BP/Shell and Mudge and Bujak, 2001) schemes and the magnetostratigraphy and absolute timescale of Berggren, et al., (1995) enables the duration of each stratigraphic interval to be determined. In the scheme of Berggren et al. (1995), deposition of the stratigraphic interval bounded by the Kettla Member and the Balder Formation represented around 5.35 My (59.4-54.05 Ma). Deposition of the Flett Formation is thought to have occurred in 0.92 My. (55.5-54.58 Ma) and deposition of the Balder Formation is thought to have occurred in 0.53 My (54.58-54.05 Ma), respectively (Berggren et al., 1995) (Fig. 3.5).

There are however, controversies and also discrepancies related to the Palaeocene-Eocene interval. The main controversy concerns the reliability of the time scale around the 55 Ma Palaeocene/Eocene boundary interval (e.g. Ali and Hailwood, 1998; Norris and Röhl, 1999). This is because the Palaeocene/Eocene boundary is based on the calibration point of 55 Ma for the calcareous nannofossil zone NP9/NP10 boundary (Aubry et al., 1996; Cande and Kent, 1995). The main problems that arise from using the NP9/NP10 boundary dated at 55 Ma as a tie-point are 1) that this date was used to estimate the ages of the C24n and C25n polarity boundaries (Cande and Kent, 1992; Cande and Kent, 1995), thus the NP9/NP10

boundary and the upper and lower bounds of chron C24r are effectively 'set-in-stone' (Ali and Hailwood, 1998) and 2) the Palaeocene/Eocene boundary was established where the zonal boundary is an unconformity of unknown duration (Aubry et al., 1996), a factor that further compounds the first problem (Ali and Hailwood, 1998; Norris and Röhl, 1999). The consequences of this are mainly that the 55.9 Ma data for the top of chron C25n may be significantly in error (Ali and Hailwood, 1998; Norris and Röhl 1999). Therefore, a chronostratigraphic calibration of the relationship between volcanic, sedimentation and tectonic events which occurred during the Paleogene, especially around the Palaeocene-Eocene boundary must be taken with care.

The late Palaeocene thermal maximum (LPTM). The Palaeocene-Eocene period with extinction of the benthic foraminifer and the rise in temperatures, has been interpreted as indications of greenhouse warming and formation of oxygen-deficient deep waters. Superimposed on this warming was a global short-term extreme warm event, termed the late Palaeocene thermal maximum (LPTM) (e.g. Zachos et al., 1993; Lu et al., 1996; Scott et al., 1996). Using an astronomically calibrated time scale, the LPTM occurred at ca. 54.93-54.98 Ma, with duration of ca. 220 Ky (Norris and Röhl, 1999; Röhl, et al., 2000) (Fig. 3.5). The LPTM event is thought to have been caused by release of ocean-floor methane hydrates and their subsequent atmospheric oxidation to isotopically light CO_2 (Dickens et al., 1997). Thus the LPTM, is thought to have been triggered by a change in ocean circulation (Röhl et al., 2000) represented by the decrease in the carbon isotope values of benthic and planktonic foraminifera and bulk carbonates (Shackleton, 1986; Zachos et al., 1993; Lu et al., 1996; Thomas and Shackleton, 1996). The resultant greenhouse climate allowed migration of some species, introduced new ones, and evolution of aquatic and marginal swamp plants occurred (Jolley et al., 2002). Furthermore the turnover in land mammals is also related to the LPTM event (e.g. Norris and Röhl, 1999).

A second controversy exists over the time scale by Berggren et al. (1995). A dating discrepancy is evidenced from Ar-Ar isotope dates, which show that the Lavas overlying palynology that represents the LPTM interval have ages between 57.5 Ma

and 60.54 Ma (Jolley et al., 2002). However, since the LPTM is 54.98 Ma (Norris and Röhl, 1999) there is an age discrepancy of up to 5 My (Jolley et al., 2002). Thus, according to Jolley et al. (2002) biostratigraphic and sedimentological evidence from the FSC (well 205/9-1) (Larsen et al., 1999) indicate that the late T40 (Ebdon et al., 1995) lava fields were erupted subsequent to the LPTM, and that isotopic evidence from both U-Pb and Ar-Ar dating systems attest to a pre-55-55.5 Ma age for the palynology and thus the LPTM (Jolley et al., 2002). The sedimentary sequence T40 is dated as 60.5-57.5 Ma and sequences T45-T50 as 56.5-53.5 Ma by Jolley et al. (2002). The Berggren et al. (1995) time scale dates sequence T40 at 55.5-54.8 Ma and sequence T45-T50 at 54.58-54.05 Ma (see further discussion in Chapter Five). Although, the discrepancy could be explain by inaccuracy of the biostratigraphical correlation or by contamination of dated igneous rocks, Jolley et al. (2002) indicate that there might be a previously undetected problem with the time scale.

Time scales are constructed on a series of assumptions that will be subject to continuous reassessment, including the Paleogene time scale (Berggren and Aubry, 1996). Thus, the above controversies indicate that a new time scale that removes all of the discrepancies, including the main ones explained above, is needed.

Paleogene Igneous activity in the FSC; The age and duration of volcanic activity

Igneous intrusions and extrusions of the North Atlantic Igneous Province (NAIP) correspond with prominent and regionally correlatable volcanic horizons and flows in offshore areas of the Atlantic Margin and the North Sea (e.g. Ritchie and Hitchen, 1996). Major igneous events are recorded in the FSC, such as the tuffs of the Kettla Member, the basalts of the Faroe Plateau Lavas Group (FPLG) and the tuffs of the Balder Formation. These igneous rocks are sometimes referred to as the British Tertiary Igneous Province (BTIP)

The Faroe Plateau Lava Group (Casten, 1973; Casten and Nielsen, 1975; Bott et al. 1974; Hald and Waagstein, 1984; Ritchie and Hitchen, 1996), consists of flood basalts that were derived from the NW (Ritchie, 1999), and reaches its maximum extent within the FSC (Fig. 3.1). The Faroe Plateau Lava Group (FPLG) has been divided into three Series, Lower, Middle and Upper on the basis of minor

unconformities (Noe-Nygaard and Raasmussen, 1968). Radiometric age dates of the onshore Faroes Lower Series sequence indicates that the lavas continued to flow intermittently between 61-56 Ma (Waagstein, 1995) (Fig. 3.5). However, paleomagnetic sampling suggests that the Lower Series were emplaced later during C26n-C25r-C25n, and the Middle and Upper Series were emplaced during C24r (Waagstein, 1988; Riisager, 2002). These magnetostratigraphic dates suggest a close temporal relation between the onset of NAIP second phase of volcanism (Chapter Two) and to the oldest rocks dated from Ar-Ar dates within the British North Atlantic Igneous province (BTIP) dated at 60.56 +/- 0.25 Ma, and the youngest dated at 58.66 +/- 0.25 Ma (Chambers and Fitton, 2000). Furthermore, intrabasaltic palynology and isotope ages in correlative rocks suggest that the Lower Series has an absolute age of 60.56-57.5 Ma (Jolley et al., 2002). A hiatus before the eruption of the Middle and Upper Series during the latest Palaeocene (Lund, 1983) resulted in a marked weathered and uneven surface of the top Lower Series and subsequent deposition of a 10-20m thick coal-bearing sequence that was deposited in an overbank floodplain environment (e.g. Rasmussen, 1990; Ellis et al., 2002). Palynological data (pollen flora) from the coal-bearing horizon on the Faroe Islands have been correlated to the intrabasaltic palynofloras recovered from borehole in the FSC (well 205/9-1) in the T40 sequence (e.g. Ebdon et al., 1995; Jolley, 1997; Naylor et al., 1999). The palynofloras recovered directly beneath and between the lava flows of well 205/9-1 have a particular diagnostic character that is seen over a wide geographic area (e.g. Ellis et al., 2002; Jolley et al., 2002). The palynofloras from 205/9-1 are comparable to the assemblages recovered from 1) the Lower Series of the FPLG coals on Suðuroy, Faroe Islands (Ellis et al., 2002), 2) the North Sea Basin (present in the Sele Formation, Unit S1b of Knox and Holloway, 1992), 3) Denmark (the Ølst Formation; Heilman-Clausen, 1985), 4) the uppermost lavas of Erlend Volcano Lava field (Jolley and Bell, 2002), 5) sediments between the Lower Series lavas of the Vøring Plateau (Boulter and Manum, 1989), 6) southern England (Lambeth Group) and, 7) the London-Paris Basin (upper Woolwich-, and upper de Varengiville Formation; Ellison et al., 1994). The correlation is furthermore enhanced by the presence of common species assemblages in the uppermost units of

the lava interval immediately above chron 25n in NW Europe (Ellison et al., 1996), the occurrence of which has been related to migration subsequent to the LPTM (Bujak and Brinkhuis, 1998).

Most of the activity associated with the Faroe-Shetland Intrusive Complex, a belt of intrusive rocks that covers an area of approximately 40,000 km2, occurred between 55 and 53 Ma (latest Thanetian-Ypresian) (Hitchen and Ritchie, 1987; Fitch et al., 1988; Ritchie and Hitchen, 1996).

The igneous intrusive centres within the FSC which represent the South Westray (Rumph et al 1993), and the North Westray (previous called the Judd) (Hitchen and Ritchie 1987) have only been detected from seismic and gravity data, and have to date, not been drilled. However, a similar seismic feature, located on the outer northern Hebrides shelf within the British Tertiary Igneous Province, was recorded in borehole 85/5B with a reliable Ar-Ar age of 55+/- 0.8 Ma. This may suggest that the centres within the FSC could be of similar age.

Volcaniclastic sedimentation consists of basalt and is predominantly derived from Fe-Ti-rich basalt precursors (Knox and Morton, 1988; Morton et al., 1988). The volcaniclastics present in the FSC are widespread and can be correlated from NE Atlantic margin across to Denmark (Knox and Morton, 1988; Morton and Knox, 1990). Two distinct phases have been recognised (Knox and Morton, 1983, 1988). The first phase occurred around 60-57.5 Ma and the second, which was the most voluminous phase, occurred around 56-50 Ma. The most extensive horizon occurs in the Balder Formation, 54.5 Ma. Eruptive (source) centres were broadly to the west of the British Isles and in the Faroe-Greenland region during the first phase of volcanic activity, but appear to have been restricted to the Faroe-Greenland area during the second phase (Knox and Morton, 1988). The voluminous deposition of the volcaniclastic sediments have been explained by being associated with the ancestral Iceland mantle-plume (Morton and Knox, 1990) and the Balder tuffs have been associated with the opening of the Atlantic (Ritchie and Hitchen, 1996).

Volcaniclastic deposits are common in offshore boreholes, and provide important correlation horizons both in the North Sea and to the northwest of Britain, including the FSC. The coarse-grained tuffites obtained from well 204/28-1, assigned

to the Balder Formation, appear to represent a distribution of ash material of more local derivation. Also, the relatively coarse-grained tuffaceous material obtained from well 209/4-1a, may be of local derivation. Geochemical and biostratigraphic analysis of offshore dredge samples recovered to the East of the Faroes (in Quadrant 6105), supported by seismic mapping, now suggest that the Balder Formation tuffs rest on the Upper Series lavas. In this case, the Middle and Upper Series predate the deposition of the balder tuffs of the Balder Formation, which represents a regional seismic marker due to its tuff content (e.g. Waagstein and Heilman Clausen, 1995).

SECTION TWO:

PALEOGENE-RECENT POST-RIFT SUCCESSION: THE FAROE-SHETLAND CHANNEL

CHAPTER FOUR

4.0. MESOZOIC STRUCTURAL CONFIGURATION OF THE FAROE-SHETLAND CHANNEL (FSC)

4.1. INTRODUCTION

The aim of this chapter is to document the main structural features and 'igneous ridges' within the southwest, south- and north-western part of the FSC. This is key information that will be built upon in later chapters of this Thesis (chapters Five, Six and Seven). More specifically, in later chapters it will be necessary to link the geometry of the Mesozoic structures and pre-Paleogene basins with distribution of the Paleogene depositional systems (chapters Five and Six) and to the orientation of inversion structures (Chapter Six). Thus an understanding of the Mesozoic structural configuration is important for these later chapters.

The predominantly NE-SW trend of the main fault-bounded ridges and the NW-SE trend of the transfer faults of the FSC is seen on gravity and magnetic data and is well documented (e.g. Ridd, 1983; Bott, 1984; Rumph, 1993; Duindam and van Hoorn, 1997) (see Chapter Three). The southwest and the northwest boundaries of the FSC, are poorly imaged seismically due to the existence of extensive volcanics, poorly mapped due to a lack of data and hence poorly understood (e.g. Ebdon et al., 1995). However, using recent acquired seismic data in this area, an attempt is made herein to interpret the main basement structures in the FSC area, in particular, the Judd Platform and the Westray Ridge, since their trend deviates from the NE-SW trend and general geometry of the Mesozoic structures within the FSC. In addition, in the area between the Mesozoic Judd Platform, the Sandøy Ridge, the Westray Ridge and the East Faroe High overlying post-rift inversion features are present (Chapter Six). Thus, the Judd Platform and Westray Ridge may have exerted significant controls on the evolution of the Tertiary depositional packages and the position of structural inversion features in the FSC. This chapter is divided into two

sections firstly, the nature/seismic character of the basement fault structures will be described then, the evolution of the basement faults will be discussed.

4.2. SEISMIC EXPRESSIONS OF BASEMENT STRUCTURES OF THE FSC

This section describes the character of the main structural elements in the FSC (Fig. 4.1). 1) The Judd Platform, 2) the Westray Ridge, 3) The East Faroe High, and 4) other deep structures in the FSC.

The Judd Platform (see Chapter Three) is a major relatively shallow (2500 ms TWT) structural element that is visible on seismic (Figs. 4.1-4.4). The Judd Platform is present in the south and southwestern area of the FSC and is characterised by a prominent subvertical northeast and northwest dipping planar fault (the Judd fault) that has up to ca. 2000 ms TWT normal displacement (Fig. 4.4). The Judd Fault that defines the Judd Platform in the FSC has two distinct strike trends, a northwest trend that abruptly bends into a southeast trend (Fig. 4.1). This bend in the fault trace is believed to correspond to the location of a major transfer fault, the Judd transfer zone (Rumph et al., 1993) (Fig. 3.1). Well data (well 204/22-1 and 204/19-1) indicates that the main rift phase occurred during the Cretaceous indicated by the stratal thickening geometry into the Judd fault (Fig. 4.4).

The Westray Ridge (see Chapter Three) is a prominent N-S trending ridge (cf. Dunian and van Hoorn, 1987) (Fig. 4.1). The fault planes defining the ridge is locally well imaged, dipping and is down-thrown into the Foinaven sub-basin to the west and the Flett sub-basin to the east (Fig. 4.1 and 4.5). A sedimentary succession is observed that thickens against the Westray fault plane indicating syn-sedimentary fault activity (Fig. 4.5). Gravity and magnetic data (e.g. Rumph et al., 1993) suggests that the Westray Ridge contains two (undrilled) igneous intrusive complexes (Chapter Three). These igneous complexes intruded into a relatively shallow level (3500 ms TWT) Westray Ridge (Duindam and van Hoorn, 1987; Hitchen and Ritchie, 1987) and can be seen on seismic (e.g. Fig. 4.6). Gravity,

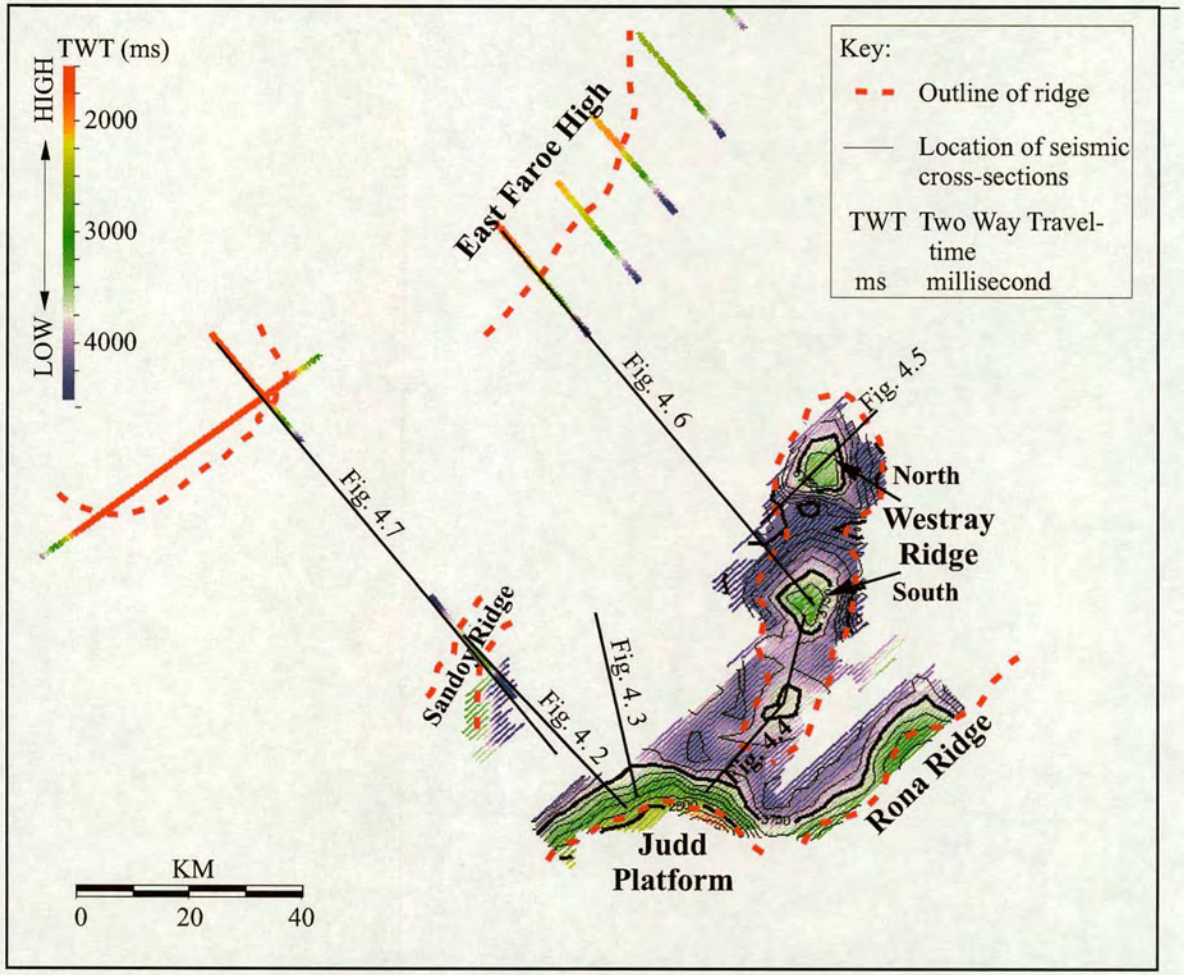

Figure 4.1. Map of the Faroe-Shetland Channel (study area) showing the main positive features, interpreted from the seismic Data (see for example Fig. 4.4).

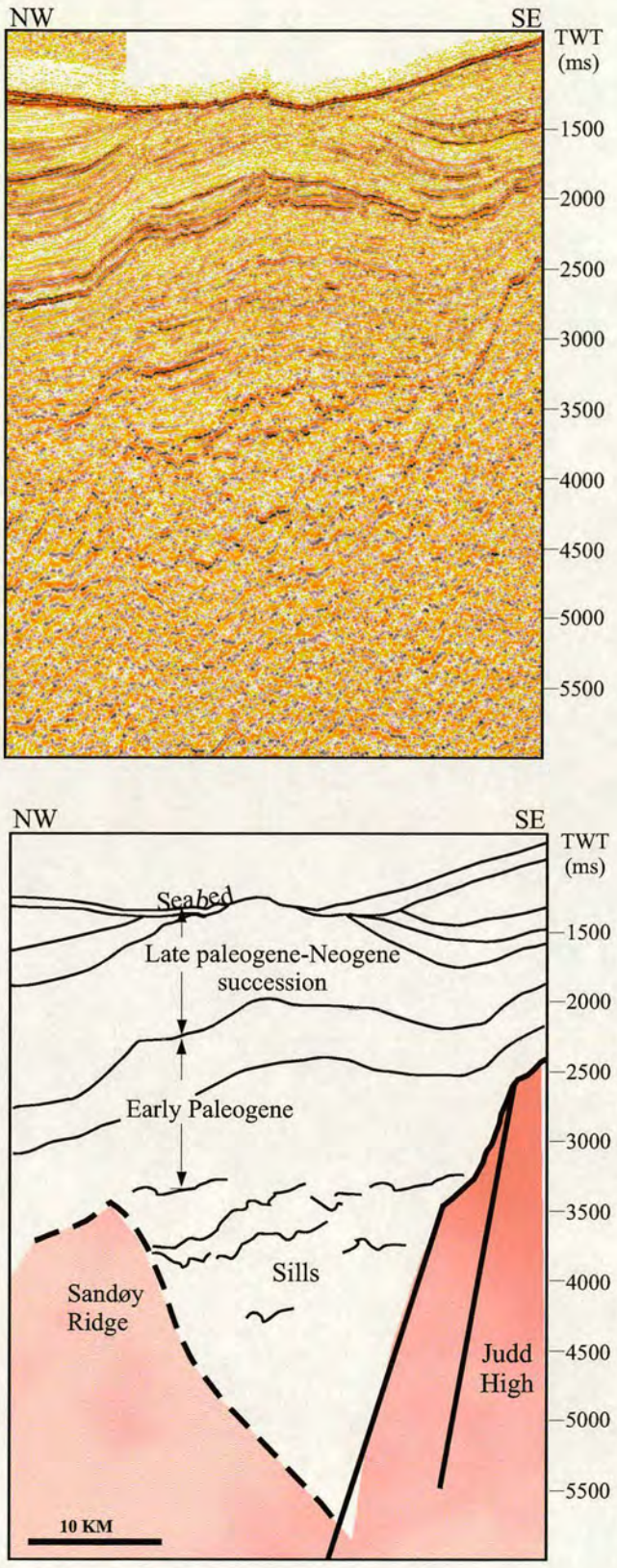

Figure 4.2. Seismic profile showing the Judd High, the Sandøy ridge and a folded stratal Paleogene to Neogene succession. Location of the profile is shown on Fig. 4.1.

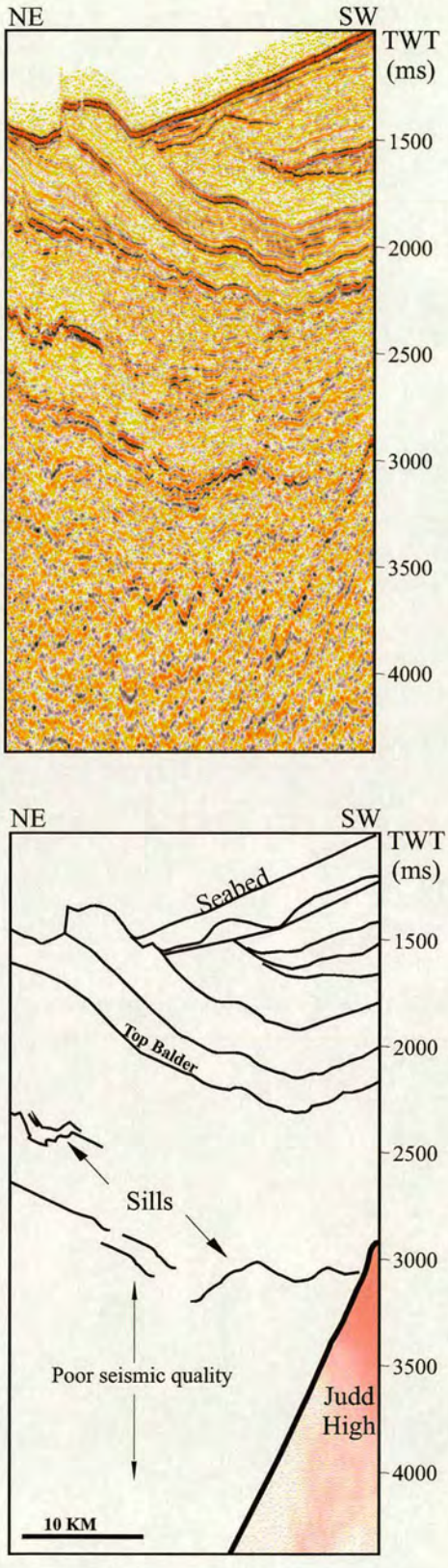

Figure 4.3. Seismic profile showing the Judd fault and the folded Paleogene to Neogene strata at a different location. Location of the profile is shown on Fig. 4.1

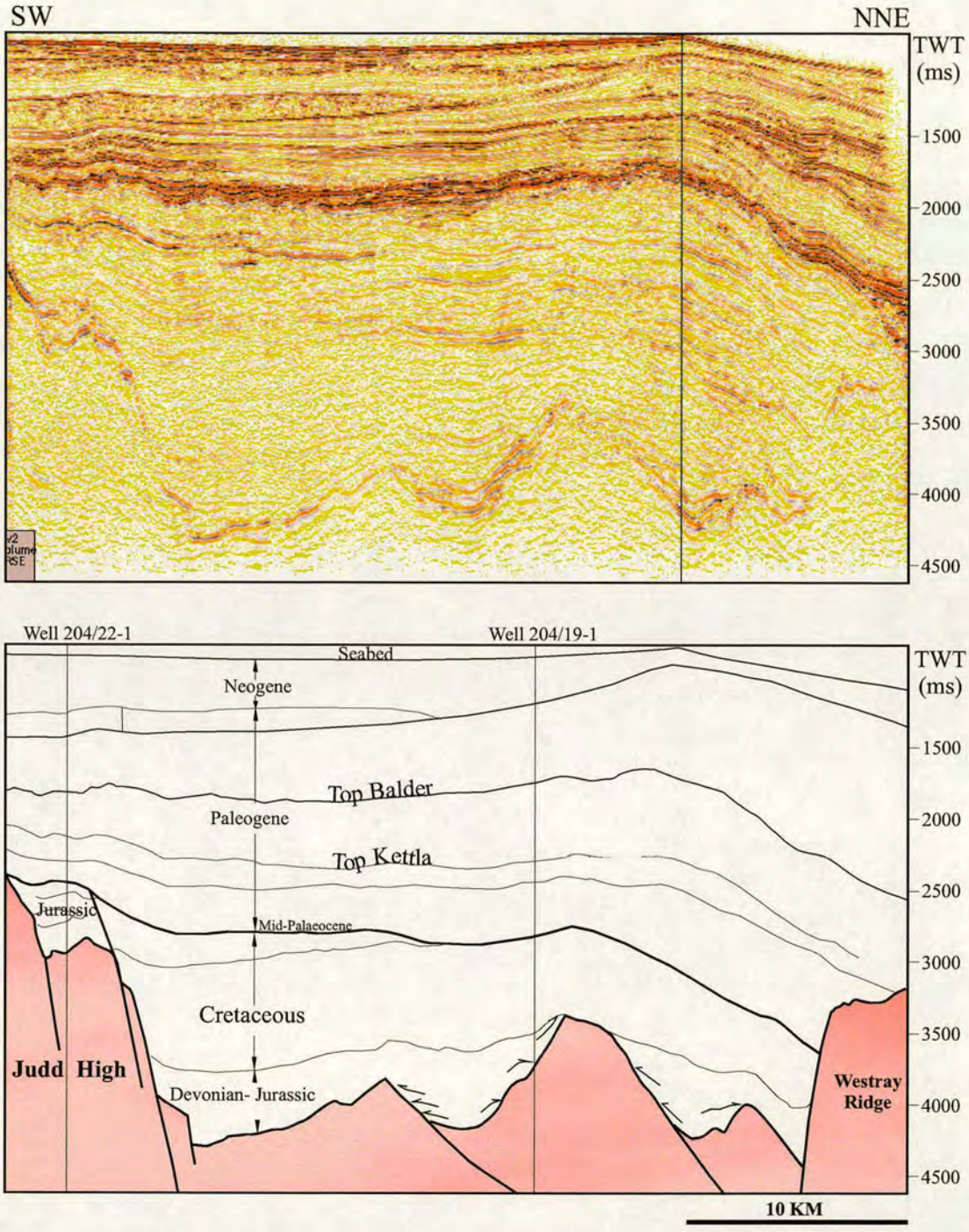

Figure 4.4. Seismic profile showing the Judd High, the Westray ridge and deeply buried rotated fault blocks. The rotated fault blocks are overlain by syn-rift and post-rift successions. Location of the profile is shown in Fig. 4.1.

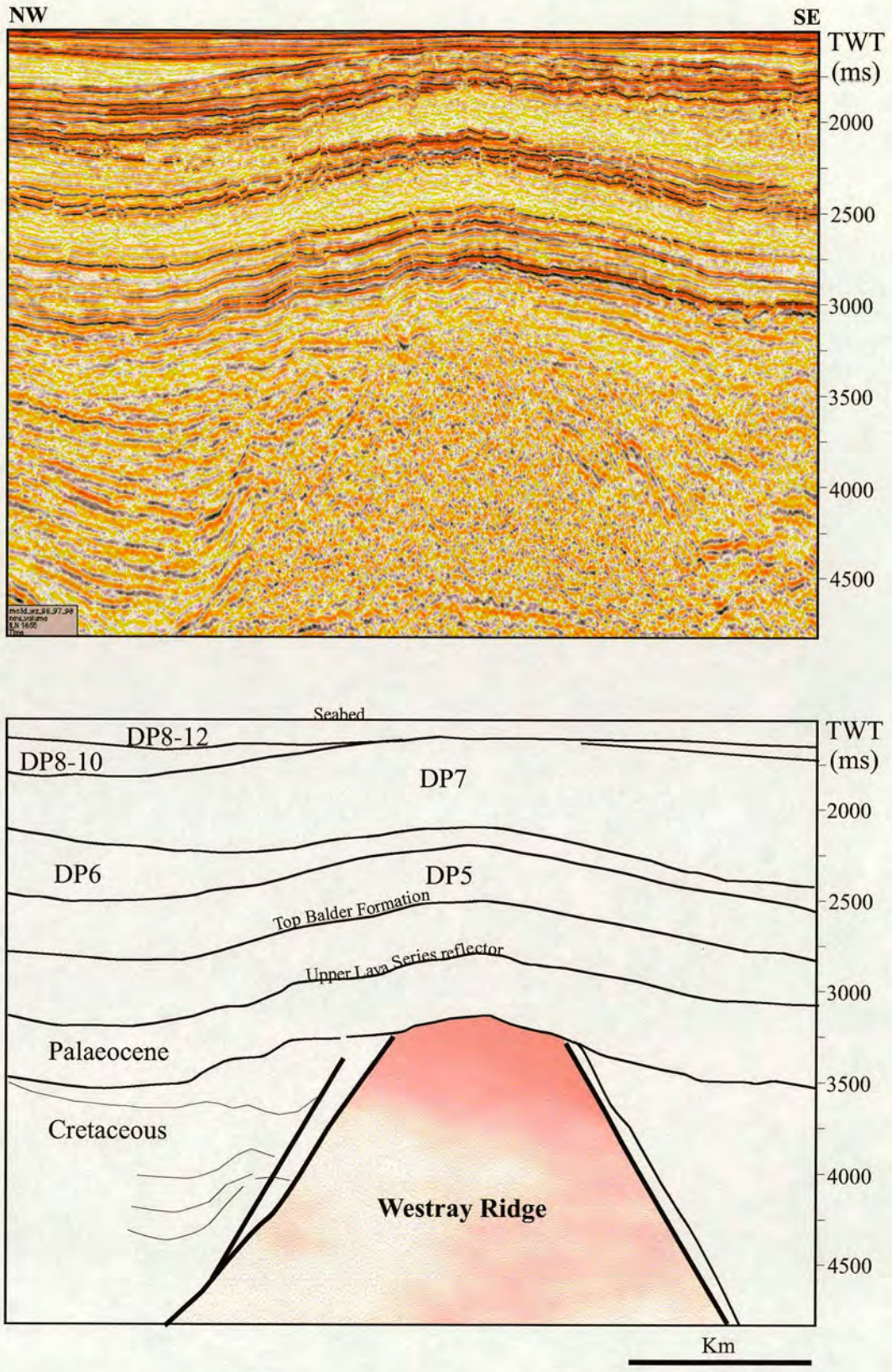

Figure 4.5. Seismic profile across the South Westray Ridge showing syn-sedimentary successions most likely of late Cretaceous age and associated with rifting. The overlying post-rift succession shows stratal geometry that indicates that the ridge has been inverted subsequently to rifting.

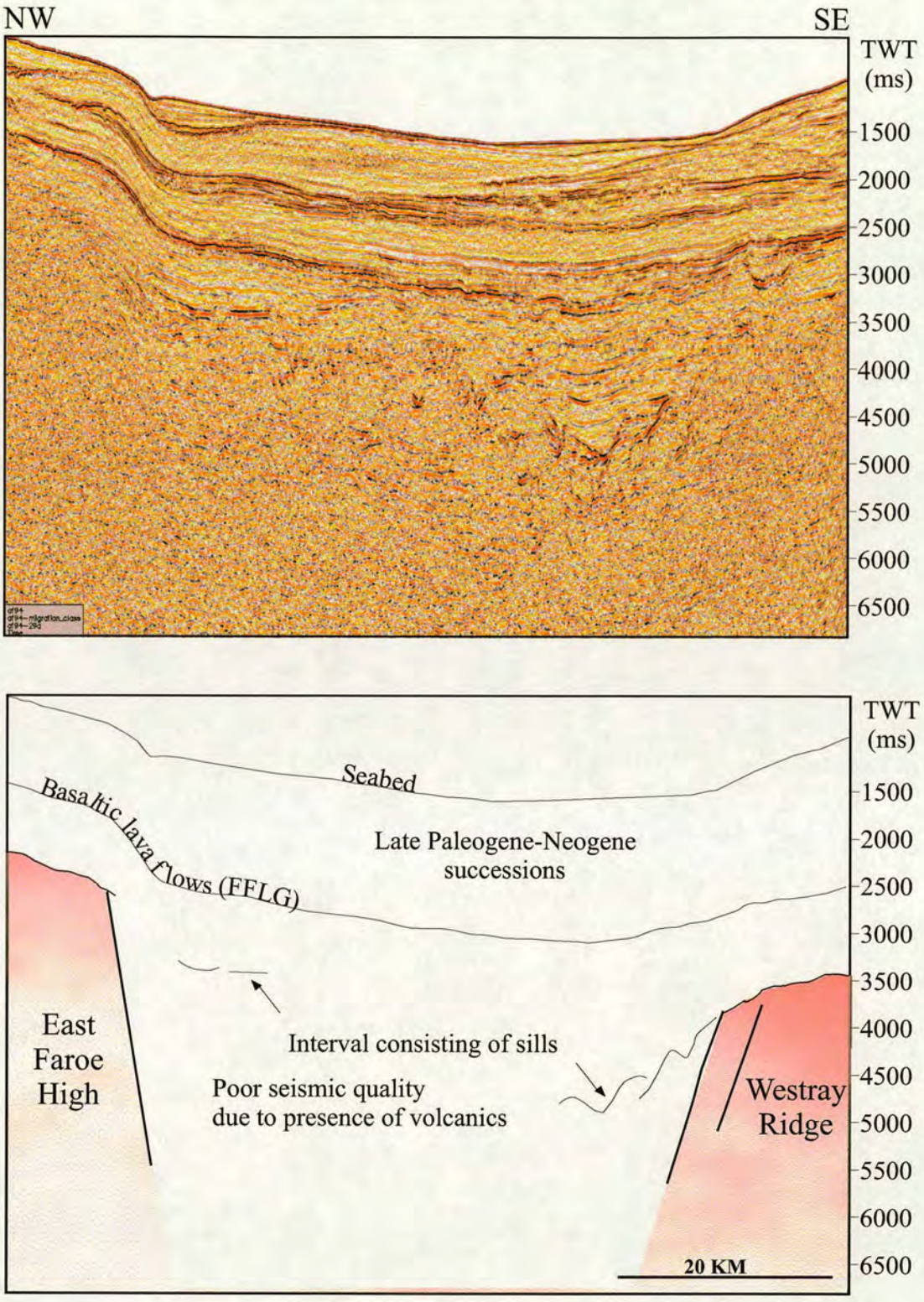

Figure 4.6. Seismic profile showing the relatively shallow East Faroe High and the Westray Ridge. The interpreted sills are thought to be intruded into the Upper Cretaceous and earliest Tertiary. The sills obscure the underlying deep structures and syn-rift succession seen in Fig. 4.4.

magnetic and seismic data suggest that transfer faults divide the ridge into at least two parts dividing the Westray ridge into the South Westray- and North Westray Ridge (Fig. 4.1).

The East Faroe High has a NE-SW trend but bends into an N or NNE trend in the north FSC (Fig. 4.1). The East Faroe High is relatively shallow (2000 ms TWT) and has a southeast-dipping fault plane bounding the southern side (fault traces are not so clear, due to poor seismic quality (Figs. 4.5, 4.6 and 4.7) that is down thrown into the Sandøy sub-basin and the East Faroe Graben (Fig. 4.1). To the north of the East Faroe High, NW dipping faults down throw into the East Faroe Basin (Fig. 3.1).

Locally, between the Judd Platform and the Westray Ridge (Foinaven sub-basin) deeply buried (>3500 ms TWT) rotated fault block structures are present that dip towards the north or NNE and strike E-W (Fig. 4.4). Deeply buried rotated fault blocks are also observed for example in the southeast FSC, for example the Flett Ridge, which forms a series of half grabens in the Faroe-Shetland Basin whilst the FSC bounding Rona ridge and the intervening Foula sub-basin also show rotated fault block geometry (Duindam and van Hoorn, 1987; Ashcroft et al., 1999) (Chapter Three).

A series of irregular, very high amplitude reflectors within the Upper Cretaceous to Early Tertiary section e.g. between the East Faroe High and the Westray Ridge and the Judd Platform, are interpreted to represent sills (e.g. Fig. 4.3 and 4.6). This is based on the seismic characteristics since no well data is available at this depth. The deep structure of the FSC is only locally detected because firstly, the deep structures are obscured by a thick (up to 2000 m) post-Jurassic succession that drapes the pre-Paleogene basins (Chapter Three), and secondly by local intrusive igneous rocks (Sill and dike complexes) (e.g. Hitchen and Ritchie, 1987).

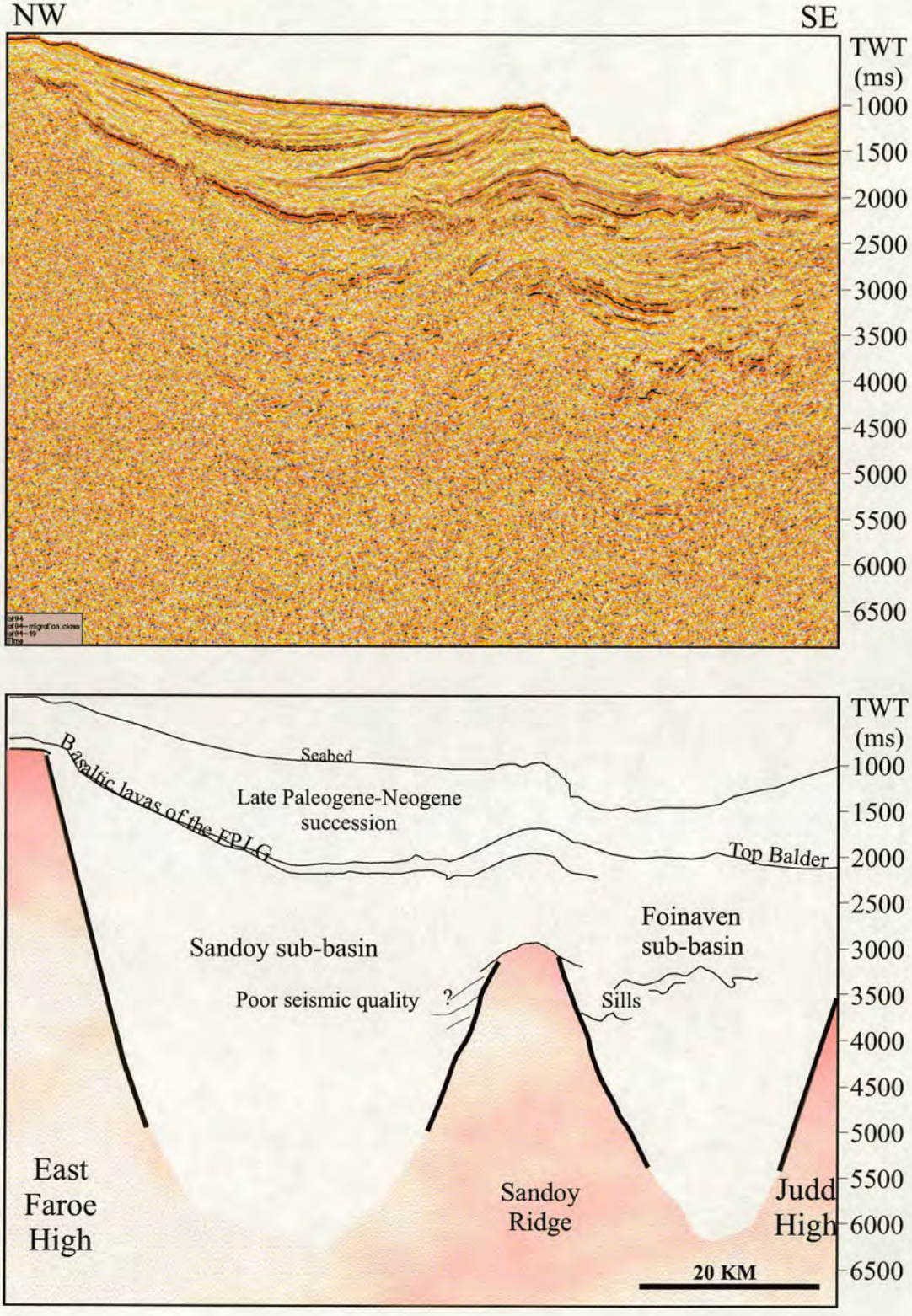

Figure 4.7. Seismic profile across the Foinaven and Sandøy Sub-basins showing the Judd High, the Sandoy Ridge and East Faroe High. The stratal geometry of the syn-rif succession is obscured under sills that have intruded the Upper Cretaceous to early Tertiary strata.

4.3. EVOLUTION OF BASEMENT STRUCTURES OF THE FSC

In the southern FSC the Cretaceous syn-rift sedimentary package is evidenced by the thickening wedge-shaped geometry (stratal expansion) into the Judd fault. This indicates that main rifting and fault-controlled subsidence occurred mainly during the Cretaceous. Evidence from fault displacements and related syn-rift sedimentary accumulation suggest furthermore that the Cretaceous rifting occurred in phases (see Chapter Three). It has previously been suggested that rifting in the southwest FSC also occurred in the early Palaeocene, evidenced by folding and faulting into the early to mid-Palaeocene (e.g. Ebdon et al., 1995). This means that the transition from fault controlled to thermal subsidence in the FSC did not take place towards the end of the Cretaceous period (Duindam and van Hoorn, 1987) but most probably in the early Palaeocene-mid Palaeocene (e.g. Ebdon et al., 1995; Carmichael et al., 1999; Dean et al., 1999) or at the latest in early Eocene at the initial North Atlantic opening and sea-floor spreading (ca. 55 Ma).

The N-S orientation of the Westray Ridge is seen to be oblique to the main NE-SW trend of the FSC. The Westray Ridge has been interpreted to involve the creation of a Late Mesozoic half graben superimposed on older, possible Palaeozoic half grabens of opposite orientation (Duindam and van Hoorn, 1987). Furthermore, the volcanic centres in the Westray Ridge have a different strength (rheology) compared with the adjacent basement structures. Thus, due to the presence of volcanic centres, the Westray Ridge may have responded differently to intra-plate stresses during the post-Atlantic opening (Chapter Three) compared with adjacent ridges, such as the Rona Ridge, the East Faroe High. Furthermore, the location and the rheology (intruded basement) of the Westray Ridge suggests that it may have acted as a barrier to intra-plate stresses, accommodating the stress that the area was subject to during the post-Atlantic opening NW of the study area (see chapters Five and Six).

Sedimentological evidence (i.e. thick depositional packages in basins, that are thin or absent on the highs) suggests that the ridges and highs of the FSC were connected during most of the numerous (mainly Mesozoic) extensional phases. The north or NNE dip of the fault blocks in the south-western part of the FSC (Fig. 4.4)

and the westward dipping fault block in the southeast FSC (the Flett Ridge) reflects a complex link between the deep structures and the adjacent ridges, such as between the Westray Ridge, the Judd Platform and the Shetland platforms to the southwest (Dean et al., 1999) and between the Flett- and Rona Ridges (Sahcroft et al., 1999). The complex basement grain is also manifested in the oblique orientation of the Westray Ridge (Fig.3.1). The complex basement grain is a result of the poly-phase extension and reactivation of pre-extension structures (Chapter Three). The deep structures that are obscured below the sill-complex in the southwest and northwest FSC may also show similarly complex trends. The igneous intrusions that form the sill-complex (Fig. 4.3 and Fig. 4.6) were intruded into the Maastrictian and the earliest early Palaeocene sediments (e.g. Hitchen and Ritchie, 1987) and thus, overly the sediments from the main extensional phase in the FSC.

The Judd Platform marks the SW limit of the Upper Cretaceous and older rift sequences in the FSC. The Judd Platform also suffered major erosion and influenced the sedimentation pattern (Ebdon et al., 1995). Differential compaction between the pre-Paleogene basin (i.e. the syn-rift Cretaceous package) and the Mesozoic basement highs influenced the sediment distribution during the Paleogene (Chapter Five).

It is suggested that a tectonic weakness may have allowed magma to be emplaced at a relatively shallow level in the Westray Ridge (Duindam and van Hoorn, 1987; Hitchen and Ritchie, 1987). Although these volcanic centres have not been drilled to date, it is thought that the intrusion occurred during initial North Atlantic ocean-floor spreading at ca. 55 Ma, simultaneous to the extrusion of the bulk of the SRDS (Larsen et al., 1994; chapters Two and Three). Flexural modelling using gravity and magnetic data suggests that the continental lithosphere was relatively thinned below the NW European margin (including the FSC) during much of its Mesozoic-Cenozoic evolution (Kimbell et al., 2004). This suggests that both the extensional and pre-extensional basement grain may have been reactivated during rifting and this is why N-S, NNE-SSW and NE-SW trending lineaments dominate in the FSC, including the oblique orientation of the Westray Ridge.

In the FSC the basins and sub-basins are thought to be separated by NW-SE trending transfer zones (Chapter Three) (Fig. 3.1). For example, the Judd Platform and the Westray Ridge are located close to NW-SE trending transfer faults (e.g. Rumph et al., 1993) (Fig. 3.1). The magnitude and sense of movement along the Judd transfer zone at different times remains unclear (Hitchen and Ritchie, 1987); however, these transfer zones are thought to have acted as major controls on sediment distribution and volcanic lava flow distribution (e.g. Naylor et al., 1999; Ellis et al., 2002). It is also likely that the transfer zones have influenced the location and orientation of inversion structures that developed in the FSC after the Atlantic break-up in the Early Eocene (ca. 55 Ma) (Fig. 4.2) (chapters Six and Seven).

4.4. SUMMARY

The predominant structural trend in the FSC is NE-SW. However, oblique trends are also present, such as the N-S trending Westray Ridge and the NW-SE and SW-NE trending Judd fault (Fig. 4.1).

The Westray Ridge contains two volcanic centres. Thus, the orientation and the different strength of the Westray Ridge (compared to ridges that do not contain volcanic centres) may indicate that the Westray Ridge acted as a barrier both in terms of accommodating stress (i.e. compressional forces) and to sediment distribution.

The Sandøy- and the Flett ridges are deeply buried compared with the Westray Ridge and the Judd Platform. Other deeply buried ridges are obscured by thick successions (locally > 2000 m thick) of pre-Paleogene sediment, and locally by sill-complexes intruded into the rift centre, such as the centre of the Faroe-Shetland Basin and the Faroe Graben).

The pre-extensional basement grain may have been reactivated during the subsequent extension, resulting in the general NE-SW extensional trend and also the less common N-S and NNE trends. These basement trends can also be expected in the deep structures in the southwest FSC that is obscured by a thick sedimentary section and igneous rocks.

The transfer zones are thought to represent an inherited pre-extensional trend (e.g. Duindam and van Hoorn, 1987; Roberts, 1989) and although it is not known when these structural lineaments have been reactivated, the transfer zones are thought to have acted as major control on sediment distribution (e.g. Naylor, et al., 1999) and volcanic lava flow distribution (Ellis et al., 2002). In addition the transfer faults may also have influenced the location and orientation of inversion structures in the FSC (Chapter Six).

CHAPTER FIVE

5.0. EARLY PALEOGENE UPLIFT AND INCISION DURING FINAL CONTINENTAL BREAK-UP BETWEEN NW EUROPE AND GREENLAND

5.1. INTRODUCTION

The stratigraphy deposited during the late syn-rift to early post-rift stage on volcanic passive continental margins records the continental break-up phase. Continental break-up of NW Europe and Greenland has been determined, from analysis of magnetic spreading anomalies, to have taken place during the Paleogene Chron24r (Vogt and Avery, 1974), ca. 56-53 Ma (Berggren et al., 1995; Eldholm et al., 2000). Immediately prior to sea-floor spreading magma appears to have been intruded into and extruded onto the continental margin within a 2000 km radius from the rift center (Fig. 2.12, A). This massive volcanic activity formed the Tertiary Large Igneous Province has been related to an ascending mantle plume that now forms the present day Iceland plume (e.g. Morgan, 1971; White and McKenzie, 1989; Duncan and Richards, 1991; Larsen, 1991, Eldholm et al., 2000). The break-up, initial ocean floor spreading, volcanic activity and the potential presence of a mantle plume, all have major implications for the temporal and spatial development and variability of the coeval transitional basin stratigraphy deposited on both the NW (NE America and Greenland) and SE (NW Europe) margins of the Atlantic spreading center. To date, evidence for plume-associated uplift and its consequences for transitional and post-rift stratigraphic development has not been fully investigated (e.g. Dam et al., 1998) and remains poorly understood (e.g. White and Lovell, 1997).

This study documents the early Paleogene (Late Palaeocene-Early Eocene) deposition history of the southern, south-western and central parts of the Faroe-Shetland

Channel (Fig. 5.1). The integration of seismic, well data and biostratigraphic data has enabled the detailed tectono-stratigraphic history of the basin to be determined. Specifically, this study has provided insights into the controls on the nature, timing and rate of deposition and direct evidence for the sedimentary response to mantle doming above the ancestral Iceland mantle plume prior to the onset of sea-floor spreading in the North Atlantic.

5.2. DATASET AND METHODOLOGY

This study utilises seven 3D seismic surveys (see Chapter One). In total 54 wells have been examined and tied with the seismic interpretation. The seismic sequence stratigraphic analysis and interpretation have been calibrated with biostratigraphic data based on a subset of 31 wells that contain complete faunal and floral analysis. The lithology and facies in the available wells have been examined using drill-cuttings, together with two short cores (from wells 204/25a-2 and well 204/25a-3) through the stratigraphic interval of interest.

Based on reflector terminations and seismic facies character a seismic stratigraphic analysis has been carried out by identifying key seismic surfaces, defined using seismic reflector termination, enabling the Paleogene succession to be divided into four main depositional packages, interpreted to be separated by key stratal surfaces which record major breaks in sedimentation. These depositional packages can be further subdivided into five genetically related depositional units based on internal seismic reflector terminations, which reflect fluctuations in relative sea level. Seismic isochron (i.e. time thickness) maps have enabled the sediment thickness distribution for each depositional package to be determined.

Interpretation of well, core and biostratigraphic data combined with seismic amplitude analysis especially root mean squared (RMS) have been integrated into the seismic stratigraphic framework in order to determine the vertical and lateral distribution of depositional environments plus the timing of stratigraphic events.

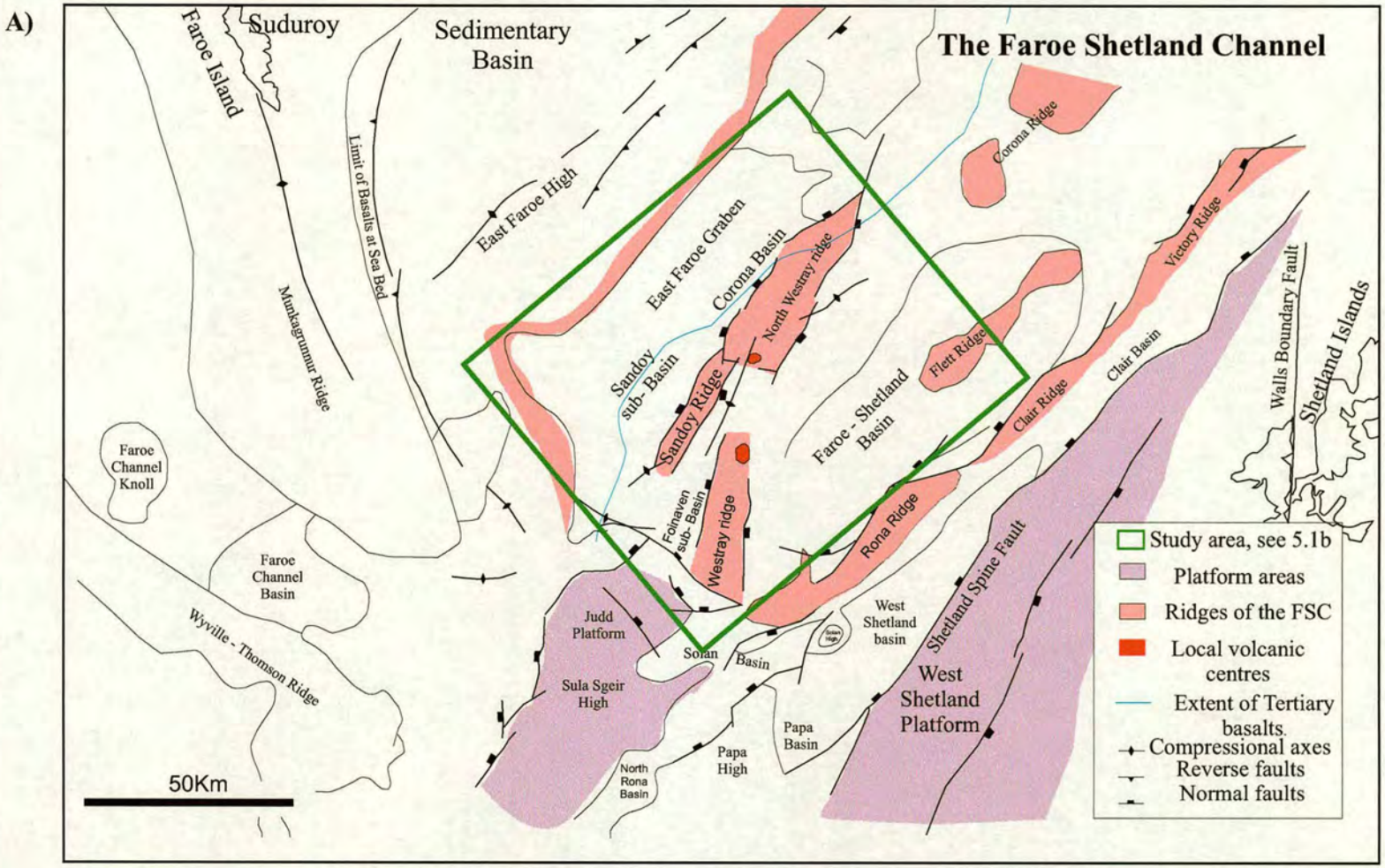

Figure 5.1. Location map of study area a) shows the structural elements and b) the seismic 2d- and 3d coverage (see figure 5.1b). The southeastern extent of the basalt of the Faroe Lava Series is modified from Ritchie et al. (1999) and Naylor et al. (1999).

B)

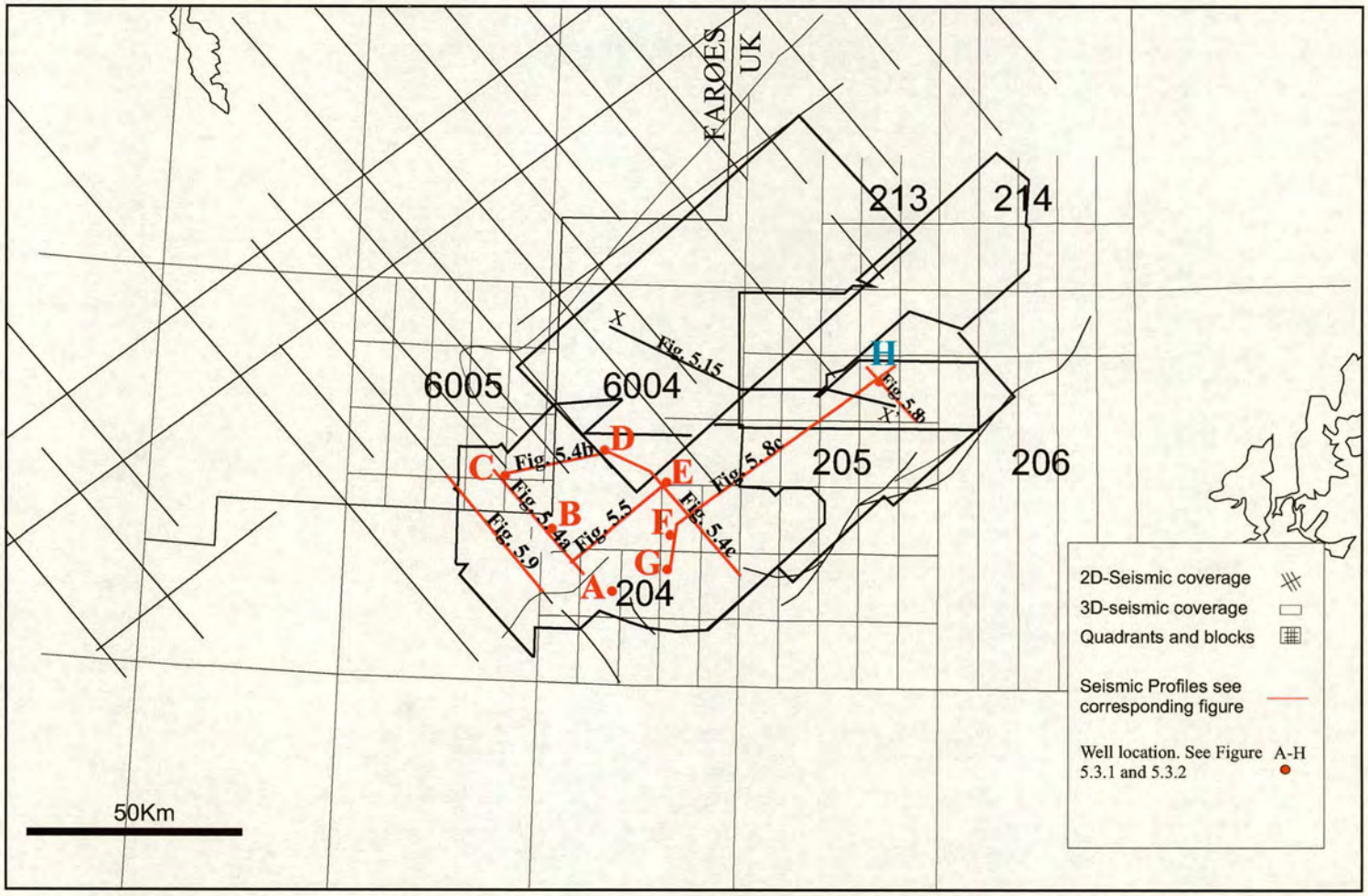

Figure 5.1B. Location map showing location of some seismic profiles referred to in the text.

An interpretation of facies successions is based largely on drill cuttings and wire-line log responses. Tying well data to seismic data allows the observed seismic response to be calibrated to lithology, enabling a general interpretation of depositional systems to be carried out (Appendix 1). The seismic amplitude extraction (RMS) has been interpreted together with well data to characterize the seismic amplitude response from specific facies associations.

It has proved possible to predict variations in the facies distribution, based on lateral variations in seismic amplitude. The amplitude analysis suggests that lignites and tuffaceous mudstone produce high amplitude seismic response, whereas sands that contain no lignites and no tuffaceous material produce a low amplitude seismic response. A heterolitic succession containing a mixture of sand, mud, lignites and tuffs produces a medium amplitude seismic response which varies in amplitude depending upon the amount of lignites and tuffaceous mudstone present. Thus, it has been possible to clearly identify high amplitude areas dominated by coals and tuffaceous mudstone and other areas where coals and tuffaceous mudstone are generally either present (moderate amplitudes) or not present (low amplitude), and the succession is interpreted to be dominated by a combination of sandstone, siltstone or non-tuffaceous mudstone.

5.3. SEQUENCE STRATIGRAPHIC FRAMEWORK OF THE EARLY PALEOGENE, FAROE-SHETLAND CHANNEL

This section describes the seismic stratigrapy of the Paleogene interval of the FSC, based on integration and analysis of 3D seismic and well data. Four main depositional packages have been identified which belong to the Faroe and Moray Group lithostratigraphic units (Fig. 5.2). Depositional Packages 1 and 2 (Faroe Group) represent fully marine mudstone dominated units deposited in shelf, slope, and basin floor environments (see Chapter Three). Depositional Packages 3 and 4, which form the focus of this study, belong to the Faroe Group and Moray Group, and represent heterolitic units deposited in a range of shallow marine to continental environments,

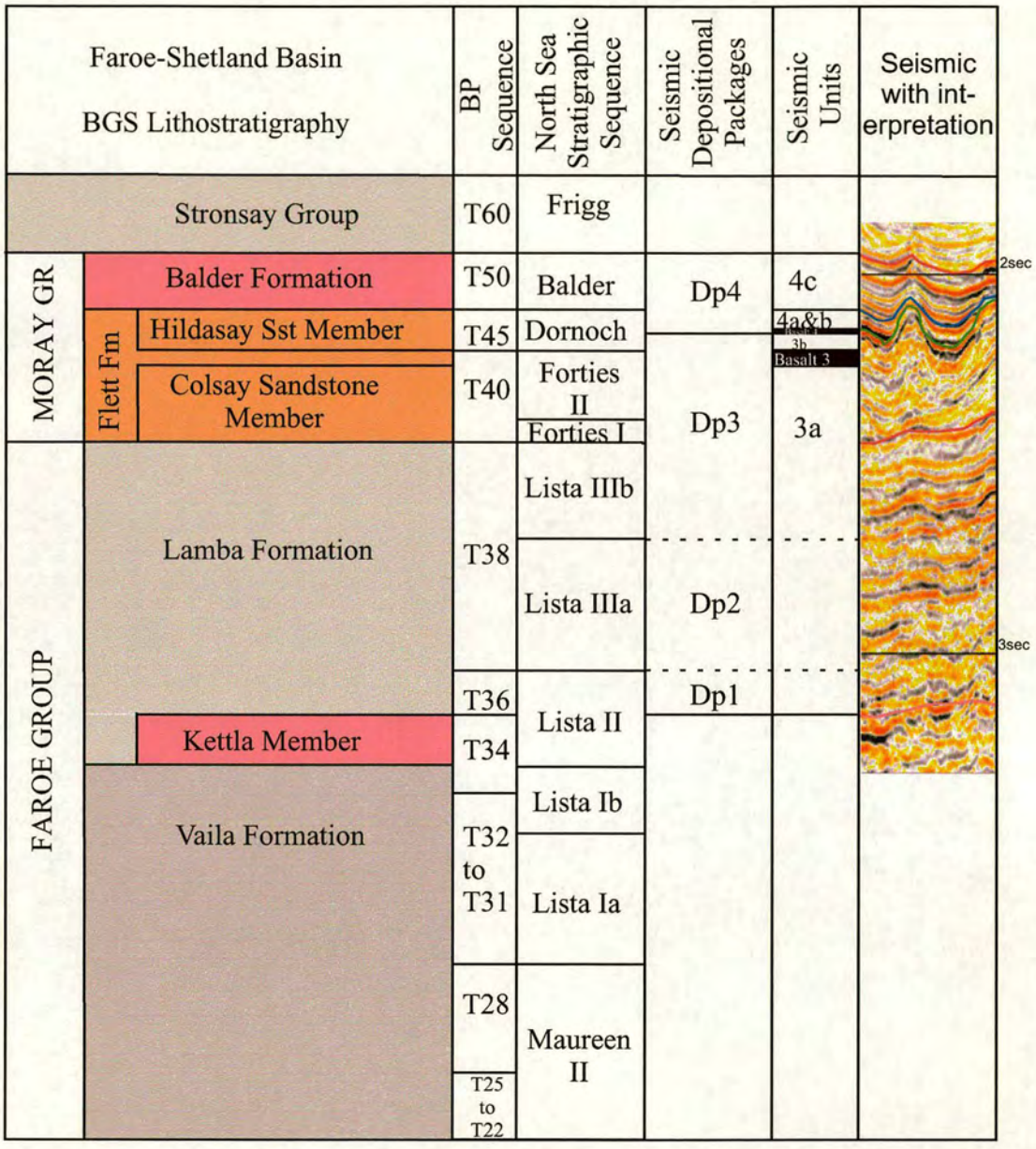

Figure 5.2. General Paleogenc lithostratigraphy in the West Shetland area (as Fig. 3.5). In addition are shown the interpreted depositional packages and the seismic characteristics related to the main surfaces. Note in particular the incision surface at the base of DP4 (see text).

during the initial stages of continental break-up and sea floor spreading (Chapter Three). Due to a lack of biostratigraphic data from shallow marine to continental deposits, it has been difficult to confidently subdivide the depositional packages 3 and 4 into Formations and Members (e.g. Knox et al., 1997). However, in this study the palynological data has been calibrated with seismic sequences and lithostratigraphy. Thus, the biostratigraphic data becomes a more powerful tool because it enables all of the wells and hence the biostratigraphy to be correlated based on key seismic "time lines" (reflectors).

Depositional Package 1 (DP1)

Depositional package 1 (DP1) is developed across the entire study area and is up to 200 m.sec thick. It is typically bounded below by a continuous, high amplitude reflector, which is interpreted to represent a tuffaceous interval developed at the top of the Kettla Member (57.5Ma) of the Lamba Formation (e.g. wells 6005/15-1, 204/14-2, 204/25a-3 in Figs. 5.3, 5.4a-c). Where the tuffs are obscured by overlying basalts (Faroe Plateau Lava Group; in wells 6005/15-1 and 6004/12-1), for example in the northwestern part of the FSC, the basal reflector is of moderate amplitude (Fig. 5.4a). In the southern area the basal reflector also becomes less pronounced (Fig. 5.4c). DP1 is bounded above by a moderate amplitude reflector which is downlapped by reflectors of the overlying depositional package (Depositional Package 2, DP2). Internally, DP1 typically consists of conformable, laterally continuous reflectors, which locally are transparent (Fig. 5.5). DP1 consist of primarily siltstone-dominated (e.g. wells 204/19-1, 204/24-1, 6005/15-1) and mudstone-dominated (e.g. well 6004/12-1, Fig. 5.3) facies (see Appendix and Fig. 5.3).

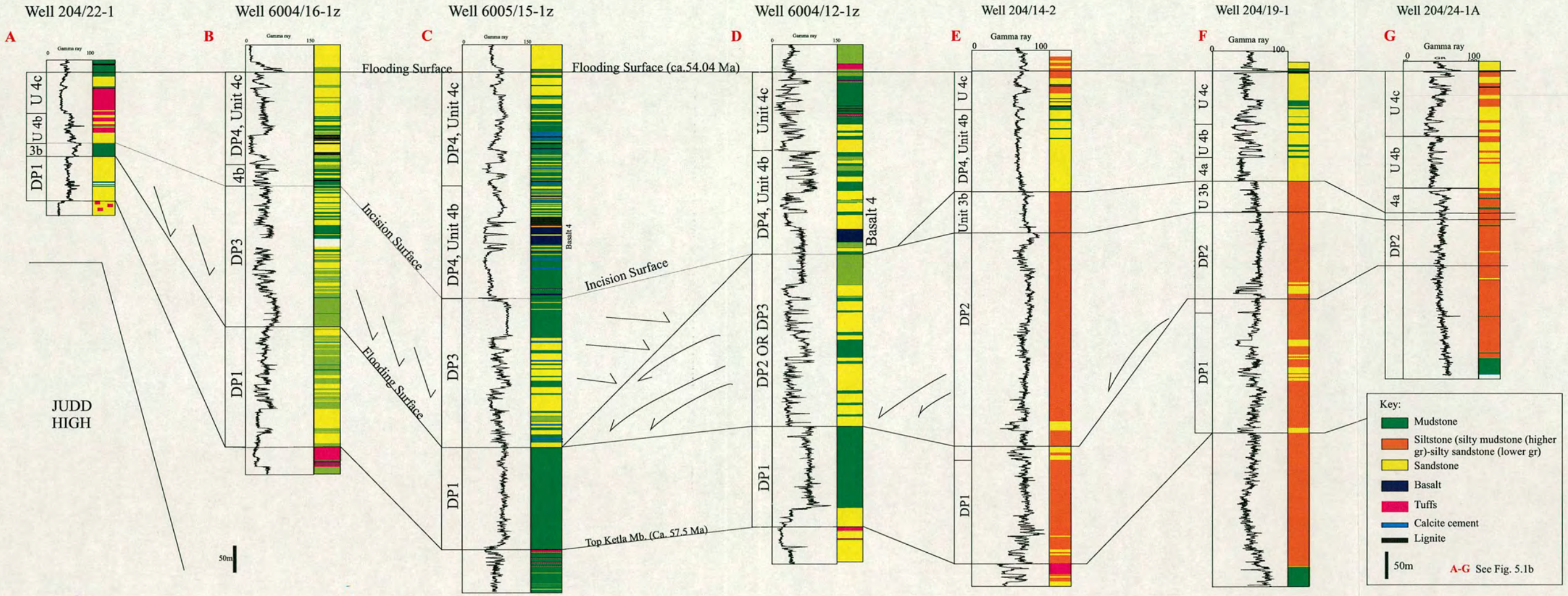

Figure 5.3 Well-correlation panel (A-G). Location of the wells (A-G) is shown on Fig. 1b. The seismic profiles (Fig. 5.4) show the seismic characteristics related to these wells (A-G).

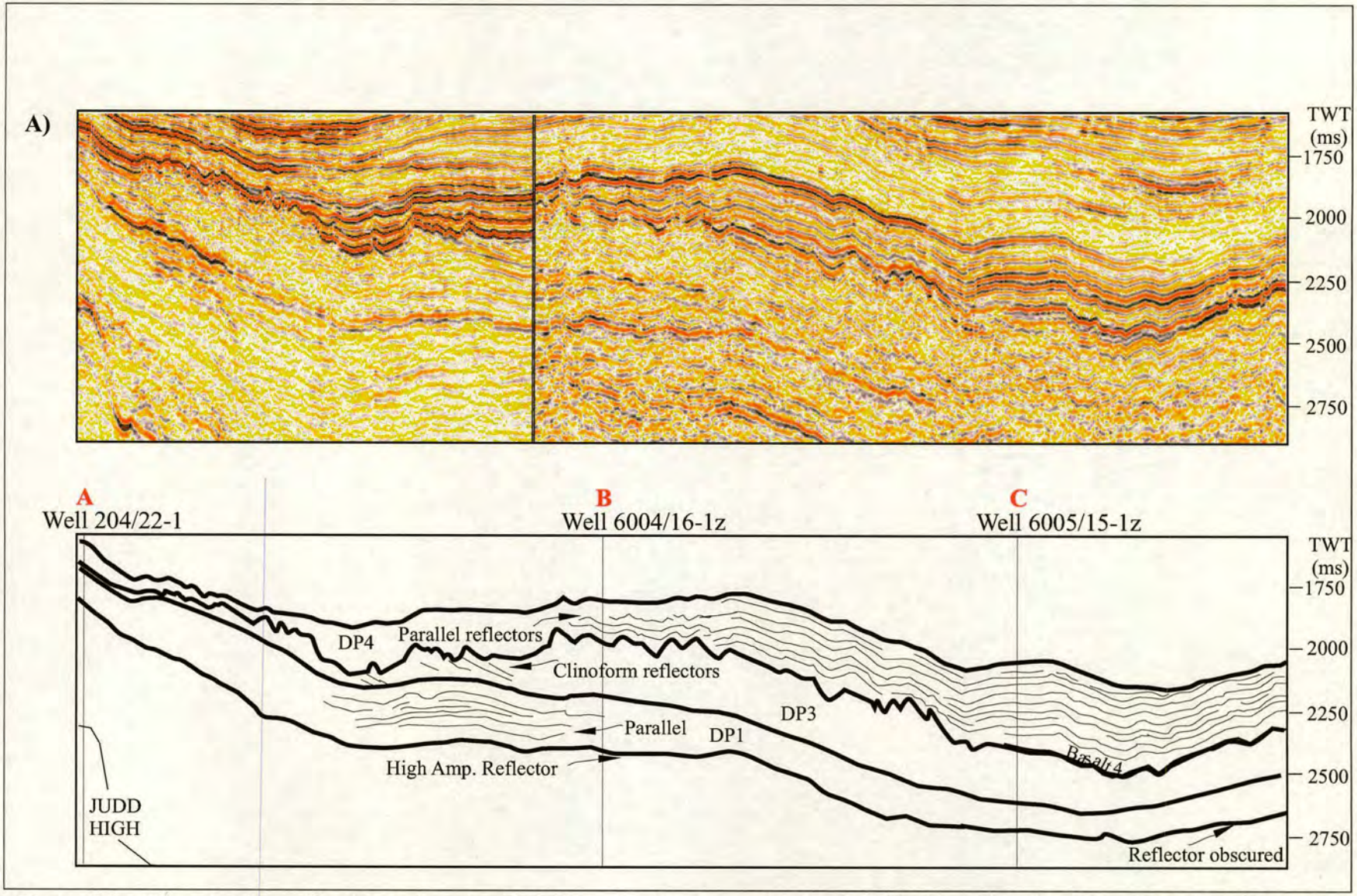

Figure 5.4a. The seismic profile shows the seismic facies and reflector terminations within depositional package DP1-DP4. The wells on the seismic section correspond with the well correlation panel (wells A-C) on Fig. 5.3.

B)

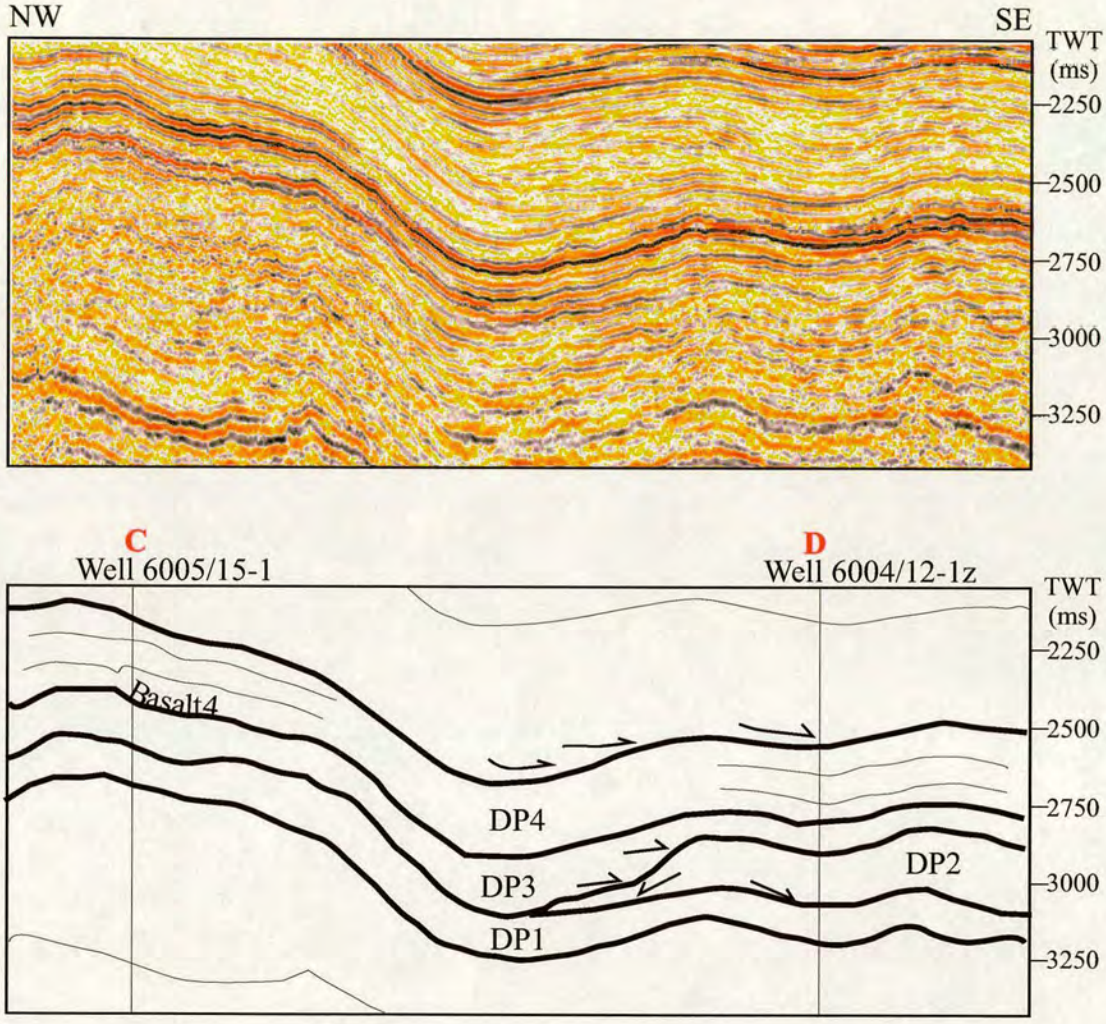

Figure 5.4b. Seismic profile showing the seismic characteristics of depositional packages DP1-4. The wells correspond with the well correlation panel (wells C-D). The main seismic characteristics are: parallel reflectors (DP1), down-lap reflectors and mound-shape facies (DP2); clinoform reflectors (DP3) that down-lap onto DP2; parallel reflectors (DP4). See discussion in text regarding an alternative interpretation in of DP2 to DP3 (section DP3).

C)

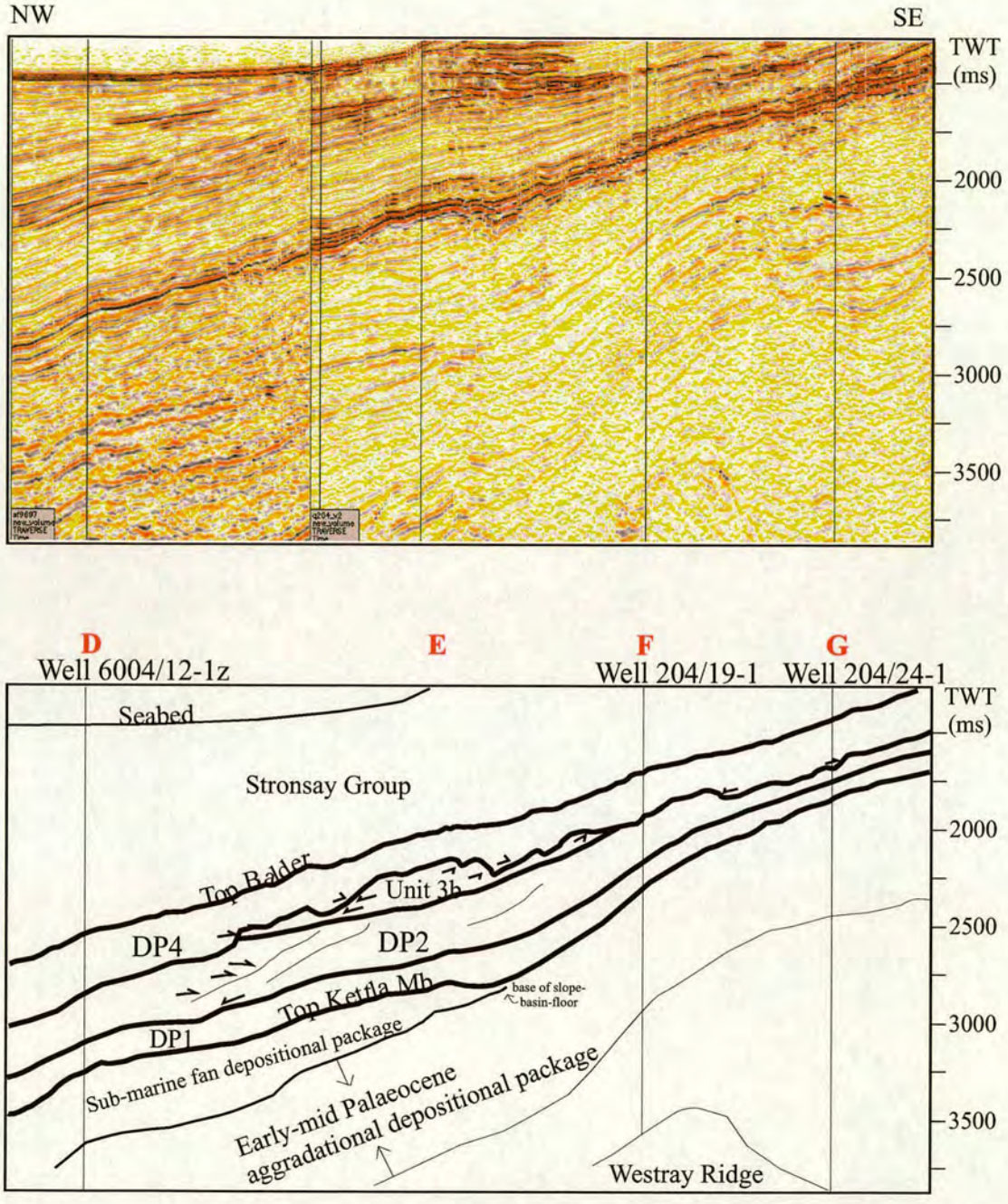

Figure 5.4c. Seismic profile showing the seismic characteristics of depositional packages 1-4 between wells D-G on Fig. 5.3. The main seismic characteristics are: parallel seismic reflectors (DP1); downlap and northwest-ward progradation and southeast onlap (DP2); Unit 3b is present locally; incision, onlap and parallel seismic reflectors (Dp4).

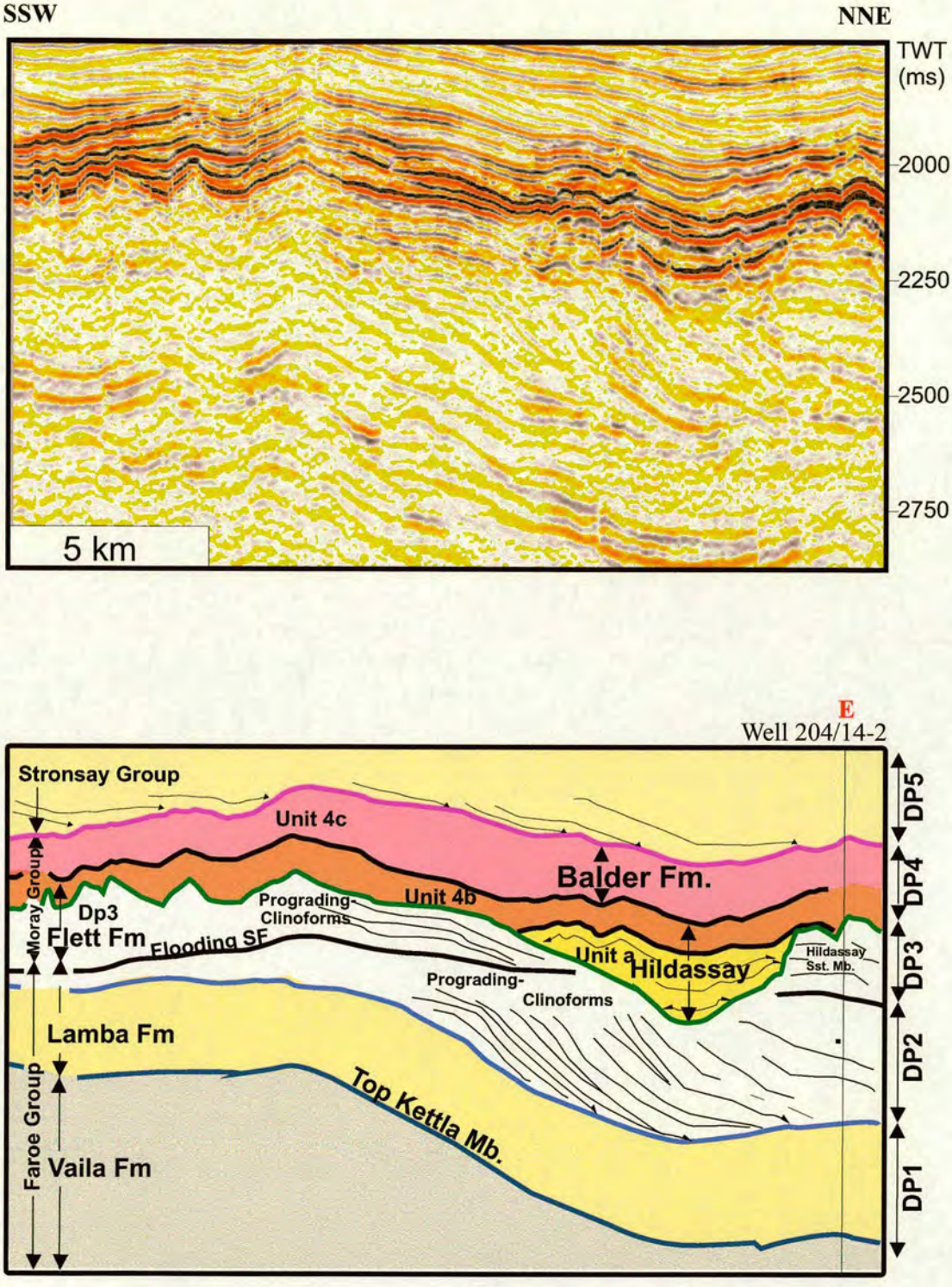

Figure 5.5. A representative seismic line showing the prominent progradational clinoform reflectors (DP2) and the erosional truncation and onlapping reflector terminations that allows the identification and correlation of the main incised surface (DP4). Location of this line is shown on Fig. 5.1b. The line intersects two wells; 204/22-2 (not shown) and 204/14-2 that corresponds to well E, on the correlation panel Fig.5.3. The wells provide direct calibration of the progradational package and of the incised valley's sedimentary fill.

Depositional Package 2 (DP2)

Depositional package 2 (DP2) is restricted to a narrow area in the southern part of the FSC, where it is up to ca. 600 m thick. It is bounded below by a moderate amplitude, lateral continuous reflector that is downlapped by overlying reflectors. It is bounded above by a moderate amplitude, lateral continuous reflector that truncates the underlying reflectors and is downlapped by the overlying reflectors (Fig 5.5). Internally, DP2 is composed of a series of clinoform reflectors that prograde towards the NNE (Fig. 5.4c and 5.5). Well 204/14-2 penetrates the lower part of the clinoform foresets, indicating that they are siltstone-dominated (Appendix and Fig.5.3, E). The gamma-ray log for this well shows at the uppermost section a 40 m thick coarsening-up unit that is overlain by 40m thick fining-up unit (e.g. well 204/14-2). Further north, beyond the area dominated by pronounced clinoform reflectors, mounded seismic bodies can be observed (Fig. 5.6). These onlap/downlap the lower parts of the clinoforms (Figs. 5.4b-c and 5.6) and correspond to box-shaped gamma ray log trends, indicating clean, well sorted sandstone facies (or conglomerates) and interbedded higher gamma ray mudstone-dominated facies (e.g. 6004/12-1z). Since the sequences that belong to DP1, DP2 and DP3, can not be mapped in this particular area due to poor seismic data, it has not been possible to produce isochron maps of each sequence, however a combined isochron map (Fig. 5.7) gives an indication of the area where most sediments mainly representing DP2 were deposited. Internally, DP2 consists of sediments of the Lamba Formation (ca. 57.9-55.5 Ma; cf. Ebdon et al., 1995).

Depositional Package 3 (DP3)

Depositional Package 3 is developed across the entire study area and is up to 300 m.sec thick. DP3 contains sediments that belong to the Lamba Formation and the Flett Formation (Colsay Sandstone member and Hildasay Sandstone Member (e.g. well 6004/16-1, 6005/15-1, 204/14-2, 204/19-1, 204/22-1, 204/25a-2 and 205/9-1) (Fig. 5.2).

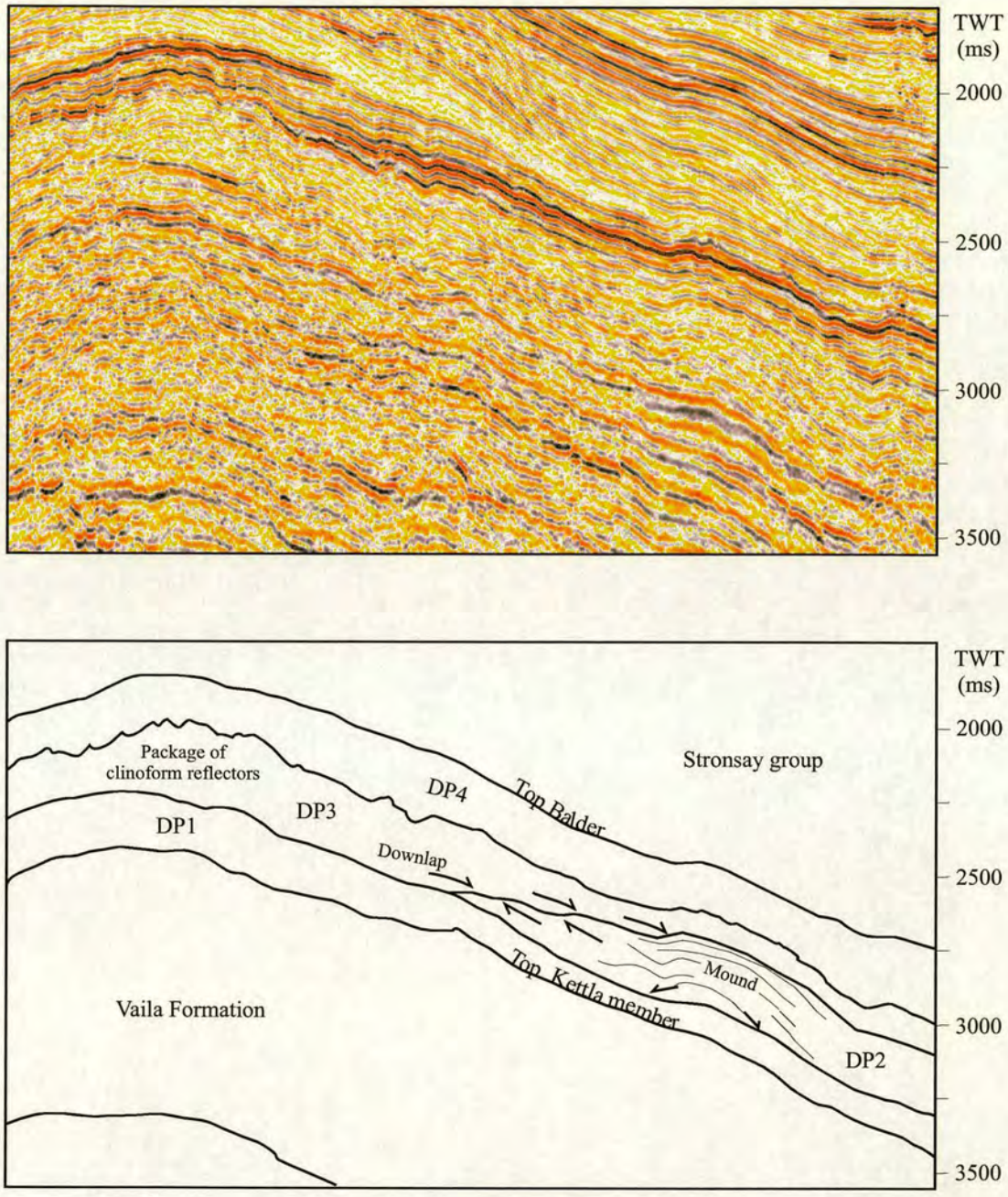

Figure 5.6. Seismic profile showing DP3, Unit 3b downlap onto the mound-shaped facies package of Dp2. See discussion in text regarding an alternative interpretation in of DP2 to DP3 (section DP3).

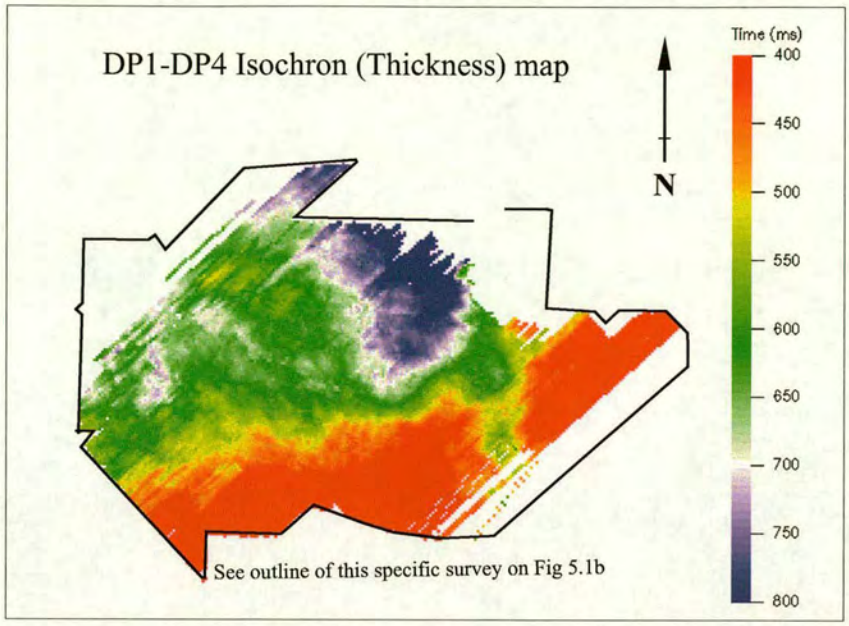

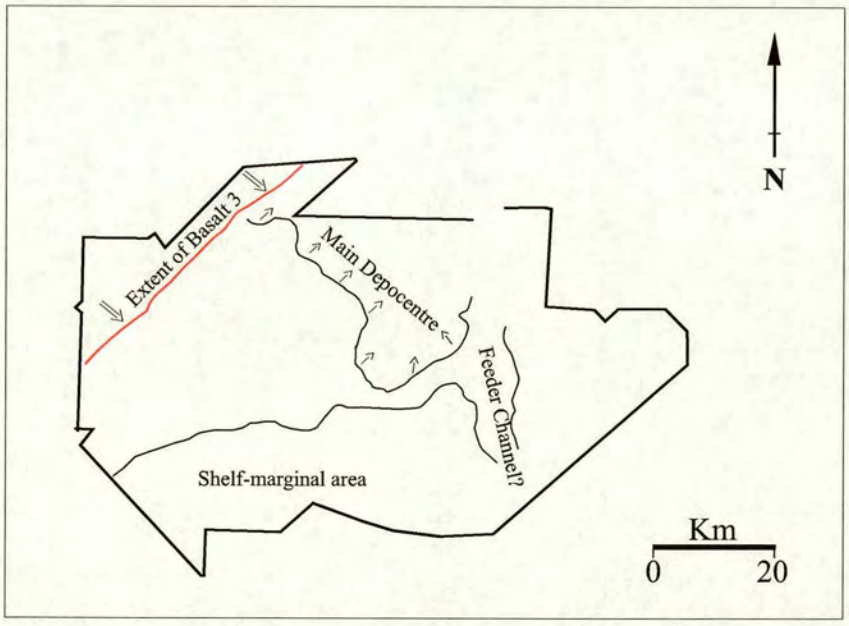

Figure 5.7. Isochron (thickness) map of DP1 to DP4 (Top Kettla to Top Balder), showing the area of greatest sediment accummulation (in dark blue), mainly representing DP2 and DP4 (see well 6004/12-1, Fig.5.3D).

In places the package can be subdivided into two units, Unit 3a and 3b, separated by a basalt unit (Basalt 3). However, this distinction can only be made with confidence where the basalt is present in the central part of the FSC. The basalt-unit (Basalt 3) is ca. 50 m thick (Fig. 5.8a) and forms a high amplitude reflector (Fig. 5.8b-c). Stratigraphically, Basalt 3 is located within the Flett Formation, at the top of the Colsay Sandstone Member (Fig. 5.8a). Geochemical analysis of Basalt 3 indicates that it originated from a different volcanic source, but is time equivalent to the uppermost section of the Lower Series lavas of the Faroe Plateau Lava Group (FPLG) (Statoil 2002, David Ellis pers. comm.).

DP3 is bounded below by a lateral continuous, moderate amplitude reflector, that is downlapped by overlying reflectors. It is bounded above by a lateral continuous, high amplitude reflector, that truncates the underlying reflectors and is onlapped by the overlying reflectors (Depositional package 4, DP4). Internally, DP3 is characterized by a series of clinoform reflectors that build-out or prograde towards the N and NNE where the reflectors downlap and DP3 pinches out onto the underlying DP2 (Fig. 5.6). In the southwestern part of the study area (Fig.5.1a), where the prograding clinoform reflectors are most prominent (Fig. 5.9), the well (well 6006/15-1) has two coarsening-upward gamma-ray log trends (Fig. 5.3,C). DP3 is capped by a mudstone (no cutting descriptions are available to add detail to this description). In the central part of the FSC, DP3 characterizes a coarsening-upward trend and consists of both sandstone-dominated facies (e.g. well 205/9-1) and mudstone-dominated (e.g. well 206/1-2) facies (see detail description in Appendix) (cf. Knox et al., 1997; Ebdon et al., 1995; Naylor et al., 1999). In the northern part of the FSC a local, thinly bedded sandstone-dominating succession is present (in well 214/28-1) (Knox et al., 1997).

A)

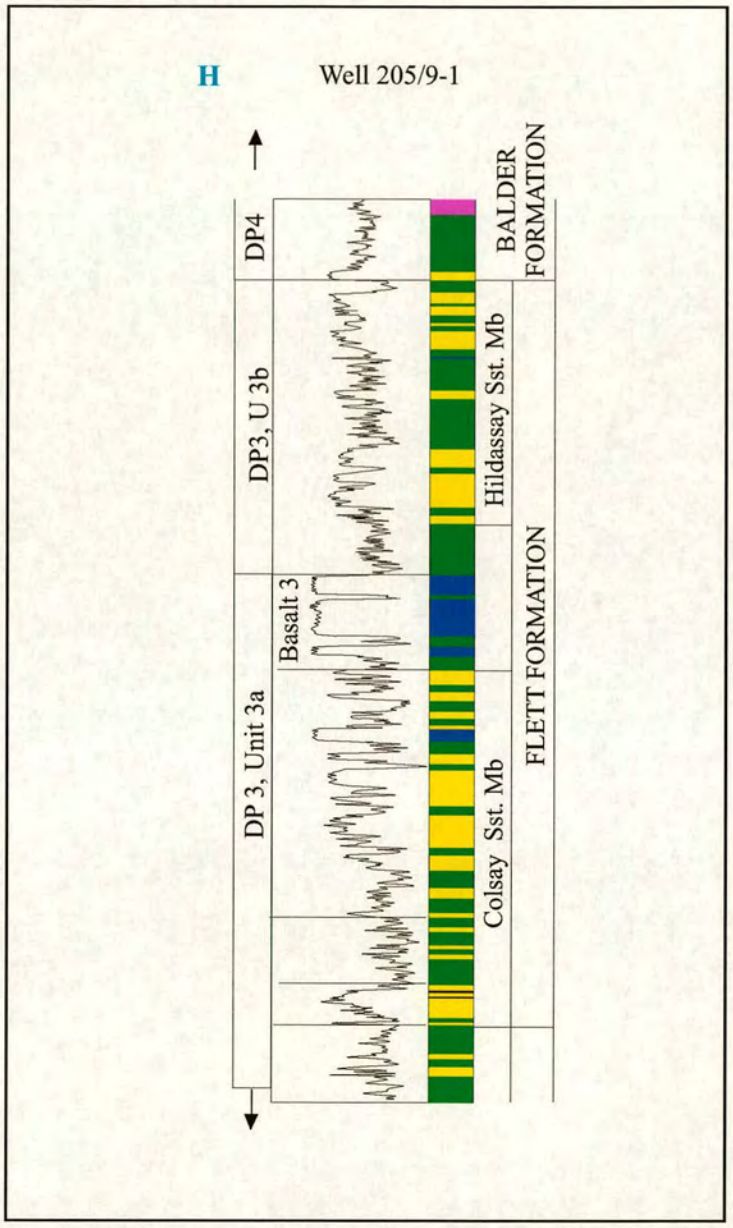

Figure 5.8a. Well 205/9-1 showing the Paleogene stratigraphy (after Knox et al., 1997) and correlation of DP1-DP4. Note that basalt (Basalt3) is within the Flett Formation and is age equivalent to the Lower Series of the Faroe Plateau Lava Group. Location of well 205/9-1 (H) and the seismic profiles (5.8 b-c) is shown on Fig. 1b.

B)

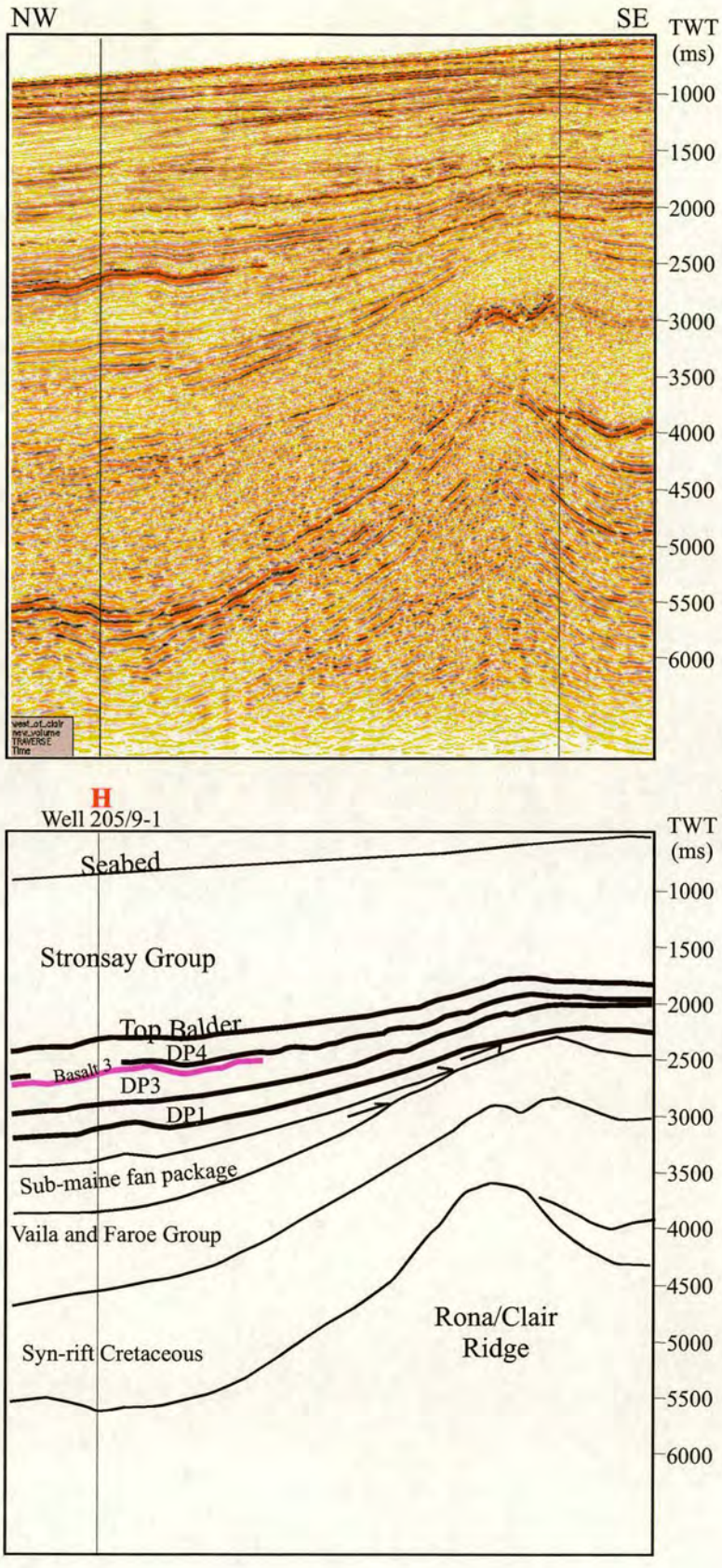

Figure 5.8b. Seismic profile showing the high amplitude reflector that represents Basalt 3, that separates Unit 3a from Unit 3b.

C)

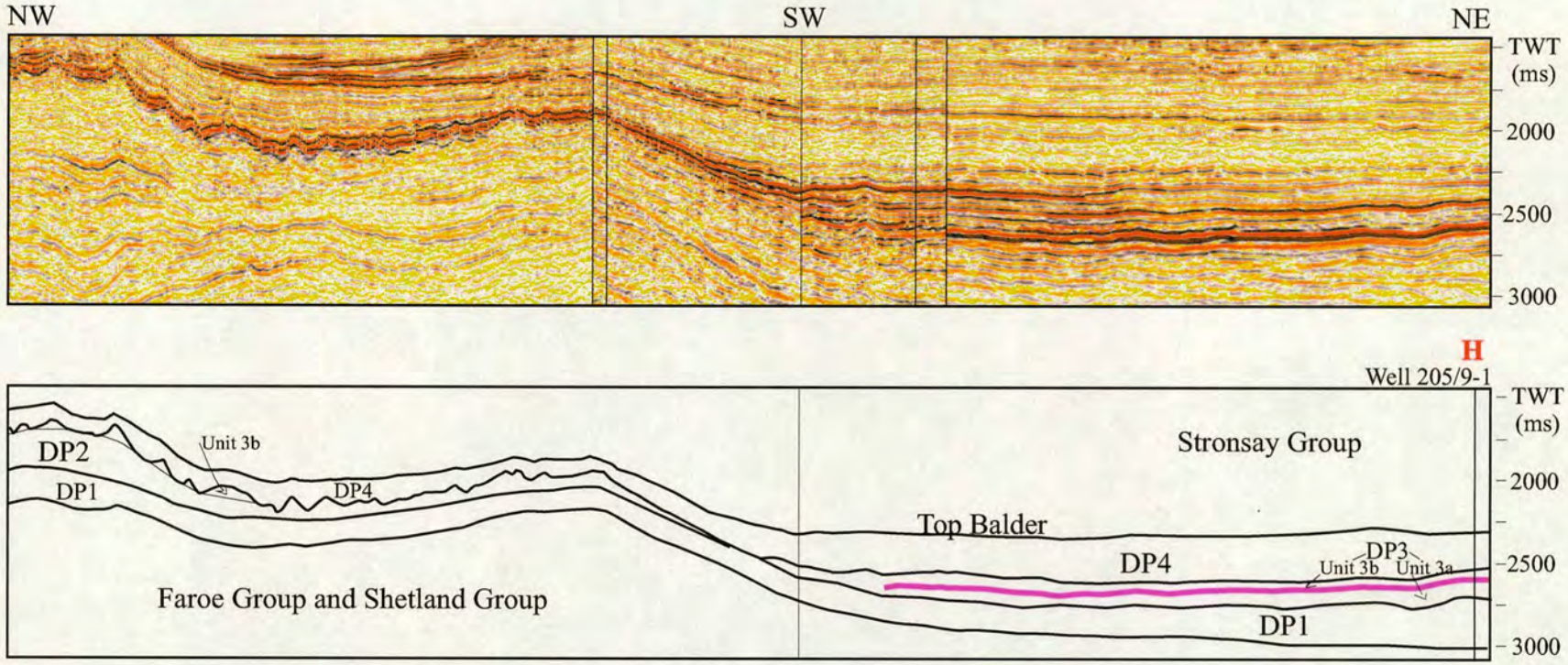

Figure 5.8c. Seismic traverse (see location Fig.5.1b) showing the correlation of depositional packages between the southern and central FSC. The local deposition of Dp2 in the southern FSC thins and pinches out to the east and thus is not present in the central FSC (Fig. 5.8b). DP3, Unit 3a and Unit 3b are present both in the central FSC and in the southwestern FSC (see Fig. 5.9), whereas Unit 3b is more extensive and present in the entire study area. The seismic profile also shows that Basalt 3 was extruded prior to incision and development of the incision surface.

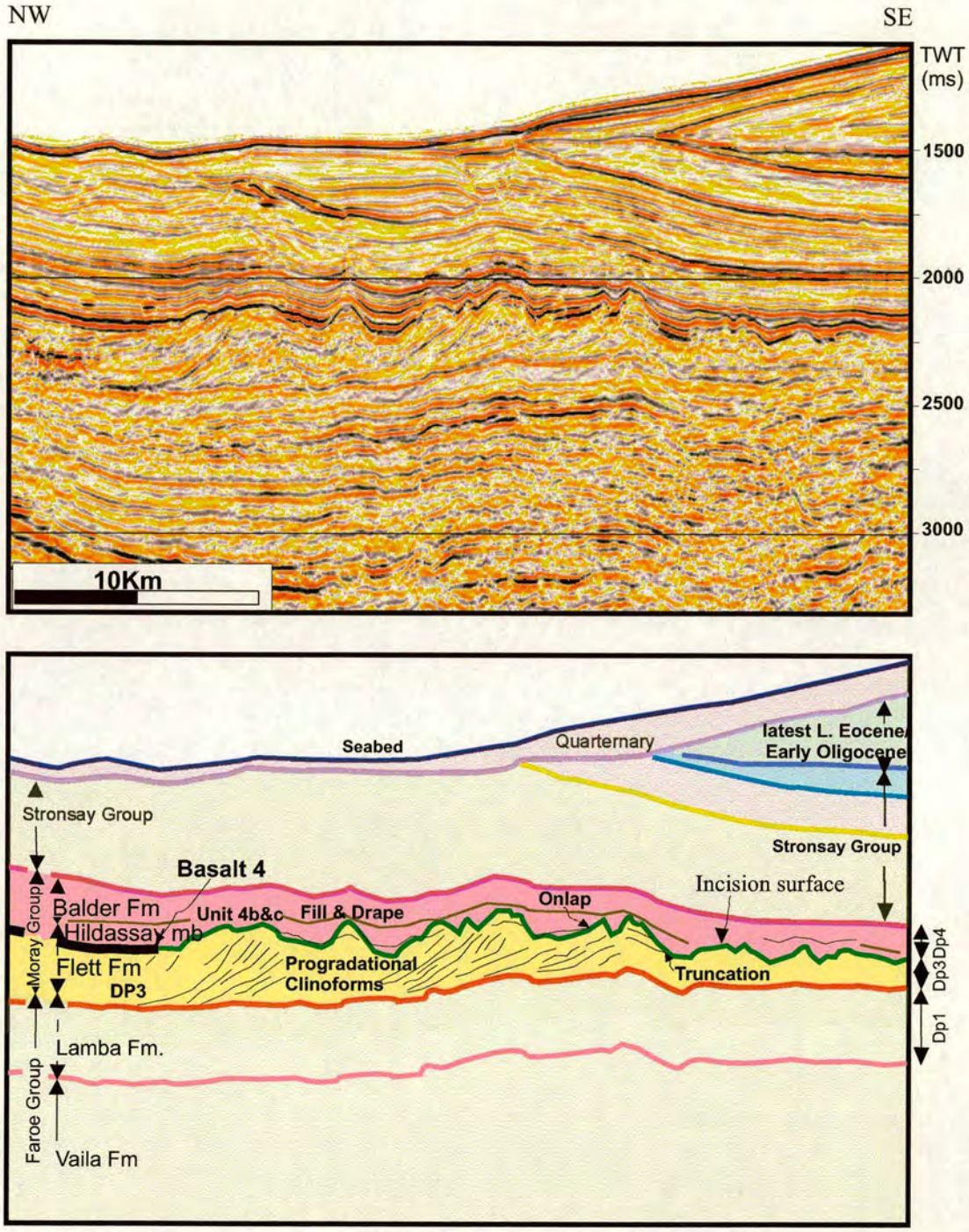

Figure 5.9. A representative SE-NW trending 2-d seismic line highlighting the clinoforms, incision and drape (DP3-DP4). Notably, DP2, which is locally present in the south FSC, is not present on this profile in the southwest FSC. Location of the seismic line is shown on Fig. 5.1b.

Depositional Package 4 (DP4)

Depositional Package 4 (DP4) extends across the entire study area where it ranges in thickness from 100-460 m (Fig. 5.10). The base of the package is defined by a prominent erosion surface. The base reflector can be mapped across much of the study area, with the exception of the northwestern part of the FSC where it is obscured underneath a high amplitude reflector. The basal surface is a prominent erosion surface which truncates DP3 and locally DP2 below. Erosional relief along the surface ranges from 10-200 m.sec, but locally exceeds 300 m.sec. An isochron map of DP4 highlights the geometry (erosional relief) of the basal incision surface (Fig. 5.11). The isochron map shows that the basal surface defines a complex incised dendritic drainage system (Figs 5.11). The valleys seem to traverse towards the SW-NE and E-W and feed into a significant centered NNW-SSE trending valley, which has an erosional relief that exceeds 300 m.sec. Taken together, the cross-sectional geometries and the plan-view map are both consistent with pronounced erosion and fill of one major NNW-SSE trending distributary channel which was fed by a spectacular ordered pattern, consisting of numerous tributaries, all of which converge to form a branching (dendritic) drainage system that extends over 2200 sq. km of the survey (Figs.5.5, 5.9,5.11). The basal surface is progressively onlapped by overlying reflectors of DP4. The seismic and the biostratigraphic evidence (see Appendix) indicates that this incised valley network has eroded and incised into the interpreted delta plain and delta front facies associations of the underlying Unit 3b (Hildasay Sandstone Member) and locally into DP2. There is no core to document lag deposits at the base of the fill, however the wire-line logs predominantly show an abrupt upward increase in gamma ray values across the basal surface (e.g. in 204/19-1) (Fig. 5.3, F&G). Therefore, this is interpreted as the incision surface.

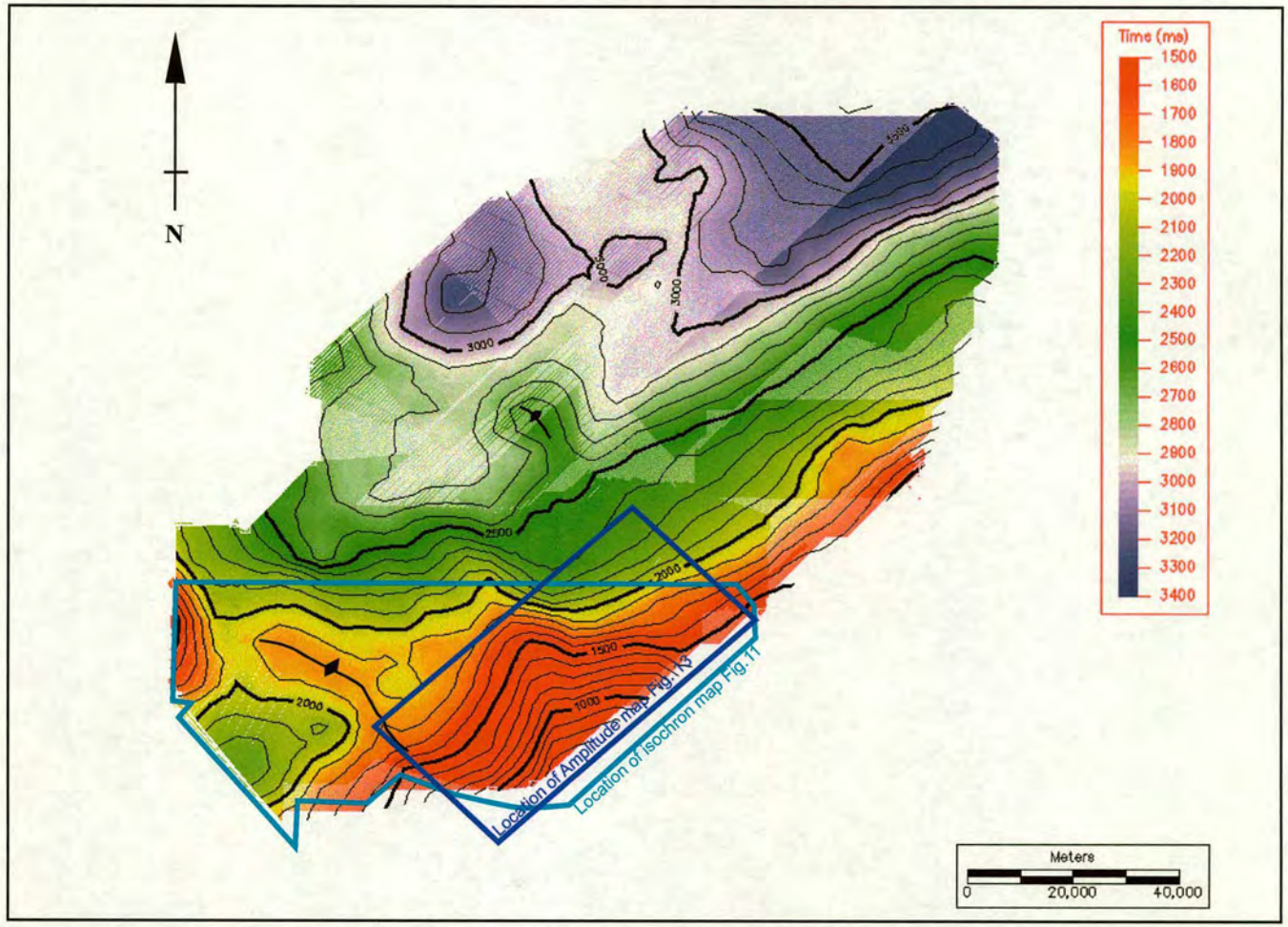

Figure 5.10. Time-map and contour lines of the Top Balder surface. The topography represents the basin-configuration after the coupled uplift-subsidence event (Dp4). The effect of younger structural inversion event is also shown on the map (shown by symbols).

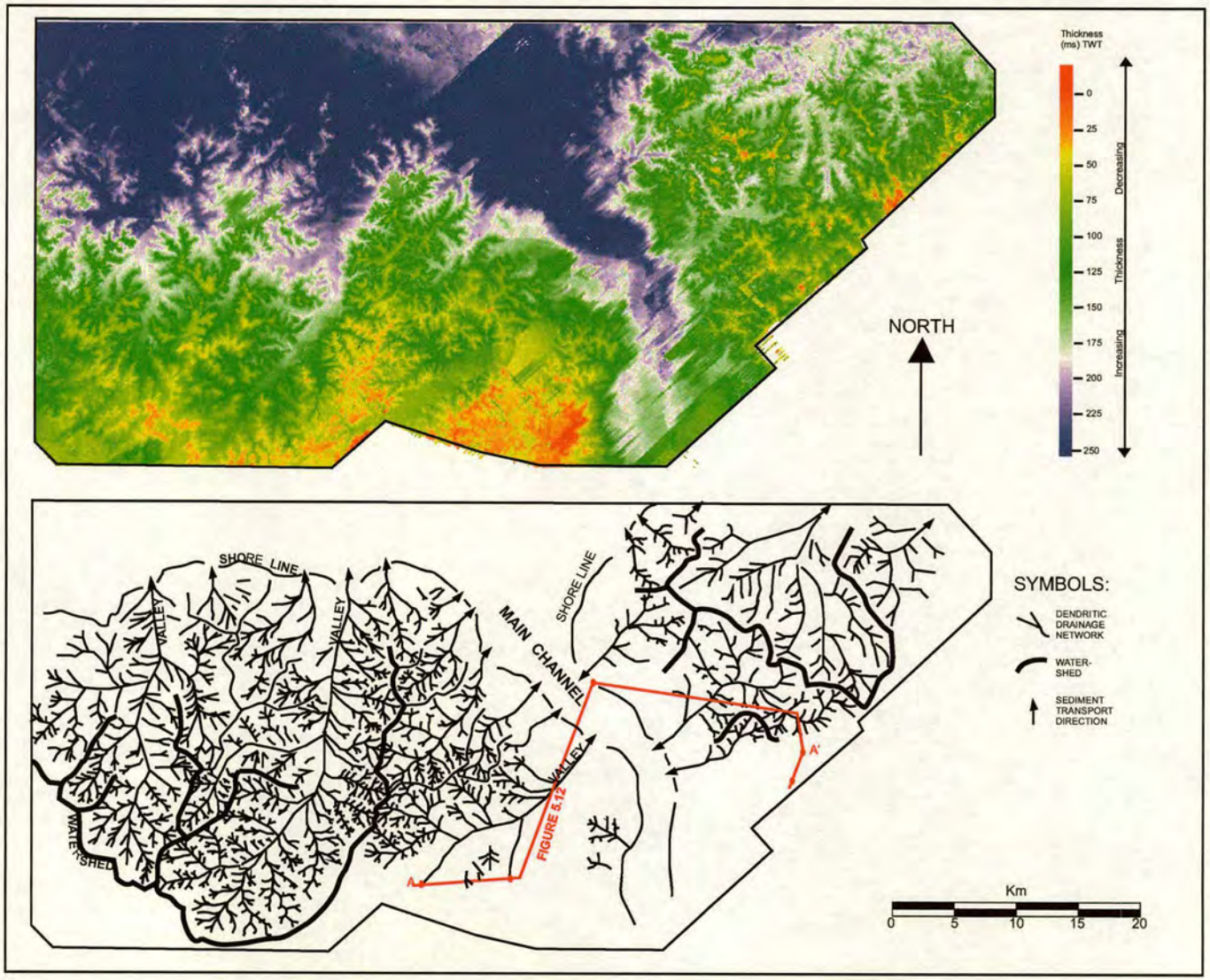

Figure 5.11. Isochron (thickness) map of DP4 and line drawing interpretation of the dendritic drainage system that characterises the south and southwestern part of the FSC. Location of the map is shown on Fig. 5.10. The map illustrates the spectacular ordered pattern of the valleys and their feeder tributaries. The NNE-directed drainage is perpendicular to underlying Mesozoic structural elements (Fig. 5.1a). The position of the well correlation panel used in Fig. 5.12 and the representative seismic section are shown in the line-drawing.

Unit 4a:

Unit 4a forms the lowermost seismic package which infills the most deeply incised parts of the valley system described above. It is up to 150 m.sec. thick and onlaps the erosional topography. Internally, Unit 4a consists of seismically-transparent, weakly conformable package of reflectors. An isochron of DP4 indicates it forms a NNW-SSE trending thick located in the central part of the southern FSC (Figs.5.1a, 5.5, and 5.12a-c). Seismic amplitude analysis indicates low amplitude reflectivity in the NNW-SSE trending body of Unit 4a (Fig. 5.13a). Unit 4a contains tropical pollen that is age-equivalent to the uppermost part of the Lamba Formation and the Colsay Sandstone Member (Lista IIIb and Forties Formation in the North Sea sequence) (David Mudge pers. comm.). Furthermore, there is biostratigraphic evidence (e.g.well 204/24a-7) that shows that Unit 4a contains reworked sediments of the Colsay Sandstone Member (Forties II). The gamma log trend and the cuttings from wells that penetrate this interval (mainly 204/19-4a, 204/24-1a, 204/24a-3, 204/24a-4, 204/24a-5 and 204/24a-7) indicate that unit 4a consist predominantly of several fining-upward cyclic successions grading from sandstone to siltstone to mudstone (see Appendix).

Unit 4b:

Unit 4b is up to100 m.sec. thick and extends across the entire study area. Unit 4b is bounded below by a moderate amplitude reflector that defines the top of Unit 4a, whereas the top of Unit 4b is marked by a continuous, high amplitude reflector. An isochron map indicates that the unit thickens to the N. Internally, Unit 4b is characterized by high amplitude, parallel to wavy reflectors (Fig. 5.4a). An amplitude map extracted from a stratigraphic level near the base of Unit 4b indicates that the main NNW-SSE trending valley is characterized by low amplitude reflectivity, whereas high amplitude reflectivity dominates laterally to the main valley (Fig. 5.13a-b). Unit 4b consists of at least five "facies"/type of mixed sandstone, siltstone, mudstone and lignites, where every component is not always present (see Appendix) with complex internal lateral variation (core data) taken through a heterolitic section and a sandstone

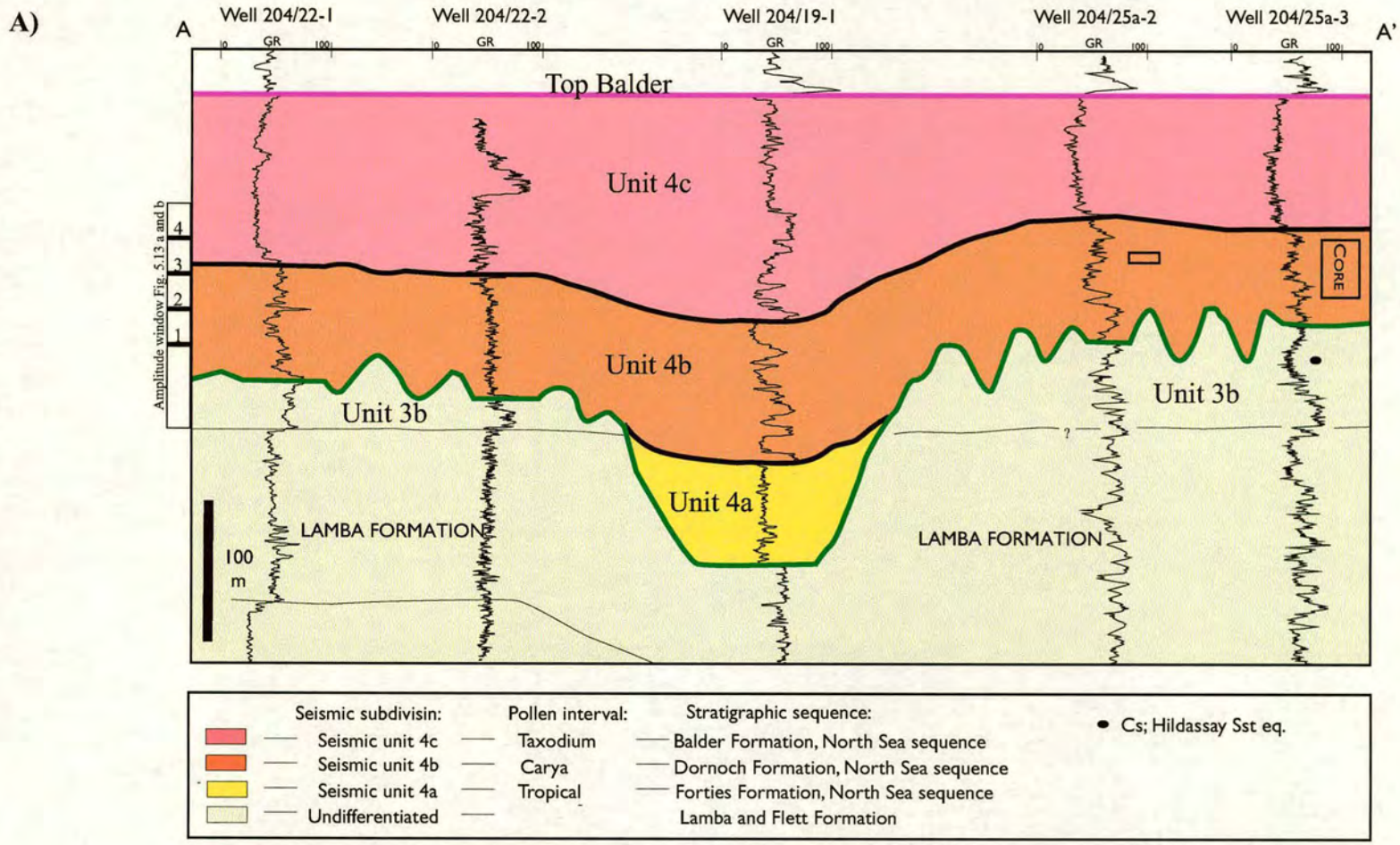

Figure 5.12a. Well correlation that has been tied with the seismic interpretation on Fig. 5.12b showing the well trends (wire-line gamma ray log), and the biostratigraphic control (in different colours) within Dp4.

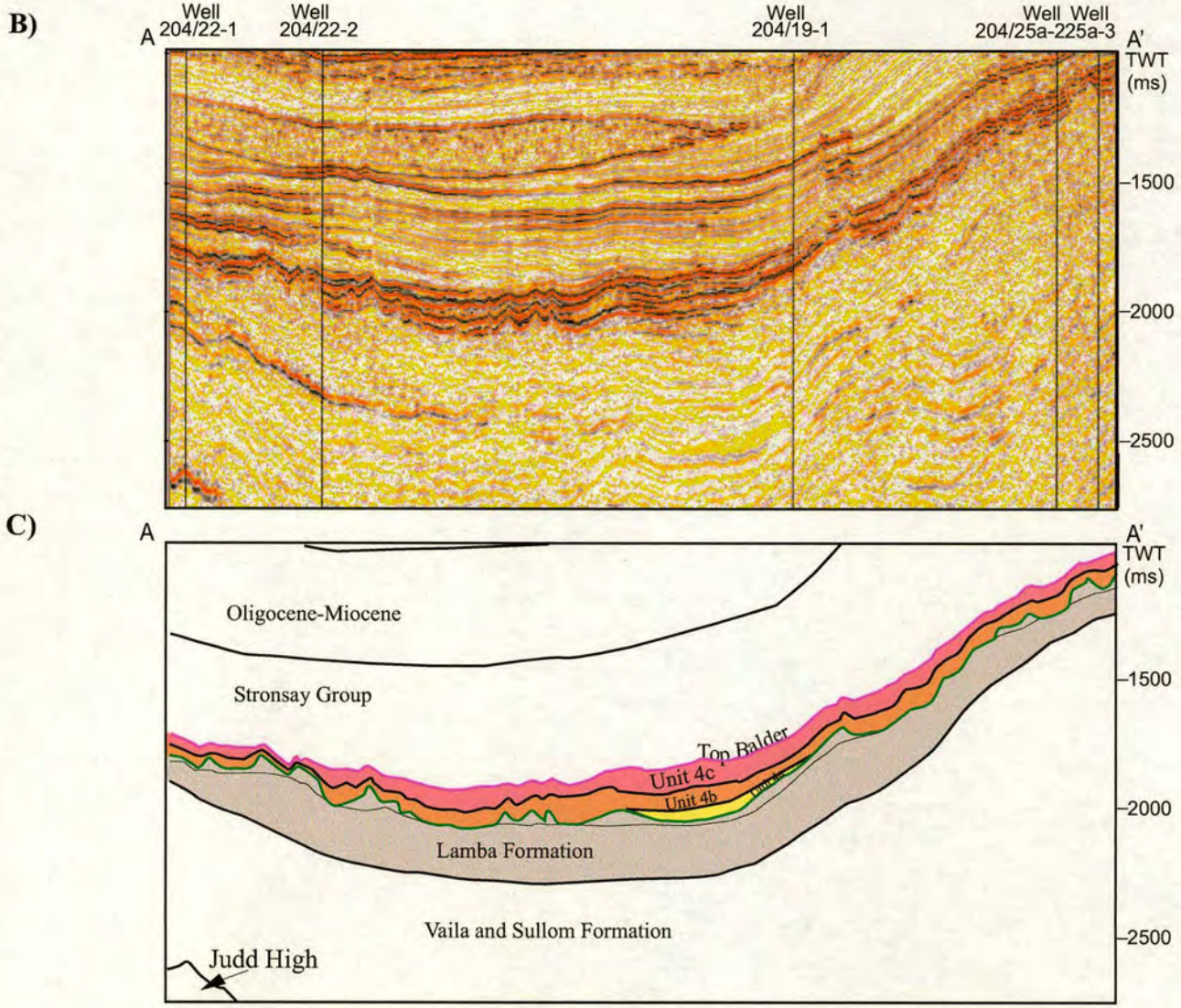

Figure 5.12b. Seismic traverse line of the well ties presented in Figure 5.12a. Location of the seismic line is shown on Fig. 5.11.

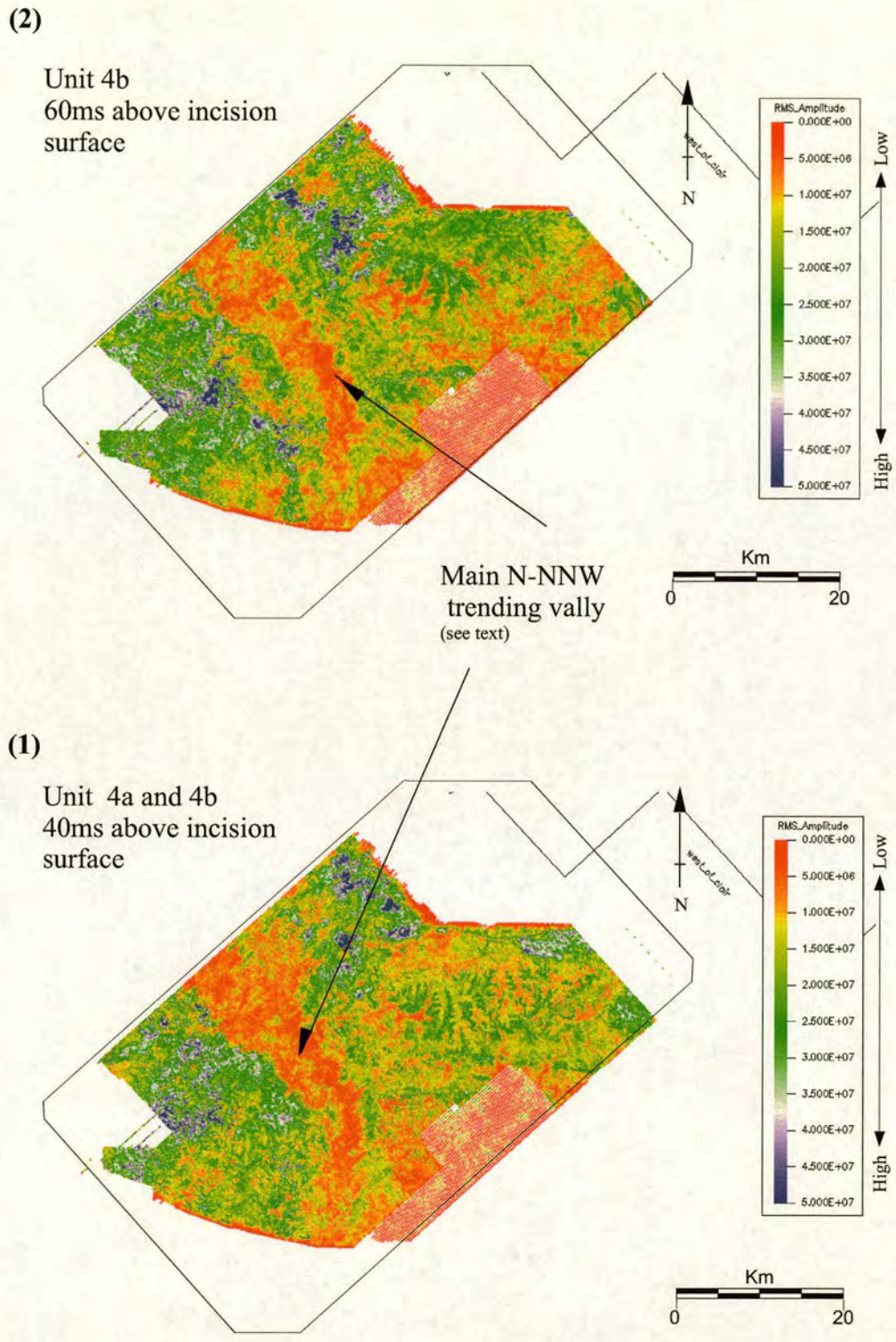

Figure 5.13a. Amplitude maps representing the lateral facies distribution of a surface within DP 4, Unit 4a and Unit 4b (see text). See Figure 5.12a for the depth at which each of the amplitude surface was extracted.

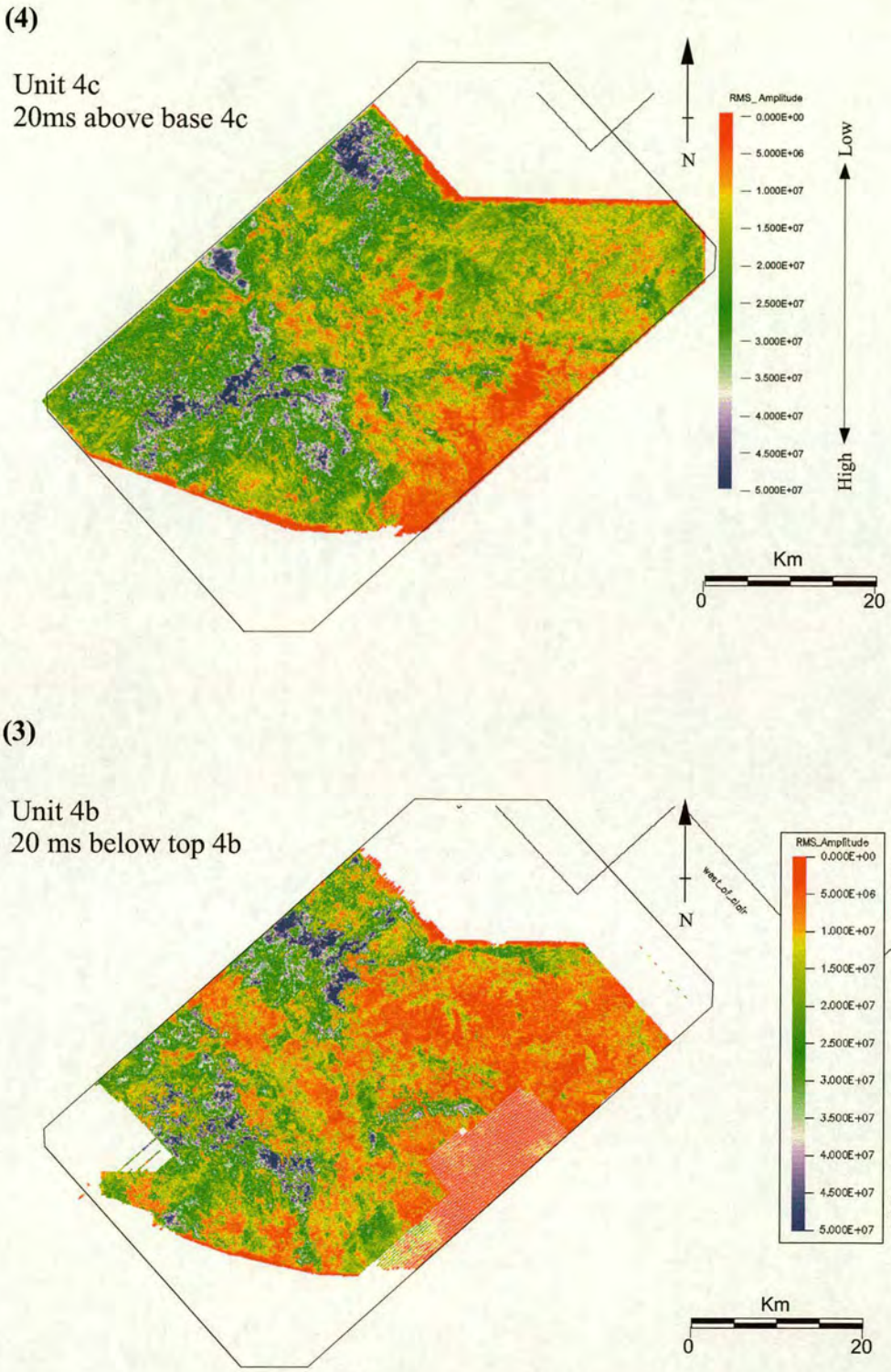

Figure 5.13b. Amplitude maps representing the lateral facies distribution of a surface within Depositional Package 4, Unit 4b and Unit 4c (see text). See Figure 5.12a for the depth at which each of the amplitude surface was extracted.

section of Unit 4b (Fig. 5.14a-b). Unit 4b contains pollen (Caryapollenites simplex; shortened to Carya; bioevent Cs; David Mudge pers. comm.), which is age equivalent to the Hildasay Sandstone Member (54.8-54.5 Ma) (Dornoch Formation in the North Sea).

Locally, near the base of Unit 4b a high amplitude, flat-lying seismic reflector is observed. It is restricted to the northwestern part of the FSC, and is demonstrated by 6005/15-1 and 6004/12-1Z to be the seismic response of a 20-35 m thick interval of basalt (Basalt 4; Figs. 5.3, C&D, Fig.5.4a and 5.9). Well data (6005/15-1, 6004/12-1Z, 6004/16-1z and 204/14-2), suggests that the boundary of Basalt 4 (extending from the Faroe Islands in the NW) is located north of wells 6004/12-1z and 204/14-2 and south of wells 6005/15-1 and 6004/12-1Z (Fig.5.1a). Basalt 4 can be correlated towards the east into the central FSC, where it extends to just north of the Westray Ridge. Stratigraphically, Basalt 4 is situated at a higher level than Basalt 3 (Fig. 5.15). Basalt 4 occurs immediately above the incision surface (base DP4) and below the top of Unit 4b, and thus is part of the fill of the incised valley network (Fig. 5.3, C&D, Fig. 5.4a and Fig. 5.9). The basalts represent the continental volcanic deposits of the Upper Series lavas of the FPLG (Statoil 2002/Ellis et al. 2002).

Unit 4c:

Unit 4c is up to 120 m.sec thick and extends across the entire study area. Unit 4c thickens to the north, and consists of a highly reflective, largely conformable sequence that drapes and infills underlying relief associated with the incision at the base of Unit 4a (Fig. 5.4a, Fig. 5.5 and Fig. 5.9). Amplitude maps indicates that Unit 4c within the NNW-SSE major valley (Fig.5.11) is high amplitude in contrast to the low amplitudes, which characterise Units 4a and 4b (Fig. 5.13b). Unit 4c consists of four different "facies"/type (see Appendix) of predominantly mudstones and lignites, but also well sorted sandstone. Unit 4a show commonly no trend and also fining-upward gamma ray trends. Unit 4c contains pollen (Taxodium) (David Mudge pers. comm.), which is age equivalent to the Balder Formation (54.5-54.04 Ma) in the West of Shetland and North Sea.

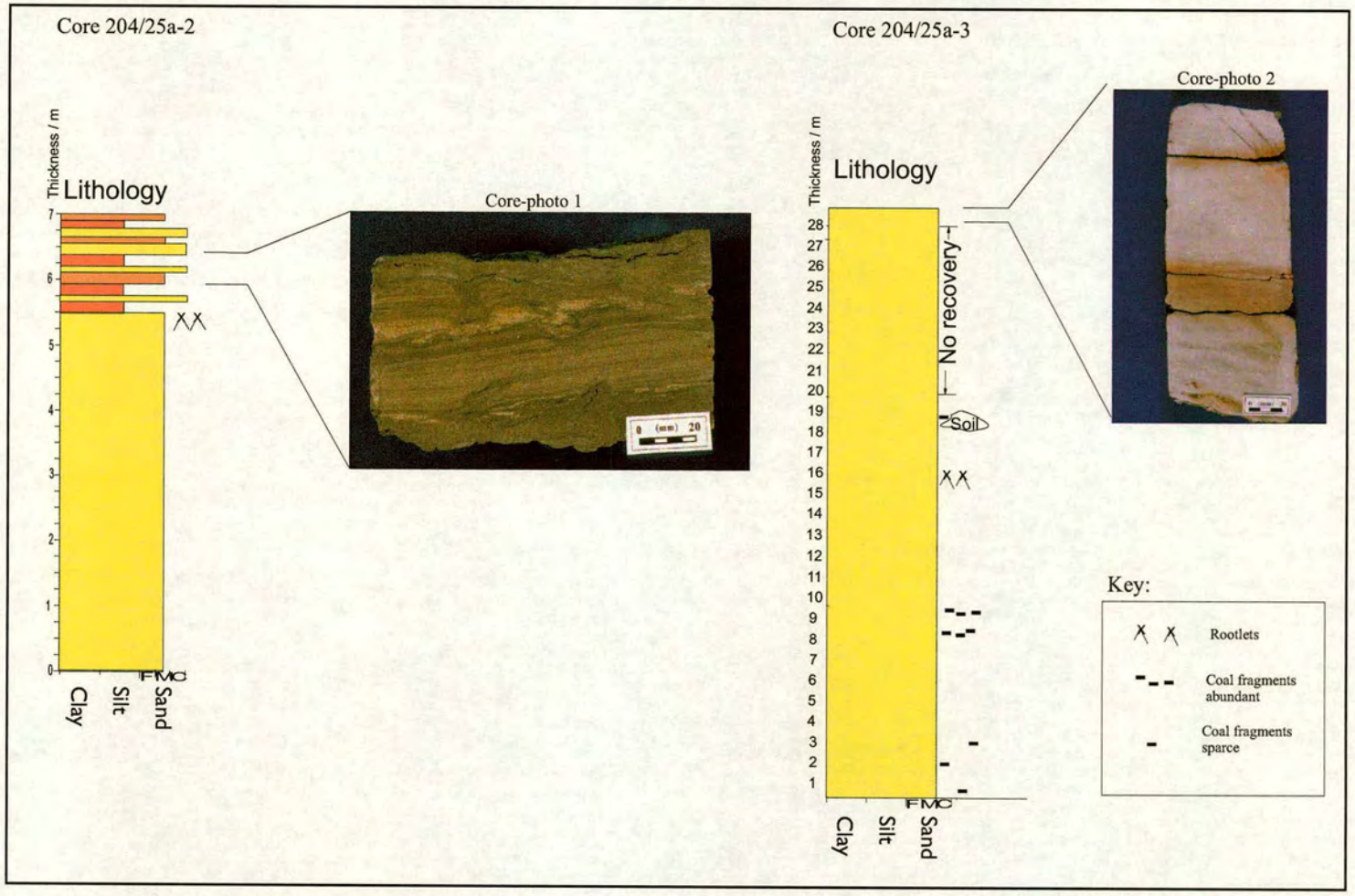

Figure 5.14a. Core 204/25a-2 and 204/25a3 (location is shown on Fig. 5.12a). Core description is shown in Appendix 1. Details of photo1 and 2 are shown in Figure 5.14b. The cores were taken within Unit 4b, see Fig. 5.12a for well location.

Core-photo 1; well 204/25a-2

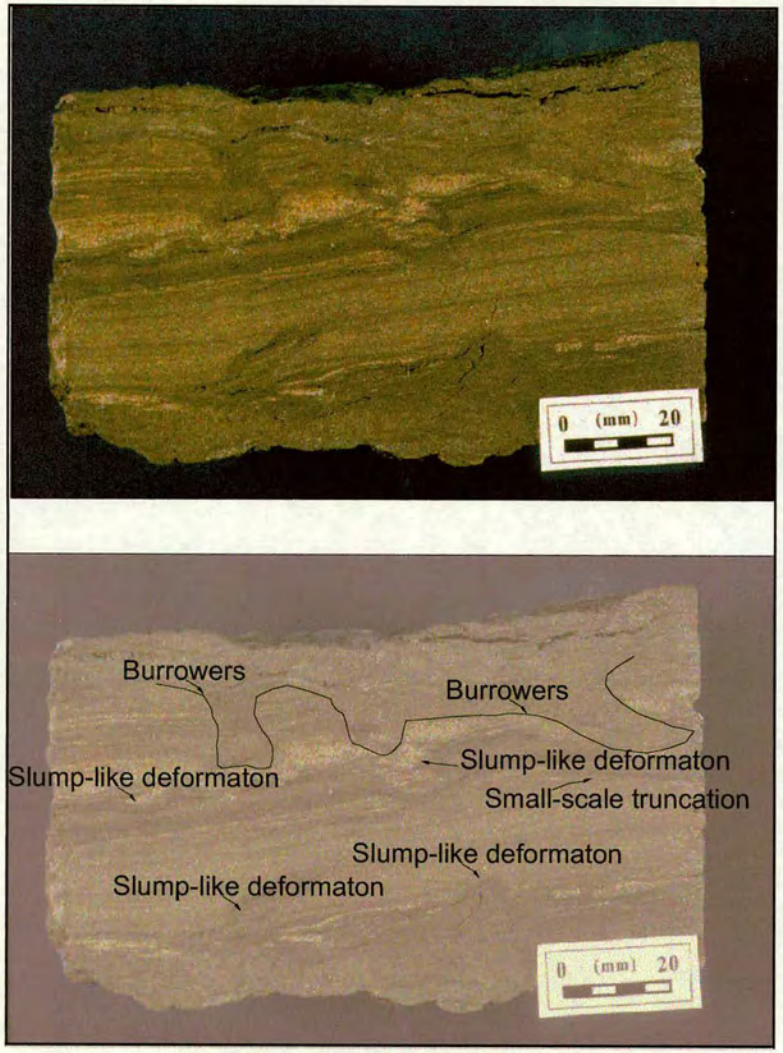

Core-photo 2; well 204/25a-3

Figure 5.14b. Photographs of cored sections (Unit 4b). A) The photo shows the heterolitic-sandstone facies encountered within Unit 4b (see Fig. 5.12a) B) The photo shows a sandstone interval within Unit 4b (see Fig.5.12a). The red bands across the sandstone are a result of secondary oxidation.

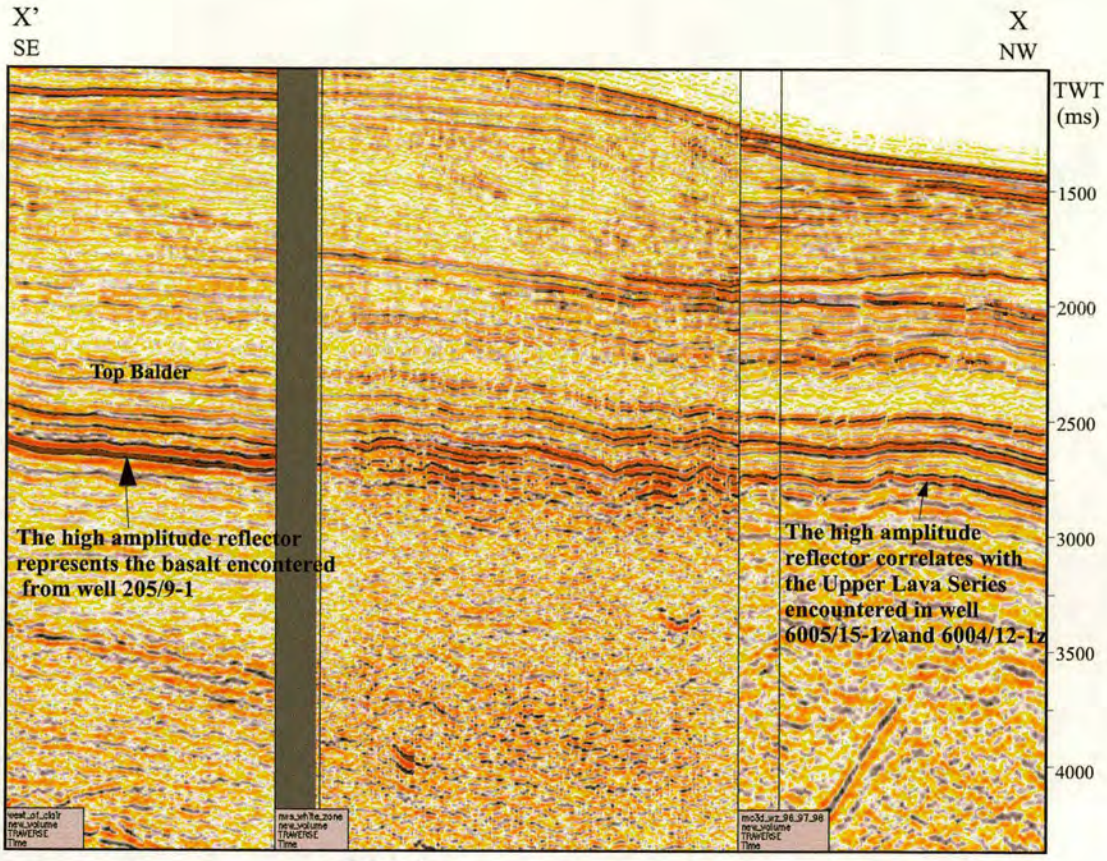

Figure 5.15. Seismic profile showing high amplitude reflectors that 1) in the southeast represents Basalt 3, which is time-equivalent to the uppermost Lower lava Series of the Faroe Islands and 2) in the northwest represents basalt 4, which is time-equivalent with the Upper Lava Series. It is apperant from the seismic profile that Basalt 3 is located at a stratigraphic level that is slightly lower than the stratigraphic position of Basalt 4. The location of this traverse-section is shown on Fig. 5.1b.

Timing of incision event

The incision surface lies at a stratigraphic level above Unit 3b (Hildasay Sandstone Member) and below Unit 4a (locally containing reworked sediments aged latest Lamba Formation–Colsay Sandstone Member) and Unit 4b (Hildasay Sandstone Member). This makes the incision surface an intra Hildasay Sandstone Member event, with an age of ca. 54.8-54.5 Ma. The timing of the incision event calibrated from the biostratigraphy and the thickness of the Flett and Balder Formations indicate that the incision event occured at 54.7 +/- 0.2 Ma.

Volcaniclastics of DP4

Depositional Package 4 and in particular Unit 4c contains tuffaceous material (called Balder tuffs). The Balder tuffs are present across the whole FSC making it an easily identified seismic marker bed. In the northwest of the basin, the Balder tuffs on-lap onto the Upper Series lavas of the FPLG (Basalt 4) (Fig. 5.16, see also Fig. 4.7)(cf. Waagstein and Heilman-Clausen, 1995; Ritchie et. al., 1999). The tuffaceous material common in unit 4c represents the deposition of Balder tuffs which was associated with a massive explosion and initial sea-floor spreading that coincident with the opening of the North Atlantic (ca. 55 Ma; Chapter Two and Three).

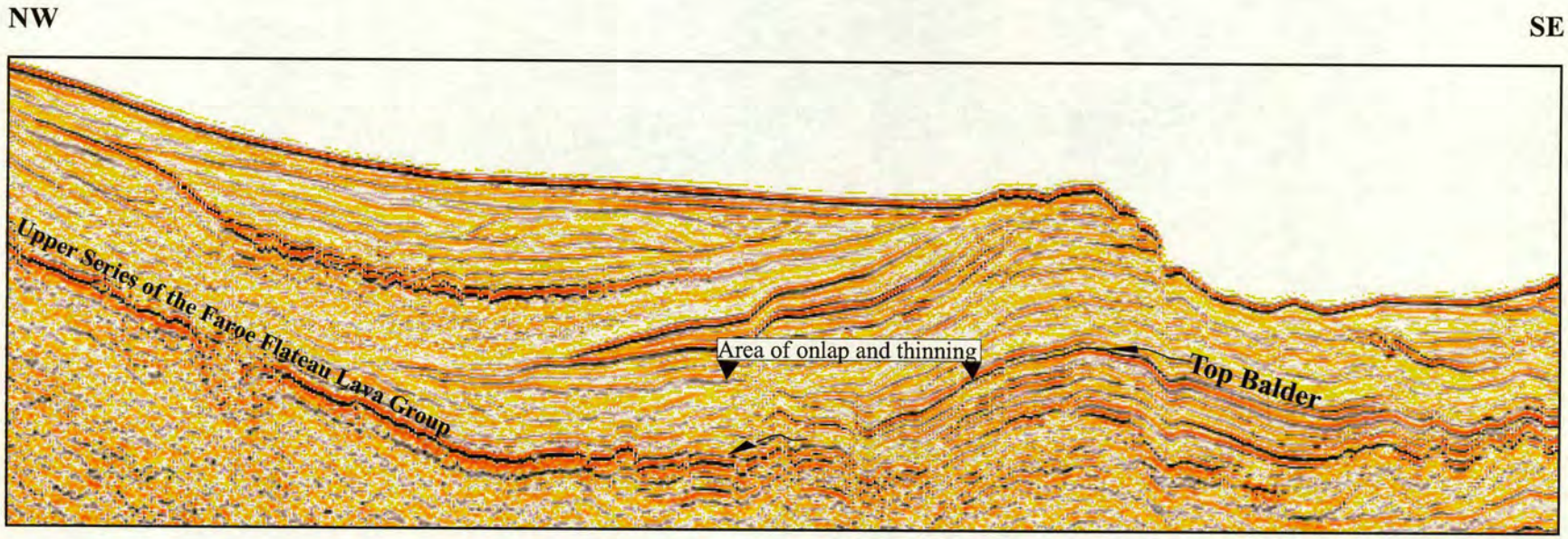

Figure 5.16. Seismic profile showing in the northwest the high-amplitude reflector representing the Upper Series of the Faroe Plataeu Lava Group and in the southeast the Top Balder reflector. The seismic geometry below the Top Balder reflector shows a seismic package that thins and onlaps towards the northwest onto the Upper Series lavas.

5.4. EVOLUTION OF THE EARLY PALEOGENE SEQUENCE STRATIGRAPHY

The seismic stratigraphic framework established and described in the previous sections has enabled the sequence stratigraphic evolution of the Paleogene succession within the study area to be interpreted.

Depositional Package 1 (DP1)

Prior to deposition of DP1 the sedimentation was characterize by onlap and downlap packages, which are restricted to the basin center north of well 204/19-1 representing submarine fan complexes (the Cuillin Package and the Kintail Package; Ebdon et al., 1995) (Chapter Three). In the FSC, following the deposition of the Kettla Member tuffs, DP1 was deposited over the former location of the slope-basin transition (Fig. 5.4c). The parallel stratified reflectors, the shelf-slope facies association recorded in wells, and the lack of seismic clinoforms geometries, suggest that the DP1 is composed largely of aggradational shelfal and slope deposits. This indicates that during deposition of DP1, sediment supply generally kept pace with the generation of accommodation space and thus the shelf-slope system built up vertically. The facies interpretation from the well data (i.e. the marginal marine shelf-slope facies) gives an estimation of the location of the shelf edge to slope transition. The shelfal facies association encountered in wells in the southern FSB indicate that the shelf was wide (ca. 20 km (cf. Naylor et. al., 1999) and based on the parallel stacking/aggradational nature of the seismic reflectors it is likely that most sediments were stored on the shelf (Fig.5.17, stage 1). With respect to the underlying submarine fans, DP1 represents a shallower shelfal facies association, indicating a basinward shift in facies.

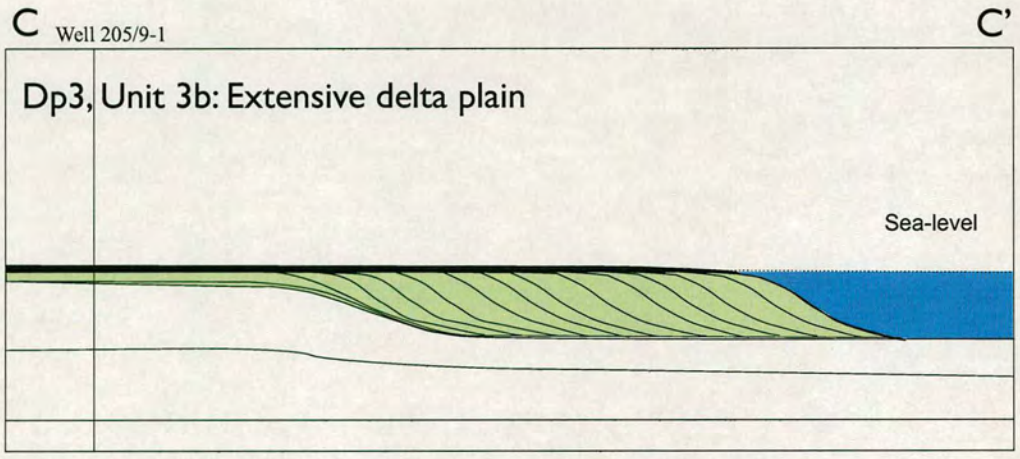

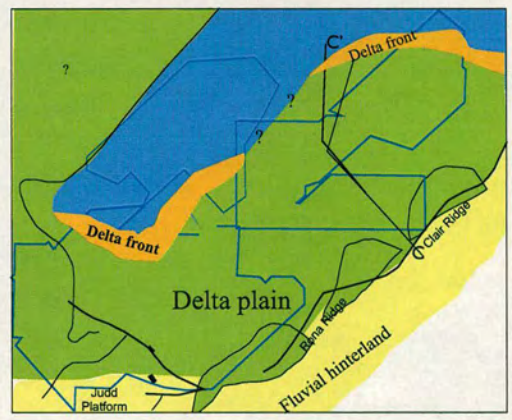

Stage 4

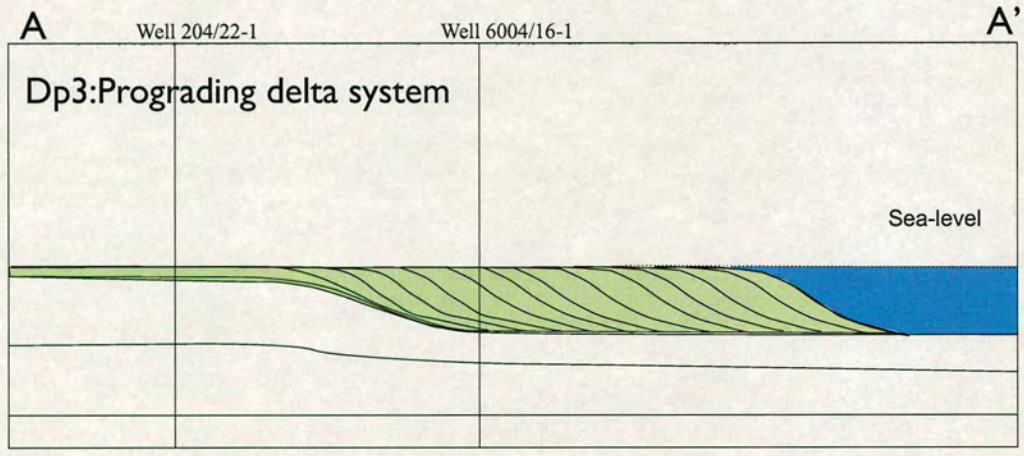

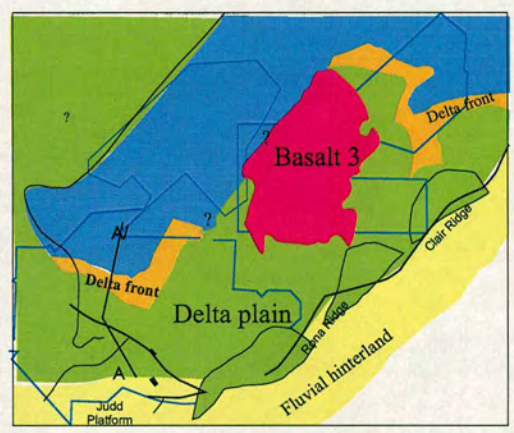

Stage 3

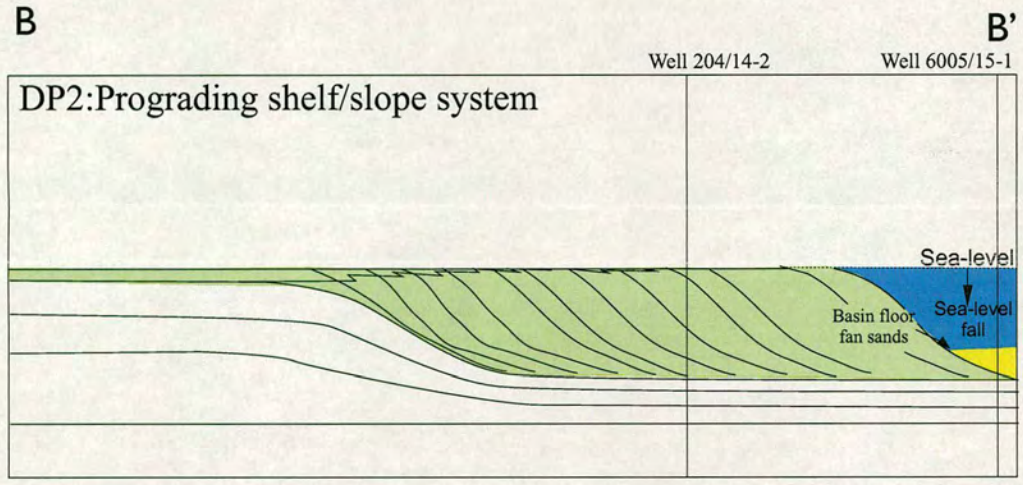

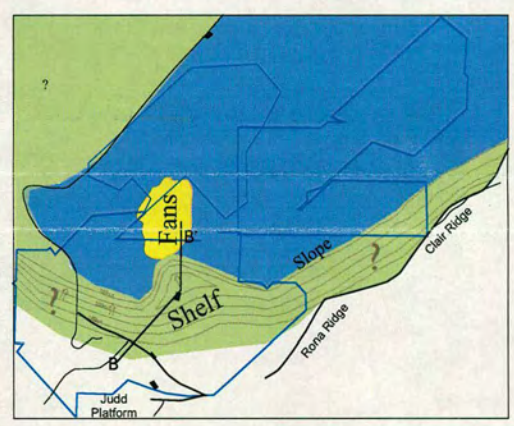

Stage 2

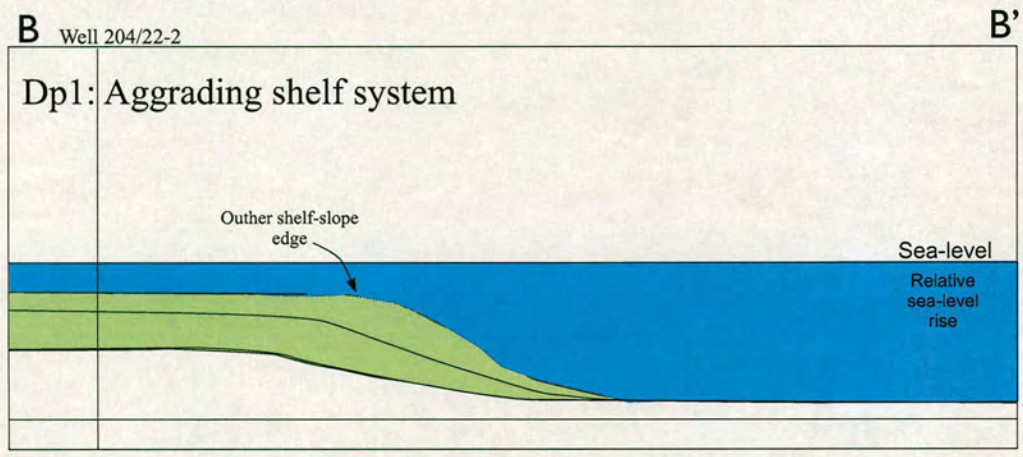

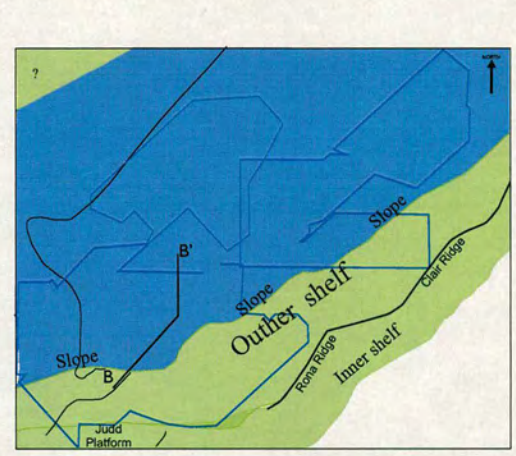

Stage 1

Figure 5.17a. Schematic evolution diagram showing stages 1-4 of the interpreted stratigraphic evolution (see text). The location of the cross sections is shown on the the corresponding plan-view map. (Stage 3 in the central FSC from Naylor et al. 1999).

Depositional Package 2 (DP2)

Reflectors in DP2 have well developed clinoform geometries and downlap onto the underlying DP1, suggesting a change in accommodation space:sediment supply ratio relative to DP1. In particular, this change in seismic geometry (strongly progradation) suggests that during the deposition of DP2 sediment supply was greater than accommodation generation and a basinward shift in facies occurred. The ca. 200 m-high clinoforms are interpreted to represent topsets, foresets and bottomsets (Fig. 5.5), indicate that water depth was up to 200m during deposition of this unit. The facies associations indicate that DP2 was deposited on a shelf-slope environment (see Appendix) in the NW part of the FSC (Fig. 5.7). The aggrading reflectors and the dominantly fine-grained lithology (e.g. well 204/14-2) indicate that the distal parts of the slope system were developed here. The coarsening and fining-upward trend in the upper part of well 204/14-2 are interpreted to reflect variations in the grade of sediment supplied down from higher up the slope (Fig. 5.3,E). It is likely that the foresets contain a coarser-grained lithology than the bottomsets, but this cannot be proven due to a lack of data. The prograding delta system was a result of either a greater sediment supply with respect to accommodation that led to the shelf slope system to prograde or that subsidence in the area was reduced, but sediment supply stayed high and the sediments were stored in land/shelf areas. The basinward shift in facies and the building out of the shelf slope break suggests a relative sea level fall, which forced deposition to occur basinwards of the previous (DP1) shelf-edge (Fig. 5.17a, Stage 2). The seismic mounded bodies and associated sandstone showing distinct box-shape gamma ray log trend and interbedded mudstone facies encountered in well (6004/15-1z;Fig. 5.3,D) are interpreted to represent submarine fans facies. The submarine fans indicate that sands were received into the basin across the narrower shelf (compared with DP1) either via feeder channels or were deposited as a consequence of slope instability, triggered by earthquakes, or storm related processes. The submarine fan facies are related to instability in the depositional environment associated with the sea level fall (Fig. 5.17, Stage 2).

Depositional Package 3 (DP3)

The boundary between DP2 and DP3 represents a normal regressive surface across which there is a shift from fine grained shelfal deposits into prograding shallow marine-terrestrial deltaic deposits (Fig. 5.5). It is probable that DP3 consists of a delta or coastal plain (e.g. well 204/22-1, 204/14-2, 204/19-1, 205/9-1) to delta front (well 6005/15-1, 206/1-2) facies association (Fig. 5.3, A and 5.3, B, Appendix, cf. Knox et al., 1997; Ebdon et al., 1995; Naylor et al., 1999). The N and NNE progradational clinoform geometries and pro-delta to delta front to coastal plain coarsening-upwards trends in DP3, are interpreted to indicate that sediment supply was generally greater than accommodation resulting in progradation of DP3 (well 6005/15-1; Appendix and Fig. 5.3, C). A maximum water depth of ca. 100 m, is interpreted based on the height of the clinoforms. The local occurrence of DP3 in the southwest and in the north FSC and additionally the facies associations (see Appendix) suggest that DP3 had at least two sediment input points and that some lobe switching may have occurred (Fig. 5.17, stage 3 and 4).

The shallow marine to non-marine delta facies association and coarsening-upward trends suggest that sediment supply exceeded the development of accommodation space. Thus DP3 prograded over the underlying shelf-slope-basinal system (DP1) and shelf-slope System (DP2). The sandstone interval in the north FSC is interpreted by Ebdon et al. (1995) to represent a major lowstand fan. In the south western FSC it is possible that the sandstone interval (well 6005/12-1, Fig. 5.3 D) could also represent a lowstand fan belonging to DP3, based on a lithostratigraphic correlation between the wells (Fig. 5.3 C and D). However, the seismic suggests that this interval could also belong to DP2, as stated in a previous section (Section: Depositional Package 2; Fig. 5.4 B and 5.6). Assigning this sandstone interval in well 6005/12-1 to DP3 would differ from the seismic stratigraphic correlation described in the previous section, that is based on the onlapping of seismic reflectors onto a wedge-shaped seismic package interpreted to belong to DP2 (Fig. 5.6). In this local area in the north west of the FSC,

the quality of the seismic data is moderate to poor, and thus, in order to unequivocally correlate the sequences improved quality of the seismic data and biostratigraphically constrained core data is required. Thus, it remains inconclusive as to whether this sandstone interval is DP2 or DP3.

During deposition of DP3, Unit 3a basaltic lavas (Basalt 3) were extruded onto the coastal plain locally in the central part of the FSB, with the flows accumulating in topographic lows (Fig 5.17, stage 3). Unit 3b was subsequently deposited across the entire study area, which at this time mostly consisted of an extensive coastal plain (much of the south and central FSC) (Fig 5.17, stage 4).

Extent of incision surface beyond the basalts in the north and northwest of the FSC

On the northwestern margin of the FSC lavas of the Upper Lava Series of the FPLG are developed (Fig. 5.18). Beneath these deposits seismic clinoforms are observed (Fig. 5.18). Although it is uncommon for clear stratal geometries to be imaged below thick lava sequences, a 2D seismic line across the northwestern part of the FSC (Fig. 5.18) shows clear SE-prograding clinoform reflectors. This is opposite to the NW-direction observed in clinoform packages of DP2 and DP3. It is possible that the clinoform reflectors in the northwestern part of the study area are age equivalent, to the delta system represented by DP2 or DP3. Thus the clinoform reflectors underneath basalt 4 (Fig. 5.18) imply that the DP2 or DP3 are present in the northwest area and furthermore that the incision surface in the "basalt free" area might extend further northwest beyond the area of poor seismic resolution underneath the volcanics of the FPLG (Fig. 5.18). It has been proposed previously (e.g. Kiørboe, 1999) that seismic clinoforms that have aggradational to progradational geometries, indicate sea level fluctuation. These progradational geometries were developed developed when the basalt of the FPLG entered the contemporary shore-line of the FSC which at present is seen on seismic as an Escarpment (the Faroe-Shetland Escarpment, e.g. Ritchie and Hitchen, 1996) (Fig. 5.1A).

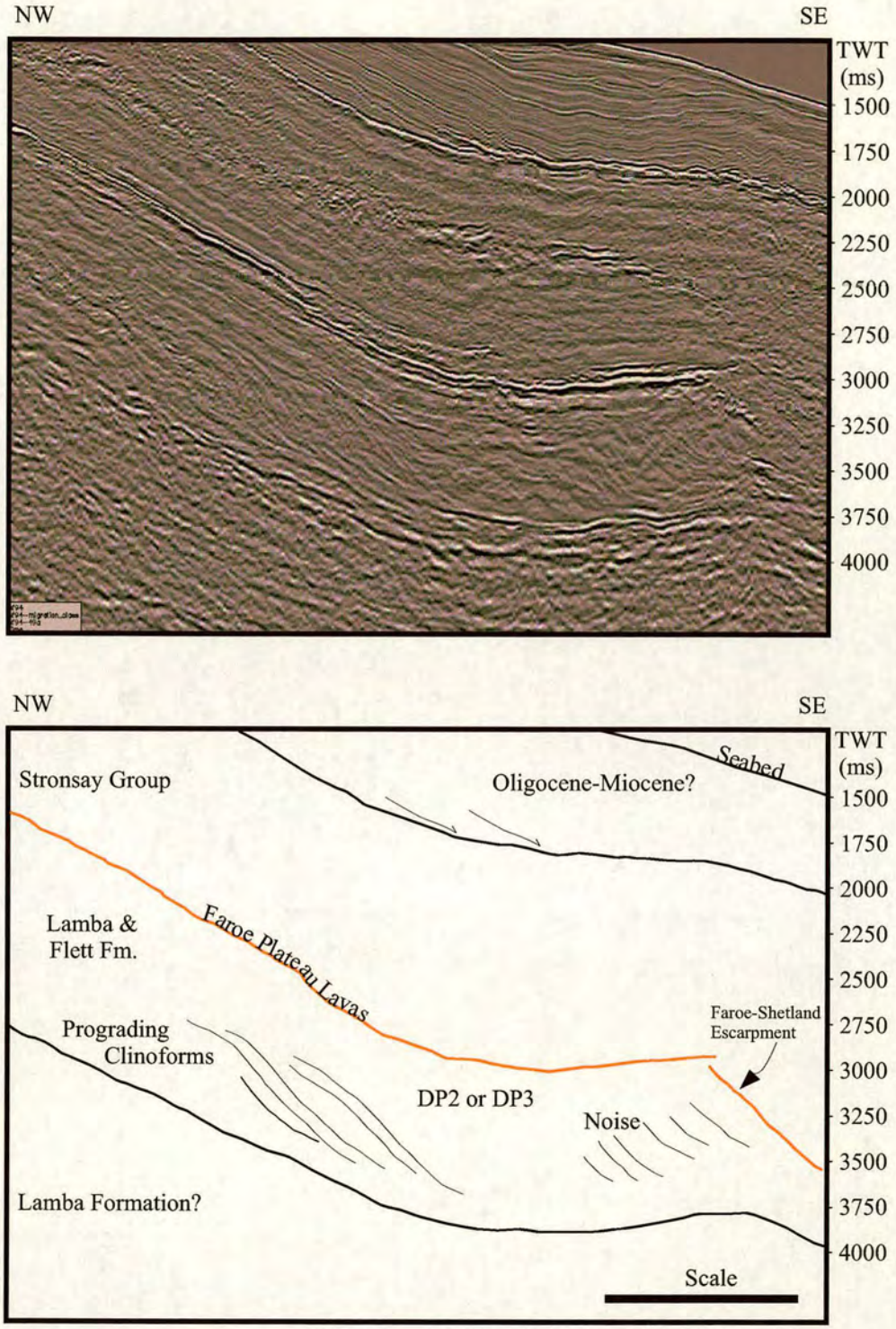

Figure 5.18. Seismic profile showing a high-amplitude reflector that represent basalt of the Faroe Plateau Lava Group. The downlapping clinoform reflectors underlying the basalt may represent a prograding delta that is part of the delta system of DP2 or DP3 (see text).

Alternatively, during the late Palaeocene-Early Eocene the northwest FSC represented a restricted shallow marine to non-marine environment (e.g. Mudge and Bujak, 1999), especially the southwest and southern FSC as indicated from this study. To date no wells have been drilled to confirm whether the clinoforms in the northwestern area of the FSC represent sediments, volcanics or volcaniclastics. It is likely, however, that the clinoform reflectors (Fig. 5.18) represent a SE prograding system located along the northwestern-northern margin of the FSC and is part of a widespread delta complex (DP3) that experienced denudation related to the ancestral Iceland mantle plume, as discussed in section 5.6.

Depositional Package 4 (DP4)

Basal surface

Incision and erosion evidenced by the basal incision surface of DP4 and the dendritic drainage pattern (Fig. 5.11) was a consequence of removal of accommodation space during relative sea -level fall and a marked basinward shift in facies. Biostratigraphy allows this event to be dated as an intra Hildasay Sandstone Member event (54.7 Ma). The valleys were incised perpendicular to the underlying fluvial distributary system evident within DP2 and DP3, and extended basinward. The products of Early Eocene (54.7 Ma) incision and erosion were transported to the N and NE and speculated to have been deposited in a series of submarine fans on the basin floor.

There was a watershed developed in the south-western and south-eastern part of study area (Fig.5.11). On the southwest margin the channels flowed to the N and NNE and on the southeast margin the cannels flowed to the NE, NW and SW (Fig. 5.11). Although drainage patterns are influenced by many factors including climate and lithology, topographical relief controlled by the location and evolution of underlying structures is considered the most important control (cf. Summerfield, 1991). It is generally accepted that dendritic drainage patterns characterise youthful systems that have developed on a substrate where there is no marked lithological or local structural control on drainage (Morisawa, 1985). Since the Paleogene drainage pattern would

have reflected the palaeoslopes developed at the time of deposition, the implication is that although local deformation did not play a role, compaction above Mesozoic structures continued to influence the pattern of drainage above the site of the Judd High and South Westray Ridge (Figs. 5.11 and 5.17, stage 5).

The lowstand submarine fan deposits associated with incision

Seismic and well data were used to document the possible deposition of LST submarine fans linked to incision (54.7 Ma). However, due to lavas and lack of well control in the NNE (where the valley systems flowed), it is not possible. As discussed above, it is evident from the valley network N and NNE flow that the erosive material, probably representing lowstand fan sandstone, is located north and north-northeast of the mouth of the valleys (Fig. 5.17, stage 5). Based on the previous seismic amplitude method, areas outside well control were tested in order to try and locate the lowstand fan sandstone associated with the incision event. However, the volcanic lavas of the FPLG north and northwest of the channel network produce very high reflectivity on the seismic profiles, so that it has not been possible to produce valid amplitude maps within the fill of this area. Therefore, it has not been possible to exactly locate the lowstand sands using this method. It is probable, that the lowstand sands are likely to be present N and NNE of the channel network (Fig. 5.17, stage 5) where the porosity and the permeability of the sandstone might have been affected by the thermal impact from the coeval eruption of the lava flows. If on the contrary, if the sandstones have not been thermally affected, the lavas could act as a potential seal to trap hydrocarbons provided that the sands are at a favorable depth for hydrocarbons to be accumulated.

The infill of DP4

Immediately after incision (54.7 Ma), extrusion of continental plateau basalts (Basalt 4) occurred. These flowed from the NW (Figs. 5.3, C&D, 5.9, 5.14 and 5.17, stage 6), and are interpreted to have filled relief associated with the incised drainage network (see later).

Unit 4a:

Onlap of reflectors onto the basal incision surface together with the fining-upward log trends in nearby wells suggest that Unit 4a was deposited during a relative sea-level rise. During relative sea level rise the incised valley system was flooded and fining-upward cycles of fluvial facies associations representing the base of the system fill indicate that estuarine condition were established in the drowned topography. Higher-frequency variation in relative sea level during transgression are indicated by small-scale coarsening-up and fining-up units. Amplitude analysis (Fig. 5.13, 1) indicates that the low reflectivity facies (sand, siltstones, non-tuffaceous and non-coal mudstones) were deposited in the main channel/channel inlets and in the mouth of the valleys and is dominated by sandstone deposition, also evidenced by the blocky-gamma ray representing a predominantly sandstone-fill (Fig. 5.12a). These sandstones could be preserved lowstand sandstone deposits associated with the earlier sea level fall (i.e. Posamentier and Vail, 1988)

Unit 4b

Unit 4b onlaps the basal incision surface, and represents the second stage of filling of topography associated with the dendritic drainage network (Fig. 5.17, stages 6-7). Ongoing transgression caused the topography to be progressively infilled by a variety of estuarine facies including distributary channel sandstones and lagoonal overbank sandstones/ siltstones/mudstones and lignites (Core Data, Fig. 5.14). Complex interbedding of the sand-rich and sand-poor facies is interpreted to reflect either high-frequency fluctuations in relative sea level or autocyclic switching of sand-rich distributary channels within the estuary.

Unit4c

As relative sea-level continued to rise, the entire area was flooded, and the remaining topographic relief associated with the incised valley system was filled by transgressive

sediments and draped (Fig. 5.17, stages 7-8). Deposition was dominated by aggradational to retrogradational sequences that stacked dominantly mudstone and lignites sequences that contain *Taxodium* pollen (David Mudge pers. com.). The fine-grained character of this interval, plus the presence of lignites and taxodium pollen indicates that coastal plain swamp conditions in a hot, humid environment were established. Amplitude maps (Fig. 5.13, 3 and 4) and well data (6005/15-1z and 6004/16-1z) indicate that sands were locally deposited in the southwestern and southeastern part of the study area (Fig. 5.3, B & C). The strong high amplitude reflectors that subdivide Unit 4b and 4c may possibly be related to a major shift in the depositional facies related to the abundant transgressive sandstone facies in that area.

5.5. CONTROLS ON THE EARLY PALEOGENE STRATIGRAPHIC EVOLUTION

The aim of this section is to discuss the controls on the stratigraphic evolution presented in the preceding sections. Focus is placed on the factors controlling fluctuations in relative sea level and sediment supply (including the accommodation space:sediment supply ratio) such as; 1) eustasy, 2) tectonics, and 3) igneous activity. When discussing eustasy, the Haq et al. (1987) long- and short-term sea level curves are used. It is, however, clear that there are limitations in using these curves in an area undergoing active tectonism and/or volcanism, as these processes are likely to exert a marked local control on relative sea level changes.

Depositional Package 1 (DP1)

Following Early to mid-Palaeocene deep-marine sedimentation, represented mainly by basinal mudstones and sand-rich basin floor fans (e.g. Lamers and Carmichael, 1999; Naylor et al., 1999), a transgression of the basin margins occurred (Chapter Three). This was associated with significant volcanism as indicated by the development of tuffaceous material (Kettla tuffs) at the base of DP1. The global short-term sea level curve indicates a sea level rise that correlates with deposition of DP1. The basinward shift in facies, indicated by the absence of sub-marine fan deposits and the aggradational nature of shelfal facies association of DP1 suggest that DP1 was not controlled by eustasy but by shallowing that occurs by a local effect most likely related to uplift but was probably controlled by thermal uplift related to the Kettla Tuffs.

Depositional Package 2 (DP2)

Depositional Package 2 was deposited in front of the previous (DP1) slope-basin transition (Fig. 4.3) as a consequence this indicates a basinward shift in facies with respect to the underlying DP1. This suggests that DP2 was forced basinwards due to a relative sea level fall. The Haq et al. (1987) global sea level curve does not record this

abrupt fall in sea level, which suggests that it is more likely to be a local event related to uplift. On seismic profiles there is no evidence for any normal fault activity. However, it is probable that the local uplift may be associated with volcanic activity in the region e.g. related to the extrusion of the Lower Series of the FPLG (e.g. Waagstein and Riisager, 2002).

The local extent of DP2, suggest that the restricted distribution of DP2 was related to local uplift creating a local sediment source area. It is evident from the sedimentary record in the FSC that the environment became more restricted as a result of progressive shallowing and infilling (e.g. Knox et al., 1997). Thus, based on the regressive sequence and the basinward shift in facies that occurred during deposition of DP2, deposition of DP2 was most likely controlled by local thermal uplift.

Depositional Package 3 (DP3)

Following the deposition of DP2, DP3 was deposited during a stable relative sea level, where there was a greater rate of sediment supply than the generation of accommodation space and thus the deltaic succession (DP3) prograded onto the former (DP1) shelf. The Haq et al. (1987) short-term sea level curve shows the onset of eustatic sea level fall that seems to correspond to the relative sea level conditions that are observed for DP3. The basinward shift in facies from the deeper water shelf-slope system (DP2) to the shallow to terrestrial conditions (DP3), suggest that during deposition of DP3 the FSC became more restricted (cf. e.g. Naylor et al., 1999), most likely controlled by uplift. On seismic profiles there is no evidence for any normal fault activity and related fault displacements. However, this uplift phase can be associated with volcanic activity and the extrusion of lavas in NW Scotland (Antrim and Skye) (e.g. Naylor et al., 1999) and continued volcanic activity with extrusion of lavas of the uppermost section of the Lower Lava Series (e.g. Waagstein, 1995).

Depositional Package 4 (DP4)

Depositional Package 4 is bounded below by a major unconformity that was created during a rapid sea level fall, which resulted in incision and erosion into underlying DP3 and locally also into DP2. The short-term curve of Haq et al. (1988) shows a eustatic low at ca.54.8 Ma that correlates with the timing of incision (basal surface of DP4, 54.7 Ma). The maximum depth of the streams and the main valleys of Depositional Package 4 never exceeds 100 m, however the main channel has a depth of 250m. Haq et al. (1987) suggest that valleys produced by eustatic sea-level fall are unlikely to be deeper than 100 m. This indicates that the rapid sea level fall that resulted in incision was not controlled by eustasy alone. In order to account for the relief created by the incision both eustasy and uplift must have controlled the creation of the incision surface of Depositional Package 4.

The timing of fill and drape (Unit 4a-4c) corresponds with the initial opening of the North Atlantic, which is evidenced from the volcaniclastic sediments present in the section that represents the fill and drape. With the opening of the Atlantic, mid-ocean ridge basalts were produced. The changes in the mid ocean ridge volumes might have had an affect on eustasy as well as the post opening subsidence and decay of the mantle plume (see discussion Chapter Seven). Furthermore, the Tertiary Large Igneous Province of the North Atlantic (NAIP) (Chapter Two) consists of large volumes of basaltic rock that have extruded onto and intruded into the crust over an extensive area (ca. 2000 km radius) (e.g. White and Mckenzie, 1989; Griffiths and Campbell, 1990). These igneous rocks comprise the SDRS, the FPLS, and additional sills, dykes and volcanic centers all of which occur in the vicinity of the FSC. The early Paleogene interval (DP1-DP4) presented in this study and the coeval volcanism directly evidenced from both the volcaniclastics and the basaltic lavas e.g. the kettla Tuffs at the base of DP1, Basalt 3 within DP3, Basalt 4 and the Balder Tuffs within DP4, indicates that considerable igneous activity, and thus thermal dynamics (Chapter Two) occurred coeval to deposition of DP1-DP4. The tuff and ash-bed equivalents of the Balder Formation (54.5-54.04 Ma) that coincident with the onset ocean floor spreading, as well

as the aerially deposited SDRS dated as 54.7+/- 1.8 Ma (Jolley, 1998; Holmes, 1998), indicate that the incision event (54.7 Ma) is closely related to the very final stage of rifting and initial opening of the North Atlantic.

The result of the current seismic interpretation shows that the sea level fall that led to incision and erosion was controlled mainly by uplift/subsidence and to a lesser degree by eustatic sea-level variations. There is no evidence for widespread normal faulting, however, the shallowing and formation of the drainage network immediately predate the extrusion of flood basalts (Upper Series of Faroe Lavas) and tuff and ash-bed equivalents of the Balder Formation, both of which are coincident with the onset of rapid basin subsidence due to equilibrium and also to eustasy related to changes in mid ocean ridge volumes. If DP4 was controlled by eustasy it is evident from the scale of incision that DP4 was indeed enhanced by plume-related uplift/subsidence associated with igneous activity that prevailed in this region.

5.6. DISCUSSION: EARLY PALEOGENE UPLIFT

The time scale proposed by Jolley et al. (2002) (see Chapter Three) suggests an age of 56.5-53.5 Ma for sequence T45-T50 (Fig. 3.5) and thus gives a time of 3 My to fill and drape the incised valley system within the study area. By contrast the time scale by Berggren et al. (1995) gives a time of 0.75 My to fill and drape the same incised valley system. The key observations from the integration of the well and seismic data are that the dendritic pattern is sharply defined, and that its channels were in-filled and their interfluves submerged before they had been degraded by the cutting back and mutual interaction of the valley systems. Thus, the time between incision and valley formation, and flooding and burial must have been relatively short. Importantly, during deposition of Unit 4a-c the sediment supply must have been high to enable the incised topography to be readily blanketed from the time that the valleys first subsided below sea level. Furthermore, the fact that units infilling and overlying the valleys are not degraded is further evidence of rapid drowning with little or no subsequent erosion (related to a base level fall). Otherwise, upper slope degradation would have continued and would have produced more widespread erosion of the valleys and interfluves. Thus, it is suggested that the time scale by Berggren et al. (1995) that gives a much quicker time for the erosion and infill event, applies better to the observations and analysis made in the study area than the time scale proposed by Jolley et al. (2002). Furthermore, evidence from other studies in this area/region (e.g. Knox et al., 1997; Saunders et al., 1997), indicate that there are some problems calibrating to the timescale of Jolley et al. (2002).

The stratigraphy within the study area is interpreted to preserve both a phase of uplift and the beginning of a phase of subsidence related to the growth and decay of the ancestral mantle plume (cf. Smallwood and Gill, 2002). Detailed biostratigraphic data coupled with seismic stratigraphic observations suggest that the uplift event associated with the mantle plume initiated during deposition of the intra-Hildasay Sandstone Member of the Flett Formation (ca. 54.8-54.5 Ma), and not at the beginning of the

Balder Formation as suggested by Smallwood and Gill (2002). For example, the pattern of incision observed is interpreted to be preserved at the palaeo-bathymetric contour, which emerged above and then subsided below sea-level during a period of a transient episode of uplift and subsidence respectively. Significantly the drainage pattern was only preserved because the shelf in to which it was incised was the last area to emerge, the first to be re-submerged and did not experience long–lived stasis in between.

With respect to erosional patterns associated with DP4, it is important to make the distinction between the timing and amount of uplift and denudation. Approximately 250m of denudation inferred from the amount of incision into the DP3 and DP2. This does not, however, mean that 250m of uplift was experienced, as the erosive cut of the distributary channels and the feeder dendritic drainage pattern can only represent the last vestige of a longer-term phase of plume-related uplift. The absolute amount of uplift is likely to be much greater as indicated from the evidence presented above (the multiple unconformities and associated shallowing-up intervals evidenced from continuing basinward shift in facies represented by the depositional packages (DP1-DP3). Because of the deep-water nature of sedimentation that prevailed earlier (DP1 and early-mid Palaeocene e.g. the submarine fan deposits) at the presumed onset of the uplift episode (early Palaeocene) it is unlikely that its magnitude is calculable in the FSC. Instead, it may only be possible to quantify dynamic uplift using data from other areas or by techniques other than seismic stratigraphic analysis. Furthermore, the overall progressive uplift reflected in the successive shallowing-up units of the sedimentary record of the FSC shows an additional complex pattern of episodes of uplift represented by unconformities. Although the timing of the intervening uplift events is complex, this study allows the final phase of uplift documented in this study related to the incision and infill of a dendritic drainage network to be constrained with confidence.

Role of the Iceland Plume in Controlling Transient Uplift in NW Europe

Analysis of burial curves from the West Shetlands showed that there is a significant perturbation of the predicted Palaeocene post-rift burial history following Mesozoic extension (Nadin et al., 1997). They calculated that the total amount of uplift was around 900 m in the vicinity of the FSC. The findings of this study are consistent with their results. In combination, all these observations suggest that dendritic pattern (base DP4) revealed in the FSC records the final stage of a greater, regional uplift event superimposed on an existing structural framework and the first stage of its decay. The regional scale of the uplift implies that similar stratigraphic patterns should be observed in Early Eocene strata in other parts of the Atlantic margin and the North Sea Basin (see discussion Chapter Seven).

Discounting Alternative Driving Mechanisms

Several other mechanisms could be responsible for the upward shoaling, incision, infill and draping observed in the Early Eocene of the FSC. For instance, because seismic observation indicate that uplift is transient, igneous underplating can be discounted as a causal mechanism because this would have produced a permanent effect i.e. uplifted topography would stay up until it was eroded. Furthermore, because the thermal time constant of normal thickness lithosphere is of the order of 70Ma (Nadin et al., 1997), a regionally extensive heat pulse, which began to decay at 55 Ma, could only do so by loss of heat upwards. This would require it to have first impinged on the base of the lithosphere in the Lower Cretaceous, a scenario, which bears no relation at all to the known history of volcanism and inferred plume activity in the region. Consequently, thermal expansion and contraction would also appear to be ruled out.

In conclusion, it is suggested that given the regional extent of uplift and subsidence, the rates involved and the synchronicity of igneous activity, the sedimentary record can be confidently ascribed to mechanical deformation of the lithosphere linked to the growth and decay of the ancestral Iceland plume. The upward motion could correspond to an increasing dynamic component of uplift and

accompanied by in-plane stresses, which would decay away following lithospheric rupture and the onset of sea-floor spreading.

5.7. SUMMARY

This chapter has investigated the Paleogene succession in the northwestern, southern and central parts of the Faroe Shetland Basin. In particular, it has demonstrated how the Paleogene basin-fill records lithospheric deformation linked to the evolution of a mantle-plume head, and the subsequent onset of sea-floor spreading. 3D seismic data integrated with well and biostratigraphic data allow the Paleogene succession to be divided into four depositional packages; DP1 consists of aggrading deeper marine shelf to slope facies; D2 is a prograding shelf-edge that was forced basinwards in front of the former shelf edge; DP3 represents a shallow marine to non-marine prograding delta system, and DP4 which represents fluvial to estuarine infilling of topography developed due to incision into DP3 and DP2. In particular, the basinward shift in facies identified between DP3 and DP4 records doming of the area linked to uplift associated with a mantle plume, and is interpreted to be coeval to the last stage of rifting and the initial sea-floor spreading in the North Atlantic. Deposition package 4 represents the stratigraphic effect of a major episode of denudation, during which time the development of a spectacular short-lived dendritic drainage network of incised valleys and subsidiary tributaries occurred. Biostratigraphic evidence indicates that the incision occurred within the Hildasay Sandstone Member (54.7 +/- 02 Ma). The pattern of drainage implies that the depositional slope created was primarily controlled by emergence of tracts influenced by underlying structure, which were within reach of sea level, rather than a pattern, which radiated away from the central uplift. Subsequent transgression led to the drape and burial of the incised valley network.

Taken together, the sedimentary, stratigraphic and volcanic relationships and chronology are consistent with the theoretical models of plume behaviour. However,

because of its coupled, transient nature, they appear to be incompatible with contemporaneous igneous underplating. Its formation is also independent of deformation resulting from structural inversion of underlying faults.

The implications are that the whole plume related coupled uplift and subsidence event in the FSC reflects not just one phase of uplift followed by subsidence, but a complex pattern involving several coupled uplift and subsidence episodes (see Chapter Seven). The incision surface is direct evidence that can be quantified to represent the final pulse of uplift and subsidence of a mantle plume that dominated the region prior to break-up and ocean floor spreading.

CHAPTER SIX

6.0. TIMING AND NATURE OF STRUCTURAL INVERSION IN THE FAROE-SHETLAND CHANNEL

6.1. INTRODUCTION

Post-rift sequences are deposited during the post-rift phase of subsidence, when initial isostatic adjustment to lithospheric stretching is followed by gradual and decreasing thermal contraction of the asthenosphere over a period of ca.60-100 million years (McKenzie, 1978). The stratigraphy and general geometric character of post-rift sequences is that of onlap onto the basin margins creating the typical 'steers head' geometry (Watts et al., 1982). During this post-rift phase, sequence geometry and stacking patterns are thought to be primarily controlled by higher frequency relative sea-level fluctuations (Watts, 1982). However in the FSC, it is apparent that "normal" post-rift subsidence has been slowed or reversed at times due to uplift (e.g. Turner and Scrutton, 1993), thought to be associated with compressional tectonics (e.g. Doré and Lundin, 1996). This has considerably implications for the temporal and spatial development and variability of the coeval post-rift stratigraphy. Consequently the basin dynamics are likely to show a more complex subsidence trend than the simple post-rift subsidence model described by McKenzie (1978).

Since the FSC is currently a focus of considerable exploration interest, understanding the structural and stratigraphic evolution is crucial to improve the chance of successfully finding hydrocarbons. It is only since the settlement of the Faroes/UK border dispute in 1999 that seismic data has been available over the entire FSC and thus the post-rift evolution of the FSC is relatively poorly understood. This study also has implications for volcanic continental margins in general.

The aim of this study is to build on Chapter Five (see aim in section 5.1, Chapter Five) and specifically to investigate the timing, nature and sedimentary

response to the growth of a prominent domal inversion structure observed within the post-rift (Eocene-Recent) succession. The structure is examined in relation to the sediment distribution and the architecture of the seismic sequences. The results are considered in a regional context in order to understand the causal mechanisms especially for the uplift. In particular, the timing is considered with respect to the contemporaneous sea-floor spreading of the North Atlantic-Labrador Sea systems and also the Alpine compressional tectonic events.

6.2. DATA SET AND METHODOLOGY

This study utilizes seven 3D-surveys (see Chapter One). In total 15 wells have been utilized (204/14-2, 204/17-99/3, 204/19-1, 204/22-1, 204/24-1A, 205/8-1, 205/9-1, 205/10-3, 205/10-4, 205/10-5A, 206/1-2, 214/27-1 &2, 6004/12-1Z 6006/16-1Z), having full or partial recovery within the Eocene to present day succession. The limited well data is due to the shallow (above top Balder ca. <2000 ms TWT) depth of the post-rift succession that was not a target in hydrocarbon exploration. The wells have been examined and tied with the seismic interpretation. The well analysis is based on drill cuttings, wire-line logs and one core (BGS 204/17-99/3 core). The cored interval is taken from 28.81m to166.0m (137.19 m) below seabed. The biostratigraphy (both microfauna and flora) from a total of seven samples show that the cored interval is Palaeogene (Eocene) in age.

The seismic sequence stratigraphic analysis and interpretation of the Eocene to present-day section allows eight depositional packages to be defined. Interpretation of the well, core and biostratigraphic data have been integrated into the seismic stratigraphic framework in order to reconstruct and temporally constrain the stratigraphic and tectonic development during stages of uplift. Biostratigraphic data from core (BGS borehole, 99-3) and well 204/22-1 are key data that has been used for calibration and determining the timing of inversion.

6.3. SEQUENCE STRATIGRAPHIC FRAMEWORK OF THE LATE PALEOGENE TO PRESENT

In this section the main structural features that have been identified, may have influenced the stratigraphic distribution are initially described. Subsequently, the depositional packages and genetically related sub-units that make up the stratigraphic framework of the post-rift succession are described. The eight depositional packages (DP5-DP12) that have been defined were deposited from the Early Eocene to present day. This was subsequent to Mesozoic rifting that led to initial sea floor spreading during Chron 24r (ca. 55Ma) time interval.

Main structural features

In the southern FSC, a structural monoclinal fold (hereafter named "Foinaven-Monocline" or shortened to FM) is defined on the seismic as a one-limbed flexure on either side of which the strata are horizontal (Figs. 6.1, 6.2a and 6.3a). The fold is trending N-S and is present locally above the Mesozoic South Westray Ridge area (Fig. 6.1). The flexure is represented by folding of Palaeocene to Late Eocene strata (Fig. 6.3a). It is possible that sediment loading since formation has enhanced the amplitude of the flexure.

In the south-western part of the FSC, a structural high is present (Fig. 6.2a, 6.4a-b), that is defined seismically by an anticlinal fold (this structure is hereafter named "Foinaven-Anticline" or shortened to FA). The anticline is 20 km long 10 km wide and trends NW-SE, but bends midways and becomes WNW-ESE (Fig. 6.1,B). The deformed beds (Palaeocene-Neogene) are locally truncated both near and at the seabed (Fig. 4a and c). The amount of uplift and deformation increases northwest along the fold axis, reflected in a northwestward truncation of progressively older strata (Fig. 6.4c). Horizontally the deformation represents 1% shortening, calculated using equation:

$e=(L_f-L_0)/L_0$, where L_f is the final length and L_0 the original length.

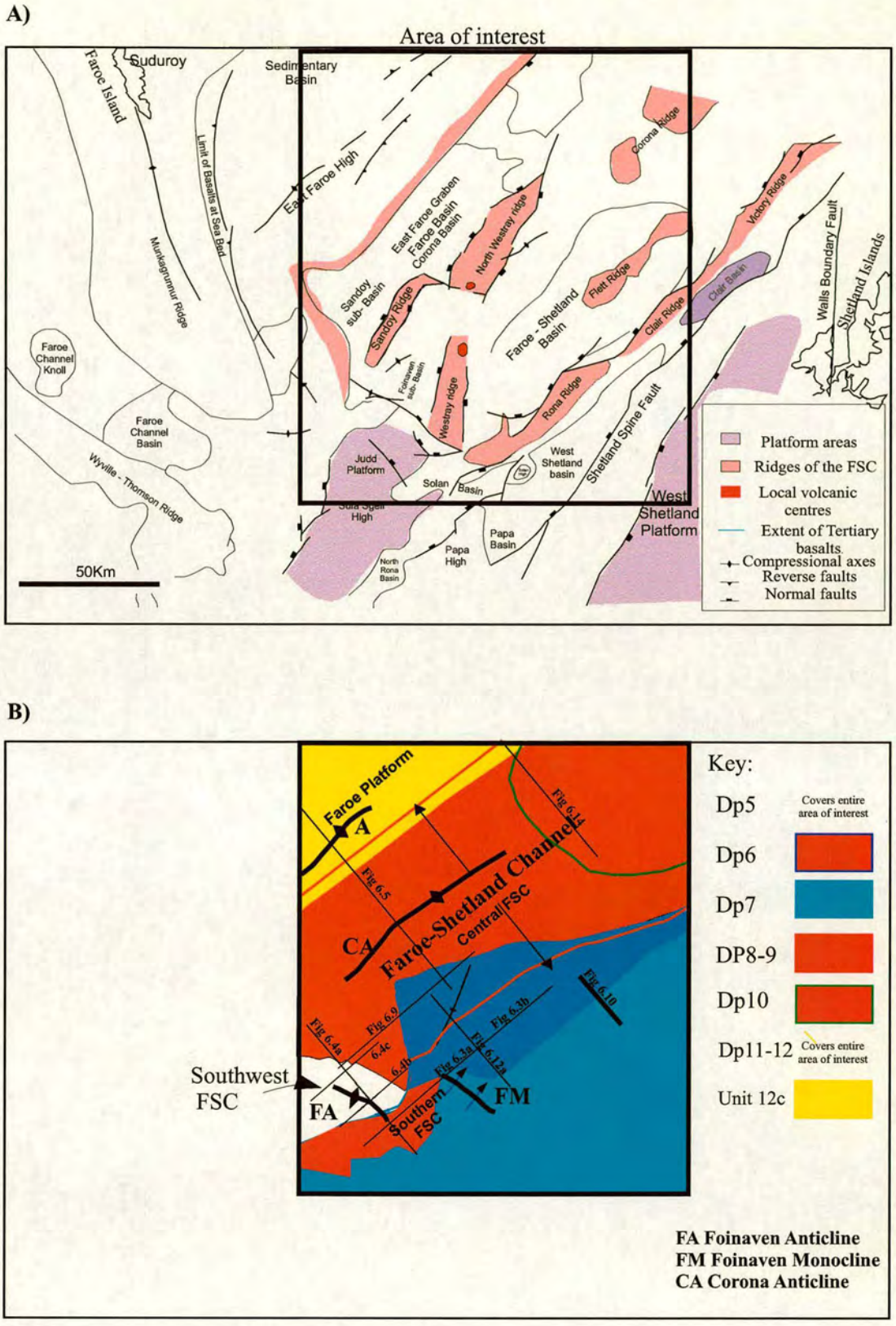

Figure 1. Location map of study area. A) Shows the structural lineaments and B) the location of main structural features and the extent of depositional packages within the Eocene to Present-day sediementary succession in the FSC.

A)

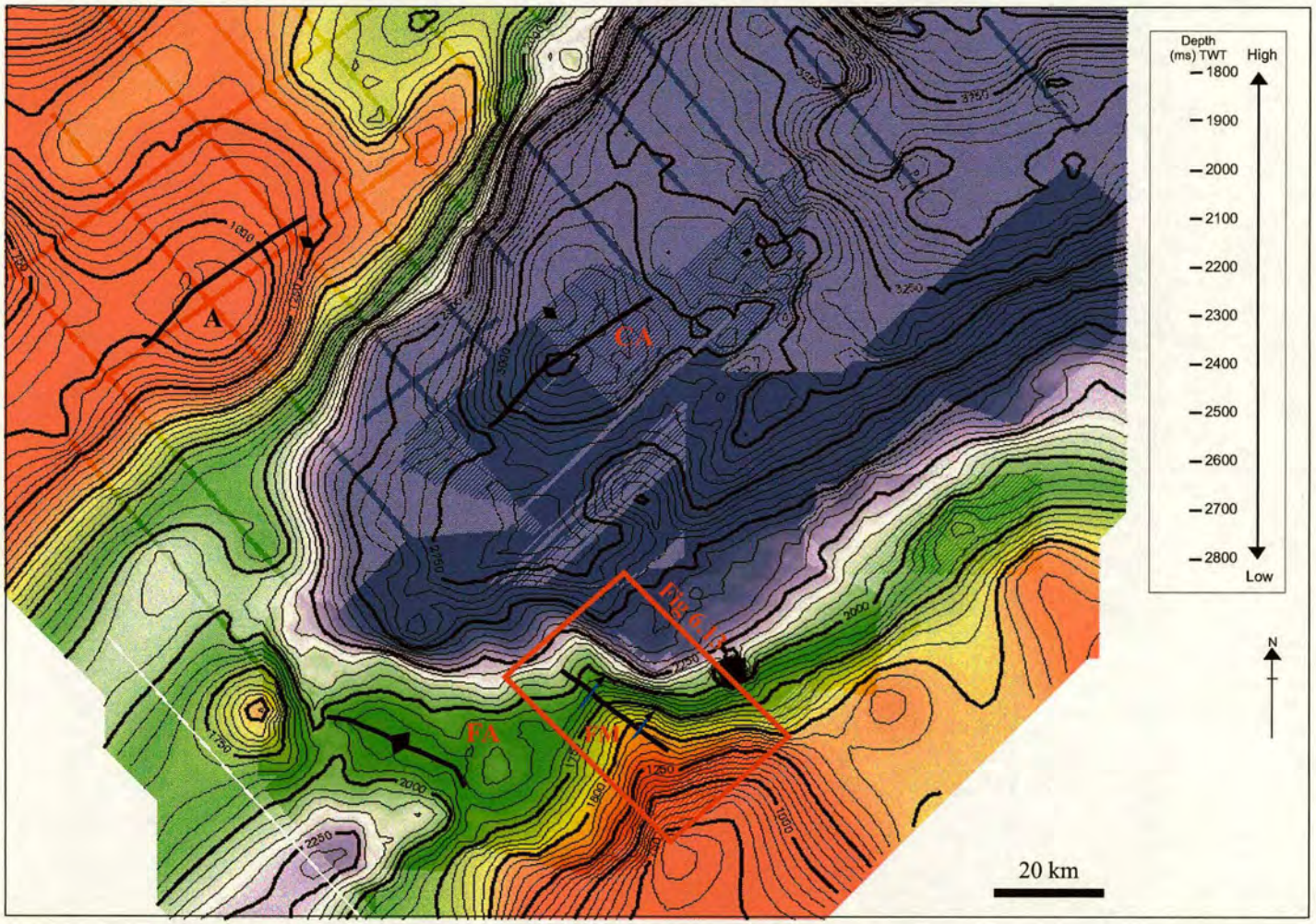

Figure 6.2a. Time-map of Top Balder/base depositional package 5, in the southern and central FSC and on the Faroe Platform showing the location of the main inversion structures FA=Foinaven Anticline, FM=Foinaven Monocline and CM=Corona Anticline.

B)

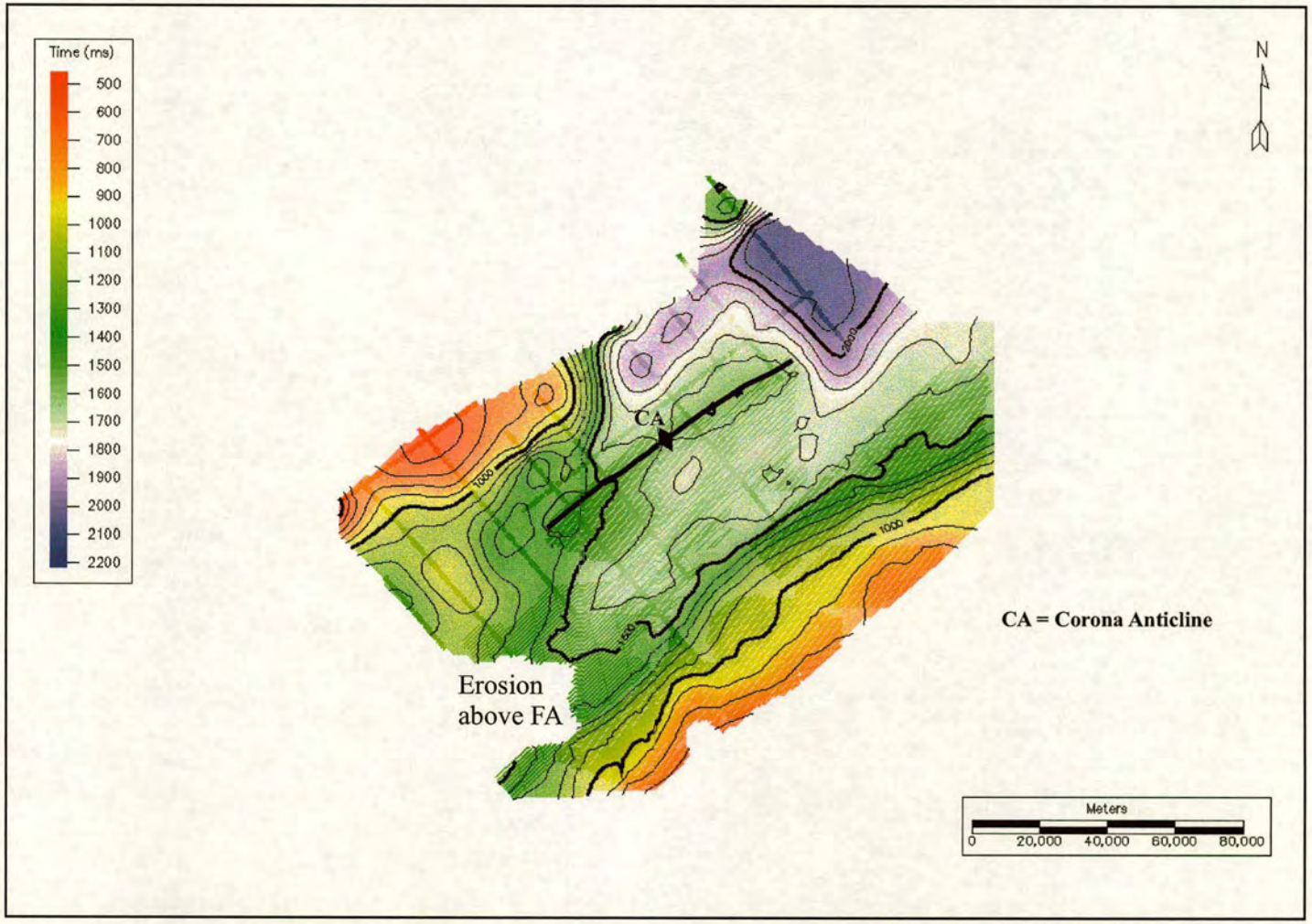

Figure 6.2b. Time map of the top DP8-10 reflector (mid-Miocene reflector) showing the Corona Anticline.

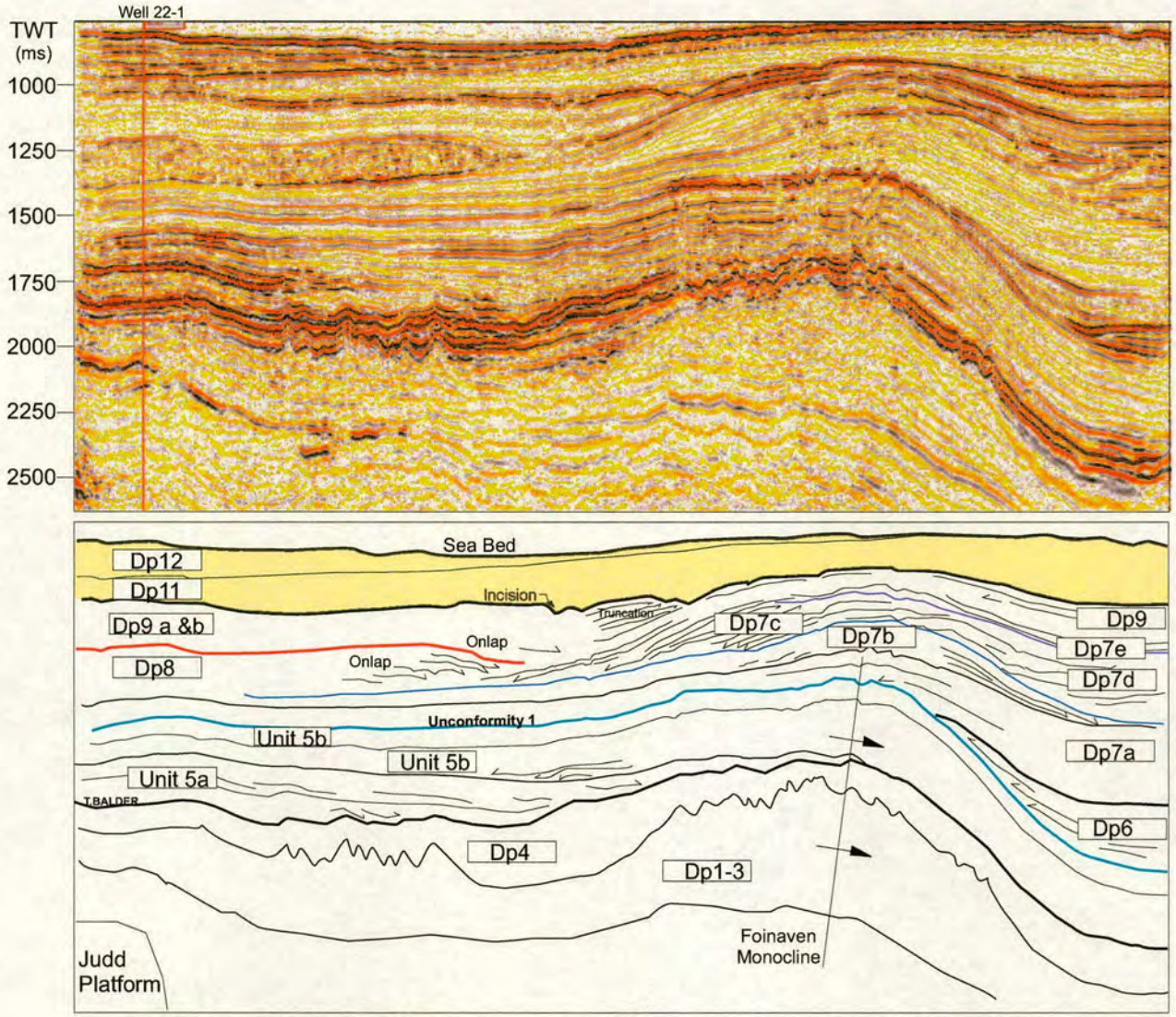

Figure 6.3a. Seismic profile of representative seismic line showing the character of depositional packages 5-12. Location of the seismic line is shown on Fig. 6.1,B.

B)

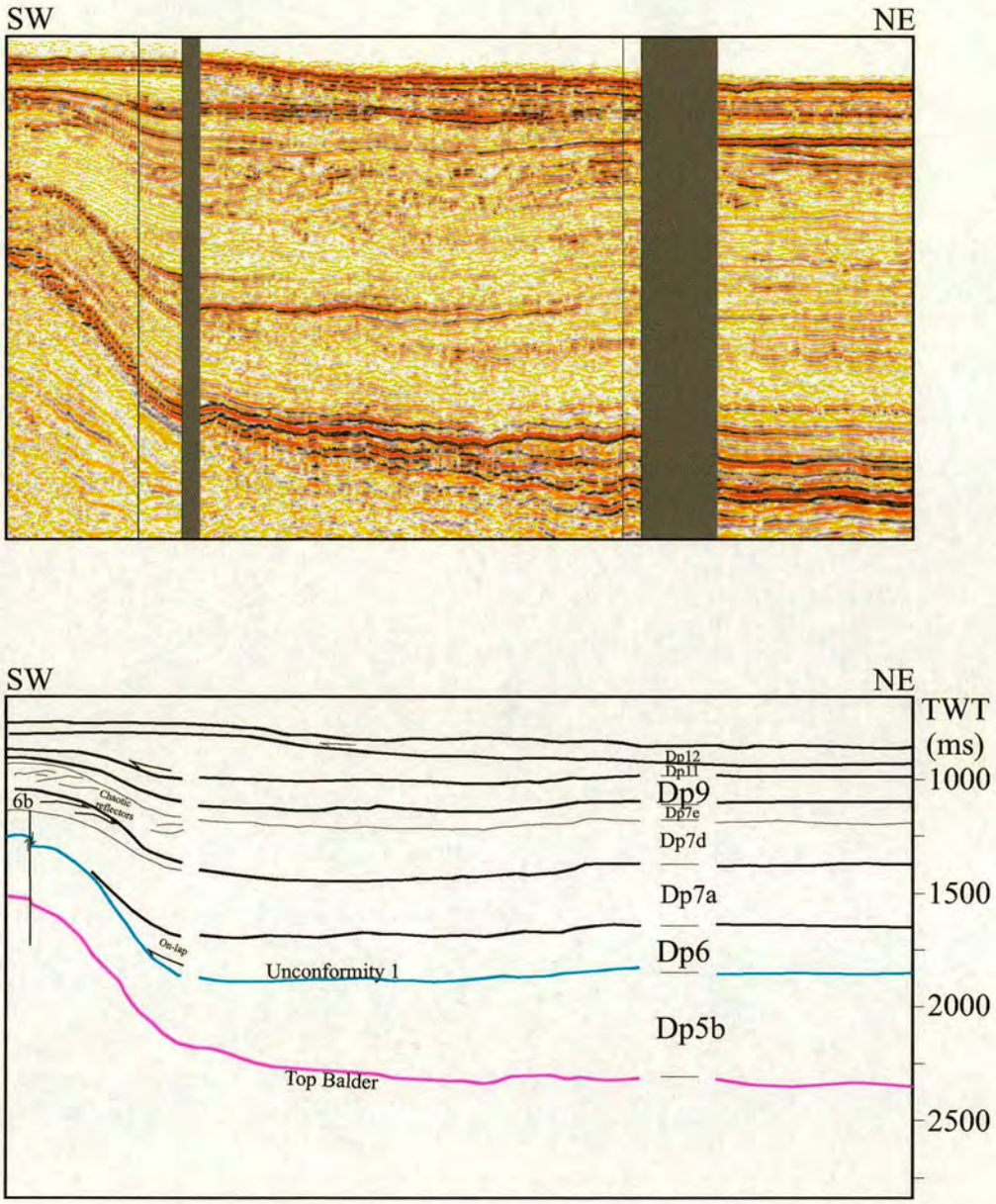

Figure 6.3b. Seismic profile of a representative seismic line showing the seismic character of depositional packages 5-12. The seismic section is an extension of Figure 6.3a. Location is shown on Fig. 6.1,B.

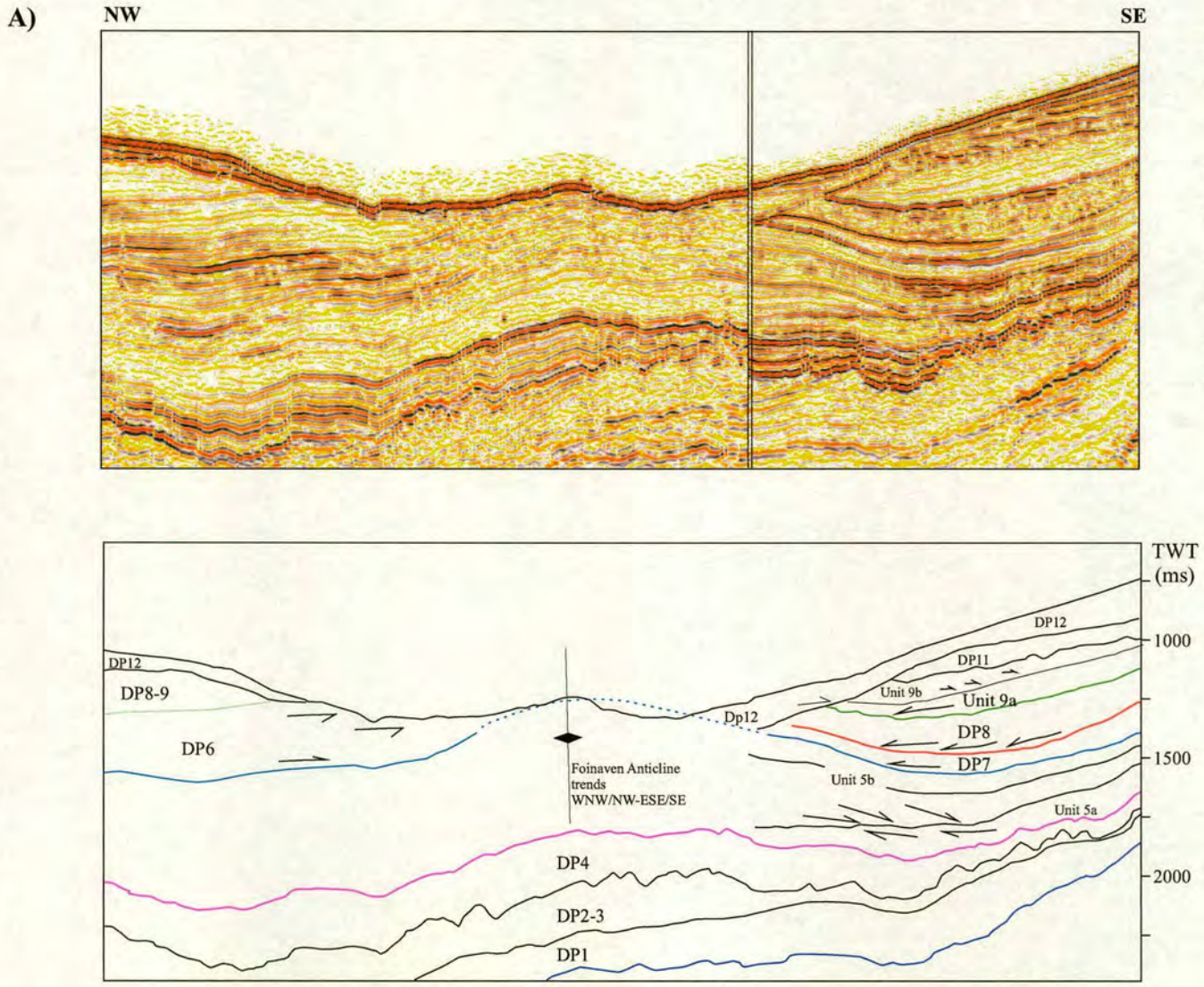

Figure 6.4a. Seismic profile showing the interpretation of depositional packages in the southwestern FSC over and around the Foinaven Anticline. Location of the seismic profile is shown on Fig. 6.1,B. Note asymmetry of units NW and SE of the Foinaven Anticline.

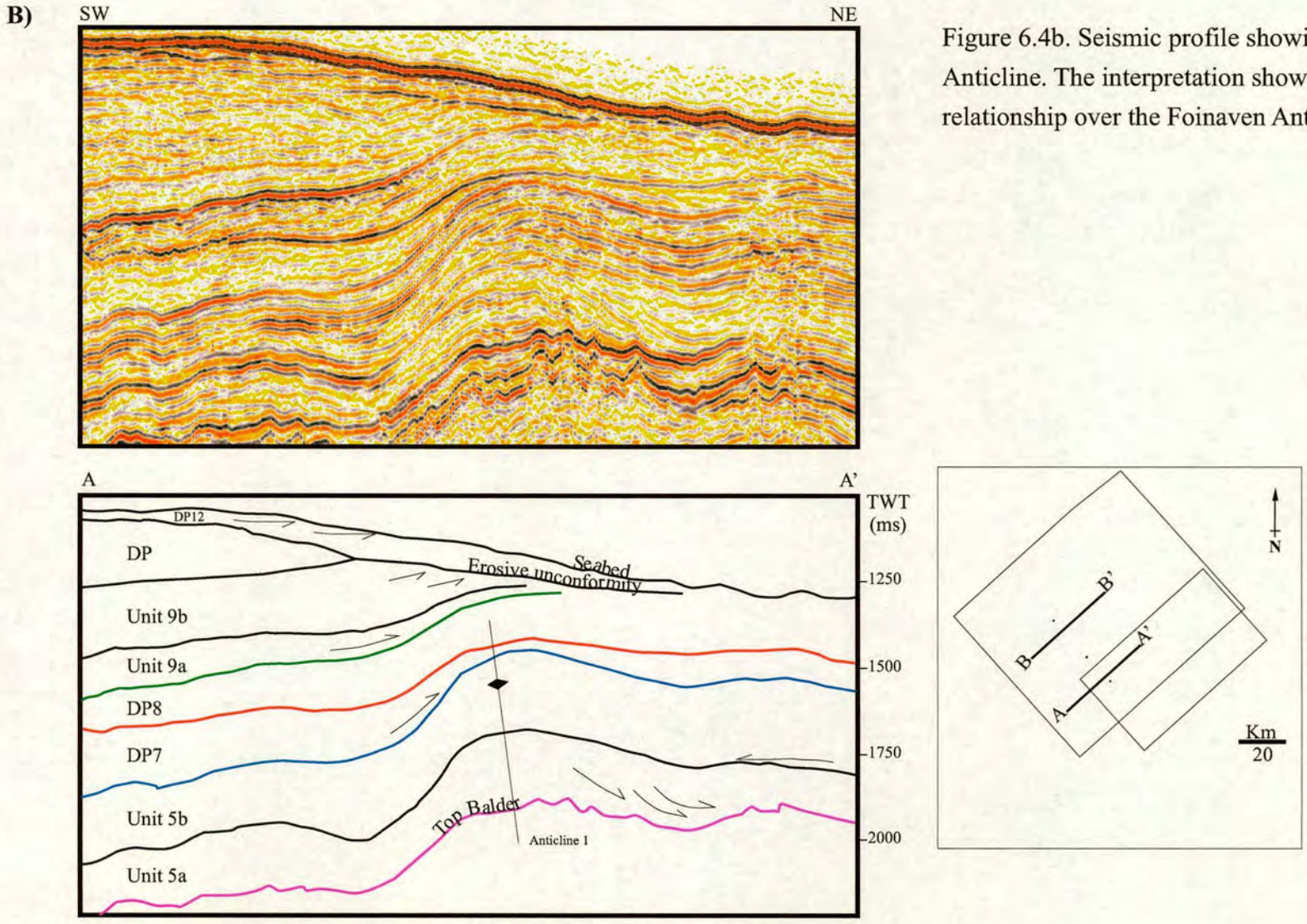

Figure 6.4b. Seismic profile showing the Foinaven Anticline. The interpretation shows thickness relationship over the Foinaven Anticline.

C)

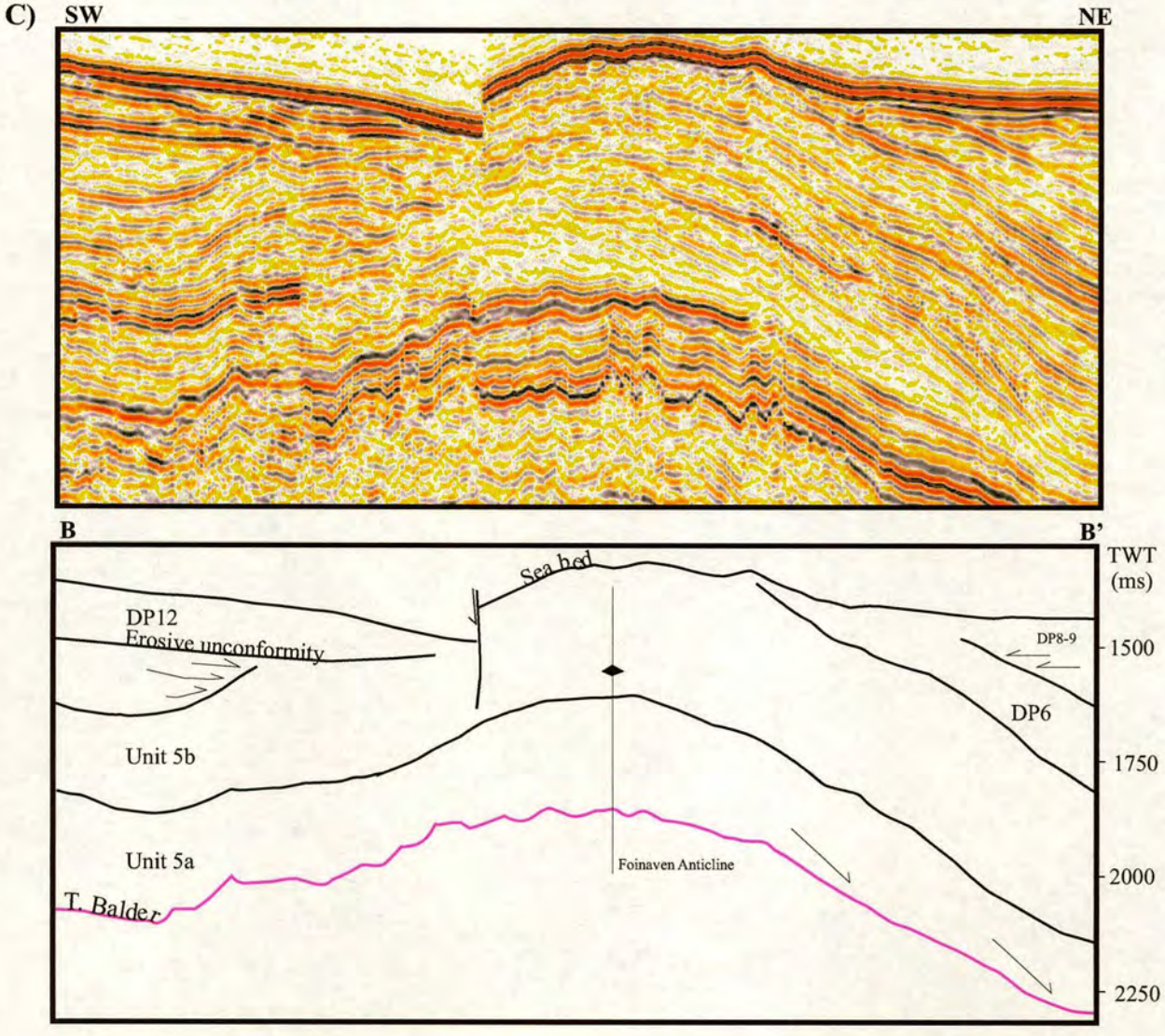
SW
NE
B
B'
Sea bed
DP12
Erosive unconformity
DP8-9
DP6
Unit 5b
Unit 5a
T. Balder
Foinaven Anticline
TWT
(ms)
1500
1750
2000
2250

In the north-western part of the FSC between the Mesozoic-East Faroe High and North Westray Ridge (in the East Faroe Graben; Corona Basin) (Fig. 6.1) a broader scale anticline is observed (hereafter called "Corona Anticline or shortened to CA) and correlates with Eocene-Miocene-age strata (Figs. 6.2b and 6.5). The Corona Anticline is elongate, 75 km long and 30 km wide, trending NE-SW, and is approximately perpendicular to the FA.

On the northwest margin of the southern and central part of the FSC, the basin bounding East Faroe High forms an anticlinal fold that has an ENE-WSE oriented fold axis (Boldreel and Andersen, 1998) (Fig. 6.5).

Sequence stratigraphic framework

In chapter five descriptions were made with references to depositional packages DP1-DP4. In this chapter the sequence of depositional packages is continued with description of depositional package DP5-DP12.

Depositional package 5 (DP5)

Depositional package 5 extends across the entire study area and in general has a relatively uniform thickness of ca. 300 m.sec. The base of DP5 is marked by a continuous, high amplitude reflector onto which overlying reflectors of DP5 downlap, whereas the top is marked by a continuous, moderate amplitude reflector onto which reflectors of the overlying packages (DP6 and DP7) onlap (Figs. 6.1 and 6.3a). Internally, DP5 can be subdivided into two units, Unit 5a and Unit 5b, on the basis of internal onlap reflector terminations (Figs. 6.3a and 6.4a).

Unit 5a:

Unit 5a has is present in the southern part of the FSC, between the Judd Platform and the South Westray Ridge extending to the northwest (Figs. 6.1,B and 6.6a). Unit 5a has a maximum thickness of ca.150 m.sec. in the south, and progressively thins and pinches out towards the northeast. Reflectors of Unit 5a downlap onto the basal surface, which is a flooding surface marking the top of the Balder Formation (54.5-54.04 Ma). Unit 5a is bounded above by a continuous, high- to low-amplitude

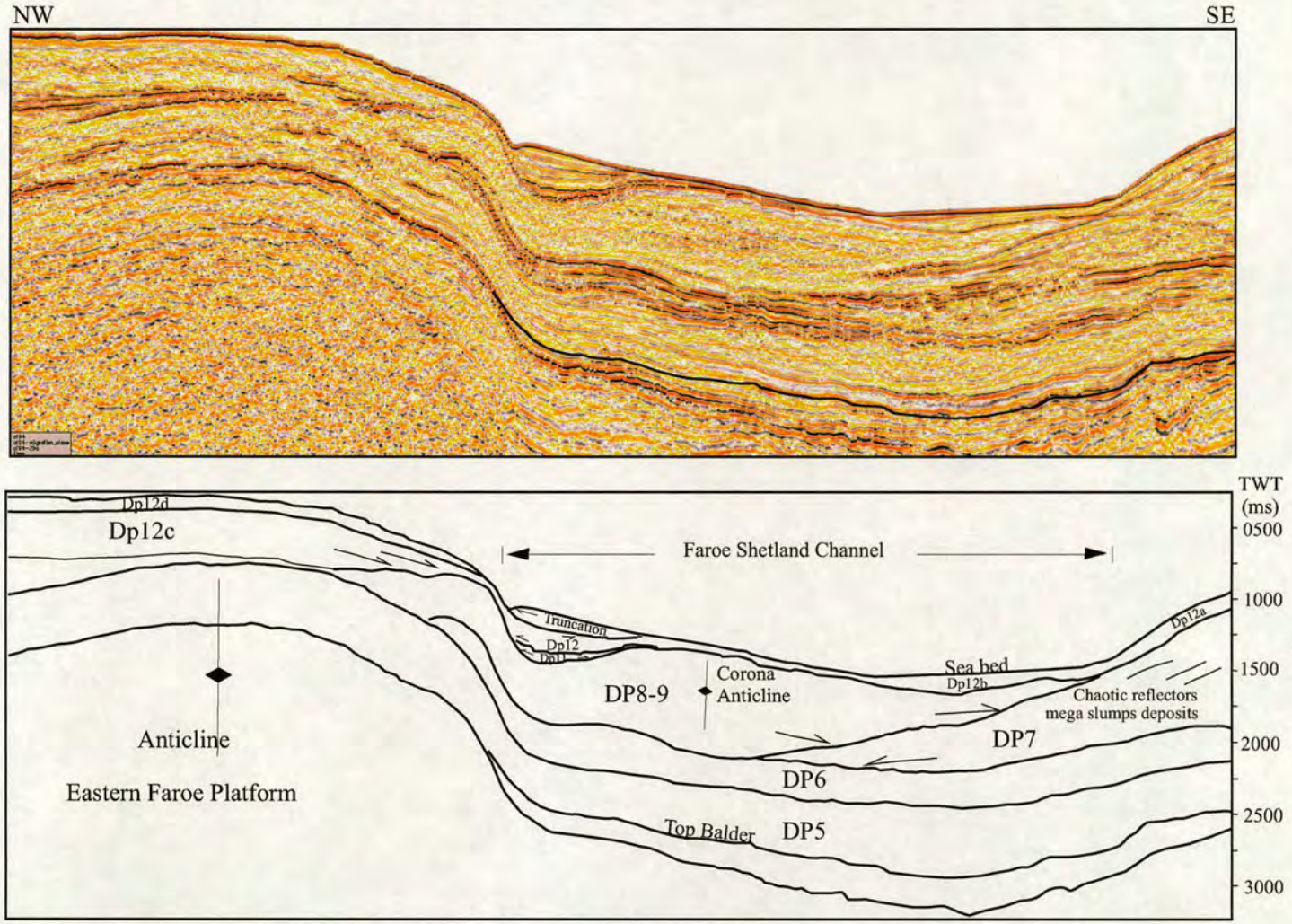

Figure 6.5. Seismic section showing the depositional packages and main structural features in the central part of the FSC and the eastern

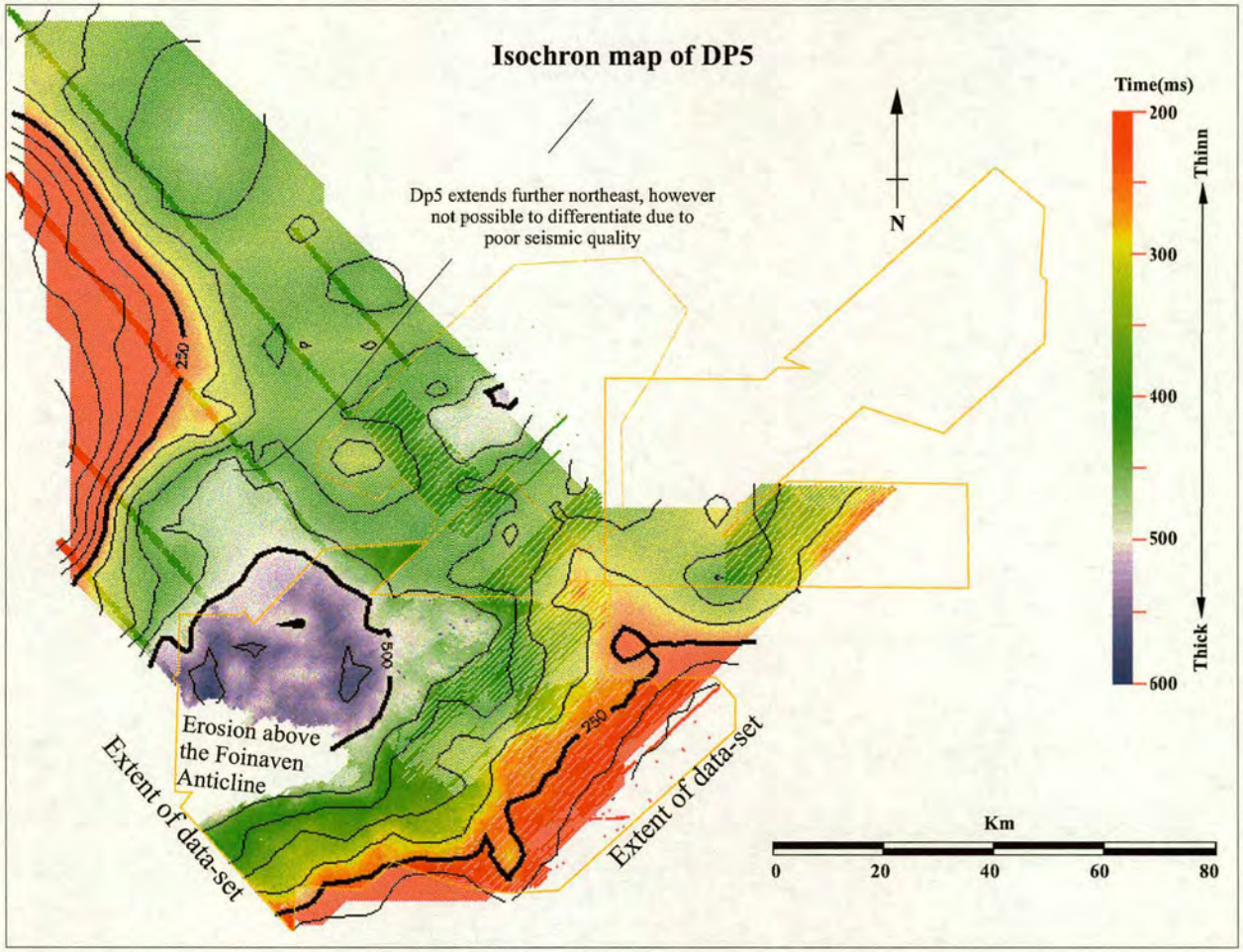

Figure 6.6a. Isochron map of DP5 showing the main depocentre occurring in the southwest area.

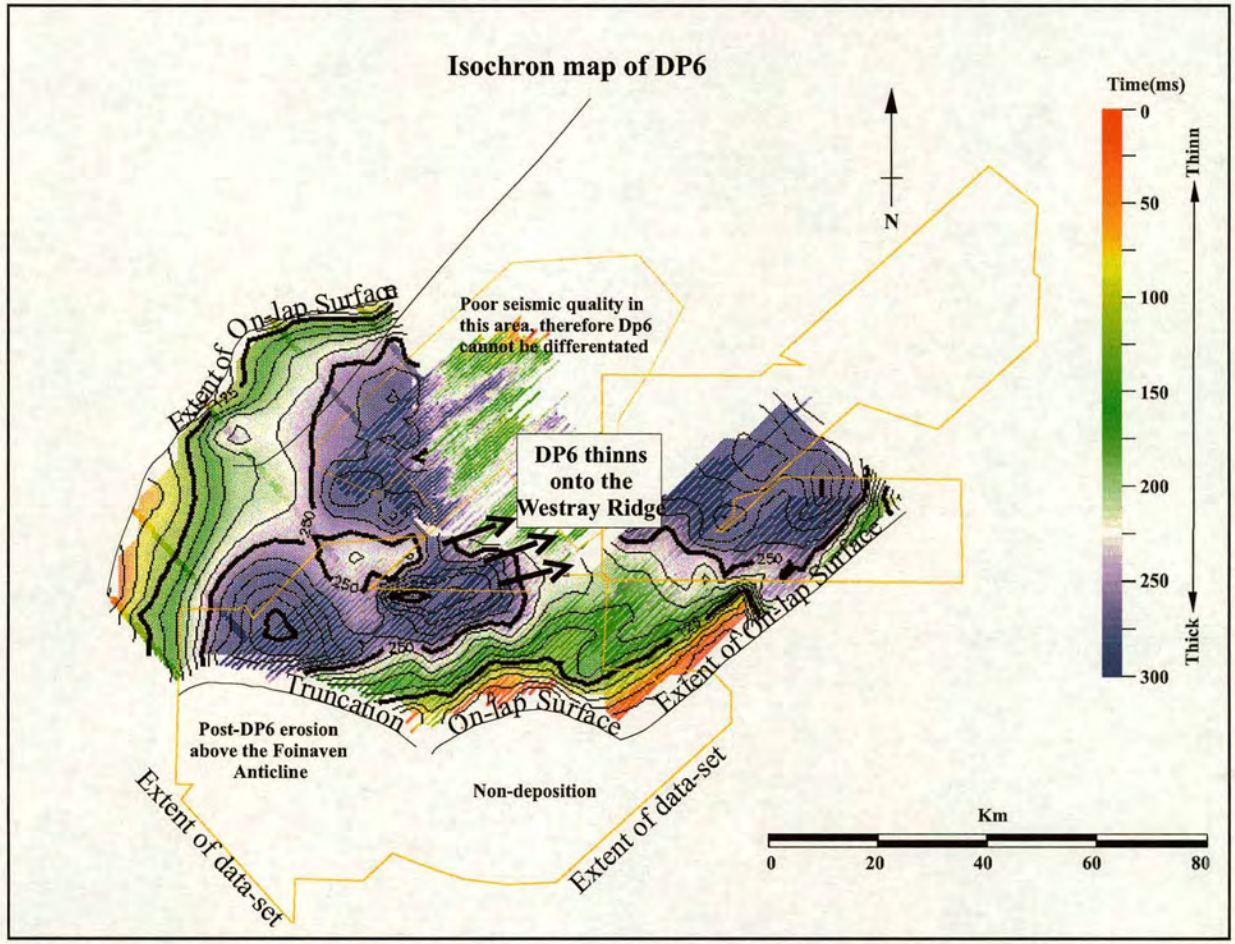

Figure 6.6b. Isochron map of DP6 showing the extent of deposition. Note that non-deposition/erosion occurs in the south, southwes and, northwest area of the FSC. Dp6 shows thinning over the South Westray ridge area (see`Fig. 4.5).

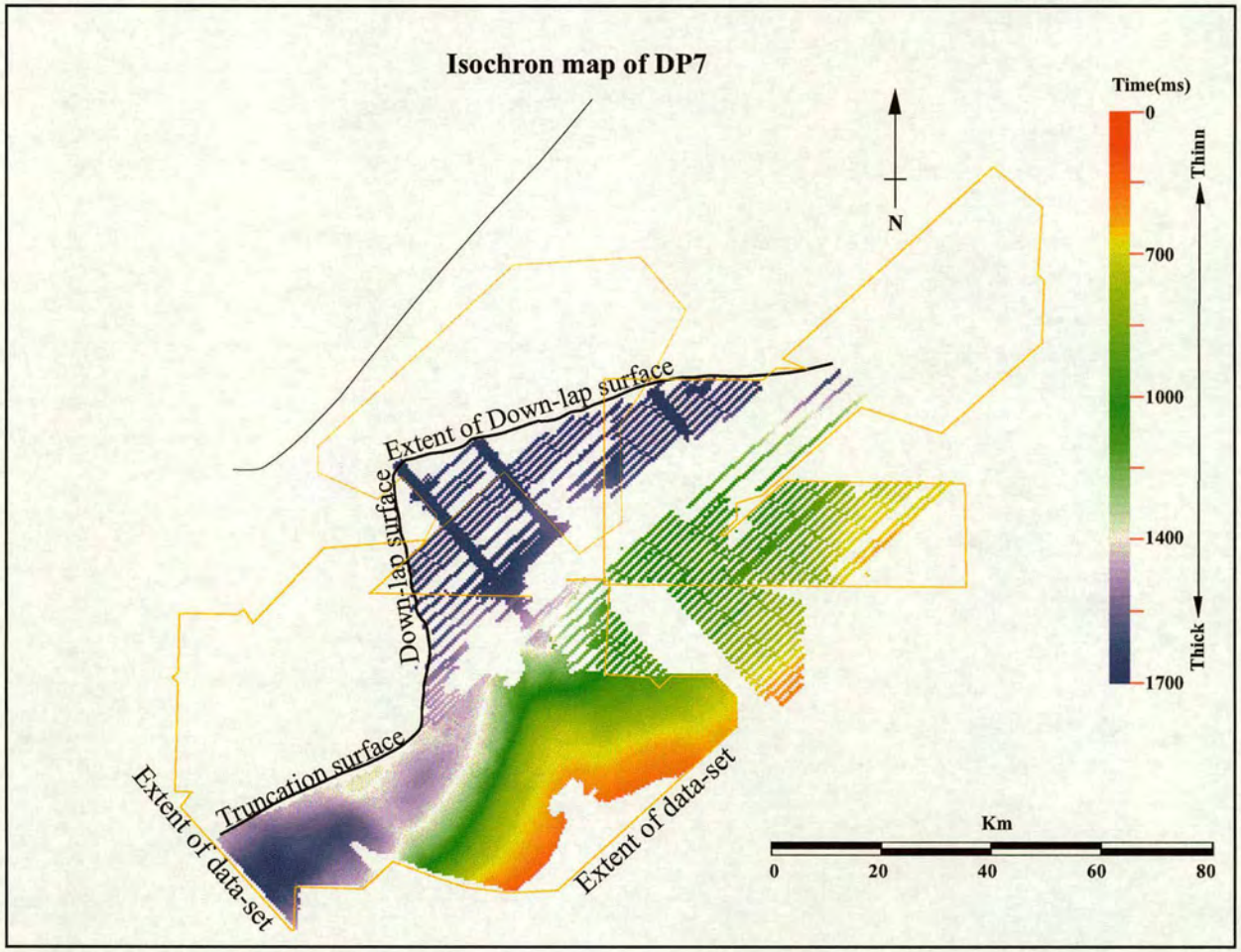

Figure 6.6c. Isopach map of DP7 showing the northwestern extent of the shelf-slope system.

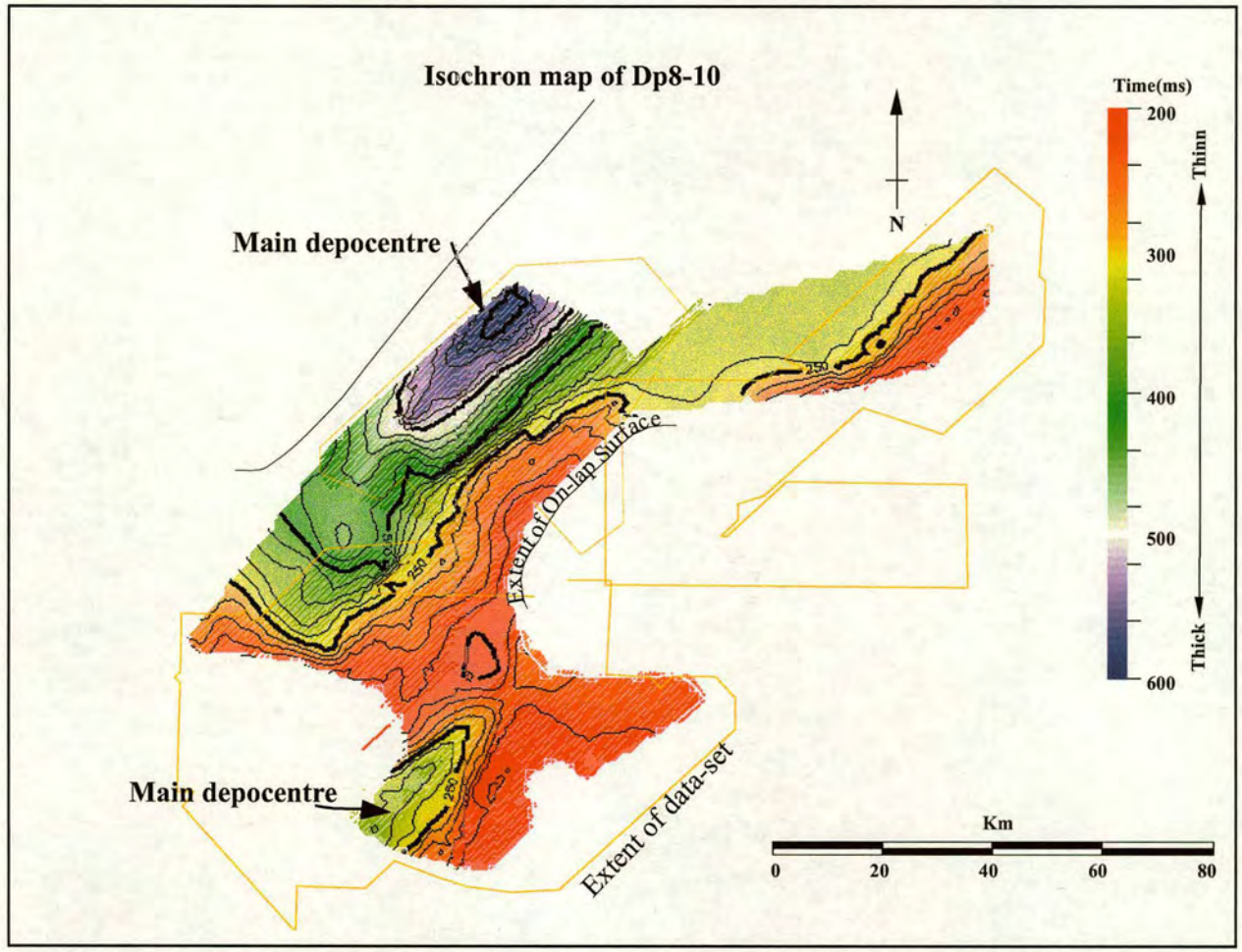

Figure 6.6d. Isochron map representing DP8-10 showing the main depocentres located in front of the underlying shelf-slope system (Dp7).

reflector (depending on location with respect to basin margin e.g. high amplitude reflector close to margin and low amplitude reflector basinwards) onto which reflectors of the overlying unit (Unit 5b) onlap. Internally unit 5a consists of a series of clinoform reflectors that dip to the northeast and have heights of up to ca. 125 m.sec. The clinoforms generally downlap and downstep towards the northeast with internal surfaces of toplap, truncation and onlap evident (Fig. 6.7).

The well data (all composite logs) indicate that Unit 5a was deposited during the Early Eocene. In general Unit 5a consists of one coarsening-upward depositional cycle (>ca. 100m thick), from claystone to sandstone, that is capped by lignite. This trend is clearly marked by the gamma ray trend (Fig. 6.8). More specifically, in the south-western area (wells 204/22-1 and 204/23-1) the unit consists of a 12 m-thick calcite and silica cemented silty claystone, that is overlain by a 110 m-thick argillaceous, very fine to fine grained sandstone containing mudstone interclasts towards the base and pebbles and calcite cement towards the top. The sandstone is finally capped by a 6 m-thick interval of lignite (well 204/22-1). In the northwest area (Well 6005/15-1z and 6004/16-1Z) the gamma ray log shows a relative low gamma ray cylindrical trend that is interpreted to represent sandstone, although the description of the cuttings was not available and thus it is not possible to confirm the exact lithologies present. In the northeast area, where the sequence is thinnest (i.e. in well 204/19-1), Unit 5a consists of a 5 m-thick carbonaceous, sub-bituminous claystone with an earthy texture.

Unit 5b:

Unit 5b has a thickness up to ca. 300 m.sec. and is developed across the entire survey. It is thus more extensive than the underlying Unit 5a. Unit 5b is thickest in the north and northeast and thins towards the southwest and west, opposite to the underlying Unit 5a, which when both units are combined gives a uniform thickness of DP5. The base of Unit 5b is marked by a continuous, high- to low-amplitude reflector that is onlapped- and downlapped by overlying reflectors. The reflectors onlap towards the southwest onto underlying Unit 5a, in the southern part of the FSC (Fig. 6.3a). The downlap reflectors however, dip towards the north and northeast

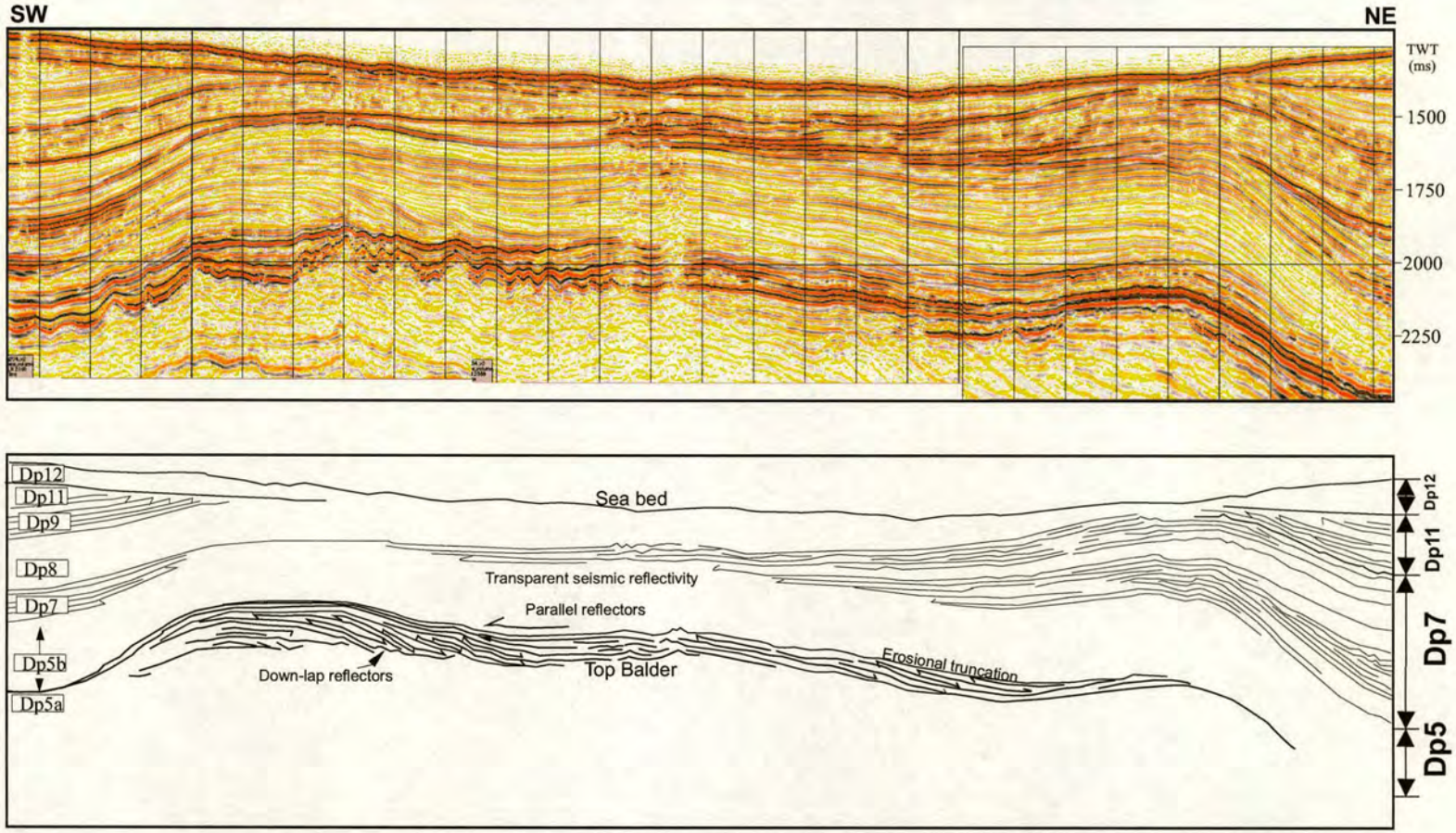

Figure 6.7. Seismic profile showing the internal downlap reflector characteristics of depositional package 5.

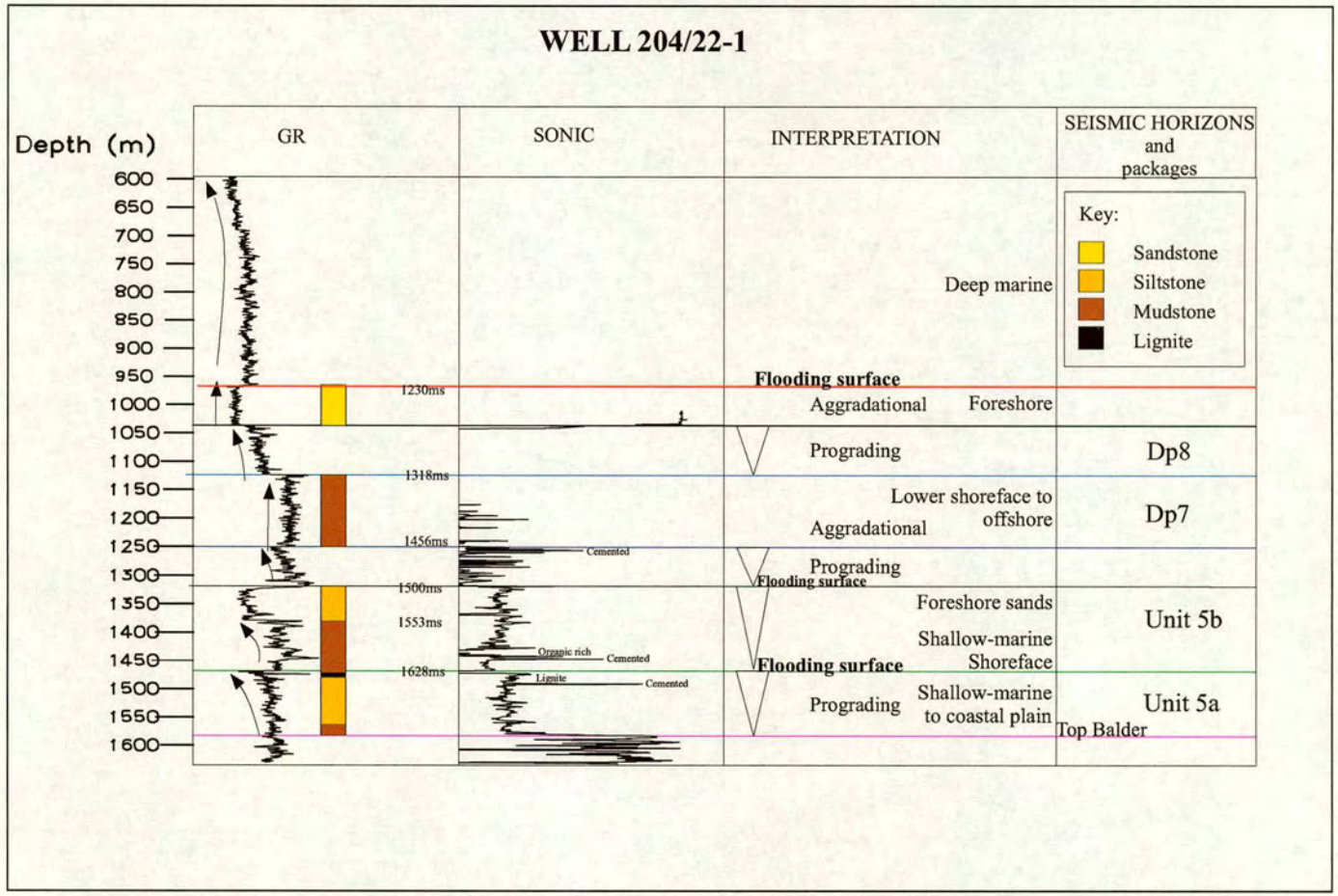

Figure 6.8. Composite log of the Eocene to Present-day succession and the interpretation of well 204/22-1.

onto the underlying Top Balder surface (Fig. 6.9). The top of Unit 5b is marked by a continuous, high amplitude reflector that is onlapped by overlying reflectors. Internally Unit 5b generally consists of parallel seismic reflectors, however, in the southern part of the FSC, the uppermost ca. 70 m.sec. interval of Unit 5b shows a distinctive uniform thickness interval that internally contains parallel seismic reflectors, but relative transparent reflectivity (Fig. 6.7).

The well data (all composite logs) indicates that Unit 5b was deposited during the Early Eocene. Unit 5b consists of, mudstone or siltstone that is interbedded with sandstone that can range from very fine to very coarse grained (well 204/22-1, well 204/19-5, well 204/19-1, 204/19-4, and 204/14-2). Glauconitic detritus and calcite cementation is common. The upper part of Unit 5b which is seismically transparent, has a box-shaped gamma-ray log trend and consists of a well-sorted sandstone that is predominantly medium grained but ranges from fine to granular (well 204/22-1; Fig. 6.8). Towards the northeast, Unit 5b has relatively constant gamma ray log values, and consists of a sandy siltstone containing glauconitic detritus and calcite cementation (well 204/14-2). The sandstone interval in the upper section corresponds with the seismic uniform thickness interval that internally contains transparent seismic reflectors.

Depositional package 6 (DP6)

Depositional Package 6 is up to ca. 350 m.sec. in thickness and is developed from the margin of the FSC in the northwest to the south Westray Ridge and Rona/Clair Ridge in the southeast (Fig 6.1, B). It is less extensive than underlying depositional package (DP5). In the south-western part of the FSC where it is thickest DP6 is truncated at the seabed (Foinaven Anticline) and gradually thins eastwards over the underlying Mesozoic North Westray Ridge (Figs. 6.1, 6.6b and 6.9). Depositional package 6 is absent in the southern part of the FSC.

The base of DP6 (Unconformity 1) is marked by continuous, high amplitude reflector that shows overlying prominent onlap reflectors, whilst the top of DP6 is a continuous, high-moderate amplitude reflectors that contains conformable reflectors of the overlying depositional package (DP7; Fig. 6.3a). The internal onlap reflectors

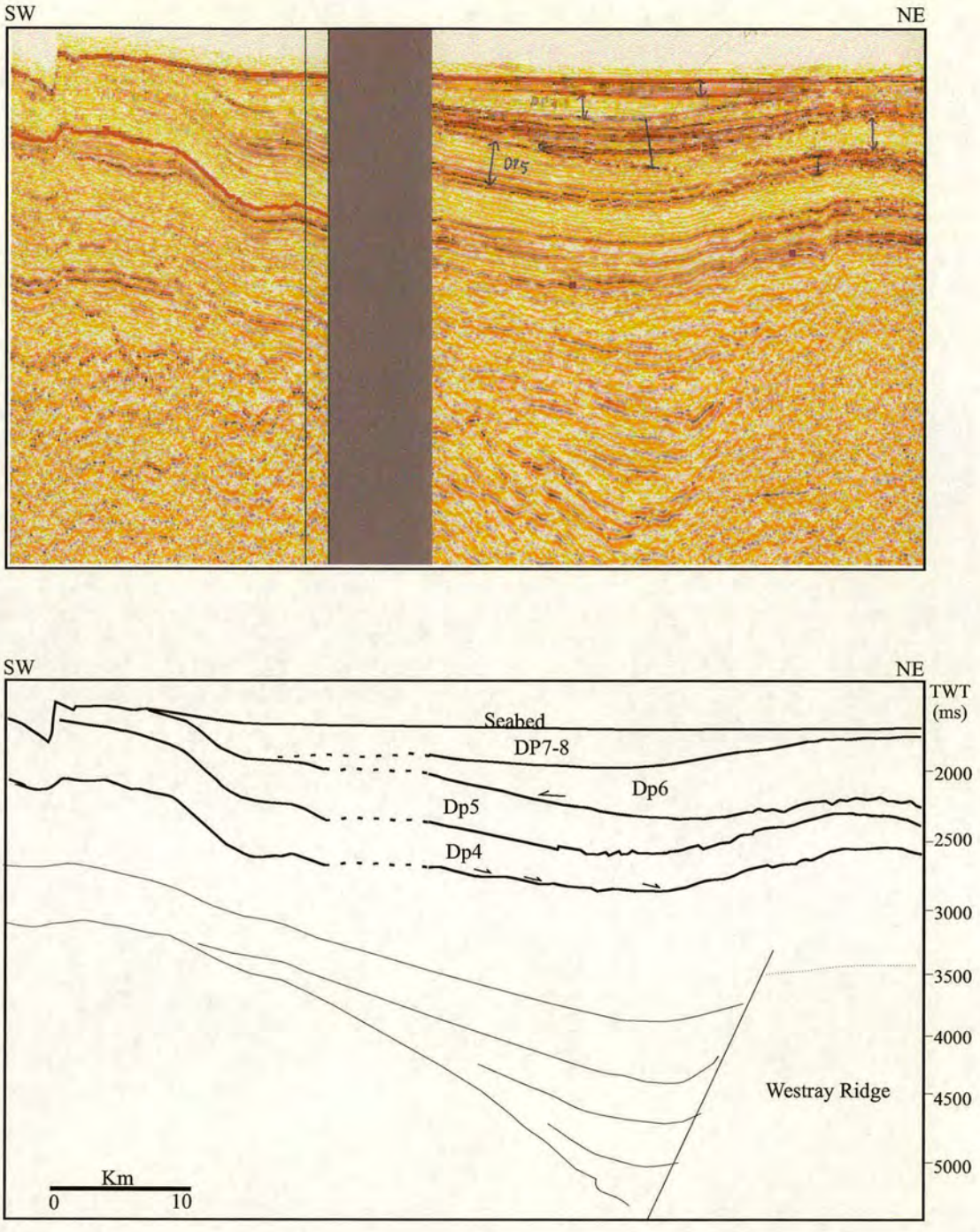

Figure 6.9. Seismic profile to showing the geometry and seismic characteristics of DP5-DP10. DP5 consists of downlap reflectors of DP5. DP6 shows gradual thickening of package towards the southwest (see Fig. 6.6a and Fig. 4.5). DP7 downlaps onto DP6. DP8-10 is truncated beneath seabed in the southwest. DP5 and DP6 are also truncated beneath the seabed in the southwest. Location of the seismic profile is shown on Fig. 6.1b.

characterise onlap both towards the northwest onto the East Faroe High (Fig. 6.5) and also towards the south onto the Foinaven Monocline overlying the Mesozoic South Westray Ridge (Fig. 6.3a). Depositional package 6 onlaps are also observed in the central part of the FSC north of the Mesozoic Rona/Clair Ridge (Figs. 6.1 and 6.10). Depositional package 6 thins in the direction of the onlaps. Internally, DP6 consists of parallel reflectors of variable amplitude reflectivity/strength (Fig. 6.5). Well data indicate that DP6 is Eocene in age. Unconformity 1, separating DP5 from DP6 or DP7 is most pronounced on the western limb of the Foinaven Monocline in the southern part of the FSC, where it divides DP5 from DP7 (Fig. 6.3a). The basal unconformity ties with a very high gamma ray value in the wells (e.g. well 204/22-1) representing a cemented surface (Fig. 6.8). Biostratigraphic data (microfauna and -flora) from BGS core 99/3 taken across Unconformity 1 (Fig. 6.11a-b) indicates a Middle Eocene age (early-mid Lutetian). The cored samples taken immediately above the seismic unconformity (Unconformity 1) contained reworked microfauna of various ages from Early Eocene age to Carboniferous and Triassic-Cretaceous ages.

Depositional package 7 (DP7)

Depositional Package 7 (DP7) varies in thickness from < ca. 100 m.sec. up to ca. 750 m.sec. and is developed along the south-eastern length of the FSC (Figs. 6.1, B and 6.6c). In the southwest, DP6 is truncated near the seabed (Fig. 6.4a). DP7 is up ca. 750 m.sec. thick and thins and pinches out mainly towards the north having a wedge-shaped geometry. Isochron map (Fig. 6.6c) shows that in the western area of its extent, the trend of the DP7 wedge (shelf-slope edge) is SSW-NNE but turns W-E over the underlying South Westray Ridge. Depositional package 7 is bounded by a continuous, high amplitude reflector with overlying downlapping reflectors and above by a continuous, high amplitude reflector onto which the overlying reflectors of DP8 and DP9 onlap (Fig. 6.12). Internally, DP7 contains high amplitude and continuity reflections showing onlap, downlap and sigmoid clinoform geometries that dip to the north and have heights of up to ca. 250-300 m.sec. (Fig. 6.12). The depositional package can be subdivided into at least six units (units 7a-7f), based on reflector terminations and seismic facies characteristics (Fig. 6.12). In addition, the

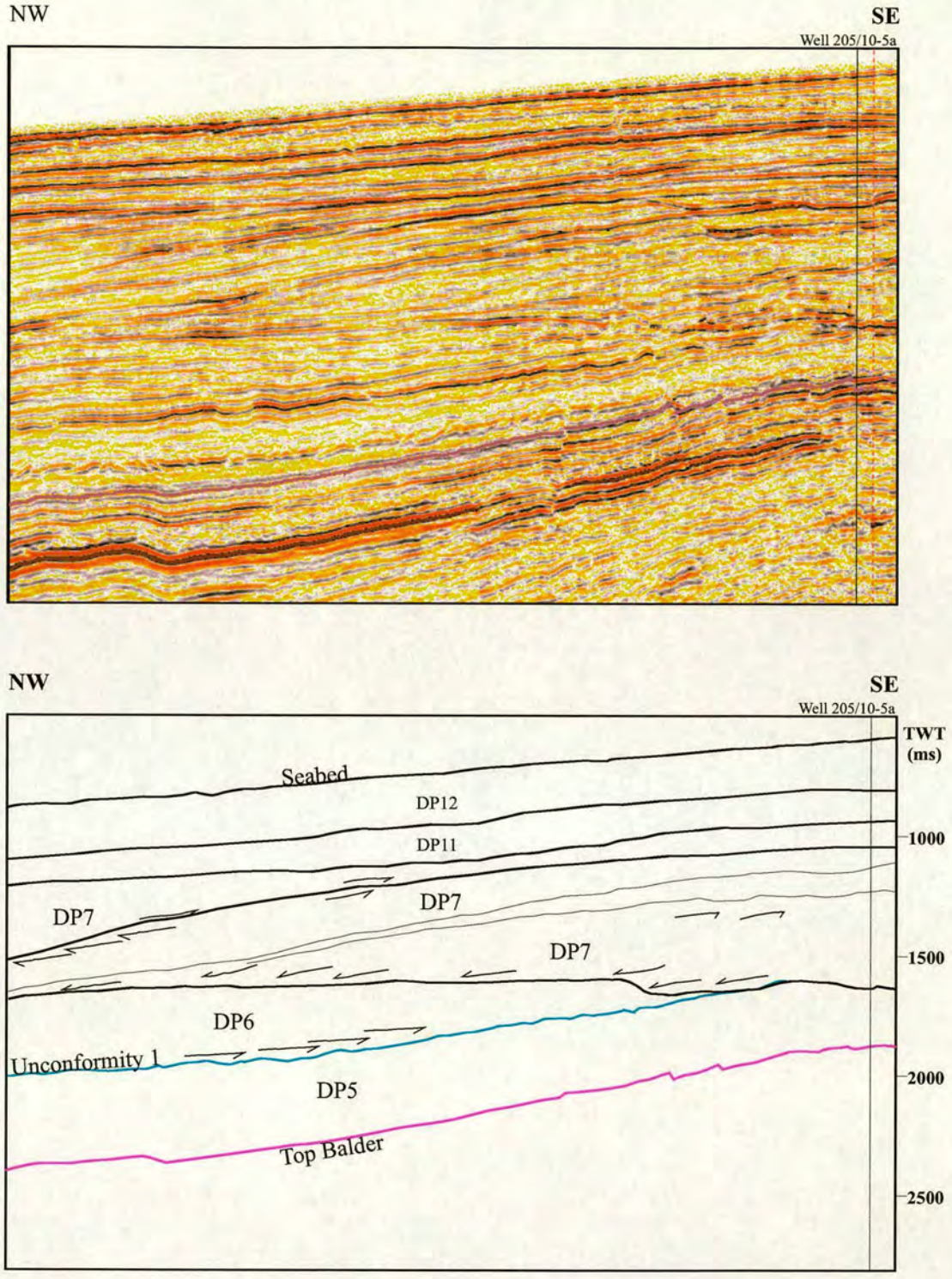

Figure 6.10. Seismic line to show the geometry and seismic characteristics of DP5-DP7 in the southeastern part of the central FSC. Location of the seismic line is shown on Fig. 6.1b.

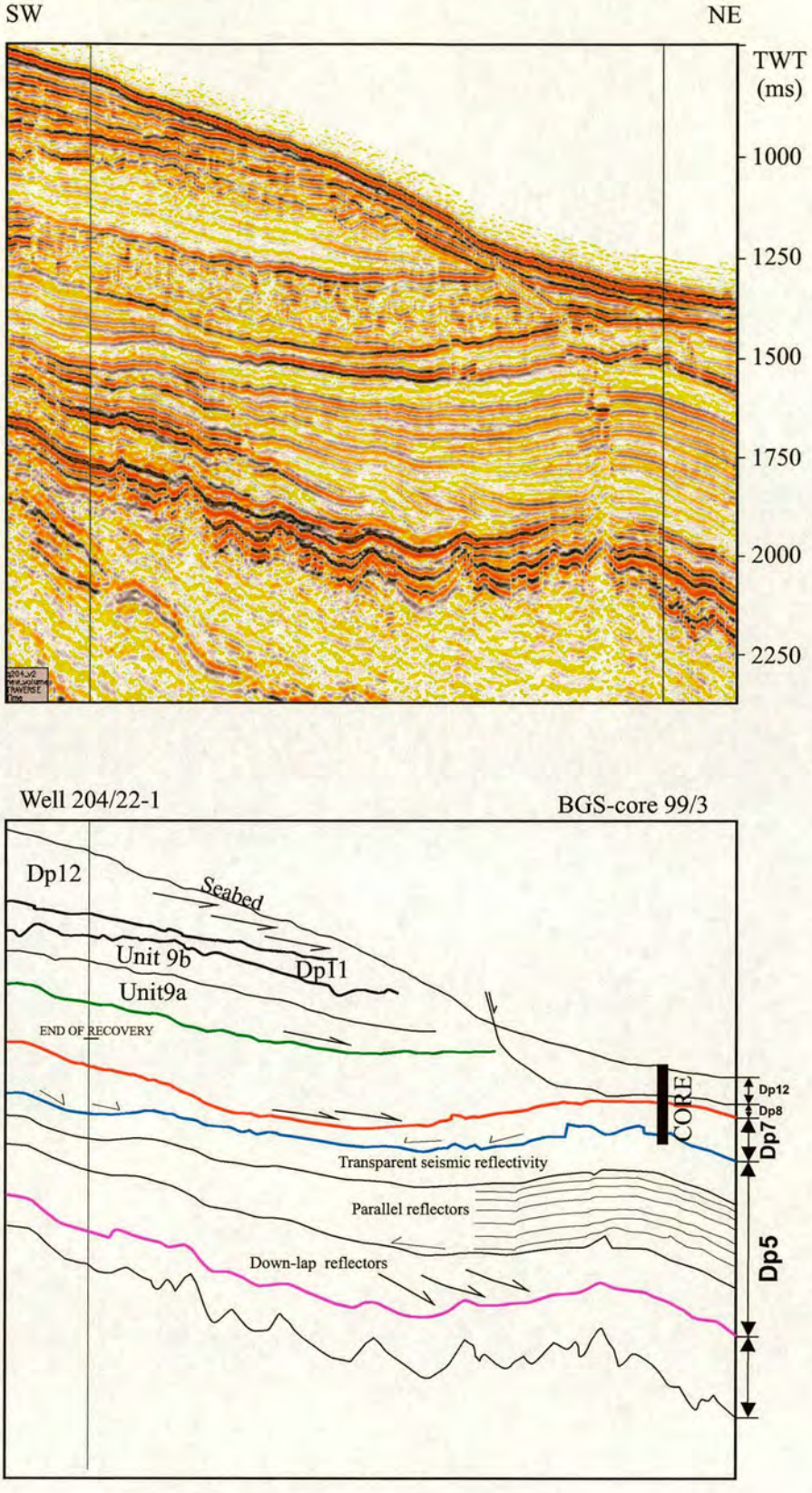

Figure 6.11a. Correlation between BGS-core 99/3 and well 204/22-1. See composite log of well 204/22-1 (Fig. 6.8) and core descriptions (Fig. 6.11b).

	Unit	Age	Palynology	Core interval	Comments	Environment
Dp8		Late Eocene	Microfauna: Foraminifera (*Uvigerina germanica*) Radiolaria	56.91-62.92m	Sample at 56.91 Allochthonous The foraminifera are fragments of the Eocene marker "Rhabdammina"	Reworking
Depositional package 7	Units 7a-7f	Middle Eocene	Microfauna: Foraminifera (diverse) Ostracods and Radiolaria Diatom (sparse)	82.4-146.6m	All microfaunal evidence consistent with a M. Eocene age Diatom: early-mid Lutetian age (sample at 134.54) Low diversity fauna in sample 134.54 above unconformity	Proximal marine setting.
	Basal surface	Middle Eocene Early-mid Lutetian	Microfauna: Foraminifera and Ostracods Microflora: Reworked Spores and Pollen	146.6m-? beyond TD (166m) of core	Spores: Carboniferous age Pollen: Jurassic-Cretaceous age (sample at 158.63) Diverse micro-fauna aged E. Eocene (samples at 158.63 and 146.6)	Reworking

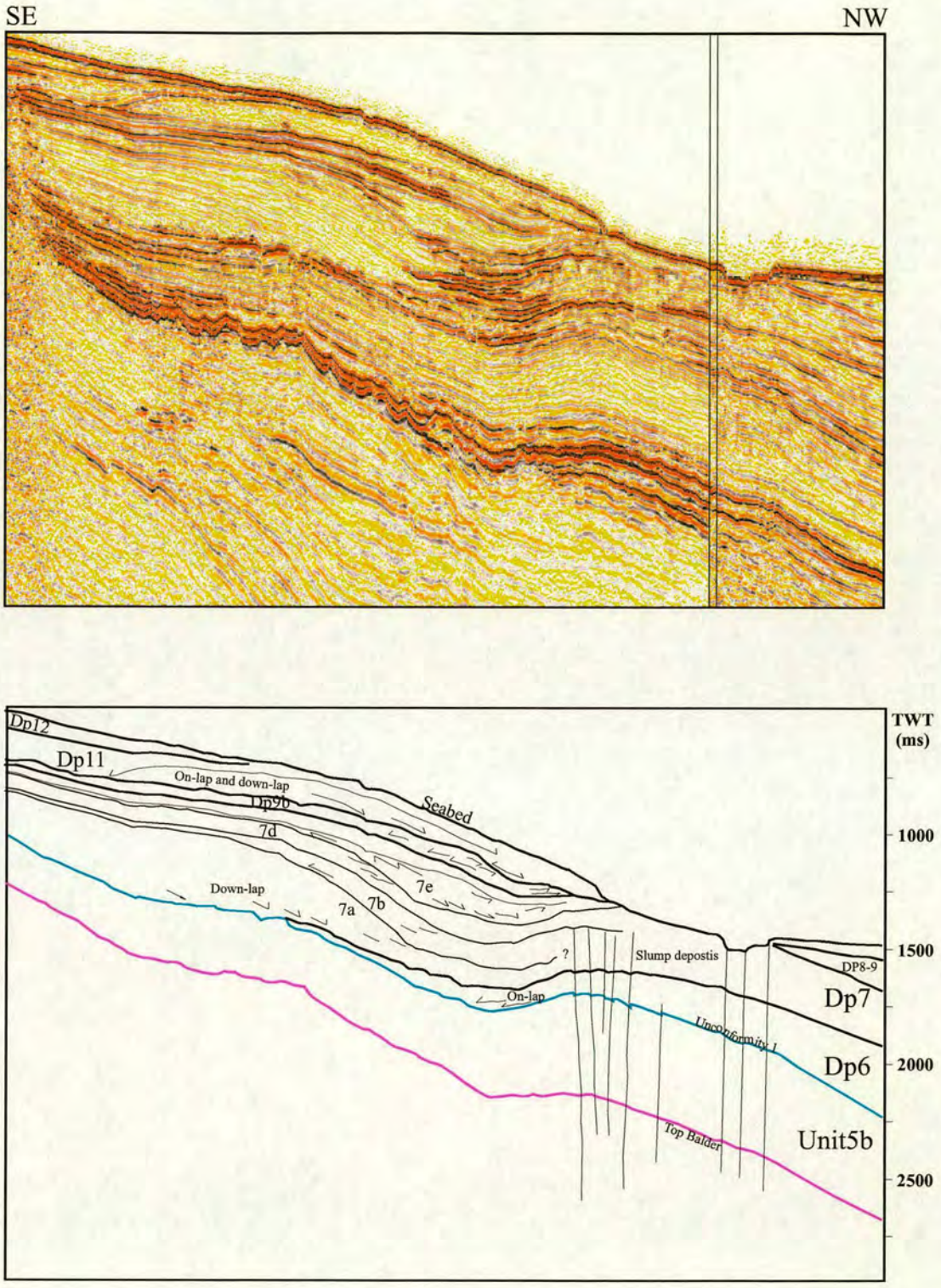

Figure 6.12. Seismic profile showing clinoform reflectors and wedge-shaped geometry of DP7. The downlapping reflectors indicate progradation mainly towards the NW.

depositional package forms a lens that internally consists of chaotic reflectors and is elongated east-west (Fig. 6.5).

Over Foinaven Anticline, in the south-western part of the FSC DP6 is characterised by onlap towards the northeast and southwest and thinning onto the anticline (Fig. 6.4b).

Unit7a:

Unit 7a extends across the southern and central part of the FSC and generally has an uneven thickness varying from ca. 0-300 m.sec. (Figs. 6.3a and 6.12). Unit 7a shows downlapping reflectors onto the basal surface, whilst it is bounded above by a surface onto which the overlying unit (Unit 7b) downlaps. Internally unit 7a contains sigmoidal clinoform reflectors, consisting of topsets, foresets and bottomsets (Fig. 6.12). Unit 7a onlaps towards the west and gradually thins onto the Foinaven Monocline (Fig. 6.3a). In the southwest area of FSC Unit 7a onlaps and gradually thins onto Foinaven Anticline (Fig. 6.4b). Well data (biostratigraphic and lithostratigraphic) indicates that Unit 7a contains sediments that are Middle Eocene in age (e.g. well 204/22-1) and consists of very silty to very sandy mudstone containing abundant glauconitic detritus and mica. The gamma ray log generally shows an irregular trend (Fig. 6.3). Core data (BGS core 99/3) from Unit 7a show that the sediments contain reworked microfauna that is overlain by a low diversity interval. The cored samples from DP7 show that all the samples contained abundant organic residues, predominantly plant tissue and wood fragments (Fig. 6.11b).

Unit 7b:

Unit 7b is up to ca. 200 m.sec. in thickness and is present only locally in the southern part of the FSB between the Judd high and the South Westray Ridge. The base of Unit 7b is marked by a surface onto which reflectors on-and/or down-lap towards the west and north (Figs. 6.3a and 6.12). The top of Unit 7b is marked by toplap surface of truncation beneath the overlying unit (Unit 7d). The downlapping reflectors of Unit 7b and the unit in general is situated further north than Unit 7a below (Fig. 6.12).

Unit 7c:

Unit 7c is up to ca. 240 m.sec. thick and only locally preserved in the southern part of the FSB. The base of the sequence is bounded by a surface onto which reflectors downlap. The top is marked by toplap and also truncation beneath the overlying unit (Unit 7d). Internally the seismic reflectors have sigmoidal clinoform reflectors that dip towards the northwest-north (Figs. 6.3a and 6.12). Although less extensive, Unit 7c shows similar characteristics as the underlying Unit 7b and 7a. The downlapping reflectors of Unit 7c and the unit in general is situated further north than Unit 7b below.

Unit 7d:

Unit 7d is up to ca. 200 m.sec. thick and extends from southwest to northeast above the flexure and eastern limb of the Foinaven Monocline (Fig. 6.3a-b) and thus is more extensive than underlying Unit 7b and and 7c. The base of Unit 7d is marked by a surface onto which reflectors onlap (the onlap reflectors are sometimes obscured due to lack of coherent reflections), with onlap occurring towards the west. In the south area over the flexure of the Foinaven Monocline the base of Unit 7d is marked by an irregular seismic surface that has up to 20 m.sec. relief. An isochron map from this particular area indicates that the irregular pattern represent small scale (15 m.sec.) incised channels trending NW (Fig. 6.13). The top of Unit 7d is marked by a surface onto which reflectors of overlying unit (Unit 7e) onlap. Internally, Unit 7d is characterised by a chaotic-fill facies pattern of discordant to wavy sub-parallel reflections (Figs. 6.3a and 6.12). Unit 7d is thickest east of the inclined north-south trending axis of the Foinaven Monocline (Figs. 6.3a-b and 6.13). The downlapping reflectors of Unit 7d and the unit in general is situated further north than Unit 7c below (Fig. 6.12).

Unit 7e:

Unit 7e is up to ca. 100 m.sec. thick and is present in the central and locally in the southern part of the FSB. The base of Unit 7e is marked by a surface onto which

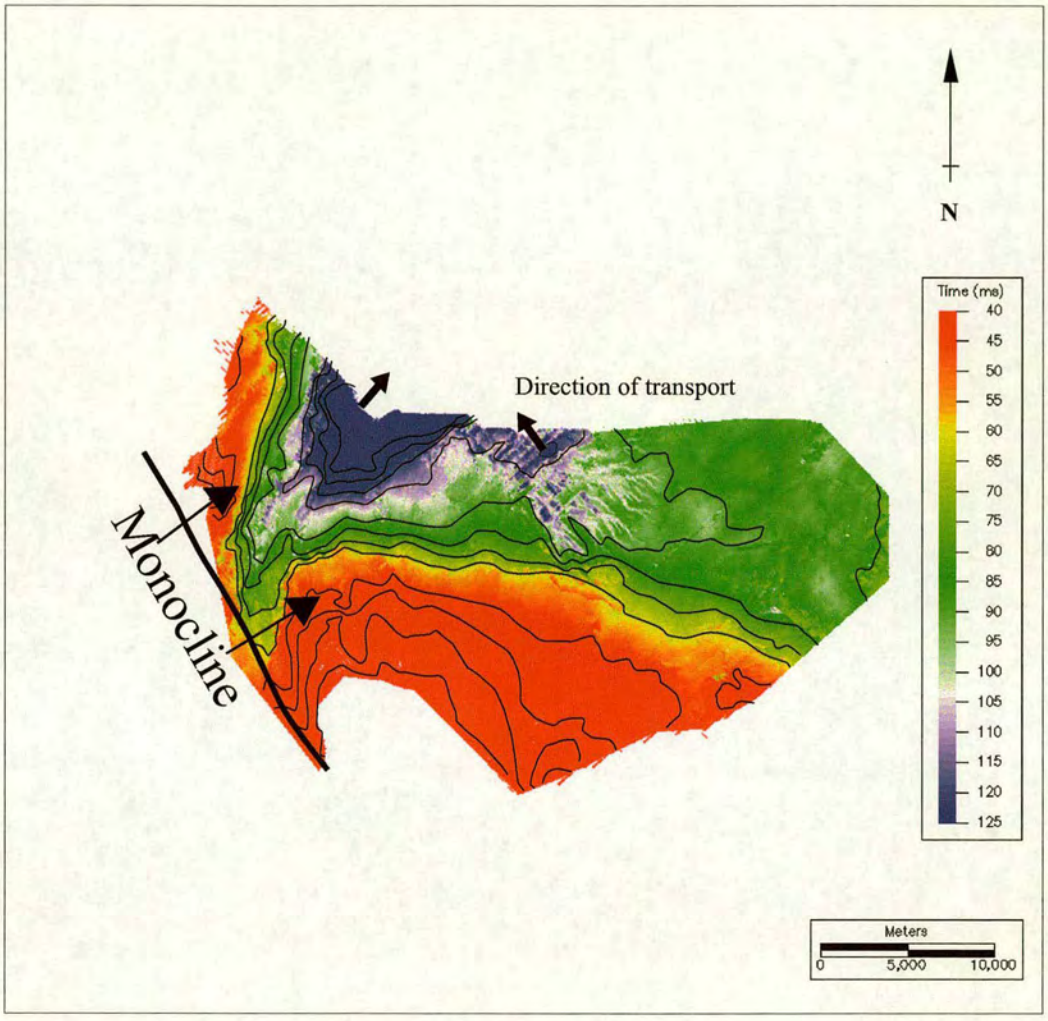

Figure 6.13. Isochron map of Unit 7d in the southern FSC. Location of this map is shown on Fig. 6.2.

reflectors downlap and onlap, whilst the top is marked by a surface onto which reflectors of the overlying depositional package (DP9) onlap and downlap. Internally Unit 7e consists of a set of clinoform reflectors that show a downward shift in onlap so that the reflectors onlap onto underlying foresets of unit 7d, indicating that during deposition of Unit 7e the wedge has progressed further north (Figs. 6.3a and 6.12).

Unit 7f

Unit 7f is up to ca. 50 m.sec. and is present locally in the southern part of the FSB. The base of Unit 7e is marked by a surface that shows truncation of underlying reflectors (Unit 7e). The top of Unit 7f is a surface onto which reflectors of overlying depositional package (DP9) onlap. Internally, Unit 7f is too thin to resolve the seismic pattern (Figs. 6.3a and 6.12).

Depositional package 8-10 (DP8-10)

Depositional Package 8-10 can only be split into three distinct depositional packages; two (DP8 and DP9) are present in the southern part of the FSC, and locally three packages in the central part of the FSC whereof only the third package (DP10) can be differentiated and thus these packages have been described as a composite depositional package (DP8-10). Each package is separates by high amplitude continuous reflectors. Depositional Package 8-10 extends along the length of the main part of the central FSC, where it is up to ca. 1000 m.sec. thick (Figs. 6.5 and 6.6d). It is also locally present in the southern part of the FSC between the Judd Platform and the South Westray Ridge, where it is up to ca. 300 m.sec. thick (Fig. 6.1, B). The base of DP8-10 is marked by a surface onto which reflectors onlap/downlap towards the southeast onto the underlying DP7 wedge, and also towards the northwest (the East Faroe High) onto underlying DP5 (Fig. 6.5). The top of DP8-10 is marked by high amplitude, irregular reflector, with shows underlying truncation and overlying onlap (Fig. 6.5). In general DP8-10 shows varied seismic character consisting of discordant, wavy to sub-parallel, and semi-chaotic-fill patterns of dominantly low amplitude reflectivity (Fig. 6.5). Furthermore, DP8-10 often contains small-scale displacement faults that terminate downwards within the

depositional package (Fig. 6.5; cf. Andersen et al. 2000). Well 204/22 and BGS core 99/3 indicates a Late Eocene-lower Oligocene age for the sediments deposited within DP8. DP8-10 is equivalent to "DPC-B.4" by Andersen et al. 2000 that is dated as early Oligocene. Whereas DP10 appears to be equivalent to package "FPC-C" of Andersen et al. (2000) and package "C2" of Davis et al. (2004) where top C2 has confidently been dated from biostratigraphy (well 214/4-1) to be Middle Miocene in age. Thus DP8-10 is Late Eocene-Middle Miocene in age.

Depositional Package 8

Within the southern part of the FSC depositional Package 8 has a uniform thickness of ca. 150 m.sec. (Figs.6.3a and 6.4b). Internally, DP8 consists of high amplitude sub-parallel reflectors that are often discordant and wavy (Fig. 6.3a).

Well data from 204/22-1 indicate that DP8 consists of moderately sorted sandstones that range from medium to granular in grain size, and contains glauconitic detritus, together with igneous rock fragments and occasional shells. The gamma ray log shows a coarsening-up interval that is overlain by a box-shaped trend (well 204/22-1; Fig. 6.8).

Depositional package 9

Within the southern part of the FSC, DP9 is ca. 150m.sec. thick (Fig.6.3a). Depositional package 9 can be subdivided into two units in the south-western part of the FSC based on reflector termination and seismic facies character. The two units are separated by a surface onto which reflectors onlap (Fig. 6.4a).

Unit 9a is up to ca. 70 m.sec. thick, contains parallel internal reflectors, that onlap/downlap towards the northwest and Foinaven Anticline. Unit 9a correspondingly thins towards Foinaven Anticline (Figs. 6.4a, 6.6c and 6.11a).

Unit 9b contains reflectors that onlap towards the south-east away from Foinaven Anticline. This thinning is opposite to that seen for Unit 9a. In the east reflectors of Unit 9b onlap onto DP7. Internally Unit 9b contains wavy parallel reflectors (Figs. 6.4a, 6.6d and 6.11a).

Depositional package 10 (DP10)

Depositional package10 (DP10) is up to ca. 200 m.sec. thick and is present in the north-western part of the FSC, where it is part of the uppermost section of DP8-10. DP10 can only be observed on one 2D-line (of94-43; Fig. 6.14) that is outside the extent of the 3D survey (Fig. 6.1). The base of DP10 lays conformably on top of DP8-9 whilst the top is marked by prominent high amplitude reflector, that shows underlying truncation and overlying onlap reflectors (Fig. 6.14). Internally DP10 generally consists of very low amplitude reflectivity.

Depositional package 11 (DP11)

Depositional package 11 consists of two units, Unit 11a and Unit 11b, that are equivalent to two components of a composite system interpreted by Stoker (2002) that was dated to a Miocene age.

Unit 11a:

Unit 11a is up to ca. 200 m.sec. thick and is present in the southern part of the central and the southern FSC (Fig. 6.1). Unit 11a progressively thins towards the southwest as a result of progressive truncation by the overlying depositional package (DP12) (Fig. 6.3a). The base of the unit is marked by an erosion surface that cuts into the underlying DP9, having ca. 50 m.sec. relief in the southern part of the FSC (Fig. 6.3a). This basal erosion surface is onlapped and downlapped by reflectors of DP11 (Figs. 6.3a and 6.12). The top of DP11 is either truncated against overlying DP12 or marked by a surface onto which the overlying DP12 onlaps (Figs. 6.3a and 6.4a). Internally, DP11a contains a series of sigmoidal clinoform reflectors (Fig. 6.12a).

Unit 11b

Unit 11b is up to 400 m.sec. in thickness and is present in the north-western part of the FSC (Fig. 6.1). The base is marked by a surface onto which reflectors onlap, and the top by a surface that shows underlying truncation reflectors (Figs. 6.5 and Fig.6.14). Internally DP11b contains parallel reflections of varying amplitude (Fig. 6.14).

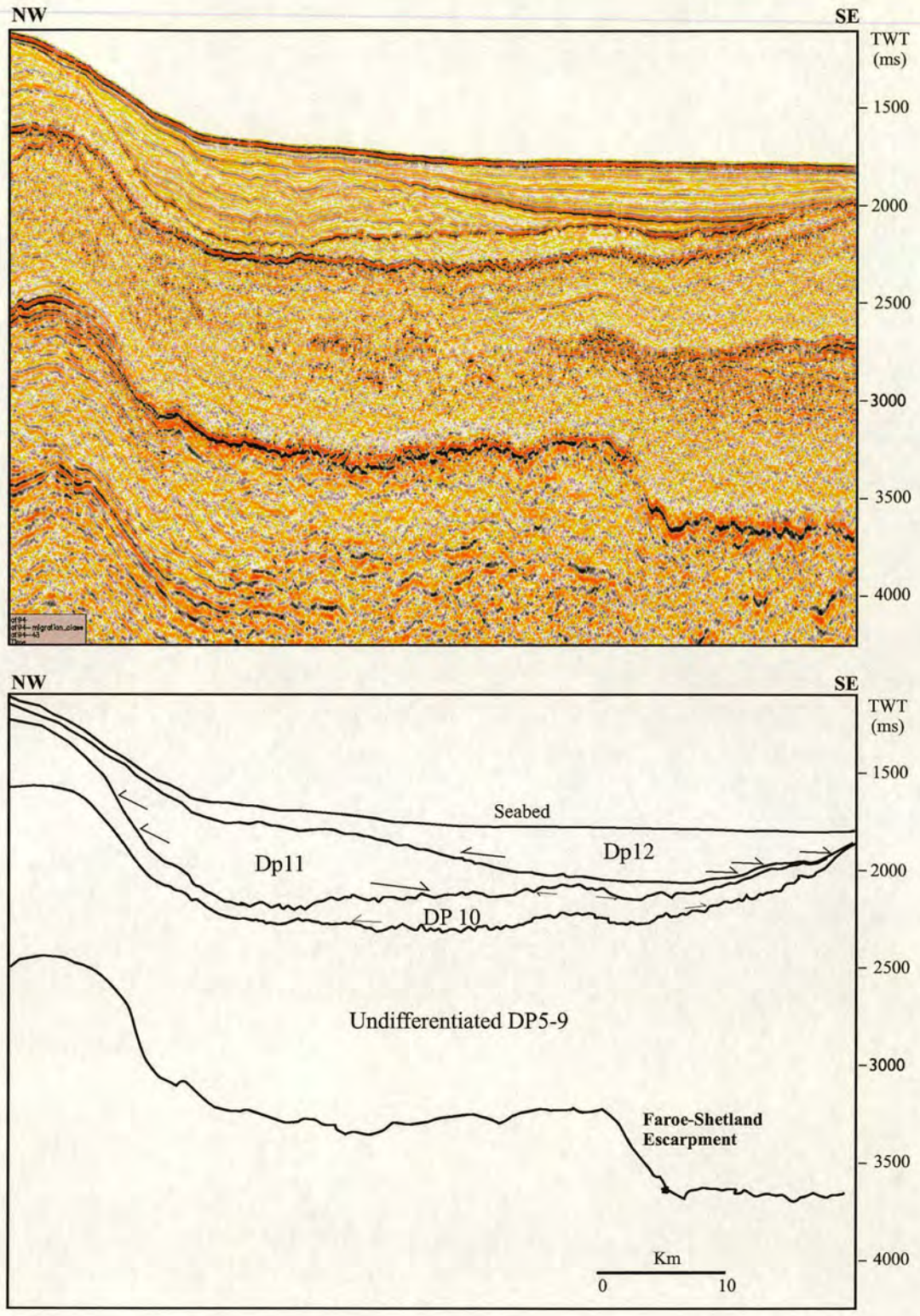

Figure 6.14. Seismic 2D-line (of 94-43) showing the nature of DP10 that has locally been deposited in this area. DP11 and DP12 is also shown. DP5-9 cannot be differentiated due to poor seismic quality. Location of the seismic line is shown on Fig.6.1b.

Depositional package 12 (DP12)

Depositional package 12 can be subdivided into four different units based on seismic character. The basal surface of DP12 is generally represented as an irregular surface, however locally on the shelf (of the Present day) in the south-western part of the FSC the basal surface is locally very flat dipping towards the northwest (Fig. 6.3a). Where the basal surface is irregular it shows local incision into underlying depositional packages (DP8-10 through to DP5, e.g. Fig. 6.4a). The basal surface is age equivalent to early Pliocene unconformity by (Stoker, 1999).

Unit 12a has variable thickness of up to 200 m.sec. and is present locally in the southwest (Figs. 6.4a and 6.11a) and in the central part of the FSC, where it is thin (Fig. 6.5). Unit 12a is marked a surface onto which reflectors downlap/onlap, whilst the top is marked by a surface that shows underlying truncation reflectors below the seabed. Internally, Unit 12a consists of parallel seismic reflectors of high amplitude (Figs. 6.4a and 6.11a). The parallel reflectors dip towards the northwest parallel to the basal surface of DP12 (Fig. 6.3a). Unit 12a is equivalent to WSD_{slope} that is part of the WSD system by Knutz and Cartwright, (2003) and contains sediments of an early Pliocene to Pleistocene age.

Unit 12b represents a variable thickness (up to 300 m.sec.) package that is present in the south-eastern part of the FSC (Fig. 6.1). Unit 12b is marked by a surface onto which reflectors onlap, whilst the top is locally truncated at present day seabed (Figs. 6.5 and 6.14). Internally, Unit 12b contains parallel seismic reflectors of variable amplitude (Fig. 6.14). Unit 12b is equivalent to WSD_{basin} by Knutz and Cartwright, (2003) and contains sediments of an early Pliocene to Pleistocene age.

Unit 12c has a wedge-shape external form that is up to 500 m.sec. thick and is present in the eastern part of the East Faroe High, extending to the southeast where it terminates against north-western margin of the FSC (Figs. 6.1 and 6.5). The base is marked by a surface onto which reflectors downlap, whilst the top is conformable

overlain by Unit 12d (Fig. 6.5). Internally, Unit 12c contains oblique clinoform reflectors that dip towards the southeast (Fig. 6.5). Unit 12c is age equivalent to FPC-D2 by (Andersen et al., 2000) and to sedimentary wedge containing clinoform reflectors on the West Shetland Shelf by Stoker et al., (2002) and contains late Plio-Pleistocene age sediments (Stoker, 1999).

Unit 12d is very thin and present locally in the northwest above Unit12c. In the southwest Unit 12c can not be differentiated or it is not present. The base is generally marked by a very flat even surface of erosion that has removed underlying unit locally (Fig. 6.5). The flat basal surface is equivalent to a mid-late Pleistocene aged glacial unconformity defined by Stoker et al. (1994) and Stoker (1995).

Seabed structure

In the south-western part of the FSC the seabed is characterised by prominent sub-vertical, planar scarps that are up to ca. 250 m high and located above the Foinaven Anticline, at the point where it has its maximum flexural folding (Figs. 6.15a-b). There are two main NW-SE trending scarps (called F1 and F2) and a series of minor scarps, which range from 1-22 km in length and occur over a 15 km wide zone (Fig. 6.15a and c). There appear to be normal faults located beneath and connected to the sea-bed scarps. These faults have their maximum height (up to 250m) at the sea bed (sea-bed scarps) decreasing downwards reaching zero displacements clearly defined at the fault tips. A displacement-length profile has been produced for seven of the faults, in order to graphically show the displacement distribution along the faults and provide insights into the evolution of the faulting (e.g. Cartwright et al., 1996; Dawers et al., 1993) (Fig. 6.15c). The main fault that is 22 km long shows steep displacement gradients at the tips of the fault (ca. 0-250 m) and a flat-topped trend of near constant displacement along much of the fault length (ca. 250 m). A similar trend is seen for the other smaller faults (Fig. 6.15c). This is consistent with displacement-length data from other normal fault populations (e.g. McLeod et al., 2000; Dawers et al., 1999). A simple depth conversion across the structure (above

F1) also preserves the offsets and downward decreasing displacement of the main fault (Fig. 6.15d). With respect to the strata around the faults, there is a greater thickness of preserved strata in the footwall than in the hangingwall, where truncation of the reflectors can be observed.

The amplitude and wavelength of the fold that makes the Foinaven Anticline (Fig. 6.2a) was calculated from the Top Balder time-map(Fig. 6.2a) to be ca. 100 m and 2.2 km respectively. In order to roughly estimate the amount of lengthening (extension) of the fold, simple trigonometry has been used, with the following equation:

$$a^2 + b^2 = c^2$$

Where a is the amplitude of the fold (100 m) and, b the half width of the fold (2.2 km). This indicates that the folding resulted in an increase in length of the deformed beds by at least ca. 4.5 m.

A)

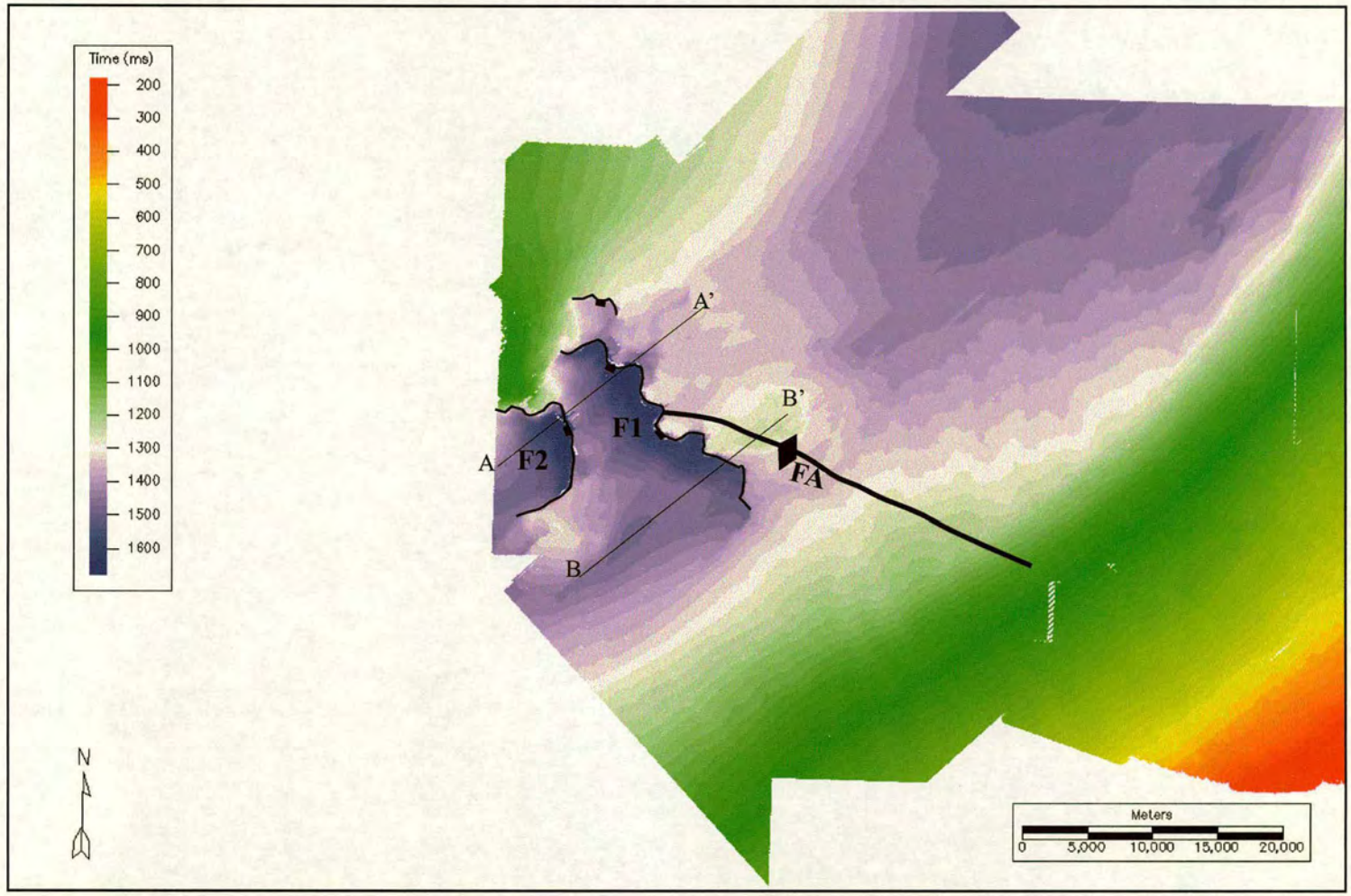

Figure 6.15a. Time-map of seabed reflector. Axial trend of the Foinaven Anticline. The anticline has its greatest deformation in the westnorthwest of its axial length, where the seabed is eroded/faulted (F1 and F2 represent the main scarps/faults).

B)

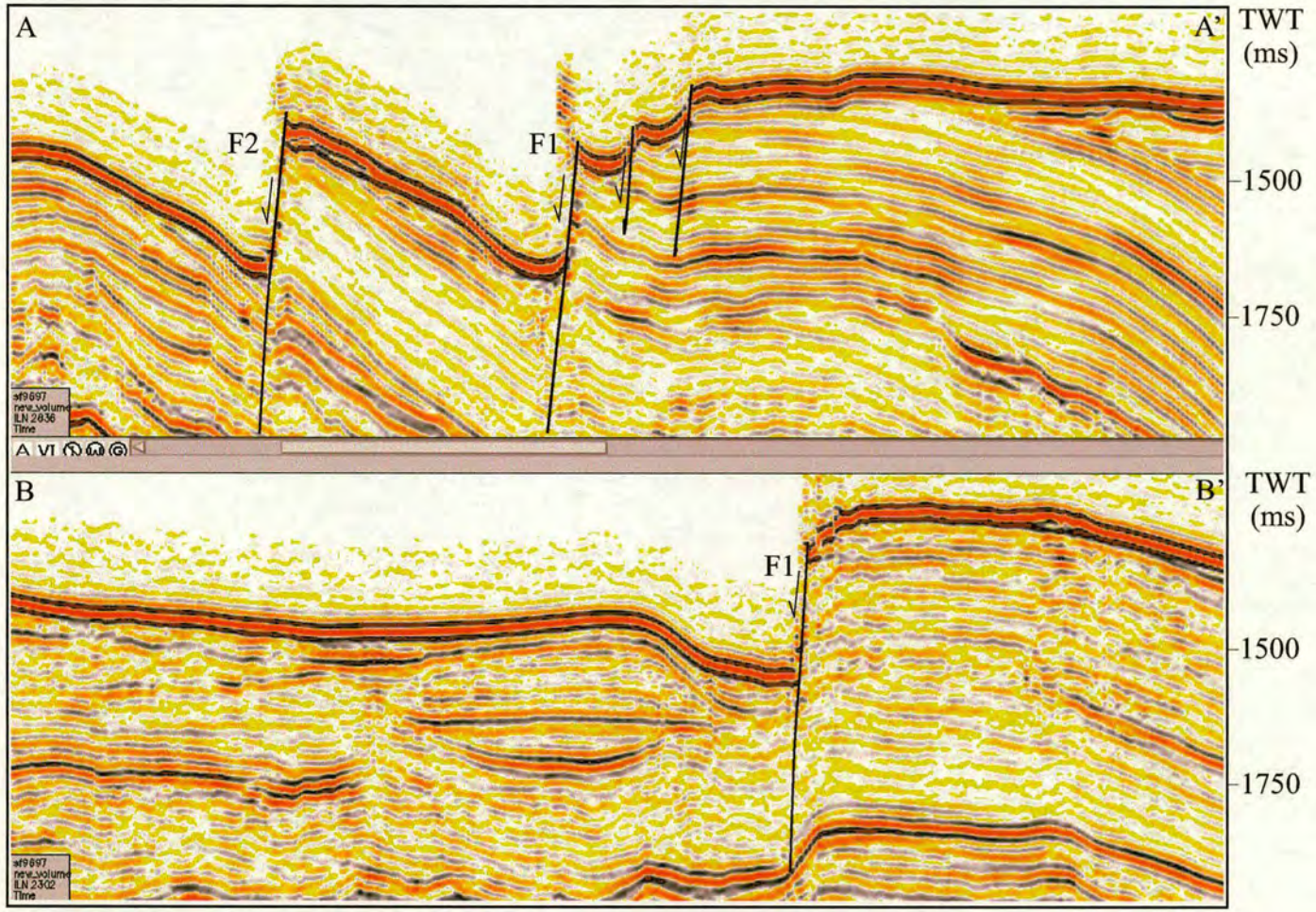

Figure 6.15b. Two seismic lines (A-A' and B-B'). Location of the seismic lines is shown on Fig. 6.15a). The seismic lines shows two main normal faults/scarps (F1 and F2) that are located where the Foinaven Anticline has its maximum flexural folding.

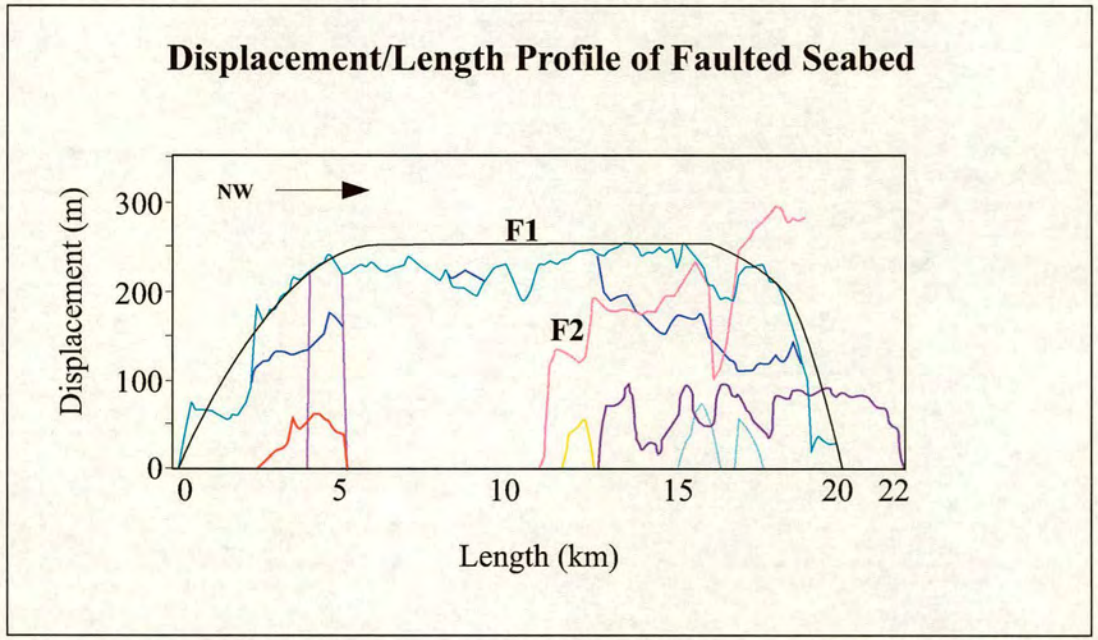

Figure 6.15c. Displacement/length profile of the extensional faults seen on Fig. 6.15 a-b. The main faults are labled F1 and F2, whereas smaller faults are not labeled. See text for discussion on faults vs. Erosion.

D)

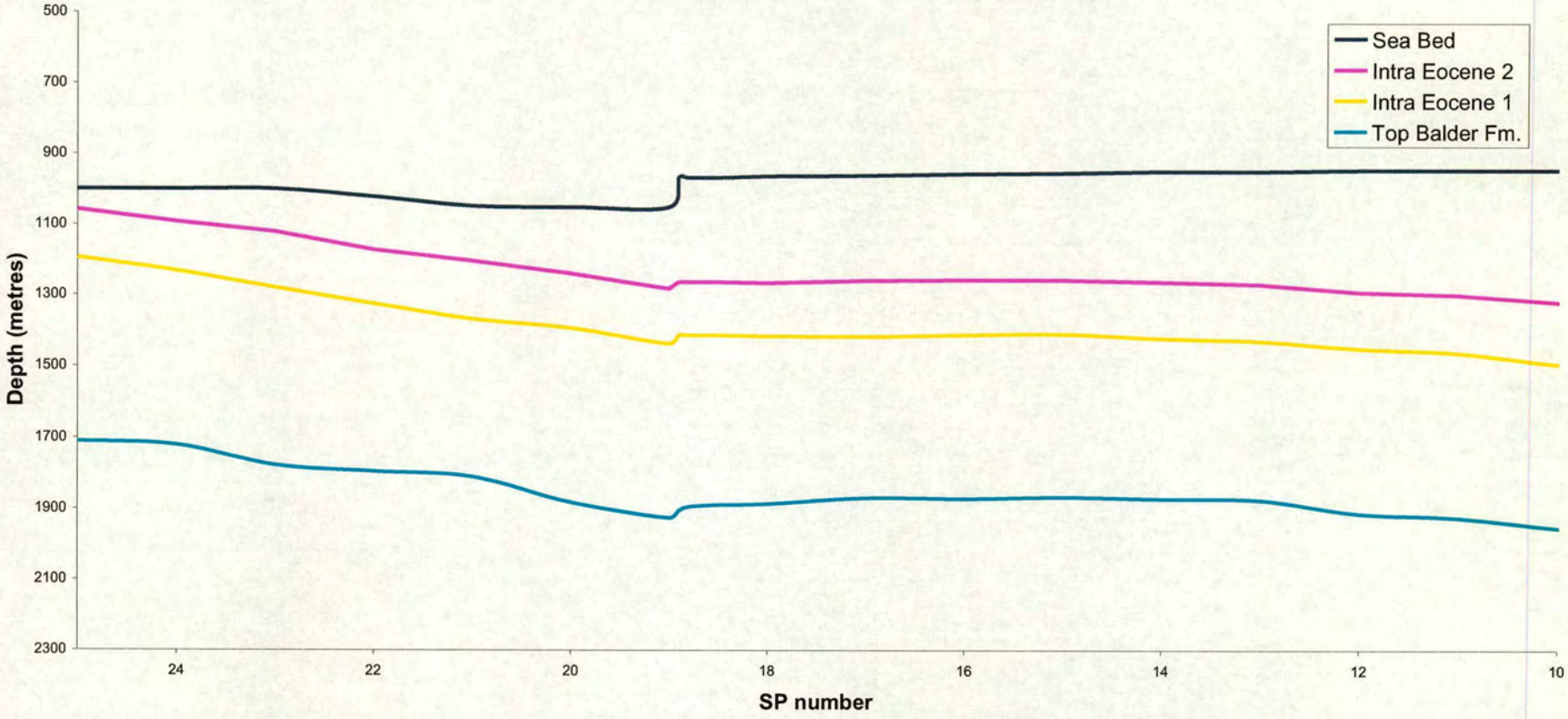

Figure 6.15d. Depth converted section across the seabed fault/scarp F1

6.4. TECTONO- STRATIGRAPHIC EVOLUTION FROM LATE PALEOGENE TO PRESENT

The seismic stratigraphic and chronostratigraphic framework described in the previous section is illustrated in figure 6.16. The aim of this section is to build upon these descriptions and interpret the temporal and spatial tectono-stratigraphic evolution of the FSC from the early Eocene to Present (Fig.6.17a and b). Each depositional package is interpreted sequentially.

Depositional Package 5 (DP5)

Unit 5a

Underlying DP4 is a terrestrial incised valley network that progressively was infilled (Chapter Five). As discussed in Chapter Five, a transgression occurred towards the end of the Paleocene during deposition of the Balder Formation. The deposition of DP4 (Unit 4c) during the Balder Formation resulted in the infilling of the drowned topography present after the flooding event. Thus immediately prior to deposition of DP5 the seabed (depositional surface) is interpreted to have had a low relief. The downlapping clinoform reflectors of Unit 5a indicate that the depositional system responsible for their formation prograded towards the north and northeast. The coarsening upward log trends further indicates northeast-ward progradation and shallowing-up of the depositional package/unit. The height of the clinoforms indicate that the depositional system prograded into water depth of ca. 125 m. The progradation resulted in a coastal plain, terrestrial environment (indicated from the lignites) capping the progradational parasequence, and overlying marine mudstone and sandstone. The coarsening up log response, the upward transition from mudstone to sandstone and lignite, and clinoforms suggests that unit 5a represents a deep marine to coastal/delta plain progradational, environment. Presumably progradation of the shelf slope system occurred as shallow marine deltaic depositional systems were transported to the shelf edge resulting in shelf-slope progradation and generation of seismic-scale clinoforms.

The prograding clinoforms indicate that sediment supply was higher than generation of accommodation space and thus the clinoforms progressively built out

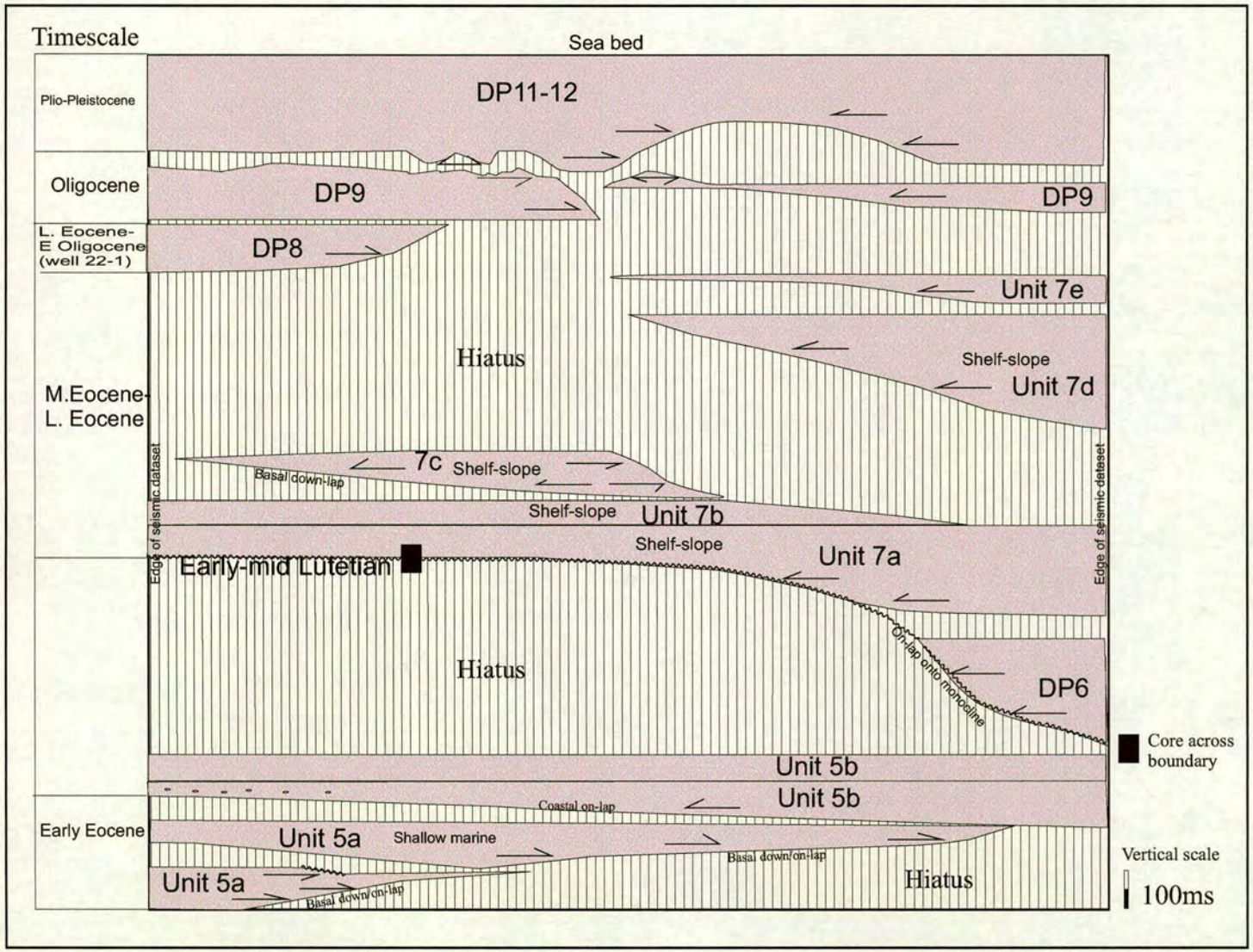

Figure 6.16. Figure 16. Chronostratigraphic diagram of the southern Faroe-Shetland Channel.

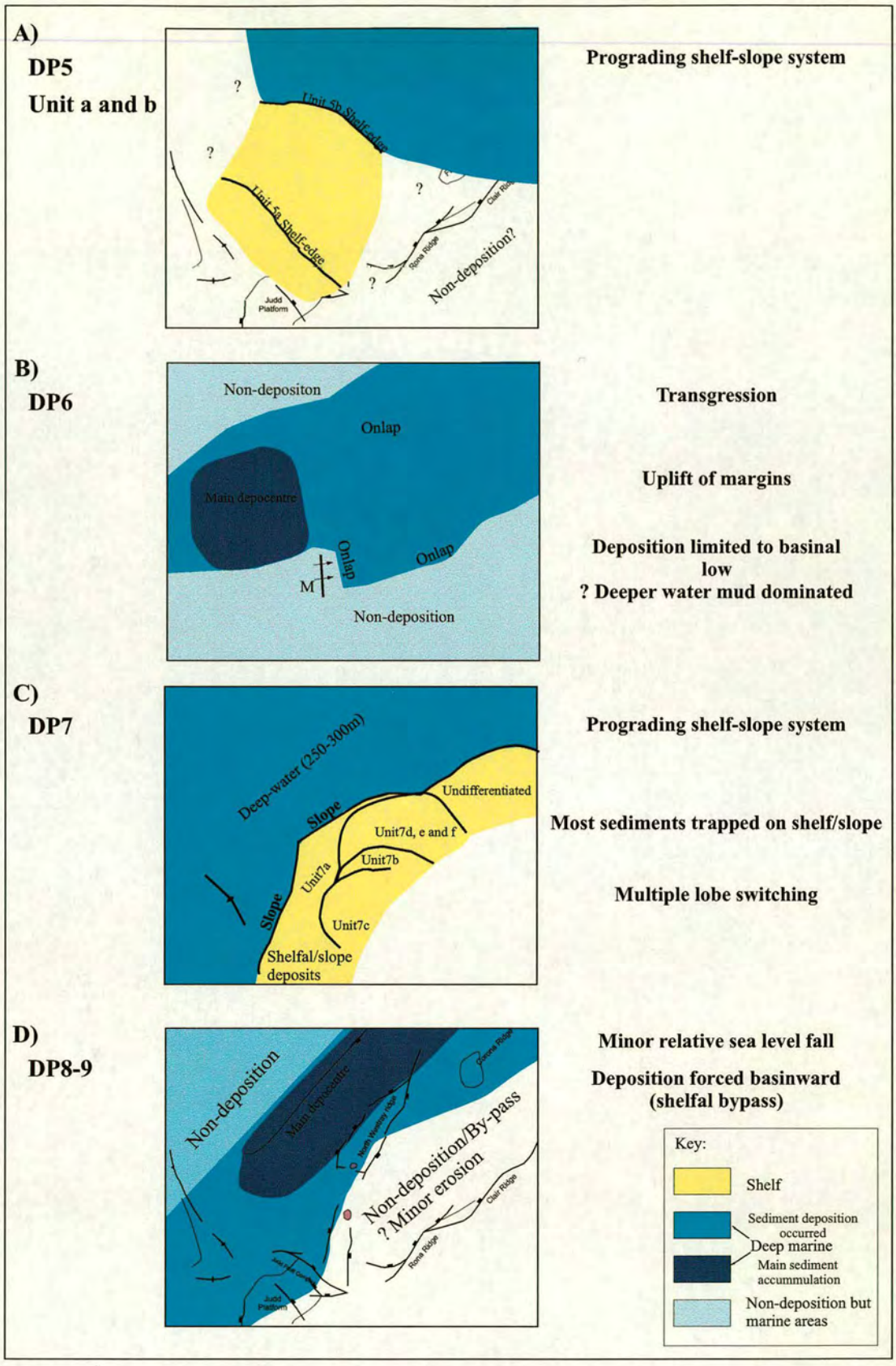

Figure 6.17a. Sketch of the evolution from Eocene to Present of the southern and central Faroe-Shetland Channel (see text for discussion).

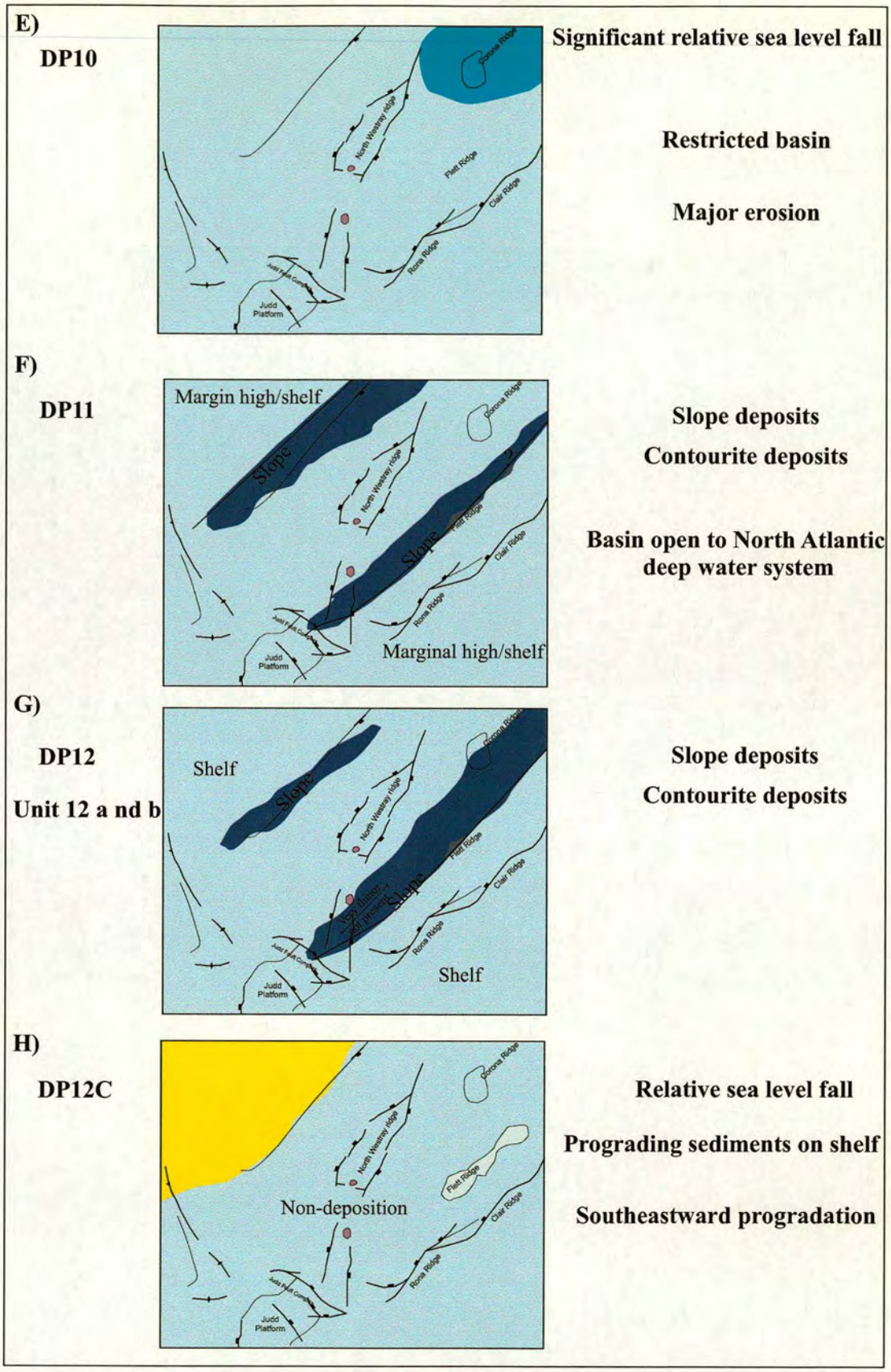

Figure 6.17b. Sketch of the evolution from Eocene to present of the southern and central Faroe-Shetland Channel. Key (as previous).

basinward. Furthermore, the downstepping of each cycle of the clinoform packages together with the internal truncation of the clinoform reflectors suggests that Unit 5a was deposited as a result of a relative sea level fall that eroded the topsets and partly the foresets. The dominantly north and northeast progradation and regression of the shoreline indicates that sediments were sourced from the south and southwest (Fig. 6.17a, A).

Unit 5b

Following the deposition of Unit 5a a relative sea level rise occurred generating new accommodation space for the deposition of Unit 5b above Unit 5a.The base of Unit 5b thus represents a flooding surface, which is also seen on wire-line log as an abrupt shift from low to high gamma-ray (Fig. 6.8). The progressive down-lap prograding reflectors of Unit 5b towards the north over the top of Unit 5a and further northwards, indicates that the unit built out or prograded (Fig. 6.9). This indicates that sediment supply was greater than generation of accommodation space. The environmental interpretation for Unit 5b, from the cuttings descriptions, the log trends and the seismic facies character, suggests a large-scale deltaic system. The well data indicates that the depositional system consisted of higher gamma ray siltstone and mudstone deposited distally, that coarsening upward with progressively more sandstone interbedded. In the upper-most proximal section of Unit 5b, clean (box-shaped log trend) sandstone is deposited representing relatively clean shallow marine sandstone facies/delta front sandstone. The extent of the prograding/downlapping reflectors indicate that the deltaic depositional system prograded a considerable distance northward. At the end of deposition of Unit 5b a very broad sandy shelf had prograded from the Judd area in the southwest to the North Westray Ridge area (Fig. 6.17a, A). Following the deposition of Unit 5b the area was flooded as indicated by the abrupt change in gamma-ray from low to high value (Fig. 6.8).

Depositional Package 6 (DP6)

The tinning and onlap of DP6 indicates that it was deposited onto relief or highs that was created after deposition of DP5. These highs consisted of the Foinaven Monocline (southern FSC), the eastern part of the East Faroe High and possibly the Rona/Clair Ridge (Figs. 6.1 and 6.17a, B). Limited deposition and/or sediment preservation occurred above these highs, with a thin layer preserved over North Westray Ridge (Fig. 6.9). The absence of DP6 above the highs suggests that during its deposition sediment distribution was restricted to the depositional lows. The gradual westward sediment thickening from the North Westray Ridge towards the Foinaven Anticline indicated that the main depocentre during DP6 was in the southwest area above this anticline, which must have formed at some time after DP6. The onlapping parallel reflectors of DP6 suggest that sediment progressively infilled relief created by uplift. The variable amplitude of the reflectors may represent some coarse-grained deposits sourced from the higher areas on both side of the FSC. The high amplitude reflectivity could also represent some igneous input (lavas) sourced from the East Faroe High in the north (e.g. Ritchie et al., 1999).

Following the considerable shoreline progradation that occurred during DP5, it is interpreted that much of the FSC basin has low relief topography. Depositional package 6 has been deposited above DP5. However, the restricted aerial extent of DP6, with onlap and thinning onto distinct highs indicates that a major structural reconfiguration of the basin physiography occurred prior to the deposition of DP6, during early-mid Lutetian. There appears to have been a change from more widespread deposition during DP5 to more localised deposition during DP6 as a result of local uplift and the formation of highs.

Depositional Package 7 (DP7)

The downlapping sigmoidal clinoform reflectors and wedge-shaped external form of DP7 indicates that it represents a progradational shelf slope depositional system. The north-westward progradation of this depositional system is evident from the progressive north-westward down-lap of the reflectors. Consequently each unit (Unit 7a-7f) of DP7 is situated progressively further to the northwest (Fig. 6.12). The

clinoforms build outwards (to the north northwest-northwest) and also upwards (parallel stacking of topsets) indicating that a component of aggradation occurred during overall progradation (Fig. 6.17a, C). The height of the clinoforms suggests water depths of up to 250-300m, indicating that the system prograded into a relatively deep marine setting. The downlapping reflectors and the progradation of the clinoforms suggest that sediment supply was greater than the generation of accommodation space. It is likely that DP7 was deposited during a slow relative sea level rise, where the high sediment supply resulted in progradation and aggradation of the depositional system. The reflector terminations between the individual units (Unit 7a-7f) of DP7 suggest that there were local fluctuations in sediment supply and/or relative sea level during the deposition of DP7.

Well (e.g. 204/22-1) and core data (BGS 99-3) record the depositional and faunal change across the unconformity boundary DP5/DP7, and indicates the nature of the out and-up-building of DP7. Above the basal unconformity DP7 contains a sparse faunal diversity and includes reworked Early Eocene, Carboniferous and Jurassic-Cretaceous material. The marked change in faunal diversity across this basal unconformity indicates a change in the basin-physiography that led to erosion and the formation of the basal unconformity. The ostracods, plant tissue and wood fragments, which occurred at the base of DP7 correspond to a terrestrial source. This suggests that terrestrial material has been eroded and transported basinward where it was deposited in a marine shelf-slope setting.

The deposition of DP7 records a progressive infilling of accommodation space mainly around and over the Foinaven Monocline, accompanied by shifts of sediment source as indicated from each unit of DP7. Unit 7a is deposited east of the Foinaven Monocline and over southern part of the Foinaven Anticline. Unit 7a thins towards southwest over the Foinaven Monocline and over the Foinaven Anticline, suggesting that during deposition of Unit 7a the Foinaven Monocline and the Foinaven Anticline represented positive relief areas. The onlaping and thinning reflectors over the Foinaven Anticline, indicates growth of the anticline during deposition of Unit 7a. The main sediment source however, was east of the Foinaven Monocline, indicated by the thickest succession of filled in accommodation space

east of the Foinaven Monocline. Unit 7b is thickest over the Foinaven Monocline and it thins over the Foinaven Anticline. This indicates that positive relief existed over the Foinaven Anticline during deposition of Unit 7b. The onlap and thinning onto the Foinaven Anticline, indicates growth of the anticline coeval to deposition of Unit 7b. Over the Foinaven Monocline however, the clear fan-shaped geometry of Unit 7b, indicates that during deposition of Unit 7b the main sediment source had moved from east further southwest on top of the Foinaven Monocline. During deposition of Unit 7c the sediment source had moved even further southwest, represented by the sedimentary thick being west of the Foinaven Monocline. The west-north-west progradational clinoforms of Unit 7c suggest that in addition to the main northwest-ward progradation of DP7, Unit 7c progrades also towards the west-north-west. Unit 7d is thickest east of the Foinaven Monocline and thins onto its crest, suggesting that accommodation space is filled east of the Foinaven Monocline. The chaotic-fill pattern of Unit 7d represents most likely slump deposits. The erosion on top of Unit 7b-Unit 7c/ base 7d on the crest of the Foinaven Monocline and the northwest trending incised channels south of the Foinaven Monocline, suggests that the slump deposits were transported off the Foinaven Monocline towards the east and from the northwest into the topographic low east of the Foinaven Monocline. The slump deposits of Unit 7d, were deposited during instability on the slope, due to a relative sea level fall or due to high rate of sedimentation oversteepening the slope, leading to slope failure. Unit 7e and Unit 7f filled accommodation space east of the Foinaven Monocline suggesting an eastern sediment source.

There appears to have been a major change in palaeoenvironment from local infilling of relief during DP6 to a prograding shelf slope depositional system during deposition of DP7.

Depositional package 8-10 (DP8-10)

Depositional Package8

In the southern part of the FSC, the main thickness of DP8 is stacked further north of DP7, with the internal reflectors of DP8 onlapping onto the former DP7 slope (Fig. 6.17a, D). Thus following the deposition of DP7 the sediment supply,

relative sea level and accommodation space clearly changed, and therefore DP8 was deposited basin-ward of the former shelf-slope system. This is evidenced by the south-eastward and southwest-ward (radiating) on-lap/off-lap onto the former (DP7) slope. The uniform thickness of DP8 and progressive onlap indicates that the main locus of sediment supply had shifted basinwards and DP8 was filling up the former relief at the base of the slope. The lack of clinoform reflectors and the shift in depo-centre, from shelf-slope outbuilding system (DP7) to slope and basin deposits (DP8), suggest that the previous shelf area was by-passed with sediment directly supplied onto the slope and into the basin. Furthermore, the basin infilling of DP8 coincides with the onset of a major coarse clastics sandstones input (sand prone interval well 204/22-1), all which indicate that DP8 may represent slope-fan deposits. DP8 was also deposited in a local area west of the Foinaven Monocline indicating that sediment was focussed into this area, where it again onlaps the base of slope of the underlying depositional package (DP7). The seismic facies and well data indicate that the influx of coarse-grained clastics continued until end of DP8, thus DP8 continued to fill in the available accommodation space. The basinward shift of sediment supply of slope-fan deposites and high sediment flux probably reflects a relative sea level fall

The coarse grained lithology and the igneous rock fragments reflects the high-amplitude "semi-chaotic" pattern and indicate that sediments were received from a proximal source from the South. In addition, volcaniclastic sandstones of Early Ologocene age have been encountered in well on the Faroe Shelf (Waagstein and Heilman-Clausen, 1995). The igneous rock fragments encountered in well 204/22-1 are age equivalent to the volcaniclastics, indicating that the rock fragments within DP8 come from a common source that has been eroded and subsequently transported probably from the north. This suggests that sediments that formed DP8 were also derived from the Faroe Platform area (Faroes shelf).

Depositional package 9

The north-eastward onlap and thinning of Unit 9a onto the Foinaven Anticline (Fig. 6.4b), indicates that the Foinaven Anticline was a relative high at this time and thus

more of the available accommodation space was filled around the anticline, especially in the southwest. The onlap and thinning of Unit 9a, records a second phase of distinct growth of the Foinaven Anticline. This growth had stopped prior to deposition of overlying Unit 9b, which is evident from the thickness relationships over the Foinaven Anticline (Fig. 6.4b).

The onlap of Unit 9b onto Unit 9a and DP7 slope represents in-fill of the topography created over the Foinaven Anticline and infill of available accommodation space in front of and onto the DP7 slope (e.g. Fig. 6.3a). Sediments of Unit 9b, which are also deposited on top of the former (DP7) outer shelf, implies that during deposition of Unit 9b generation of accommodation space over the former outer shelf (DP7) is available for sediment accumulation again for the first time since Middle Eocene. The lack of chaotic-fill pattern suggests a different less high energy environment compared with underlying DP8, indicating that DP9 may represent a finer-grained, more background sedimentation, as opposed to slope/basin floor fan deposition. This may be as a result of a progressively deeper marine setting.

Depositional Package 8-10

A large thickness (> 1000 m.sec.) of sediment accumulated in the central area of the FSC, along its axis. A considerable amount of accommodation space must have been in this area compared with the south-western FSC where limited accommodation space was available over the Foinaven Anticline. It is possible that sediments accumulated over the Foinaven Anticline and was later eroded. Erosion has clearly occurred over the Foinaven Anticline, however it is not possible to quantify how much was eroded.

The transition from the shelf-slope environment during DP7 to the base of slope deposition during DP8-10 suggests a marked change in basin configuration that reflected the sediment distribution pattern. The restricted aerial extent of DP10 is interpreted to be a result of relative sea level fall and DP10 was deposited as local lowstand fan. There appears to have been a change from more widespread deposition and high sediment flux focused in the central FSC during deposition of DP8 and DP9 to deposition further north-eastwards as a result of a relative sea level fall (DP10).

The faults seen within DP8-10 are similar to the configuration of dewatering faults in the Tertiary of the North Sea (e.g. Cartwright et al., 1994). Andersen et al. (2000) interpret the faults to be dewatering faults that were active during early burial. Furthermore, Andersen et al. (2000) suggest that the faults may have been caused by overpressure in a sand-shale succession, and the faults penetrating through the overlying successions could have been escape routes for fluids.

Subsequent to deposition of DP8-10 the successions was folded. This is evident in the northwest (e.g. 2d-line of94-43, Fig. 6.14), where folding of depositional package DP8-10 has occurred. Parallel unfolded progressively onlapping and infilling reflectors of overlaying depositional package (DP11), indicates that folding occurred prior to deposition of DP11. An alternative interpretation is that DP8-10 represents mega slumping of the shelf (East Faroe High). In the Northern FSC the surface that represents DP10/DP11 is equivalent to a Middle Miocene unconformity by Davis et al. (2004), who have documented seventeen anticlines that formed during the Middle Miocene (Davis et al., 2004). Also the East Faroe High was folded into an anticline (Andersen et al., 2000) during the Middle Miocene.

Depositional Package 11 (DP11)

The restricted aerial extent of DP11 in the north-western and south-eastern part of the FSC, and the lack of sediment accumulation in the centre of the FSC, suggests a marked change in depositional environment after the Middle Miocene. This change resulted in a shift in sediment distribution from the main locus of deposition being in the centre of the FSC (basin in-filling) during DP8-9 and DP10 to deposition along narrow zones of the margin of the FSC (Fig. 6.17b, F). The shift in sediment distribution might be due to a relative sea level rise and/or starvation of sedimentation during DP11. The seismic character and the location of DP11 however, seems to be equivalent to the previously interpreted Miocene drift deposits by Stoker (2002). Since Middle Miocene times the FSC, that had previously since Early Eocene been a restricted marine area, became influenced by the Atlantic deep-water circulation (Berggren and Schnither, 1983; Thiede, 1983). Therefore, the

change in depositional environment that is observed after deposition of DP11 is likely to be associated with transport facies that are deposited as contourite drift deposits, at the foot of the slope and upslope, which is according to e.g. Knutz and Cartwright (2003) due to changes in the velocity of deep-water bottom currents.

Depositional Package 12

The incision that characterises the early Pliocene basal unconformity of DP12 is a major erosion surface (Figs. 6.3a and 6.14). In the southwest the basal unconformity of DP12 erodes into underlying depositional packages (DP9, DP8, DP7 and DP4, Fig. 6.4a). The geometry of the surface that truncates these packages forms a shelf-slope feature. This shelf-slope is north of the underlying shelf-slope edge of DP7. It is therefore likely that the processes that formed the basal surface of DP12 and the new position of a shelf-slope were responsible for the reconfiguration in the southwest part of the FSC probably due to preferential erosion. This preferential erosion was possibly associated with the location of the Foinaven Anticline and also to the underlying Mesozoic basin alignment (the Judd Platform and the soft sediment successions off the Judd Platform). The basal surface that dips towards the northwest and the internal reflectors of DP12, which truncates at the seabed, suggests that that it has been tilted after deposition of DP12. The basal erosion surface has previously been interpreted to represent a major angular unconformity landward on the margin that separates Miocene strata from younger Pliocene-Pleistocene strata (Stoker, 2002). This tilting event was coeval to a change in the oceanographic circulation pattern that has altered pattern of deep-water sedimentation in the FSC (Stoker 2002).

Unit 12a

In the southwest the north-westward dipping basal surface and the north-westward dipping internal parallel reflectors of Unit 12a and the truncation against the seabed suggest that Unit 12a has been tilted in the southwest. The north-west-ward tilt is only observed in the present day shelf area, in the basin however, the parallel seismic reflectors suggest that the basin was not affected by this tilt (Figs. 6.3a and 6.17b, G).

The tilting is possibly related to postglacial margin rebound and additionally Unit 12a has probably been eroded/modified by high velocity deep water-bottom currents, indicated from the truncation reflectors at the seabed.

Unit 12b

The parallel internal reflectors and the onlapping onto DP8-10 indicates that Unit 12b represents aggradation and infilling of sediments. The restricted deposition along the margin of the FSC, and at the foot of overlying present day slope (Figs. 6.14 and 6.17b,G), has previously been interpreted to represent contourite drift deposits (Stoker, 2002; Knutz and Cartwright, 2003).

Unit12c

On the East Faroe High in the northwest the downlapping oblique clinoform reflectors of Unit 12c indicates that it represents a progradational shelf-slope depositional system. The south-eastward progradation of this depositional system is evident from the progressive south-eastward downlap of the reflectors. The clinoforms build outwards to the southeast (Figs. 6.5 and 6.17b,H). The height of the clinoforms suggest water depth > 250 ms. The downlapping reflectors and the progradation of the clinoforms suggest that sediment supply was greater than generation of accommodation space. The Pliocene-Pleistocene aged sediments of Unit 12c indicate that Unit 12c was deposited during a relative sea level fall most likely related to glaciations.

Following deposition of contourite deposits of Unit 12a in the basin and upslope in the FSC of Unit 12b deposition of a prograding shelf-slope depositional system during Unit 12c indicates a marked change in depositional environment. This change could be related to a relative sea level fall possibly associated with the glaciations that prevailed during the Plio-Pleistocene or the change could be related to sea level fall related to uplift. The basal surface of DP12 shows evidence for tilting suggest that the area must have been uplifted during the early Pliocene, the progradation of the Pliocene-Pleistocene shelf-slope depositional system could have been deposited as a result of this uplift and tilting event, but with a slight time-

delayed component (cf. Stoker, 2002). Unit 12c is equivalent to prograding clinoforms that downlap towards the northwest and are present outside study area on the NW British Shelf (Stoker, 2002). A similar shelf-slope depositional system is present off mid-Norway that is equivalent in age (Eidvin et al., 2000). This indicates a regional change in depositional environment.

Unit 12d

Unit 12d is separated from underlying units by the flat mid-late Pleistocene glacial unconformity. Unit 12d is thin and only locally present in study area. The abundant occurring truncation reflectors of Unit 12 below the seabed indicate that the area has been affected by erosion. The restricted presence of Unit 12d is therefore due to erosion possibly related to uplift associated with isostatic rebound as a result of glaciations. Glaciations occurred on the NW British Shelf and created the glacial unconformity during mid-late Pleistocene (e.g. Stoker, 2002). In addition to glacio-isostasy, erosion has also been modified by deep-water bottom-currents that persist at present day.

Seabed Structure

These scarp features may be a result of either 1) normal faulting related to uplift and local stretching (outer arc extension) of the seabed in response to growth of the Foinaven Anticline, 2) erosion related to deep-water bottom currents (e.g. Smallwood, 2002), or 3) a combination of both normal faulting and erosion.

The scarps have many characteristics of normal faults, such as the planar cross-sectional and plan form geometry, displacement characteristics, drag/folding of the beds against the fault scarps and rotation of bedding (Fig. 6.15a). The downward decrease in displacement indicates that the faults most likely nucleated at or near to the seabed and propagated downward and laterally. The zigzag plan form geometry of the faults together with highs and lows seen along the displacement-length profile (Fig. 6.15a-b) suggest that the faults may have developed by linkage of smaller segments (cf. Cartwright et al., 1996). The fault-displacement decreases both laterally and downwards from a maximum level at the seabed to a zero tip at depth.

However, the greater thickness of strata in the footwall of the faults (scarps) and the seismic reflector-truncations in the hangingwall, suggest that incision/erosion occurred in the hanging-wall (Fig. 6.15b). Whilst the scarps show the characteristics of normal faulting, the amount of outer-arc extension (>4.5 m) expected to have resulted from the uplift, is unlikely to have generated fault displacements of ca. 250 m. Rather, this degree of extension may only have generate metre-scale faulting, and therefore it is unlikely that faulting alone was responsible for forming the high scarps that can be observed at the seabed (Fig. 6.15a and b).

On the basis of the incision and correspondingly thinner, truncated stratal packages in the "hangingwall" of the scarps, it is more probable that the scarps were largely formed by erosion, related to deep-water bottom currents (e.g. Smallwood, 2002, Stoker, 2002). It is postulated that small offsets of the sea-bed by normal faulting, created depressions along which sea-bottom currents were focussed, and thus, the fault controlled depressions were subsequently enhanced by considerable erosion in their hangingwall (Fig. 6.15b). The lack of incision over the scarps in the footwall (Fig. 6.15b), despite the sand prone lithology (e.g. well 60005/15-1), suggests that preferential erosion occurred parallel to the fault scarps, along the fold axis of the Foinaven Anticline (Fig. 6.15a). However, it remains unclear why the erosion has resulted in the formation or preservation of such planar, fault-like scarps, rather than creating more rounded and lower angle margins (in cross-section).

6.5 CONTROLS ON STRATIGRAPHIC EVOLUION

The aim of this section is to determine the structural and other control that are exerted on relative sea level, basin physiography, drainage development, sediment supply and sediment distribution, and thus controlled the stratigraphy development outlined previously.

Depositional Package 5 (DP5)

The sea level fall and the progressive northeast-ward regression of the shoreline that lead to sub-aerial exposure is likely to be local and probably controlled by uplift in the southwest, since there is no indication of a eustatic sea level fall, based on the sea level curve by Haq et al. (1987). Uplift due to compression has been documented to occur during the Early Eocene to the west, northwest and northeast of the study area (Andersen and Boldreel, 1995; Boldreel and Andersen, 1993, 1998). This uplift phase, termed post-basalt compressional phase one (after Boldreel and Andersen, 1993), is evidenced by originally parallel-bedded basalt (Faroe-Rockall Plateau Lava, Fig. 6.1) have been folded into large anticline structures e.g. the Wyville-Thomson Ridge Complex, the Munkagrunnar Ridge, the northern flank of the Faroe Bank and possibly the Fugloy Ridge (Fig. 6.1). In the southwest and northwest FSC equivalent aged basalts (part of the Faroe-Rockall Plateau Lava) to those that have been folded, are present immediately below the Top Balder Formation, within an incised valley fill, ascribed to the Hildasay Sandstone member of the Flett- and Balder Formations (see Chapter Five). Depositional package 5a down-laps onto the Top Balder marker bed and thus post-dates the basalt. A regional post-basalt compressional tectonic event that occurred in the Early Eocene has been related to horizontal compression, associated with sea floor spreading in the North Atlantic and, stresses related to the Alpine orogeny of northwest Europe (Boldreel and Andersen, 1998).

Following the uplift and compression that led to the progradation of Unit 5a there was a relative sea level rise. However, sediment supply remained greater than the sea level rise and thus during deposition of Unit 5b progressive north- and northeast-ward progradation continued. During the deposition of Unit 5b there was a component of aggradation and parallel stacking of topsets. Aggradation suggests that

uplift had ceased or was much reduced at this time. Generation of accommodation space is interpreted to have been mainly controlled by post-rift subsidence, with no indication of a eustatic sea level rise (cf. Haq et al., 1987).

Depositional package 6 (DP6)

The relative sea level rise and deposition of sub-marine fan deposits together with a lack of shelfal deposition occurred during DP6. At the end of deposition of DP5 the south-western part of the FSC represented a low relief shelfal area (Fig. 6.17a). The seismic character and restricted sediment distribution of DP6 was probably caused by major structural movements in the northwest and south of the study area, perhaps along the fault-complexes uplifting and folding deep Mesozoic structures. This uplift of the shelfal area in the south forced sediment basinward where it onlaps onto folded underlying strata. There is evidence that the uplift was associated with compressional tectonics, and coeval mechanical folding of the strata, best observed in the southern part of the FSC where the Foinaven Monocline was formed.

Depositional Package 7 (DP7)

In the southern FSC, a transgression occurred following deposition of DP6 creating accommodation for the progradation and aggradation of DP7. Progradation and aggradation of the shelf-slope system that forms DP7 and in particular the aggradation represented by parallel stacking of topsets, indicates that the relative sea level rise was controlled by either (1) a eustatic sea level rise, (2) post-rift subsidence, sediment loading and compaction or, (3) a combination of all. The onlap and thinning of DP7 onto the Foinaven Anticline, suggest that this anticline was a positive relief feature formed by structural growth and basin inversion. This is based on thickness relationship of the packages below and above the Foinaven Anticline, which indicates that deposition of DP7 was locally influenced by the growth of this structure. It is not possible to correlate the growth of the Foinaven Anticline and the cyclicity of Unit 7a-7f (i.e. the shifting of the locus of deposition) with the short-term sea-level curve of Haq et al. (1987) due to limited well constrain on each unit. However, since the long-term sea-level curve (Haq et al. 1987) shows a general sea

level fall during Middle Eocene, eustasy is not thought to have controlled the relative sea level rise during the deposition of DP7.

The relative sea level rise is therefore more likely controlled by post-rift thermal subsidence. In this case, it is interpreted that generation of accommodation space that is controlled by subsidence is at times locally reversed due to flexural folding (of the Foinaven Anticline) occurring in the deep-marine basin, controlled by horizontal compressional forces. The erosion and chaotic-fill reflectors of Unit 7d could indicate a minor relative sea level fall related to a pulse of compression, associated with the growth of the Foinaven Anticline, that affected the otherwise subsiding basin.

Depositional Package 8-10 (DP8-10)

The relative sea level fall, that lead to the abandonment of the progradation of the shelf-slope (DP7) and the change in local depocentre could be controlled by an eustatic change in sea level or by uplift. This led to the by-pass of the shelf and the deposition of basin-floor deposits. The uniform thickness and the radiating on-lap reflectors onto the slope of DP7 and onto the Foinaven Anticline, indicates that DP8 was deposited during tectonic quiescence. The fall in relative sea level correlates with first-order eustatic sea-level curve of Haq et. al. (1987). Suggesting that this could have been a controlling factor.

The on-lap and thinning of Unit 9a onto the Foinaven Anticline indicates a second phase of growth of the Foinaven Anticline probably controlled by horizontal compressional forces. The timing of this inversion occurred sometime during the Oligocene. Oligocene compressional tectonics has been documented southwest and south-southwest of the study area, in the Wyville-Thomson Ridge Complex (Boldreel and Andersen, 1993) and West Lewis basin (Earle et al. 1989; Boldreel and Andsersen, 1993). Off mid-Norway, compressional tectonics, with a late Oligocene-Miocene age, is also documented, for example the Nalgfar and Vema Domes (Hjelstuen et al., 1997). Oligocene inversion is furthermore, contemporaneous with the second phase of the Alpine orogeny of the northwest Europe (e.g. Ziegler, 1988)

for example in the Weald and Central Channel basins in southern England (Chadwick, 1985), and in the West Netherlands Basin (Bodenhausen and Ott, 1981).

As was interpreted for DP7, the compressional forces that prevailed during the deposition of Unit 9a only affected a local area over the Foinaven Anticline, where there is local thinning. As a result, deposition in the area east of the Foinaven Anticline was not effected by compressional deformation/uplift. Instead, a relatively even thickness of sediment was deposited controlled by post-rift thermal subsidence. This post-rift subsidence correlates into adjacent area. For example in the Wyville-Thomson Ridge Complex, Late Eocene and Oligocene sequences fills pre-existing lows (Boldreel and Andersen, 1993).

The Late Eocene/Early Oligocene (DP8-10) was marked by a rearrangement of the basin configuration compared to during the deposition of DP7. Apart from the local inversion during the deposition of Unit 9a (the Foinaven Anticline) slow post-rift subsidence controlled. The locally deposited DP10 was related to a marked sea level fall controlled either by eustasy or uplift. DP10 can be correlated with a glacial event recorded at the Oligocene/Miocene boundary (ca. 23.7 Ma) by Miller et al., (1996) that also correlates with a eustatic low (Haq et al., 1987) (Chapter Three). Thus DP10 may be related to this eustatic low (cf. Andersen et al., 2000).

The high volume of coarse-grained sediments that were shed into the basin during deposition of DP8-10, suggest that sediment supply may have been controlled by coeval uplift of adjacent land areas. This suggests that uplift of landmasses and/or basin margins occurred at the same time as post-rift basinal subsidence. This controversial mechanism has been proposed by (Jaspen and Chalmers, 2002). While the mechanism responsible for the uplift remains uncertain, Early Oligocene margin uplift of Fennoscandia (Norway, Sweden and Finland) has been reported (e.g. Eldholm, 2002), in addition the NW margin of Britain (e.g. Jaspen, 1997; Galewsky et al., 1998) and the Irish Sea Basin (Green et al., 2001) show evidence of Neogene uplift, that might have begun earlier in Paleogene times (Clausen et al., 2000).

Following the deposition of DP10, the FSC was yet again affected by compression, locally uplifting the Corona Anticline and the anticline of the East Faroe High. Miocene compression has been interpreted in the FSC (e.g. Andersen et

al., 2000; Ritchie et al., 2003 and Davis et al., 2004) and in adjacent areas, such as the Wyville-Thomson Ridge, Ymir Ridge and Bill Bailey Bank (Boldreel and Andersen, 1993, 1994). In addition, in the area off mid-Norway Miocene compression is thought to have resulted in the formation of dome and arch structures, such as Ormen lange Dome, Helland-Hasnsen Arch (Doré & Lundin 1996), Nalgfar- and Vema Dome (Doré, 1999). However, Hjelstuen et al. (1997) suggests a late Oligocene-Miocene age for the latter two anticlines. Miocene compressional deformation in East Greenland (e.g. in Jamesonland) of Late Miocene age (Price et al., 1997) have been observed. These evidence, suggest that compressional forces affected a wide area of the NE Atlantic margin, resulting in the formation of mainly local "uplift structures" including the Corona Anticline and the anticline of the East Faroe High in the FSC.

Depositional Package 11 (DP11)

The seismic character of Unit 11a suggests that deposition was controlled by distribution of bottom sediments with no direct input of continental sediments.

Depositional Package 12 (DP12)

The marked change in deposition and associated angular unconformity landward on the margin is likely related to tilting of the NW British shelf (Stoker, 2002). Thus the uplift, erosion and input of sediments during deposition of DP12a and 12b was mainly controlled by tectonic forces rather than eustasy. A significant eustatic sea level fall occurred at c. 4.1 Ma (Vail and Hardenbul, 1979). However, this eustatic fall does not explain the seaward tilting of the successions or the change in oceanographic circulation pattern in the basin (Stoker, 2002). The high energy nature of the progradational wedge (Unit 12c) is thus most likely related to tectonic uplift and tilting. Similar prograding wedges have been reported in the Norwegian continental margin (e.g. Eidvin et al., 2000; Stoker, 2002). Coeval to margin uplift, accommodation space was available in the basin and the slope for contourite sediments to be deposited. This indicates that despite the adjacent margins being uplifted, the basin continued to subside controlled by post-rift subsidence.

During the Pleistocene widespread glaciations affected the northern hemisphere (Stoker, 2002) and thus it was a eustatic sea level low. The deposition of Unit 12d during the Pleistocene and Holocene, was thus mainly controlled by glacio-eustasy and also glacial-isostasy/rebound. Glacial rebound, occurring after the ice-sheet started to melt, has controlled deposition and erosion since glaciations by uplifting sedimentary source areas in the hinterland. The tilt of the basal bounding unconformity of DP12 and truncation against the seabed may also have been enhanced by glacial rebound. Bottom-current processes that continue to be active at the present day (Howe, 1996; Masson et al., 2002) have eroded sediments on the seabed in the FSC, in particular in the southwest FSC.

6.6. DISCUSSION: STRUCTURAL INVERSION OF THE FSC

This section discusses the timing and nature of the inversion structures, which have been defined in the previous sections. The aim is to give a collective overview of the development of the inversion features in the FSC with respect to age, trend, orientation (with respect to the underlying structural lineaments; Chapter Three), and to regional stresses. This is in order to understand the evolution of the features and hence find driving mechanisms for their formation.

Timing and Nature of Inversion Structures

Four main phases of uplift and compression of the basins within the FSC occurred during the Middle Eocene, Oligocene and Middle Miocene. Each of these main phases is discussed below.

Phase 1: The formation of the NW-SE trending Foinaven Monocline occurred in the southern FSC over the South Westray Ridge, during the early-mid Lutetian. The development of the Foinaven Monocline (i.e. folded strata) suggests that the uplift was associated with compression, and it is likely that the coeval uplift of other highs (e.g. the East Faroe High and the North Westray Ridge) were also accompanied by folding.

Phase 2 and 3: The basin inversion that formed the NW-SE trending Foinaven Anticline occurred during the Middle Eocene, post early-mid Lutetian (Phase 2) and also during the Oligocene times (Phase 3). It is possible, that the Foinaven Anticline was subsequently affected by additional compressional forces, which is indicated by the considerable erosion of the Eocene and younger strata over the Foinaven Anticline, evidenced in the southern length of its axial length (Fig. 6.4a).

Phase 4: In the Middle Miocene the central part of the FSC was affected by compressional forces that lead to basin inversion and folding above/over Mesozoic Highs. The Corona Anticline was formed and the Mesozoic East Faroe High was folded into an NE-SW trending anticline (Andersen et al., 2000), which on the basis of above (Phase 1) must represent a second phase of uplift and compression of the East Faroe High. In the northern part of the FSC seventeen Middle Miocene aged small-scale anticlinal folds have been identified, that predominantly trend NE-SW

(Davis et al., 2004). Also Ritchie et al. (2003) has identified NE- and NNE trending anticlines of early-mid Miocene age in the FSC.

Obvious physical relationships between the Foinaven Anticline and the Corona Anticline can be compared, although it seems that more dissimilarities can be detected. In both cases depocentres have been inverted and no faults are obvious. In contrast, they have formed at different geological time and the axial trends are largely perpendicular to one another. Each anticline was also developed during very different geological settings and depositional environments as indicated by the syn-tectonic strata. The Foinaven Anticline was developed in a shelf-slope environment not long after initial opening of the North Atlantic. The Corona Anticline however, was formed in a deep-marine setting that had undergone the main part of post-rift subsidence farther away from spreading centre of the North Atlantic. It is apparent that the position and orientation of the Foinaven Anticline is related to the underlying basin-configuration that previously during Phase 1 had been uplifted; the Foinaven Monocline in the south, the Judd Platform situated to the southwest, the East Faroe High in the northwest and the Westray Ridge to the northeast, all formed a "barrier" to subsequent sediment distribution (DP6). The interrelationship between basement configuration (Chapter Three) and trend of the Foinaven Anticline is also apparent by the subtle bend in the axial trend of the anticline in the south, from NW-SE to slightly WNW-ESE. Where this change in orientation occurs, the Judd Platform that is aligned parallel to the axis of the Foinaven Anticline, extends no further north (Fig. 6.1, B). Therefore, the Foinaven Anticline is most likely to have formed due to restraining bend as a result of compressional forces that pushed/buttressed the soft Early Paleocene sediments against the harder Mesozoic rocks (see chapter Seven; discussion and Fig. 6.13). It is possible that the compression was associated with the reactivation of normal faults, although evidence for this is obscured beneath lavas that have adversely affected the seismic profile (Chapter Three). Compressional features have been documented in the Faroe-Rockall area that shows WNW-ESE and NW-SE axial trends, similar to the Foinaven Monocline and the Foinaven Anticline. An example is the Wyville-Thompson Complex and the Munkagrunnar Ridge, which formed initially in the Early Eocene (Boldreel and Andersen, 1998). These structures

seem to be located close to the NW-SE Judd transfer system, suggesting that the anticlinal features might have been controlled by transfer faults (see discussion in Chapter Seven and Fig. 7.7). The Corona Anticline, has an axial trend approximately perpendicular to the NW-SE directed sea-floor stress regime, indicating that the formation of the Corona Anticline was related to compressional forces associated with the North Atlantic spreading (cf. Boldreel and Andersen, 1993).

Ruling-out that the anticlines in the FSC are caused by sediment loading

This section discusses whether the inversion structures discussed above could be an artifact associated with sediment compaction and thus sediment loading.

In the FSC during the development of the Foinaven Anticline in the southwest, coeval progradation of a major (750ms thick) delta system occurred in the south. The orientation of the anticline axis is parallel to the direction of progradation and sediment transport of the delta. Furthermore, the location of the anticline is west of the main depocentre of the delta and maximum uplift of the anticline is in the northern part of its axis. If they were related it would be expected that main compression and uplift was in the south, in front of the main depocentre, with the fold axis trending perpendicular to the sediment transport direction. This is thought to be the case with the Helland-Hansen Arch where folding has been interpreted to have occurred as a result of sediment loading (e.g. Skogseid and Eldholm, 1989). However, the second phase of inversion of the Foinaven Anticline in the southwest, occurred during a different depositional setting, deep marine basinal deposition compared with the build out of the delta system during the first phase. On the basis of the timing-, location- and characteristics-of the inversion feature in the southwest FSC the basin inversion is unlikely to be linked to the build out of the delta and thus sediment loading is unlikely to have been a cause of inversion in the FSC.

On the Norwegian margin, the N-NE trending Helland-Hansen Arch, which is the largest anticline on the margin, has previously been interpreted to be a result of differential subsidence due to a large Pliocene-Pleistocene wedge prograding from

the east (Skogseid and Eldholm, 1989; Stuevold et al., 1992). However, this has been ruled out by Lundin and Doré et al., (2002) because of the complex evolutionary pattern of the anticline, which cannot be the result of differential loading.

In general, it is unlikely that sediment loading is a major mechanism for the inversion features on the North Atlantic continental margin since it fails to explain the complex development of the structures. Furthermore the widespread occurrence, the orientation and the development of these inversion features that apparently occur in phases suggests that these features cannot be explained in terms of sediment loading (see Chapter Seven). Thus sediment loading is ruled out as a generic mechanism although it might have a local modifying effect. For example, in the FSC sediment loading subsequent to folding may have enhanced the flexure of the Foinaven Monocline.

The generic link of the inversion features in the FSC to for example the ocean-floor history and to mantle-plume will be addressed in Chapter Seven.

6.7. SUMMARY

This chapter continued from Chapter Five the investigation of the Eocene to Present succession in the study area (Fig. 6.1). The available data allowed the Eocene to Present interval to be divided into eight depositional packages; DP5 represent a widespread N and NE prograding delta system; DP6 represents infilling of basin topography; DP7 is a NW prograding shelf slope system; DP8-10 consists of slope fan and basin-floor deposits and marks a shift in depocentre from shelf-slope progradation (DP7) to slope and basin deposition (DP8-10); DP11 and DP12 represents of deposition along a narrow zone of the FSC margins and consists of contourite drift deposits (e.g. Stoker, 2002; Knutz and Cartwright, 2003). However, the uppermost units consist of glacial deposits e.g. Unit 12c consists of a SE prograding shelf slope system deposited during relative sea level fall controlled by tilting and uplift. The onset of tilting in the early Pliocene pre-dates, and may have been a cause of widespread continental glaciations (Stoker, 2002).

It is evidenced from the stratigraphic interpretation that the depositional packages (DP5-DP12) were deposited during thermal post-rift subsidence; however, the generation of accommodation space that is controlled by subsidence is at times locally reversed due to flexural folding occurring in the deep-marine basin, controlled by horizontal compressional forces.

This study has identified compressional structures and demonstrated the timing and nature of these. Inversion occurred in at least four phases; in the Middle Eocene (early-mid Lutetian and post early-mid Lutetian), the Oligocene and the Middle Miocene.

Formation of the NW-SE trending Foinaven Monocline occurred in the southern FSC over the South Westray Ridge, during the early-mid Lutetian. The marked change in sediment distribution related to DP5/DP6 suggests furthermore that Westray Ridge and also the East Faroe High were uplifted during this compression phase that also indicates a marked change in basin-physiography.

The NW-SE trending Foinaven Anticline developed in the south-western part of the FSC during the Middle Eocene, post early-mid Lutetian (Phase 2) and also during the Oligocene times (Phase 3). The scarps above the Foinaven Anticline are interpreted to be normal extensional faults, that formed in response to uplift and local stretching (outer arc extension) of the seabed in response to growth of the Foinaven Anticline, that later became enhanced by considerable erosion by deep-water bottom currents.

The compressional forces that prevailed during deposition of DP7 (Phase 2) and Unit 9a (Phase 3) only affected a local area over the Foinaven Anticline, where there is local thinning. As a result, deposition in the area east of the Foinaven Anticline was not effected by compressional deformation/uplift. Instead, a relatively even thickness of sediment was deposited controlled by post-rift thermal subsidence.

The Corona Anticline was formed in the north-western part of the FSC during Middle Miocene.

SECTION THREE:

DISCUSSION AND CONCLUSIONS

CHAPTER SEVEN

7.0. DISCUSSION: DRIVING MECHANISMS

7.1. INTRODUCTION

The main objective of this chapter is to discuss the Tertiary (early Palaeocene to Present) tectonic and sedimentary response to the dynamics (vertical motions) associated with the evolution of the VPCM of the FSC. The main observations documented in Chapters Four to Six will be integrated with other relevant studies carried out in this area and the major implications discussed. The chapter is divided into two sections. The first section discusses the sedimentary response to late Palaeocene-earliest Eocene (early Paleogene) uplift, especially the uplift event associated with incision (Chapter Five). The time-constrained uplift events in the FSC are compared to uplift events on a regional scale (such as in East and West Greenland and in Southern England) and the temporal and spatial interplay between sedimentation, erosion and igneous activity is discussed with respect to the evolution of a mantle plume, related to the LIP's of the North Atlantic, that is thought to have influenced the dynamics of the North Atlantic VPCM in the early Tertiary (e.g. Eldholm, 2000). The second part of this chapter discusses the possible mechanisms forming the inversion features identified in the FSC that developed in phases during the Middle Eocene and Middle Miocene post-rifting (Chapter Six). The time constrain on each inversion event (Chapter Six) and the axial orientation of the inversion features with respect to underlying basement structuration (Chapter Four and Six) is discussed and compared with the temporal and spatial development of other inversion features present both on the NE and NW Atlantic margin (e.g. Lundin and Doré, 2002) in order to understand their generic mechanisms.

7.2. EARLY PALEOGENE UPLIFT: SEDIMENTARY RESPONSE TO MANTLE PLUME

The most important observations that emerged from Chapter Five is: 1) that deposition of the Paleogene stratigraphic interval DP1-DP4 occurred coeval to volcanic activity. This is evident from the volcanic and volcaniclastic content of DP1-DP4 (the kettla Tuffs present at the base of DP1, Basalt 3 within DP3, Basalt 4 and the Balder Tuffs within DP4). Thus, thermal dynamics occurred coeval to deposition of DP1-DP4 and 2) The evidence that relative sea level fall associated with the incised drainage network (consisting of numerous tributaries that fed into a major 400 meter deep NNW-SSE trending channel), cannot be caused by eustasy alone. Furthermore, since there was no fault activity and given that incision occurred immediately prior to extrusion of the Upper Series of the FPLG, it is likely that the incision represent an episode of thermal uplift related to a mantle plume. These observations (1-2) indicate that the sediment erosion and distribution related to DP1-DP4 allow a direct look at the surface expressions related to mantle plume evolution. This section discusses: 1) evidence for mantle plume, 2) evidence for plume in the sedimentatary record in the North Atlantic region, 3) the effects on sedimentation patterns due to plume emplacement and upward displacement of the lithosphere 4) comparing plume models to the interpreted sediment history in the NE Atlantic/Faroe Shetland Channel.

1) Evidence for mantle plume

There have been controversies about the mantle plume theory that was initially developed by Morgan (1971). Some workers object to the plume theory (e.g. Mutter et al., 1988; Anderson et al., 1992, 1998). However, it is generally accepted that the igneous distribution of the North Atlantic Igneous Province (NAIP) present within a pre-drift radius of 2000 km (Fig. 7.1) and the evidence for simultaneous eruption within this radius cannot be explained by simple mantle convection, but is more specifically associated with a mantle plume. Furthermore, geochemical evidence indicate, that the basalts from the Baffin Islands have a mantle plume source (Stuart et al., 2003). In addition, the presence of thermal-, gravity-, geochemical-, and

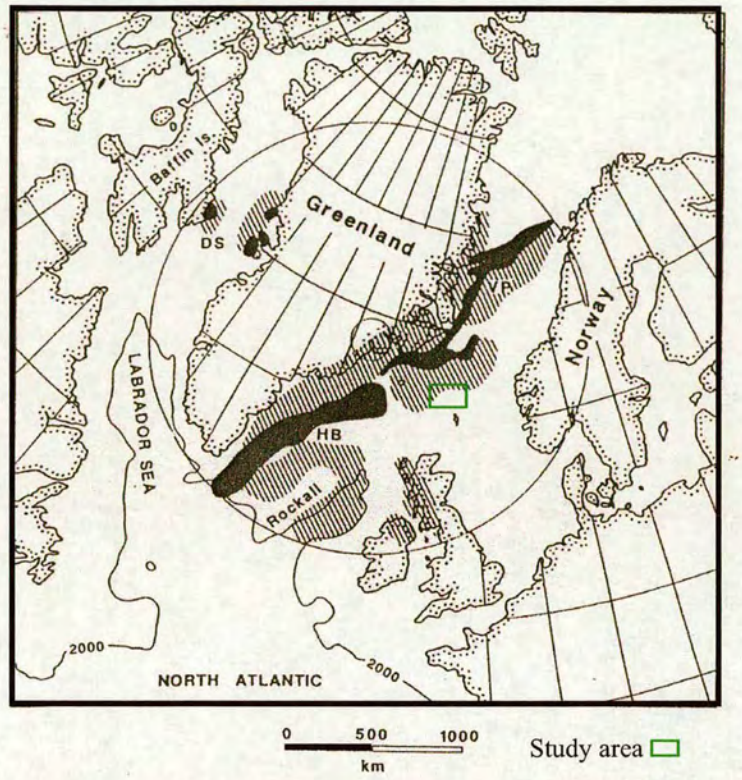

Figure 7.1 Reconstruction of the North Atlantic region, just after the onset of oceanic spreading (c. 55 Ma). The circle shows the extent of early Tertiary volcanism, that occurs within a radius of 2000 km (solid shading and hatching). The volcanism has been associated with the Iceland mantle plume, that was beneath East Greenland at the time of break-up (from White and McKenzie, 1989).

topographic-anomalies beneath present day Iceland lends powerful circumstantial support for similar anomalies existing in the past (Saunders et al. 1997). Moreover, the thick oceanic crust associated with Iceland and the Greenland-Iceland-Faroes Ridge (Fig. 7.2) is convincing evidence that a thermal anomaly, presumably a mantle plume, resides beneath Iceland (e.g. Saunders et al., 1997). On the basis of the above, evidence for an ancestral mantle plume and the independent evidence from the sedimentological history of the FSC (this study) supports the mantle plume theory.

2) Evidence for plume in the sedimentatary record in the North Atlantic region

Evidence for mantle plume-related uplift in the sedimentary record on a regional scale

This section discusses the early Tertiary sedimentary response to the uplift history related to a mantle-plume that is thought to have affected the North Atlantic region between NW Europe and Canada (e.g. White and McKenzie, 1989) (Fig. 7.1 and 7.2). The main aim is to put into context the sedimentary history, in particular the regressive-transgressive sequences observed in the surrounding region (e.g. West Greenland and East Greenland; Dam et al., 1998) and in the FSC (Chapter Five) to the transient history related to a mantle plume.

The response in the sediment record to vertical movements (i.e. uplift of the earths surface) is the formation of major unconformities; due to erosion, peneplanation and incision (e.g. Rainbird and Ernst, 2001). Another response is deposition of this material into the adjacent lows/basins. Vertical movements that result in uplift of the continental crust, are primarily controlled by crustal shortening, extension or epeirogenic movements, the latter being related to underplating or a hot, ascending mantle plume (e.g. McKenzie, 1984).

Field studies in West and East Greenland have documented the presence of incised valley systems (termed the Paatuut and Tupaasat valley fills; Dam et al., 1998) that are thought to have been created and filled/preserved through a phase of coupled uplift and subsidence during the Early Palaeocene. The drainage network is particularly well exposed along the south coast of Nuussuaq in West Greenland where the Early Palaeocene Quikavsak Formation fills and drapes individual incised

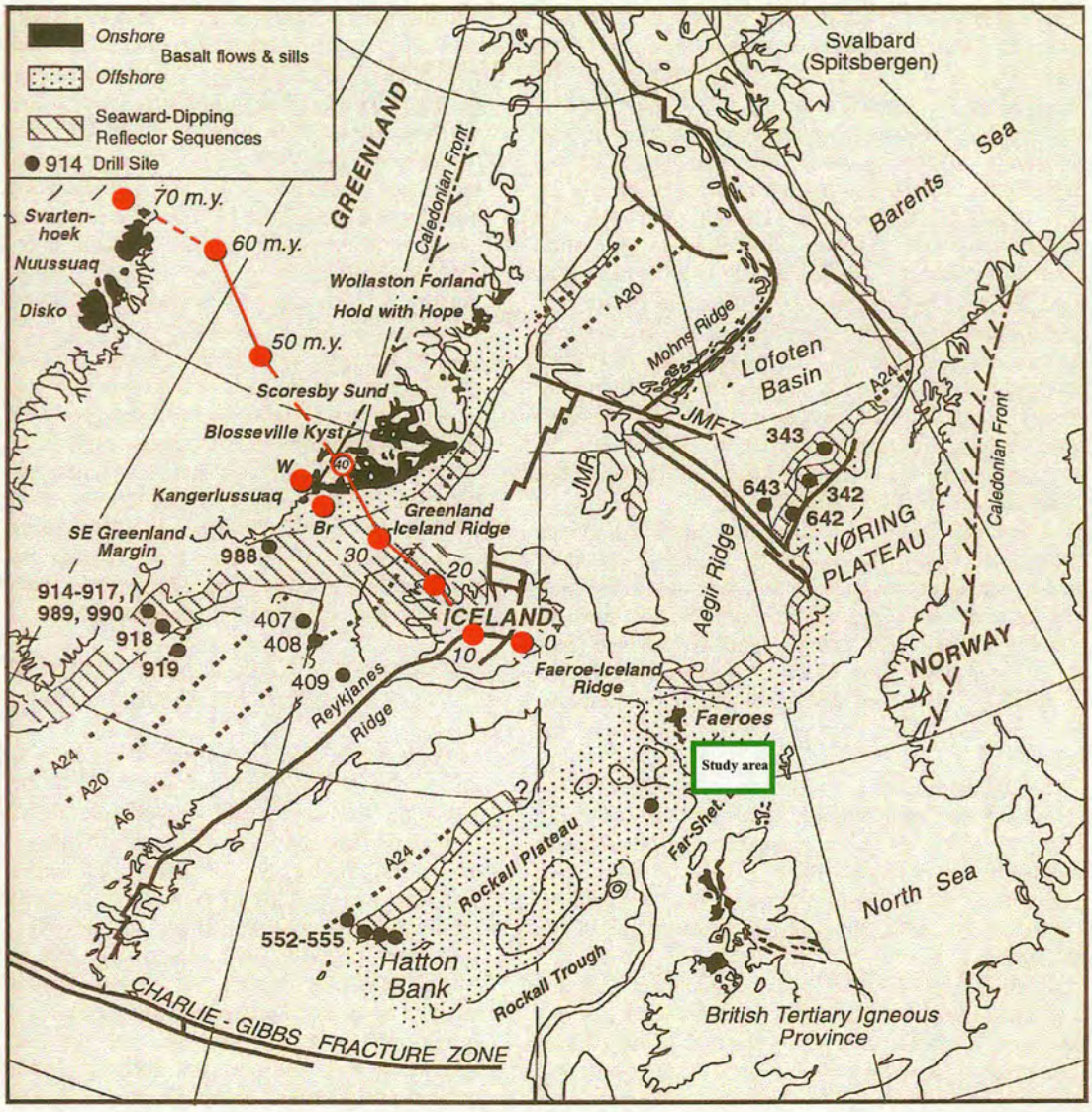

Figure 7.2. Map of the North Atlantic region showing the extent of the NAIP, and the assumed locations (in red, full circles) of the ancestral Iceland mantle plume by Lavwer and Muller (1994). Alternative location of plume axis (White and Mckenzie, 1989) are shown (in red, open circle) by W, at anomaly 24 times (from Saunders et al. 1997).

valleys that locally cut down up to 200 m into the marine sediments ascribed to the Atane Formation (Dam et al., 1998) (Fig.7.3). Significantly, the palaeo-valley system of East Greenland occurs immediately below transgressive marine mudstones, hyaloclastite breccias and flood basalts that form the lower part of the Upper Palaeocene volcanic pile. This stratigraphic relationship indicates that uplift that drove the incision was followed by a phase of rapid subsidence prior to extensive volcanic activity at ca. 61 Ma (Chalmers et al., 1995b). Recognition of the stratigraphic relationships and the close temporal link to the volcanics led Dam et al. (1998) to interpret their formation and preservation to a coupled uplift and subsidence associated with the ascending Iceland mantle plume.

The major question that arises from the genesis and timing of the coupled uplift and subsidence in the West and East Greenland locations is whether their occurrence is linked in any way to the incised drainage network developed in the Early Eocene of the FSC (Chapter Five).

Given the Early Palaeocene age of the formation and fill for the West Greenland incised valley system and the Early Eocene age of the incised valley system for the southern FSC, there would appear to be no temporal link between the two systems (Fig. 7.3). However, their striking similarity in stratigraphic, sedimentological and volcanic relationships suggests that there may be a generic causal mechanism. On the basis of the coeval presence of a mantle plume and its dynamic characteristics that affect the surface above its axis, the most obvious mechanism is coupled uplift and subsidence associated with the mantle plume. These relationships, allows one to speculate that the valley incision, fill and drape events represent the sedimentary response to *two* episodes of transient uplift and subsidence. The first episode occurred in the Lower Palaeocene (between ca. 63-61 Ma) and had the greatest effect in West and East Greenland; the second/final episode occurred in the late Upper Palaeocene-Early Eocene (between ca. 56-54.7 Ma) and was most marked in the FSC.

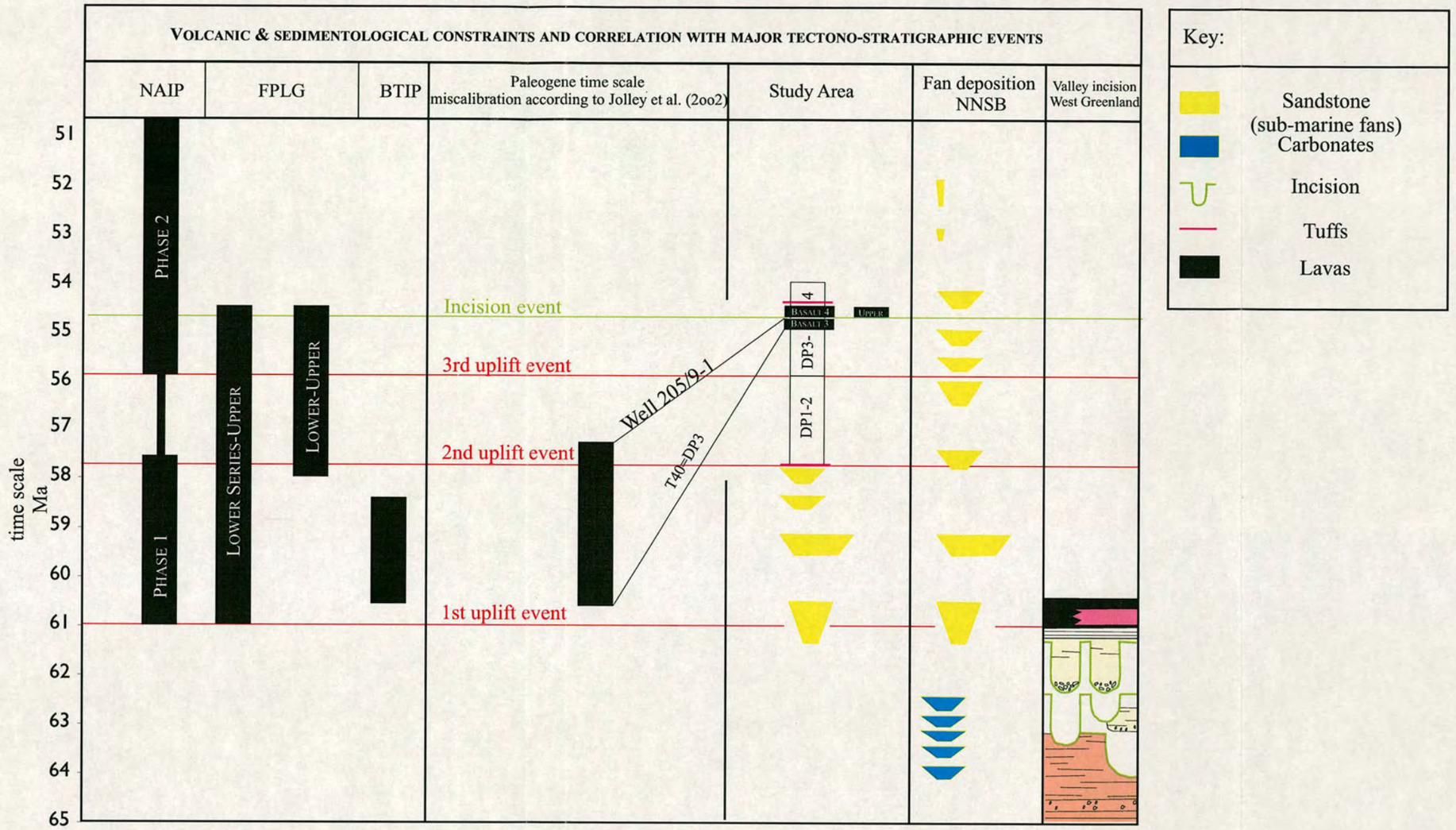

Figure 7.3. Event and correlation chart, showing from left to right: 1) presumed ages of the NAIP=North Atlantic Igneous province, from Saunders et al., 1997, 2) Ar-Ar age dates and magnetostratigraphic age dates for the FPLG=Faroe Plateau lava Group respectively, from Waagstein, 1996; Waagstein and Riisager, 2002, 3) presumed ages of the BITP, from Chambers and Fitton, 2000 4) the proposed age for volcanics equivalent to Basalt 3 and the T40 sequence of Ebdon et al. (1995) from Jolley et al., 2002, 5) depositional packages and inter-related Upper Series of the FPLG, Basalt 3 and Basalt 4, the kettla tuff and the balder tuff encountered in the Paleogene interval of sudy area (see text), 6) submarine fan deposition in the FSC and NNSB, from White and Lovell, (1997) 7) deposition of shallow marine and terrestrial sediments, incision and volcanism, example from West Greenland, from Dam et al., 1998. In solid lateral lines (in red) is shown the timing of proposed uplift events of this study (see text).

Evidence for mantle plume related uplift in the sedimentatary record the FSC and the Northern North Sea area.

The study carried out in previous chapters Three and Five, indicate that at least three phases of uplift occur, during (i) the Early Palaeocene (e.g. Naylor 1999), (ii) the mid Palaeocene, and (iii) the late Upper Palaeocene/early Eocene (Fig. 7.3).

The first and final episodes of surface uplift can easily be constrained by the sedimentology, stratigraphy and volcanism (in East and West Greenland and in the FSC). In the FSC the clastic sediments and the contemporaneous volcanics and volcaniclastics of depositional packages DP3-DP4, indicate that the Paleogene stratigraphic interval can be temporally constrained with the second phase of volcanism of the NAIP, identified by Saunders et al., (1997) (Fig. 7.3). The igneous activity related to the NAIP has furthermore been independently linked to the evolution of a mantle plume, suggesting that the uplift is related to a mantle plume. Dam et al. (1998) suggested the uplift (related to the first uplift phase) that drove the incision and the following phase of rapid subsidence and volcanic activity was in accordance to the plume theory by Campbell and Griffiths (1990) (see Chapter Two). The depositional history of DP3-DP4 in the FSC (Chapter Five) indicates that the uplift associated with the second phase of volcanism is more complex (i.e. the presence of Basalt 3 and Basalt 4) and may be related to more than one uplift episode, the incision being part of the last uplift phase. Each uplift phase from observations in the FSC (Chapters Three and Five) and in the NNSB will be discussed in the following section.

3) The effects on sedimentation patterns due to plume emplacement and upward displacement of the lithosphere

First Phase of uplift

The Early Palaeocene depositional system in the FSC and NNSB records a major change in deposition, from carbonate- to clastic-dominated, mainly submarine fan complexes (Fig. 7.3). This change has previously been associated with uplift and exhumation related to the onset of magmatism (e.g. Parker 1975; Rochew, 1985, Naylor et al. 1999; Morton, 2000). Furthermore, White and Lowell (1997) suggested

that the repeated influx of coarse clastics form the sub-marine fan complexes in the FSC, were associated with pulsing of the ancestral mantle-plume. They argued that each pulse of clastic input was linked with a discrete phase of volcanic activity based on their similar age relationship. Apatite Fission Track Analysis (AFTA) on fan sandstones in the FSC indicate that the main sediment source was from the Shetland Platform, thus indicating that uplift of the NW British region occurred during the Early Palaeocene (e.g. Roberts, 1989; Morton, 2002). The main plume axis of the ancestral mantle plume was according to Lawver and Müller (1994) located beneath West Greenland during the Early Palaeocene (Fig. 7.2). Thus, the FSC and northern North Sea basins (NNSB) were situated in a more "distal" position relative to the plume axis during the Early Palaeocene. If the plume was situated beneath West Greenland, the coeval uplift recorded in NW Britain implies that the surface uplift associated with the plume did not simply decrease radically away from a central plume axis (beneath West Greenland). Rather, plume uplift was manifest by a central maxima (West Greenland during Early Palaeocene) with additional smaller plume/magmatic related uplifts occurring in the surrounding region (NW Britain region). Volcanics that are of the same age are found in both West Greenland and NW Britain (e.g. Saunders et al. 1997) (Fig. 2.13 and 7.3). This suggests that they are part of the same volcanic event (related to mantle plume) and thus have the same source. Coarse clastic sediments were thus not simply radiating away from a central bulge, rather sediment transport was also coming from additional highs. In the case of the FSC, sediment transport also occurred from NW Britain region, during the Early Palaeocene.

Second Phase of uplift

Following deposition of the deep marine fan system in the FSC during the Early Palaeocene, the change in basin-configuration and local deposition of a major delta system during the Mid-Palaeocene (ca. 56 Ma) is related to uplift (Chapter Five). Although the stratigraphy indicates no direct temporal link of volcanism, the marked shift in depositional environment from deep marine fan complexes to a shelf-slope delta system, the massive progradational fine-grained sediment input (ca. 750 m.sec.

thick interval) and the restricted occurrence locally in the southern FSC, can best be explained by a sediment source deriving from a locally uplifted region in the NW, as indicated from the dip of the seismic clinoforms of the delta. Stratigraphically this sequence is time-equivalent with basalt flows of the Lower Lava Series of the Faroe Islands (Fig. 7.3). Thus it is likely that this local uplift event was related to mantle plume uplift.

Earliest Eocene

In the FSC progradation of a deltaic depositional system occurred during the Late Palaeocene-early Eocene (during uppermost Lamba Formation and Colsay Sandstone Member and Hildasay Sandstone Member of the Flett Formation). Subsequently the delta system was incised (during the intra Hildasay Sandstone Member) and following a transgression, the incised valley system was filled with estuarine deposits (Chapter Five). The interpreted stratigraphic interval recording uplift and subsequent subsidence indicates that this event occurred over a total time interval of ca. 2 My (Fig. 5.19). However, the presence of two basalt intervals (Basalt 3 and Basalt 4) within this stratigrapic interval (DP3 and DP4), especially the locally sourced lavas of Basalt 3 (Chapter Five), suggests that this uplift event that ultimately led to the incision may represent a complex history of at least two pulses of uplift. The first uplift event resulted in a basinward shift in facies and progradation of the delta system, subsequently covered by Basalt 3, a regional event that led to the widespread extrusion of lavas (e.g. in Scotland and the Faroes). The area was subsequently incised and Basalt 4 was extruded into the valleys. The extrusion of this younger basalt (Upper lava Series, Basalt 4) may have been related to a second discrete uplift and thus the uplift and incision of the valley system may have occurred in a period of less than 1 My.

The depositional delta system (DP3) predates the incision/unconformity. The deltaic interval belonging to the Colsay Sandstone Member (DP3) also contains a basalt interval (Basalt 3); locally present seismically and encountered in well 205/9-1. Biostratigraphic assemblages of the interval immediately beneath and above Basalt 3 in well 205/9-1 is comparable to assemblages of the coal-bearing

horizon in the Faroe Islands which is part of the uppermost Lower Lava Series and overlain by the Middle Lava Series (Ellis et al., 2002). It is also identical with the assemblages seen in the uppermost basaltic lavas of the Erlend lava field in the northern FSC (Jolley and Bell, 2002) and to the palynofloras of the upper Woolwich Formation, and upper Formation de Varengiville of the London-Paris Basin (Ellis et al. 2002). Furthermore, this horizon correlates with a period during the late Paleocene Thermal Maximum (LPTM) by Bujak and Brinkhuis, (1998) (see Chapter Three). The overlying interval of the prograding delta system (DP3) belongs to the Hildasay Sandstone Member is more extensive and leading up to the ultimate uplift and incision documented across the southern and central FSC evidenced in this study.

Within the incised valley fill, basalt flows (Basalt 4) equivalent to the Upper Lava Series of the Faroe Islands are present; imaged seismically and encountered in wells 6005/15-1 and 6004/16-1. Field studies in the Faroe Islands examining the flow-top vegetation of the Upper Lava Series show evidence of terrestrial palynoflora (e.g Taxodium; Ellis et al., 2002). These are comparable to the palynoflora recovered within the fill of Depositional Package 4c in the FSC (this study, see Chapter Five). Thus evidence from the stratigraphic relationship of the sedimentology and the volcanics in the FSC indicate that the shallowing and formation of the incised valley immediately predates the extrusion of the subaerial flood basalts (Upper Lava Series of the Faroe Islands, Basalt 4) and tuff and ash-bed equivalents of the Balder Formation.

Similar patterns of deposition characterize other parts of the Atlantic margin and the North Sea Basin. For example, in the North Sea Basin, in the Bressay area, the coeval stratigraphy show evidence of progradation and incision followed by infilling and drape of a large deltaic complex ascribed to the Dornoch Formation (e.g. Deegan & Scull, 1977; Milton et al., 1990; Jones & Milton, 1994; Underhill, 2001). In SE England the coeval stratigraphy also shows shallowing and incision followed by subsidence. Marine- (Upnor Formation) to continental facies (Reading Formation) are followed by incision (the basal erosive unconformity of the Harwich Formation) that forms a planar or slightly undulose discontinuity

(Knox et al. 1994). Subsequent to incision the Harwich Formation deposits consist of bioturbated fine-grained clastic deposits that at the top are marked by a marine transgressive event (the base of the London Clay Formation). The Harwich Formation also contains volcanoclastics and above the transgessive surface the volcanoclastics are related to the main Balder Formation phase of volcanism (Knox, 1983). This is similar to observations of the fill and subsequent drape of the incised valley network in the FSC.

Based on the correlation of a prominent unconformity (i.e. the incision surface) as discussed above, indicates that the shallowing that led to terrestrial conditions in the FSC (evidenced form the incised valley network and subsequent infilling and the subaerial extrusion of the Upper Faroe Lava Series) can be correlated from the Faroe Islands to at least as far as SE England.

Time scale calibrations

According to Jolley et al. (2002), volcanism in the FSC region occurred during sequence T40, which their time scale dates at 60.56-57.5 Ma (Fig. 7.3). The T40 sequence represents the Flett Formation and thus, is located above the Lamba Formation. It is at the base of the Lamba Formation that a regional marker bed (prominant tuffaceous interval) of the Kettla Member occurs (Fig. 3.5). This indicates that volcanic activity in the FSC region occurred prior to sequence T40. Furthermore, the Isotope dated extinction event related to the Late Palaeocene Thermal Maximum (LPTM), dated at 54.93-54.98 Ma by Norris and Röhl, (1999) and Röhl, et al. (2000) (Chapter Three) is present within T40 (e.g. Ebdon et al., 1995). If the timescale of Jolley et al. (2002) is used, the LPTM is located below Basalt 3, that is correlated with the Lower Series of the FPLG (e.g. Ellis et al. 2002), and thus using the Jolley et al. (2002) timescale would give an age discrepancy of >5 My compared to other studies. Overall the timescale by Jolley et al. (2002) does not seem to fit with the other studies in this area and regionally (e.g. Saunders et al., 1997). However, because of the controversies about the time scale by Berggren et al. (1995), in particular around the 55 Ma boundary (see Chapter Three) it is likely that with new data in the future, revisions to this timescale might be necessary

Evolution of the ancestral mantle plume:

Studies of the NAIP show that immediately prior to continental break-up the hot mantle plume reached its maximum radial extent at c. 55 Ma when magmatic productivity was 2 to 3 times greater than it is at the present day in Iceland (Saunders et al. 1997) (Fig. 7.4). During the time of break-up the mantle plume axis was situated in East Greenland (Lawer and Muller et al. 1994) (Fig. 7.2). The uplift event related to the incision surface (at 54.7 Ma) in the FSC immediately predates the extrusion of SDRS (Chapter Two) in addition to the Balder tuffs all which are related to the continental break-up and initial spreading event. The wide extent of the incision surface in the FSC has been related to uplift and not eustasy in the FSC (Chapter Five). Instead, the unconformity that can be correlated to SE England is related to mantle plume uplift and most likely is a response to the more expanded nature of the plume during the final stage of continental rupture and thus creating a wide uplift region in NW Europe. Furthermore, the fact that the area during late Palaeocene/early Eocene time characterises a more restricted and marine to terrestrial environment (e.g. Mudge and Bujak, 2001) compared with the previous deeper marine environment (e.g. Naylor et al., 1999) is consistent with the nature of the plume, based on the NAIP (e.g. Saunders et al. 1997), indicating that the plume axis initially was less expanded and less focused to the rift zone, but later showed more local effects as seen in the FSC during the second phase of uplift. In contrast, uplift that corresponds to the stratigraphic intervals leading up to continental rupture was more widespread.

Early Tertiary Burial History

Analysis of burial curves by Nadin et al. (1997) from the West of Shetland and Northern North Sea sedimentary basins show that there is a significant "perturbation" of the predicted Palaeocene post-rift burial history following Mesozoic extension, which can only be explained by regional uplift followed by decay to the present-day. Nadin et al. (1997) have calculated that the total magnitude of the uplift increased towards the northwest and was around 900m in the vicinity of the Faroe-Shetland Basin and 375m in the Moray Firth (Nadin et al.,

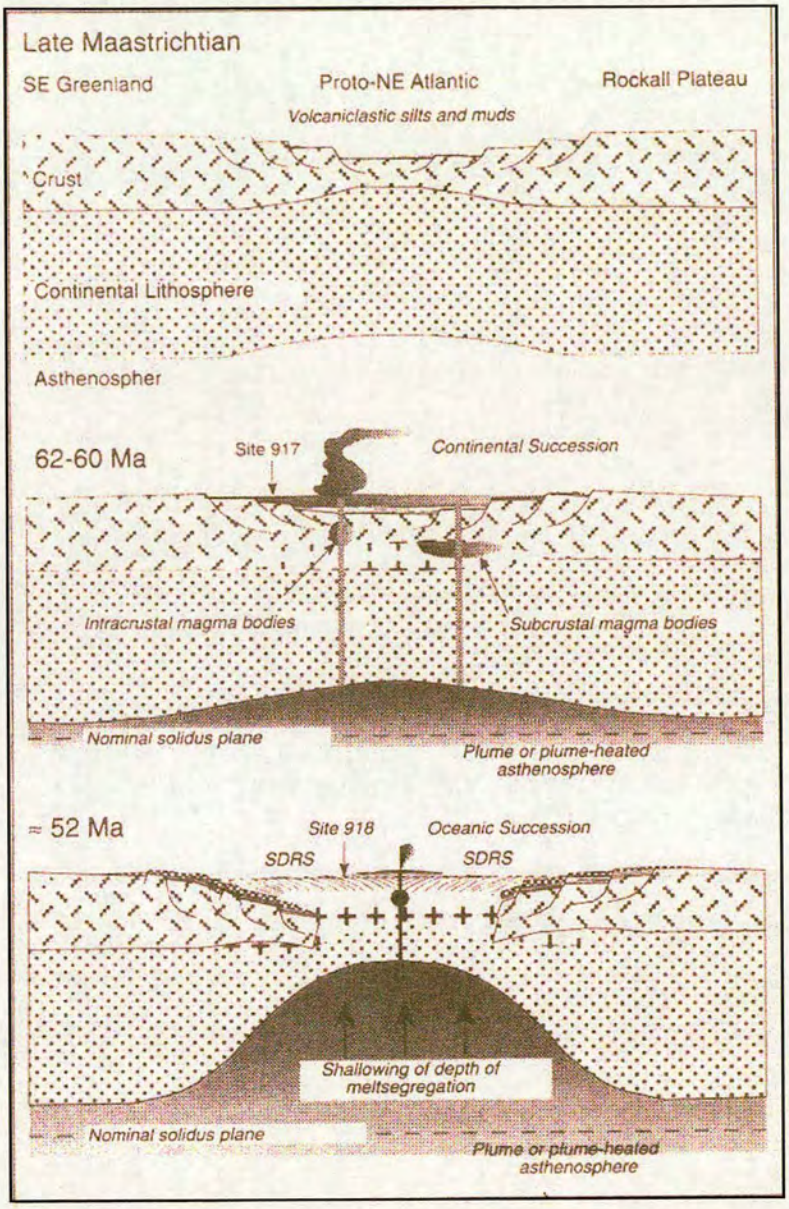

Figure 7.4. Schematic reconstruction of the southern northeast Atlantic during the Paleogene,showing the development of the rifted margin and the contemporaneous magmatism. (from Saunders et al. 1998).

1997). The uplift has been interpreted to be the result of the ascending Iceland mantle plume. The findings of their study suggest a decreasing uplift away from the plume axis. The apatite fission track analysis of the early Paleaocene, suggesting uplift of the Shetland Platform (NW Britain) and sediment transport towards the plume axis may be compatible with their results, but suggest a more complex uplift pattern. Regardless, all these observations suggest that the incised valley network revealed in the southern FSC records the final stage of a greater, regional uplift event superimposed on an existing structural framework, and the first stage of its decay.

4) Comparing plume models to the interpreted sediment history in the NE Atlantic/Faroe Shetland Channel; Generic mechanisms

Transient plume uplift provides an attractive means to explain the departure that the burial history curves show from that expected by classic post-rift basin subsidence following Late Jurassic rifting (Bertram & Milton, 1989; Milton et al., 1990; Barr, 1991; Nadin & Kusznir, 1995). The interpretation discussed above is consistent with this conclusion, albeit with the important caveat that the deflection can now be thought to be the result of at least two well-defined phases of plume-related transient uplift and subsidence.

Given the regional extent of uplift and subsidence, the rates involved and the synchroneity of igneous activity, the sedimentary record can be confidently ascribed to mechanical deformation of the lithosphere linked to a mantle plume. This is based on the stratigraphic study of the FSC (Chapters Three and Five) and the regional correlation of the early Tertiary sedimentary succession and the extent, nature and timing of volcanism. The upward motion of the plume could correspond to an increasing dynamic component of surface uplift and accompanied by in-plane stresses, which would decay away following lithospheric rupture and the onset of sea-floor spreading. There are two alternative models for the fluid dynamic nature of the plume. These are (1) the theoretical fluid dynamic model by Campbell and Griffiths (1990) that predicts uplift, followed by subsidence and volcanism and that significant uplift begins 10-20 m.y. before onset of volcanism and (2) that the

volcanism exploited lines of weakness (e.g. thinspots) in the lithosphere, so that channeling of hot mantle into pre-existing thinspots restricted magmatism to localised areas (e.g. Graham et al., 1998; Storey et al., 1998; Saunders et al., 1998) (Fig. 7.5 and 7.6). The Palaeocene-Early Eocene regressive mega-sequence of the FSC (Duindam &van Hoorn, 1987), which this study (chapter Five) has documented to shows evidence of discrete phases of uplift and subsidence evidenced by a series of shallowing-up sequences overlain by transgressive sequences separated by an unconformity. This could be explained to have occurred as a result of episodic or pulsing uplift events. In addition, the main sediment input from NW Britain, including the drainage direction of the incised channels in the FSC during the early Eocene supports channelling and local uplift along zones of weakness. Pulsing of the plume has previously been suggested from studies of the NAIP (e.g. Saunders et al. 1997; White and Lowell, 1997; O'Connor et al. 2000). The fact that the plume has shown variation in flux through time is consistent with magmatism occurring widespread but also in restricted localised areas (Saunders et al. 1997). Furthermore, this is consistent with the model of "ultrafast" mantle plume by Larsen et al. (1999) and Larsen and Yuen, (1997). They show evidence of very focused magmatic activity and subsequent calm periods, with pulses ranging from a few My to 10 My In addition, O'Connor et al. (2000) suggest on the basis of dredged samples from three Rockall seamounts that volcanic activity took place in pulses on a timescale of 5-10 My dating back to the late Cretaceous. Examination of the extensive and complex sedimentary horizons (ash beds of Rasmussen and Noe-Nygaard, 1970) within the Faroes Lower Series reveals patterns similar to those seen in the British Province, where volcanic activity was markedly pulsed over the time interval 62-56 Ma (Jolley, 1997; Bell and Jolley, 1997). It is therefore possible that the Faroes Lower Series represents a composite sequence of (discontinuous) pulses spread over c. 5 My or less. In the FSC at least three phases of uplift (Chapter Five) with an interval between the first and second uplift phase of ca. 3 My, while an interval of ca. 2 My occurred between the second and the third phases of uplift. Within the third uplift phase there may have been two discrete pulses of uplift as evidenced by the relationship between Basalt 3,

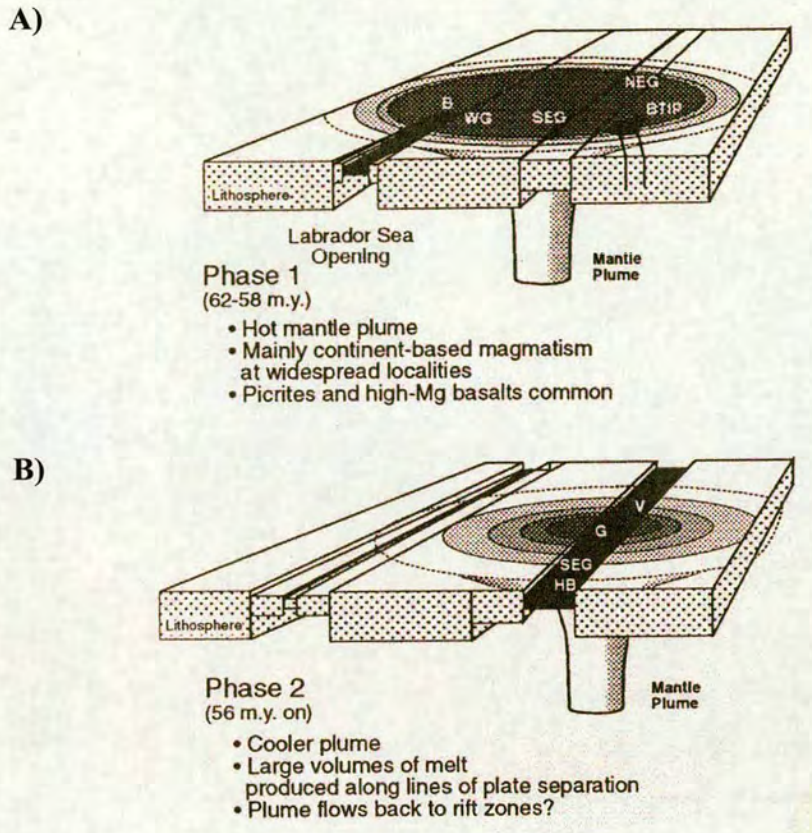

Figure 7.5. A) Schmatic model of the arrival of the ancestral Iceland mantle plume at c. 61 Ma and B) the retreat of the ancestral Iceland mantle plume to the North Atlantic rift axis after break-up at c. 55 Ma (from Saunders et al., 1998).

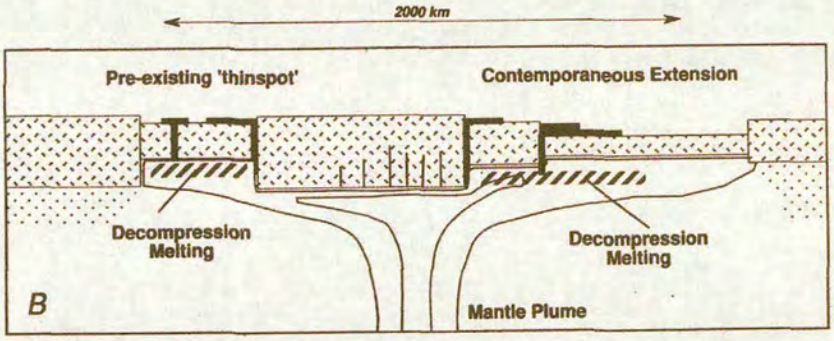

Figure 7.6. Schematic diagram of possible mechanism responsible for excessive melt formation at volcanic rifted margins. A mantle plume, originating from either the 650-km discontinuity or the lower mantle, incubates beneath the continental lithosphere. The lithosphere has a pronounced topography along its underlying surface. Decompression, allowing melting, occurs when the lithosphere is pulled apart (1 and 2) or when the plume mantle or plume-heated mantle ascends into preexisting "highs" or "thinspots" (=young basins at the surface) (from Larsen et al., 1994).

Basalt 4 and the incision surface (see earlier discussion). Thus the results from the FSC (Chapter Five) are compatible with the model suggested by several (e.g. Graham et al., 1998, Storey et al., 1998; Saunders et al. 1998, Larsen et al., 1999), where magma exploits zones of structural weakness. Furthermore, the mantle plume that migrated eastwards across Greenland during the Paleogene (65-50 Ma; Lawver & Müller, 1994) (Fig. 7.2), and the nature of the plume (becoming restricted in the Early Eocene to the rift axis; Fig. 7.4 and 7.5) is consistent with results from the sedimentary history of this study. The last phase of uplift that was most marked in the FSC occurred during the Early Eocene (54.7 Ma). The expansion of the plume head affected a wider area at the time coming up to final rupture, evidenced from the regional correlation of the unconformity of the third phase of uplift that drove the incision. The magma associated uplift/subsidence extended at least as far as the SE of England. This is also consistent with markedly greater volumes of volcanics intruded and extruded. Importantly, as neither incision or fill were evidently associated with a permanent uplift, igneous underplating (favoured by other workers; e.g. Clift et al., 1995; White & Lovell, 1997) is effectively ruled out as a causal mechanism during the Palaeocene-Early Eocene. Instead, if underplating occurred, it must have occurred much later, for example in the Oligocene (e.g. Dam et al., 1998). The evidence from the discussion above suggests instead, that the sedimentation pattern reflects the dynamic vertical movements of a plume in a local variable manner depending on distance from axis of the plume and the nature of the plume. The sedimentology (the shallow marine and terrestrial Early Palaeocene sediments in West Greenland compared with deep-marine fan sands in the FSC and NNS) suggests that the initial uplift phase was most marked in West Greenland closest to the supposed plume axis in West Greenland, whereas during the final uplift phase sedimentation pattern are increasingly affected by the expansion of the plume prior to plate rupture (e.g. shallow to terrestrial sediments in FSC extending to SE England) that finally lead to incision in the FSC. The results presented in the discussion above are also compatible with the evidence from the sediment input areas and drainage direction. It is apparent that the sediment record indicates a source input towards the north

and northwest directed from NW Britain. Maximum uplift is assumed to be above the plume axis decreasing towards its periphery. Thus drainage is expected to also be radiating away from the maximum uplift region (the bulge). Instead, since the plume material is channelled into zones of weaknesses (fault zones, e.g. ridges) this would explain the drainage direction into the FSC from the south and southwest This indicates that the Cretaceous-Tertiary sedimentation history of the basins offshore of Europe are coeval to the intrusion and extrusion of the volcanic deposits of the NAIP apparently in response to the mantle plume and apparent fluctuations in the flux (episodic pulsing).

7.3. INVERSION FEATURES ALONG THE NORTH ATLANTIC MARGINS: CONTROLLING MECHANISMS

Inversion features are common on the continental margin off mid-Norway (e.g Doré and Lundin, 1996; Doré et al., 1999), off NW Britain (Boldreel and Andersen, 1998, Roberts et al., 1989) and in East Greenland (Jameson Land, Traill Ø and Geographical Society Ø region; Price et al., 1997). These inversion features typically occur as domes, arches and reverse faults, indicating that they formed due to intraplate stresses (e.g. Lundin and Doré et al., 2002). The axial trend of the inversion features can be separated into three groups with respect to ridge push direction from the mid-ocean ridge (Fig. 7.7). These are (i) parallel (NE-SW), (ii) oblique (ranging between WNW-ESE through to ENE-WSW) and (iii) perpendicular (NW-SE). The most common orientation is NE-SW. Following the opening and subsequent ocean-floor spreading of the North Atlantic during the Early Eocene, the stress direction in the NE Atlantic margin area changed from divergent- to convergent forces (e.g. Doré and Lundin, 1996). After break-up of Greenland and NW Europe the resulting volcanic passive continental margin became part of a regional compressive regime. Controversies continue about the genesis of these inversion structures. The formation of the most common NE-SW trending inversion structures along the NE margin has been explained by orthogonal NW-SE compression associated with the mid-ocean ridge sea-floor spreading (e.g. Doré and Lundin, 1996) and the Alpine orogeny (e.g. Vågnes et al., 1998). However, the anticlines that are at an angle sub-parallel with the main ridge push direction (i.e. oriented from NWN-ESE through to ENE-WSW) are less easy to explain, and the mechanisms responsible for their development remain unresolved. The range of orientation of the inversion features (both sub-parallel and orthogonal to ridge push) indicates that a complex interaction of forces acted successively upon the North Atlantic passive margin causing the Tertiary development of inversion structures. Mechanisms that have previously been proposed to explain the development of the oblique trending inversion features, include (1) the change in relative plate motion during the initial break-up between Greenland and NW Europe, (2) the separation of Jan Mayen from Greenland which occurred around the Eocene-Oligocene transition,

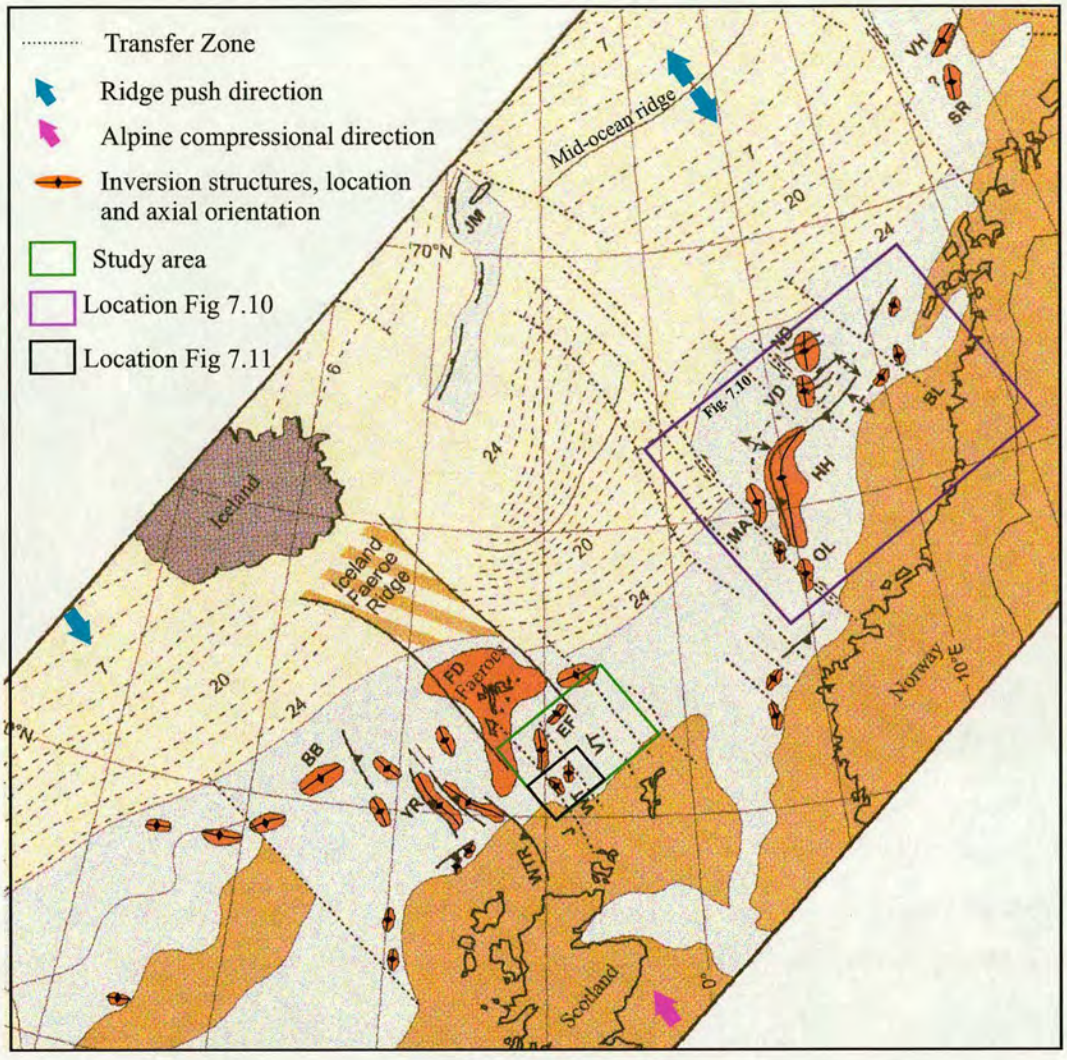

Figure 7.7. Map of intra-Cenozoic inversion structures (shown in red) showing the location and orientation of the main inversion structures along the NW European Atlantic margin. Note the probable relationship between compressive domes and major transfer zones such as the Judd Transfer (J), Wyville-Thompson Ridge (VTR) and the Jan Mayen Fracture Zone (more detail is shown on Fig. 7.10 and 7.11). More detail on stress directions is shown on Fig. 7.9 (modified from Dore et al., 1999).

caused by a shift in the position of spreading ridge segments, (3) changes in relative plate speed (e.g. Hjelstuen et al., 1997; Doré et al., 1999), and (4) variations in plume flux, enhanced by changes in mid-Atlantic-ridge interaction (Doré et al., 2002) (Fig. 7.8).

Main control on the location and orientation of the inversion features

The predominantly NE-SW, N-S and NW-SE axial trend of the inversion features closely resembles the orientation of the main underlying structural lineaments, that date back to the Caledonian Orogeny, the transtensional development of Devonian intra-mountain basins, and the subsequent Late Palaeozoic and Mesozoic extensional rift tectonism (e.g. Lundin and Doré, 1996). This is consistent with the model by Lowell (1995), which predicts that inversion is dependent on pre-existing basin configuration and that the primary position and geometry of the inversion features is favourably oriented along inherited structures. In addition, the pre-Atlantic opening sedimentation of the Mesozoic basins and sub-basins along the NW Atlantic margin is different as a result of the complex structural histories and the influence of the pre-existing structure (Chapter Two and Three). Consequently, inherited structures and differing basin evolution makes each inversion feature unique. The inversion features developed in a complex pattern during distinct phases between the Eocene and Miocene (e.g. Lundin and Doré et al., 2002) and although each inversion feature is unique and neither temporally nor spatially linked, they must have a common main formation mechanism which potentially works in concert with other secondary, but important mechanisms. This is suggested by their widespread occurrence, orientation (predominantly perpendicular to the maximum ridge-push direction of the rift axis) and common 1-3 % shortening (mild compression).

In the FSC it is evident from the analysis of the underlying basement structure (Chapter Four) that structural lineaments are predominantly oriented NE-SW with the exception of the Judd Platform and the Westray Ridge. The N-S trending Westray Ridge, which has been intruded and locally contains two intrusive centres evidenced from gravity and magnetic data (e.g. Rump et al., 1993), indicates

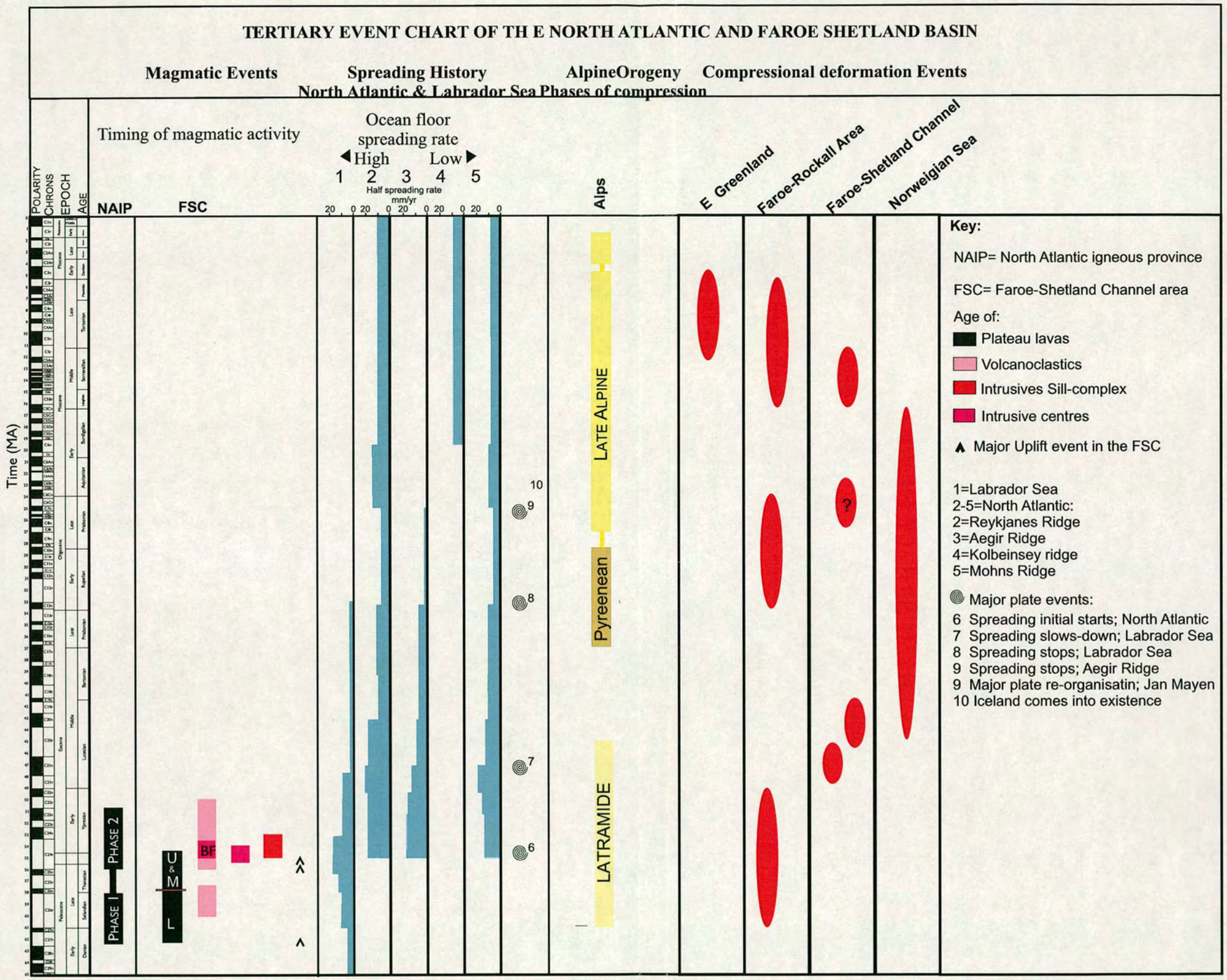

Figure 7.8. Time scale and tectono-magmatic event chart for the North Atlantic in general and the Faroe-Shetland channel. Major events (see text). Spreading rates from Roest and Srivastava (1999); Mosar (2000).Timing of inversion features off mid-Norway from Lundin and Dore, (2002). Timing of doming in the Faroe-Rockall area from Boldreel and Andersen (1993). Timing of doming onshore East Greenland from Price et al. (1997). Timing of magmatism from Saunders et al. (1997).

that in addition to the fundamental different orientation, the rheology of the Westray Ridge is stronger in places where it has been intruded. It is apparent from the location of the inversion features in the FSC (this study, and Boldreel and Andersen, 1993, 1994; Andersen et al., 2000; Ritchie et al., 2003; Davis et al., 2004) that no inversion features are present beyond the south eastern side of the Westray Ridge and thus the Westray Ridge seems to have acted as a "barrier" between inversion occurring in the southern, south-western, north-western and north-eastern FSC and a shadow zone southeast of the Westray Ridge of no post-Atlantic-opening deformation. Thus the Westray Ridge was probably accommodating strength and thus acting as a limit to compression (buttress).

Primary plate-boundary forces

From the Cretaceous to Present day the study area has been affected by two main plate-boundary forces, the Alpine Orogeny and the mid-Atlantic ridge push force. Although ridge-push is not a plate boundary force, it produces significant stresses within the plates (e.g. Artyusthkov, 1973; Molnar, 1978; England and McKenzie, 1982). In addition, when the mid-ocean ridge is associated with a hotspot, as in the case of the North Atlantic and the Iceland plume, the normal ridge push forces may increase by more than double (Bott, 1993). Furthermore, ridge push force related to the presence of a plume could considerably accelerate plate motion (Bott, 1993). At present, the vector of compression in the Alps is broadly parallel with the vector of ridge push force from the spreading ridges in the North Atlantic (e.g. Ahorner 1970, 1975, Müller et al., 1992), whilst the compressional stress field in NW Europe has a NW-NWN direction (Müller et al., 1992). A model proposed by Gölke (1996) suggests that such forces (ridge push and Alpine compression) are presently interacting constructively in northwestern Europe. The far-field stress form the Alpine orogeny are thought to be transmitted long distances, of up to 1300 km to the north of the Alpine collision front (Ziegler, 1987e) with a declining effect away from the plate boundary (e.g. Cloetingh et al., 1990).

At the time of opening of the North Atlantic, relaxation of tensional stresses related to continental break-up may have allowed the compressional stress from the ongoing Alpine Orogeny to propagate northwards resulting in the initial contractional deformation (Vågnes et al., 1998). However, this could only have been a relative temporary effect and would not explain the development of inversion features from the opening (break-up) in the Early Eocene through to Late Miocene (Fig. 7.8).

Force related to the Alpine Orogeny

The Alpine Orogeny, from the late Cretaceous up to the present day has occurred in four main phases and each phase represents focussed compressional activity with intervening calm periods. These are (1)'sub-Hercynian' Phase in the late Turonian-Senonian, culminating in the Santonian-Campanian, (2)'Laramide' Phase in the Paleocene, (3)'Pyrenean' Phase in the Eocene-Early Oligocene and (4)'late Alpine' Phase in the Miocene (Fig. 7.8). Evidence for structural inversion is seen in the inverted sedimentary basins in NW Europe, for example, the Broad Fourteens Basin in the Southern North Sea and the Iberian Basin in Spain (Ziegler, 1989, 1990). Inversion in these basins occurred perpendicular to the stress direction of the Alpine orogenic events.

In the Faroe Shetland Channel the Alpine Orogeny (Pyrenean Phase) does not satisfactorily explain the Middle Eocene inversion that first occurred in the southern FSC during the early-mid Lutetian and secondly occurred in the southwest FSC post early-mid Lutetian. The inversion features that developed during the Middle Eocene in the FSC do not link to the orientation and seem to have occurred over shorter intervals than the 'Pyrenean' compression phase (Eocene-Oligocene) (Fig. 7.8). The Alpine Orogeny neither explains the Oligocene phase of renewed compression in the southwest FSC. Although the presence of transmittable plate boundary force cannot be completely ruled out, both the timing and the orientation of the inversion features in the FSC do not favour an Alpine generic mechanism for the inversion features during the Middle Eocene and the Oligocene. The Miocene inversion phase fits both

in time and orientation (perpendicular to stress) and thus may be linked to the Alpine Orogeny (Fig. 7.8).

The Alpine orogeny, however, cannot explain the inversion features on the NE Greenland margin, since it is difficult to transmit stresses across the spreading axis. Thus Lundin and Doré et al. (2002) do not favour an Alpine origin to explain the compression and inversion on the North Atlantic margin although this is not totally excluded since the Alpine Orogeny and the ridge push stress sources are likely to have acted continuously throughout the Late Cretaceous-to the present day, and cannot be mutually exclusive (Doré et al., 1999; Lundin and Doré, 2002). However, the Alpine and the ridge push forces do not always satisfactorily explain the inversion features on the North Atlantic margin. The ridge-push direction and the far-field stress related to the Alpine Orogeny do not account for the WNW- and NW-trending anticlines for example the Wyville-Thompson and Ymir Ridge in the Rockall area and the Foinaven Anticline and the Foinaven Monocline in the FSC. Therefore, there must be additional mechanisms to explain the formation of this trend of inversion features.

Inversion and timing of major plate reorganisations

There have been two major episodes of changes in the plate-configuration in the NE Atlantic. Firstly during the early Eocene at the initial opening of the North Atlantic, and secondly, during the late Eocene-Late Oligocene (A13-A7) when sea floor spreading of the Labrador Sea ceased (Srivastava and Tapscott, 1986, Roest and Srivastava, 1989) and in the North Atlantic, north of the Faroe Islands, the stepwise reduction in sea-floor spreading rates led ultimately to the extinction of the Aegir Spreading Ridge and the start of spreading in the Kolbeinsey Ridge (Srivastava and Tapscott, 1986; Ziegler, 1987) that resulted in the Jan Mayen being separated from Greenland (Figs. 7.8 and 7.9).

At the initial opening of the Atlantic the stress direction was NE in the Labrador Sea and SE in the North Atlantic (Roest and Srivastava, 1989) (Fig. 7.9). Coeval inversion occurred locally along the NE Atlantic margin, for example in the

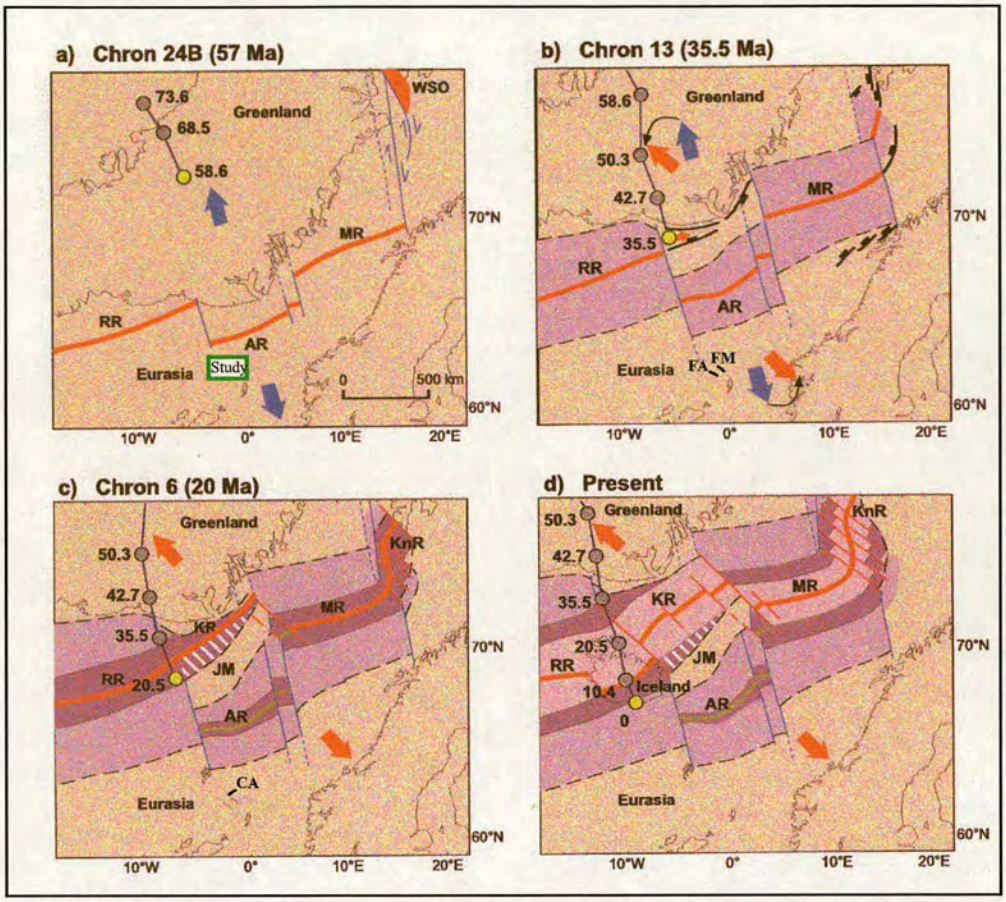

FA=Foinaven Anticline
FM=Foinaven Monocline
CA=Corona Anticline

Figure 7.9. Plate tectonic evolution of the North Atlantic. The position of plume is marked by circles. The yellow circles mark the approximate position at each reconstruction and the grey circles mark previous positions. a) Initiation of seafloor spreading. The relative stress direction is shown as blue arrows. b) Major plate reorganisation and change of relative separation (from blue to red arrows). c) The Kolbeinsey Ridge propagated northward in East Greenland (between chron 13 and 6c) and eventually separated the Jan Mayen microcontinent from East Greenland. The Aegir Ridge was abandoned. d) The plate configuration at Present (Modified from Lundin and Dore, 2002).

Rockall area, the ESE-trending Westray Ridge Complex, the SE trending Munkagrunnar Ridge, and the ENE-WSW trending Fugloy Ridge (Boldreel and Andersen, 1998). During the late Eocene-Oligocene, inversion features developed on the mid-Norwegian margin that have been related to dextral movement associated with the complex rotation in the late Eocene-Oligocene (A13-A7) of the Jan Mayen micro-plate. The orientation of the resulting inversion features during the late Eocene-Oligocene was both oblique and perpendicular to spreading direction of North Atlantic (e.g. Andersen and Boldreel, 1993; Doré and Lundin, 1996 (Fig. 7.7 and 7.9).

The changes in stress that resulted in rotation of plates and the resulting changes in plate- configuration have been thought to trigger inversion and cause reactivation of transform faults and rotation of inversion features (e.g. Doré and Lundin, 1996) (Fig.7.10). However, the inversion features in the FSC that formed during the Middle Eocene, Oligocene and Miocene cannot be explained simply by any of the major plate reorganization in the North Atlantic. Firstly, because the approximately 45° shift in orientation of the major stress axis between early Eocene and late Oligocene that is thought to have resulted in a complex shift of sea floor spreading from the Aegir Ridge to the Kolbeinsey Ridge in the same period (Ziegler 1988, 1990), would produce a final N-S or NNW-SSE ridge-push direction. Since the axial orientation of the Foinaven Anticline and the Foinaven Monocline requires a NNE and NE compression, rotation of plates does not explain their development. Secondly, a shift in plate motion is thought to have no affect on the push force unless the spreading axis is dramatically reorganised (Vågnes et al., 1998), and this is not the case in the Oligocene (e.g Srivastava and Tapscott, 1986). However, the planar curvature of the southern part of the Aegir Ridge may suggest asymmetric spreading and thus oblique ridge push (see next section). Thirdly, in the North Atlantic no major plate reorganisation events have been recorded since the latest Late Oligocene-Early Miocene (Fig. 7.8 and 7.9) and since inversion features have developed in the mid-Miocene their generic mechanism has to be explained from a different source.

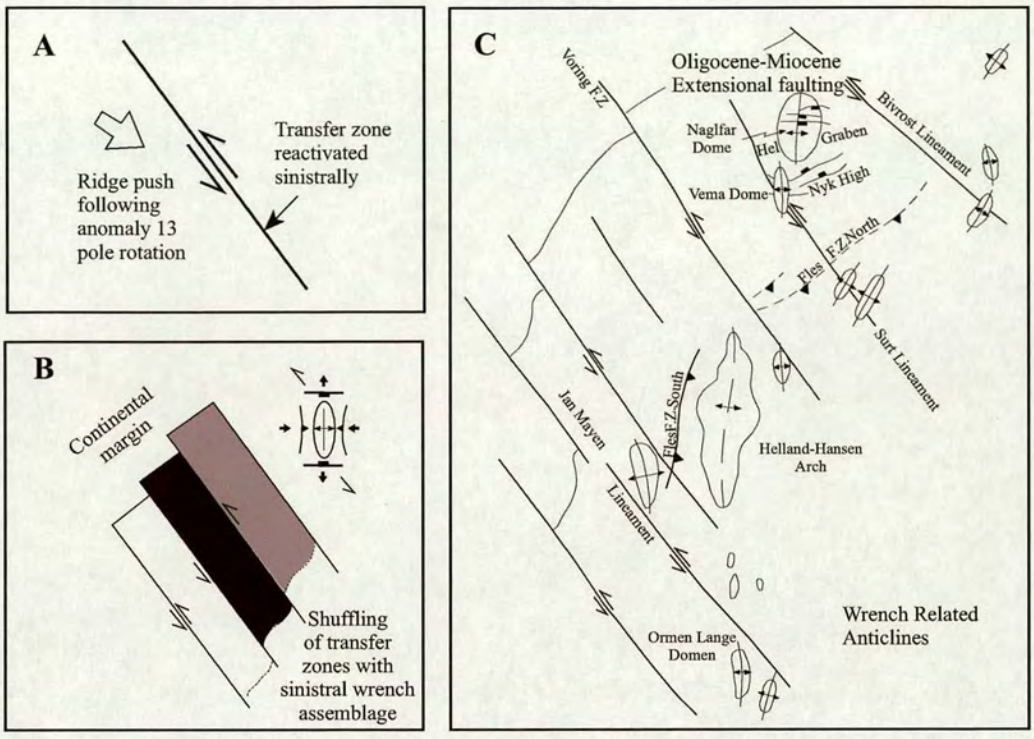

Figure 7.10. Conceptual model for sinistral activation of transfer zones during mid-Cenozoic spreading reorganization. A) Change in spreading direction imposes oblique ridge push on 'fixed' continental transfer zones. B) Continental margin adjusts by rotation 'shuffling' along transfer zones with sinistral offset. Small inset: structural trends associated with sinistral wrenching. C) Application of the model to observed Cenozoic structures offshore Mid-Norway (from Dore and Lundin, 1996).

Reactivation of Transfer system

One causal mechanism for the development of inversion features parallel to the ridge-push direction could be the reactivation of transfer faults that have a slight curvature or bends in the platform fault trace. Strike-slip movement on such faults would form Restraining Bends and could cause zones of compression (buttressing) and thus is not primarily dependent on the push-direction (Fig. 7.11). In the southwest FSC and southern FSC both the Foinaven Anticline and the Foinaven Monocline are located close to and sub-parallel to the Judd transfer and the Westray transfer, that have been interpreted from gravity and magnetic data by Rumph et al. (1993). On seismic profiles the transfer zones appear as complex fuzzy seismic zones probably of multi vertical oblique-slip faults. Compression is observed between them (Dave Ellis, 2004 pers. com.). Some authors have interpreted the transfer faults to have controlled the pre-opening sedimentation distribution (e.g. Naylor et al., 1999) as well as the distribution of the lava flows of the Faroe Plateau Lava Group (Ellis et al., 2002). Since these features, are zones of pre-existing weakness, it is possible that they could have played an important role in basin reactivation (e.g. Ziegler et al., 1995). The transfer faults could have been reactivated during compressional tectonics, during the Paleogene, and thus the different stress regime, post-opening of the North Atlantic, could have reactivated these lineaments at different times related to their orientation with respect to the principal stress direction.

In order to reactivate such faults the angle of compression must have been oblique to the transfer fault. It is suggested by Andersen and Boldreel (1995) that dextral motion along the NW trending Denmark Strait Fracture Zone (DSFZ) took place during the Early Eocene related to spreading of the Aegir Ridge. Spreading of the Aegir Ridge occurred until late Oligocene, when it became extinct (Fig. 7.8). Thus, it is possible that oblique stress force from the Aegir Ridge spreading axis could have caused strike-slip movements of the Judd- and the Westray transfer zones. Furthermore, the development of the Foinaven Monocline instead of an anticline was probably influenced by the orientation, location of the Westray Ridge complex.

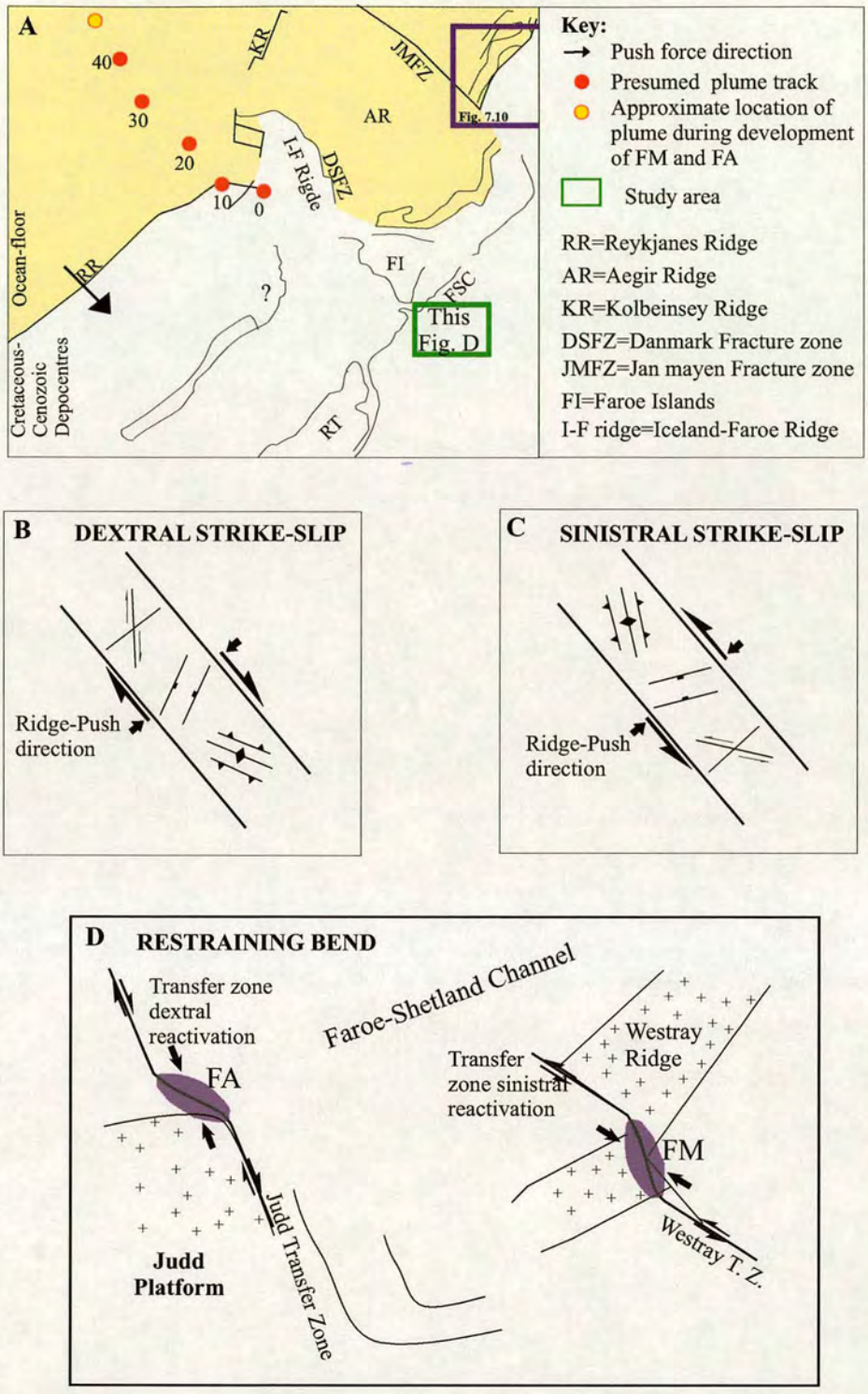

Figure 7.11. Models for the reactivation of transfer zones. A) Area of study with respect to major fracture zones (e.g. DSFZ). B and C) Conceptual models for dextral and sinistral transfer zones. D) Model showing influence of fault trace geometry on the location of inversion structures (FA=Foinaven Anticline and FM=Foinaven Monocline) within the FSC.

Inversion caused by changes in Spreading rates.

In the FSC the initial uplift and compression corresponds in age to the highest spreading rates on the North Atlantic ridge (Mosar et al., 2002) and could have triggered the inversion (Fig. 7.12). However, the high spreading rates do not correspond with the other phases of inversion identified in the FSC. This result corresponds with the study by Lundin and Doré et al. (2002), who found that the lowest value of spreading rate corresponds with the major Oligocene plate reconfiguration during which time inversion structures developed off mid-Norway. Thus, there seem to be no relationship between changes in spreading rate and timing of inversion. In addition, numerical modelling suggests that for a slow spreading ridge, changes in spreading rate by as much as 400 % (from 1.5 to 6.0 cm/year half-rate) have no influence on ridge push forces (Bott, 1991). Therefore, changes in spreading rates are unlikely to generate forces capable of causing compressional deformation (Lundin and Doré et al., 2002). Consequently, high rates of spreading are unlikely to have triggered inversion in the FSC or in the adjacent area and are thus ruled out as a causal mechanism for inversion features on the North Atlantic margin.

Inversion and timing of major plume flux variations

There is strong evidence from the age constraints on the stratigraphic interpretaion and the sediment thickness relationships that the compressional features in the FSC have developed in phases/pulses (this study, Chapter Five). This is consistent with the formation of inversion features in an adjacent area, on the mid-Norwegian shelf (e.g. Lundin and Doré et al., 2002) and in the Faroe-Rockall area (e.g. Boldreel and Andersen, 1993, 1994), which developed in multiple phases between the Eocene and Early Miocene (Lundin and Doré, 2002).

The size and magnitude of the inversion features on the NE Atlantic margin are subtle and they have undergone only mild compression, compared to the 1-2 km of domal uplift of the landmasses of southern Norway, Finnmark and northern UK. The uplift of the landmasses is interpreted (e.g. by Rohrman and van der Beek, 1996)

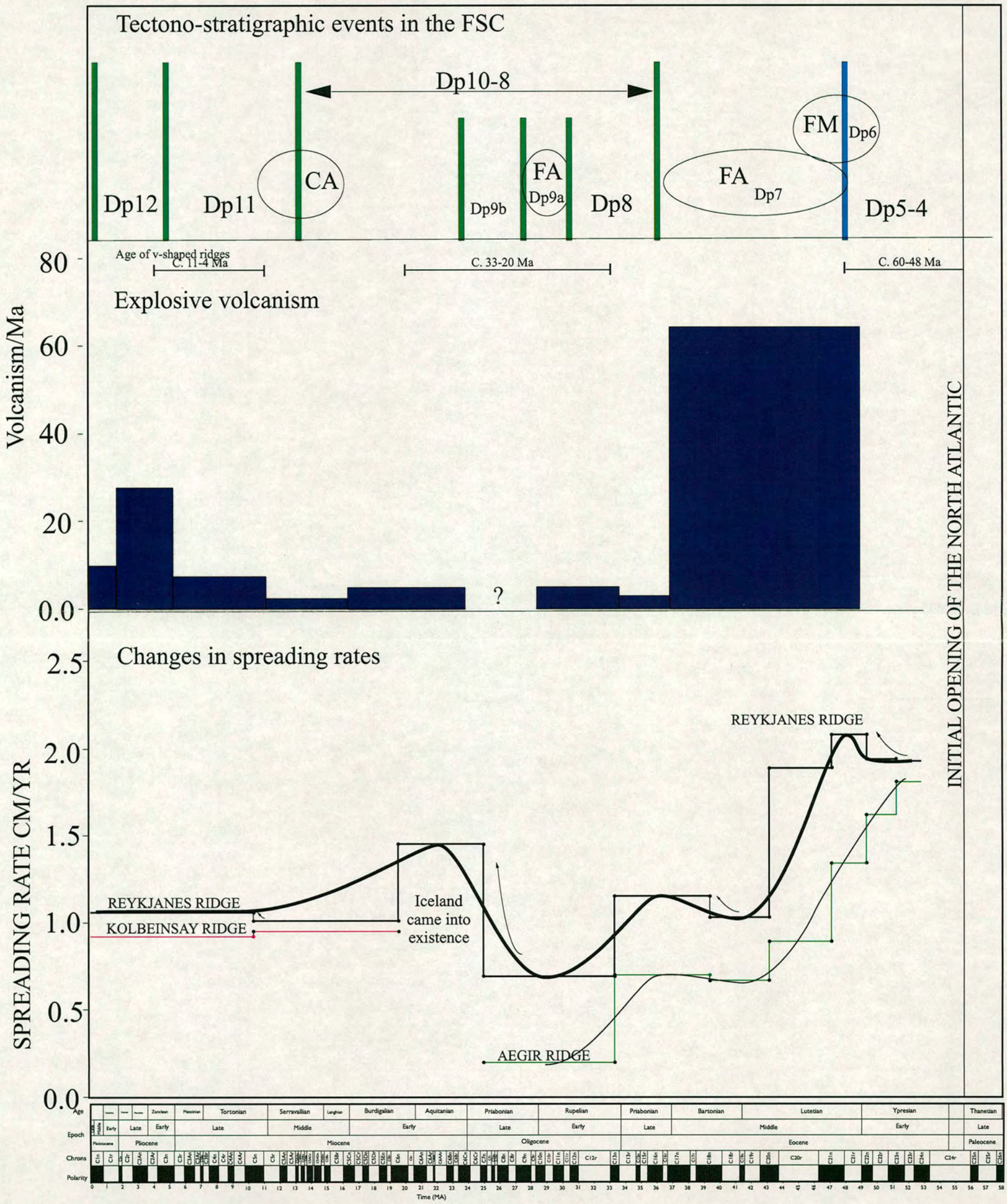

Figure 7.12. Chronologic diagram illustrating the timing of compressional doming versus major events. Spreading rates from Mosar et al. (2002). Iceland plume pulses from White and Lovell (1997). Rates of explosive volcanism from Donn and Ninkovich (1980).

to have initiated during the Neogene but prior to the onset of glaciation, whereas other workers have suggested a Paleogene age for the uplift of Fennoscandia (e.g. Clausen et al., 2000; Eldholm et al., 2002). It is much easier to explain the local inversion features on the NE Atlantic margin as an intraplate deformation, whereas it is not a likely mechanism for the Neogene uplift (Skar van Balen and Cloetingh, 2000).

The axial orientation of the inversion features in the FSC that are parallel-sub parallel to ridge push direction may be a consequence of reactivation of the transfer faults (Judd transfer and the Westray transfer zones) causing inversion in the local area of restraining bends (Fig. 7.11). The axial orientation of the inversion features that are perpendicular to ridge push direction, those mainly formed in the Miocene, can easily be explained either by ridge push, alpine stress forces or a combination of both. However this does not explain the timing of the inversions with respect to fluxes of mantle plume thought to have arrived underneath the lithosphere at ca. 65 Ma (Lawer and Müller, 1994) and fluxes from the plume present since Iceland came into existent (latest Oligocene/early Miocene) to Present. A mechanism proposed for the development of the inversion features along the NW Atlantic by Lundin and Doré et al. (2002) is the fluctuation of mantle plume flux that caused a combined ridge-Plume interaction. The timing of the development of anticlines on the NW Atlantic margin indicates that the development of anticlines in the Faroe-Rockall area broadly correlate with the timing of different fluxes on the mantle plume, whereas the anticlines on the mid-Norwegian shelf show a less obvious link, however, more data is needed to analyse this in detail (Lundin and Doré et al., 2002). At the initial spreading of the North Atlantic the mantle plume axis was situated beneath East Greenland. Greenland moved NW relative to the stable plume as oceanic lithosphere was created, so that during the early Oligocene the plume was located beneath East Greenland and Iceland and during the early Miocene beneath NW Iceland (Lawer and Müller, 1994) (Fig. 7.2). During the initial break-up, the retreat of the mantle plume to the rift axis may have enhanced the convection process (Saunders et al., 1997) and thus triggering inversion. This did not however, reactivate and form inversion features in the FSC. In the FSC, the different inversion phases, the initial

phase of compression and the formation of the Foinaven Monocline and subsequently the Foinaven Anticline correlates in time with major explosive volcanism evidenced form ash samples around Iceland (Don and Ninkovich, 1980) (Fig. 7.12). The Miocene phase corresponds broadly in time with the emergence of Iceland. Furthermore, all phases correlate broadly with the development of v-shaped ridges identified south of Iceland (White and Lovell, 1997) (Fig. 7.12). In addition, White and Lovell (1997) implicate time-varying conditions within the Iceland mantle plume to explain the North Atlantic deep water exchange (NADW), variations identified by Wright and Miller (1996). All of the above suggests that the Iceland plume is likely to have had a significant role in the development of the inversion features in the FSC. Significantly, changes in the flux of the plume triggered the inversion that led to updoming and basin inversion and controlled the timing of reactivation of weakness zones.

This is consistent with the pattern of inversion phases along the NE Atlantic margin. Although the mid-Atlantic rift axis propagated northwards, inversion still occurred south of the Norwegian Sea in the FSC and the Faroe Rockall area. Despite a lack of precise timing on the evolution of the mantle plume since break-up, the uniqueness and sporadic phases of inversion in the surrounding area on the continental margin probably reflects the complex and episodic nature of the flux of the plume. In addition, it is not an unusual character for a plume to be pulsing and episodic, as during the early Tertiary the chronology and the widespread local occurrence of the NAIP as well as the sedimentary response to mantle plume in the FSC give evidence of a pulsing nature of plume (see the first section of this chapter).

In summary; it is apparent from the orientation and timing of the inversion events in the FSC and elsewhere on the NE Atlantic margin that although the inversion structures have clearly been influenced by underlying structure and developed sometimes in relation to major plate reorganisation events or have been triggered by major volcanism associated with plume, there is no mechanism yet for the development of inversion structures that can fully explain them on their own.

7.4. GENERIC IMPLICATIONS

This section discusses the key results that have come out of this thesis that may have implications for other passive continental margins. In particular how relevant is the West of Shetland in understanding other passive continental margins with or without the presence of a plume or plumes.

1) In the Faroe-Shetland Channel it is evident that the location and the orientation of the inversion structures is closely linked to the alignment of the underlying Mesozoic major structural lineaments (see Chapter Four). Thus the structural configuration is a local, but important generic mechanism for the inversion structures characteristics. Thus, in other passive continental margins, an understanding of the pre-inverted basins is crucial when analysing younger structural inversion features.
2) The timing of inversion in the Faroe-Shetland Channel, is broadly related to major ocean plate reorganisation during the Eocene and Oligocene. These events are believed to be the major driving mechanism for the development of the inversion features. Thus the spreading history that will affect the timing of inversion needs to be understood before studying inversion in other passive continental margins.
3) In the Faroe-Shetland Channel the underlying occurrence of a mantle plume has been an additional driving mechanism and is thought to both have triggered and influenced the timing of inversions. Detailing the episodic flux of plume material which reaching the earth surface should be fully understood in order to study inversion on margins that are affected by plumes. Inherently passive continental margins that are affected by plumes have a more complex evolution than margins that have not been affected by plumes.
4) The generation of sediment source areas, erosion and subsequent distribution of sediments is clearly influenced by the location and orientation of inversion features. In the FSC the deposition of sediments was focused in the area where inversion was not occurring. Depositional packages onlapped and thinned over areas affected by inversion. Thus, an understanding of the

geometry of inversion features has implications with respect to predicting the likely distribution of sediments and in particular sand prone depositional systems.

5) Post-rift subsidence seems to have occurred coeval to local inversion and sedimentary deposition. This also has implications for predicting the evolution of a sedimentary basin because the main areas of accommodation will be away from the inversion structures.

6) Stratigraphy within the inversion structures often represents local depocenters that existed prior to uplift.

CHAPTER EIGHT
CONCLUSIONS

The following conclusions relate to the specific objectives set out in Chapter One.

1) The Paleogene to present day stratigraphic succession has been investigated in the northwestern, southern and central parts of the Faroe Shetland Channel (FSC) (Chapter Five and Six). 3D seismic data integrated with well and biostratigraphic data have allowed the Paleogene succession to be divided into twelve depositional packages (DP1-DP12); DP1-DP4 were deposited during early Paleogene uplift, resulting in a progressive basinward shift in facies and shallowing-up sedimentary packages. DP1 consists of a deeper marine, shelf-slope system; D2 is a prograding shelf-slope, situated basinwards of the former shelf edge; DP3 consists of a shallow marine to non-marine prograding delta system; and DP4 consistes of fluvial to estuarine deposits that infill topography developed due to incision and erosion into DP3 and DP2. DP5-DP12 were deposited during late Paleogene-Neogene thermal subsidence, with local compressive deformation and uplift occurring. DP5 is a laterally extensive prograding delta system; DP6 consists of marine deposits that infill basin topography, created during coeval compressional movements; DP7 is a prograding shelf slope system; DP8-10 consists of slope fan and basin-floor deposits that developed in front of the former shelf-slope (DP7); DP11-12 represents deposition that occurred along a narrow zone of the FSC-margins and consist of contourite drift deposits (e.g. Stoker, 2002; Knutz and Cartwright, 2003), apart from the uppermost units that consists of glacial deposits. For example Unit 12c that consists of a SE prograding shelf slope system deposited during relative sea level fall associated with glaciation.

2) The Paleogene stratigraphic interval (DP1-DP4) commonly contains volcanic and volcanoclastic material (e.g. the kettla Tuffs at the base of DP1, Basalt 3 within DP3, Basalt 4 and the Balder Tuffs within DP4) indicating that deposition occurred coeval to considerable igneous activity. Therefore, it is possible that thermal dynamics (i.e. an incubating mantle plume and channeling of hot mantle into pre-existing weak zones) occurred coeval to deposition of DP1-DP4. This contemporaneous igneous activity correlates with the second phase of volcanism of the NAIP and has independently been linked to the evolution of a mantle plume.

3) Uplift during deposition of DP1-DP4 led to a progressively restricted basin that finally became sub-aerial, resulting in incision, erosion and the formation of a prominent incision surface. Furthermore, the preservation of the incised valley network indicates that uplift must have been followed relative rapidly by subsidence to allow infilling and hence preservation. Excellent age constraint of the sediments shows that the incision event (base DP4) occurred at 54.7 Ma. Based on biostratigraphic dating of the sediments above and below the incision surface it is apparent that the vertical motion (i.e. uplift and erosion; subsidence and burial) was transient, coupled and relatively fast, occurring in less than 1 My.

The depth of maximum incision (400 m) on the valley network indicates similar magnitude of relative sea level fall. This suggests that the development of the incised drainage network cannot be caused by eustasy alone. Since there was abundant contemporaneous igneous activity (NAIP), the incision it is more likely to represent an episode of thermal uplift related to a mantle plume. Furthermore, there was no active faulting occurring.

The plume related coupled uplift and subsidence event related to the incision surface in the FSC reflects not just one phase of uplift followed by subsidence, but a complex pattern involving several coupled uplift and subsidence episodes beginning with DP2 and marked by more minor unconformities and volcanic activity. The incision surface is direct evidence that can be quantified to represent the final pulse of uplift and subsidence of a mantle plume that dominated the region prior to break-up and ocean floor spreading.

Taken together, the sedimentary, stratigraphic and volcanic relationships and chronology are consistent with the theoretical models of plume behaviour. However, because of its coupled, transient nature, they appear to be incompatible with contemporaneous igneous underplating. Its formation is also independent of deformation resulting from structural inversion of underlying faults. The final coupled uplift and subsidence is compatible with and thus related to the final continental rifting between Greenland and Europe, when the plume head expanded to its maximum, before decaying as ocean-floor spreading initiated.

(4) The incision surface can be correlated into the northern North Sea (Bressay area) and to SE England where progradation and incision followed by infilling and drape of large deltaic complexes occurred coeval to that in the FSC. This indicates that uplift related to the incision event in the FSC was widespread.

5) The incised valley network revealed in the southern FSC records the final stage of a greater, regional uplift event superimposed on background thermal post-rift subsidence, and the first stage of its decay. This is consistent with burial history curves expected by classic post-rift basin subsidence. However, it is consistent with that expected from volcanic passive continental margins. However, following rifting (e.g. Bertram & Milton, 1989; Milton et al., 1990; Barr, 1991; Nadin & Kusznir, 1995) albeit with the important caveat that the deflection (uplift) can now be thought to be the result of at least two well-defined phases of plume related transient uplift and subsidence. The greatest effect was in West and East Greenland during the early Palaeocene and in the FSC during the late Palaeocene/early Eocene episode of uplift.

6) Depositional packages 5-12 (DP5-DP12) were deposited during overall thermal post-rift subsidence. However, the generation of accommodation space that is controlled by subsidence was at times locally reversed due to flexural folding evidenced by stratal thinning of depositional packages controlled by horizontal compressional forces.

At least three compressional inversion in the FSC. Biostratigraphic evidence from the stratal depositional packages indicates that inversion occurred in four phases, 1) during the Middle Eocene (early-mid Lutetian); 2) post early-mid Lutetian; 3) the Oligocene and 4) the Middle Miocene.

Formation of the NW-SE trending Foinaven Monocline occurred in the southern FSC over the South Westray Ridge, during the early-mid Lutetian (Phase 1). The stratal thinning related to DP5/DP6 suggests furthermore that Westray Ridge and also the East Faroe High were uplifted during this compression phase resulting in a marked change in basin-physiography.

The NW-SE trending Foinaven Anticline developed in the southwestern part of the FSC during the Middle Eocene, post early-mid Lutetian (Phase 2) and also during the Oligocene times (Phase 3).

The compressional forces that prevailed during the deposition of DP7 (Phase 2) and Unit 9a (Phase 3) only affected a local area over the Foinaven Anticline, where there is local thinning. As a result, deposition in the area east of the Foinaven Anticline was not effected by compressional deformation/uplift. Instead, a relatively even thickness of sediment was deposited controlled by post-rift thermal subsidence. The Corona Anticline was formed in the northwestern part of the FSC during Middle Miocene.

The locations of the Foinaven anticline and monocline above the transfer zones indicates that their formation could be linked to the reactivation of existing transfer zones. The Foinaven anticline may have developed as a result of buttressing during reactivation of the Judd fault/transfer zone and compressional forces that accommodated at a compressional restraining bend in the Judd fault/transfer zone. The Foinaven monocline developed probably as a result of a similar process above the Westray transfer zone.

7) The link of these inversion features to the ocean-floor evolution and to plume has been addressed. The Foinaven Monocline developed along the NW-SE trending Westray transform fault and the Foinaven Anticline developed parallel to the Judd transform fault. Thus the orientation of these structures is parallel to the main coeval

compressional forces exerted by the Alpine Orogeny and the North Atlantic sea-floor spreading (ridge push force) and therefore the inversion structures cannot be explained primarily by these forces.

The results from this study indicate that the inversion features in the FSC cannot be explained simply by any of the major plate reorganization that occurred in the North Atlantic during the Paleogene and Neogene. Thus the driving mechanism is complex and most likely works in concert with several forces.

The stratigraphic and tectonic evolution indicates that the Foinaven monocline and the Foinaven and Corona anticlines are governed by pre-existing inherited structures and their location. The effect of compression related to reactivation of transform zones can explain the orientation of the Foinaven anticline and monocline.

Strike-slip movements on the Judd transfer and Westray transfer zones was associated with the dextral motion along the NW trending Denmark Strait Fracture Zone (DSFZ) related to spreading of the Aegir Ridge, during the Eocene to late Oligocene. The major volcanism and the development of v-shaped ridges south of Iceland suggest that the plume is likely to have had a significant role in the development of the inversion features in the FSC.

Although a common mechanism for the development of the inversion features on the NE Atlantic remains enigmatic, the orientation and the timing of inversion features in the FSC indicates that the ocean-floor history and evolution of mantle plume play a dominating role for the development of inversion features in the FSC.

8) The widespread occurrence of inversion structures along the length of the NE Atlantic margin, their orientations and common 1-3 % shortening (mild compression), suggests that the inversion structures have a common main formation mechanism. However, the relationship between the inversion structures in the FSC and regionally along the margins indicates that each inversion structure is unique and neither temporally nor spatially linked.

9) The early paleogene uplift events together with the uplift related to compressional inversion of the post rift succession in the FSC, indicates that post-rift subsidence stops at times when there is local uplift as a result of in-plane stresses related to mantle plume and/or compression and this is likely to be common on volcanic passive continental margins in general

APPENDIX

Depostional Package 1

Seismic facies:

Predominantly parallel reflectors.

Drill Cuttings Descriptions:

Type 1) Siltstone and/or silty mudstone-mudstone with thick up to 10m sandstones interbeds (e.g. 204/19-1, 204/24-1, 205/9-1).

Type 2) Predominantly very fine to very coarse sandstone that is poorly sorted (e.g. well 204/22-1). The sandstone contains thin (up to 0.5m) thick slightly silty and carbonaceous mudstone inter-beds.

Type 3) Predominantly mudstone (wells 6004/12-1z, 6005/15-1z; no drill cuttings descriptions available).

Wire-line log trend:

Large-scale (full package): The overall wire-line log trend is irregular indicating no particular trend.

Small-scale (up to 50 m):

The sandstones show both fining-upward and box-shaped log trends.

Interpretation:

The parallel reflectors and the predominantly fine-grained lithology with common calcite cemented layers are common shelf deposits. The sandstones indicate marginal areas, such as shelf edge to slope environments.The uniform mudstone lithology (Type 3) is interpreted to represent basinal environment.

Environment:

Shelf-slope-basinal facies association.

Depostional Package 2

Seismic facies characteristics:

Wedge-shaped package tha contains clinoform reflectors. The foresets-bottomsets show prograding to aggrading characteristics.

Drill Cuttings Descriptions:

Type 1) Predominantly siltstone (well 204/14-2, 204/19-1, 204/24-1a). The siltstone contains shell fragments (e.g. well 204/14-2) and common carbonaceous calcite cemented layers (well 204/24-1, 204/24-3, 204/19-1). The siltstone contains common (up to 10 m thick) sandstone interbeds.

Type 2) Mudstone beds that range from 2m to 35m in thickness. The mudstone is interbedded with sandstone beds that are up to 50m in thickness (Well 6004/12-1Z; no cuttings describtion is available). The mudstone to sandstone boundary is sharp.

Wire-line log trend

Large-scale (full package):
Irregular trend indicating no particular log trend
Small-scale (up to 50 m):
Type 1) Coarsening-upward trend, that is overlain by, a similar thickness (ca. 40m) fining-upward trend, indicating a symmetrical log trend. Two symmetrical trends, are confined to the upper section in well 204/14-2.

Type 2) Box-shaped trend, indicating clean, well sorted sandstone (or conglomerates)(e.g. 6004/12-1z).

Interpretation:

Type 1) The irregular log trend, the fine grained lithology with common calcite cement layers represents shelf deposits. The sandstone beds indicate a more marginal shelf-slope deposits. The coarsening-upward to fining-upward trends, represent variation in grade of sediment supplied from the foresets/slope.

Type 2) the high gamma ray mudstone interbedded with low gamma ray box-shaped log trend indicate either turbidite facies or sub marine fan facies. The relatively high content of sandstone and the relative thick sandstone bedding indicate that type 2 lithology more likely represents sub marine fan deposits.

The DP2 wedge that contains the seismic clinoform facies are confined to the area with type 1 lithology. Type 2 lithology is present in front of the wedge. The clinoforms and the type 1 lithology indicate a slope edge that is building-up vertically. Type 2 lithology in front of the prograding to aggrading wedge is interpreted to represent sub-marine fans that are either slumped down from the slope edge or are received via feeder channels (not clear on seismic).
The lack of seismic mound facies with internal hummocky configuration makes it not possible to interpret the fans this is due to poor seismic quality in this particular area.

Environment:
Shelf-margin facies association and basinal submarine fan facies

Depostional Package 3
Seismic facies characteristics:
Consists mostly of sandstone and mudstone. In the southwestern area where the prograding clinoform reflectors are most prominent, the well log (well 6006/15-1) shows a funnel shaped gamma-ray log trend. This corresponds to a coarsening-upward facies, from mudstone through siltstone and sandstone. The unit is finally capped by a mudstone (no cutting descriptions are available for any further detail of the lithology) (well 6005/15-1).

Drill Cuttings Descriptions:

Wire-line log trend:
Large-scale (full package):
Coarsening-upward
Small-scale (up to 50 m):

Coarsening-upward

Interpretation: The clinoforms, the coarsening-upward lithology indicate could represent progradation of a distributary mouth bar in a wave dominated delta, or offshore muds into shore face coastal barrier sands. However based on xx interpreted to be delta front facies associations

Environment:
Delta front and delta top/plain facies association

DP3 in the central FSC
Seismic facies characteristics:
Parallel/obscured beneath basalt.

Drill Cuttings Descriptions:
Mudstone,siltstone and sandstone showing a thickening-upward. The sandstone range between 5-30 m in thickness (e.g. well 205/9-1).

Wire-line log trend:
Large-scale (full package):
Coarsening-upward
Small-scale (up to 50 m):
Coarsening upward cycles (8m thick). Box-shaped trend (30m thick)

Interpretation: Delta plain Sandstones, could be mouth bars, tidal flats. On the basis of the coarsening upward trend indicate delta front and the coals indicate delta or coastal plain deposits.

Environment:
Delta front and delta or coastal plain facies association

Depostional Package 4
Unit 4a
Seismic facies characteristics:
On-lap reflectors

Drill Cuttings Descriptions:
Predominantly composed of several fining-upward cyclic successions grading from sandstone to siltstone to mudstone, where every component is not always present in one fining-upward cycle (Wells 204/19-4a, 204/24-1a, 204/24a-3, 204/24a-4, 204/24a-5 and 204/24a-7).

Wire-line log trend:
Large-scale (full unit):

The log characteristics shows commonly a fining-upward (retrogradational) trend for example in well 204/24a-3 and 204/24a-5.

Small-scale (up to m):

Cyclic fining-upward trends.

Interpretation:

The on-lap reflectors onto the deeply incised channels together with the overall fining-upward trend indicate a sea level rise and the resulting generation of accommodation space and infilling. The small-scale fining-upward trends indicate that there is a fluctuating sea level within the overall transgression.

Based on the above descriptions the Unit is interpreted to represent a tide dominating delta or an Estuary. Since the seismic profile shows an incised valley network that is being back-stepped and filled up, it is most likely representing an Estuary. The current available data and the lack of core this interpretation is based on models. Depending on weather the Estuarine is wave or tide dominating the following facies could represent the fining up-ward cycles seen in the wells; 1) Alluvial channel and overbank, bay head delta, inner straight tidal-fluvial, tidal meanders.

Environment:

Estuarine facies association.

Unit 4b

Seismic facies characteristics:

On-lap

Drill Cuttings Descriptions:

Type 1) alternating mudstone/silty mudstone and lignite layers (e.g. in wells 204/19-1, 204/20-3, 204/23-1, 204/24a-3, 204/22-1 and 204/24a-5). The gamma-ray logs show an irregular and heterolitic trend.

Type 2) mudstone interbedded with thin(0.5 and 10m) thick fine-coarse sandstone layers (well 204/19-1, 204/19-5, 204/23-1, 204/24a-3, 204/24a-5). Gamma-ray log signature shows irregular trend,

Type 3) sandstone showing cleaning-upward log trend Well 204/22-2,

Type 4) sandstone that grade into argillaceous and very silty sandstone that show a dirtying-upward log trend (e.g. well 204/19-4).

Type 5) massive sandstone ranging between 20m and 50m in thickness with a few thin (up to 3m) mudstone interbeds (well 204/19-4 and 204/19-5). This facies occasionally shows a sharp box-shaped log trend (204/19-4) depending on how dirty the sand is where it is not as well pronounced (well 204/20a-6, 204/20-3, 204/24-1).

Core A:

In well 204/25a-2 a short core (7,6 m, 55% recovery) was taken from the uppermost part of unit 3b. The core consists of a fine-medium sandstone layer, and an overlying sucession that consists of silt-very fine-fine sandstone. The sedimentology has both a similar log signature and lithology as division 5 above, however, the core provides much more detailed of the sedimentological data and allows two main facies to be identified within

the division.

Facies 1 consist of a brown-green changing to light grey sandstone (thin-section indicates medium-coarse grained sandstone (quarts arenite), poorly sorted with sub-rounded grains).

Facies 2 shows a cyclic interval showing a number of upward coarsening intervals, from siltstone into very fine sandstone and fine sandstone. Facies x shows wavy sandstone laminations up to 3 cm thick. The base of facies2 is sharp and marked by abundant needle like fragments of black lignites. At the lowest most part some cm scale slump structures and oval shaped 1,2x0,4cm nodules of ?calcite? can be seen.

Core B:

In well 204/25a-3, three short cores (in total 19.5m, 95% recovery) were taken from unit 3b. The core contains a sandstone (it is not possible from the core to divide the sandstone into facies since the core only contained loose sands). The sandstone is fine-medium grained (thin-section indicates a well rounded and well sorted very clean quarts (<99%)) and frequently contains coal fragments that are generally very small (mm) but can be large up to 2cm. In the uppermost part of the core there is a thin cm scale red brown nodule of a paleosol. In the upper most part of the core the sandstone is red from oxidation, indicated from a geochemical analysis, which suggest no traces of tuff. The geochemical analysis additionally showed a high content of kaolinite.

Wire-line log trend:

Large-scale (full Unit):

No particular set trend

Small-scale (up to m):

1) Irregular trend, indicating no trend, containing heterolitic material.
2) fining-upward trend
3) coarsening-upward
4) box-shaped log trend

Core: cyclic coarsening-upward trends

Interpretation:

Seismic facies and well data indicate following:

Type 1 and 2. Heterolitic including lignites, sometimes sandstones, irregular log trend. Interpreted as marsh/swamp area. Sandstones represents channels, intertidal sand bar/flat. Depositional system, Estuarine (valley fill).

Type 3,4and 5. Depending on the location of the well with respect to the valley network (on the isochron map Fig. x) the sandstones represent either i) intertidal sand/bar. Depositional environment Eustarine (valley fill) or ii) marginal bar, tidal inlet, marginal spit. Depositional Environment Eustarine mouth.

Core: cyclic coarsening-upward trends are common in estuarine facies association.

The many different cycles of varying trends indicate the complexity of the Estuarine system and also indicate that the fill is forming during transgression, but within several cyclic fluctuation stages.

Environment:
Estuarine facies association

Unit 4c
Seismic facies characteristics:
Parallel

Drill Cuttings Descriptions:
Type 1) alternating layers of tuffaceous mudstone and lignites (wells 204/19-5, 204/20-3, 204/20a-6, 204/22-1 and 204/22-2, 204/23-1 and 205/16-2).
Type 2) mudstones, silty mudstone, siltstones and lignites (wells 204/14-2, 204/19-1 and 24a-3).
Type 3) mudstone layers with very thin siltstone and/or sandstone interbeds (well 204/19-5, 204/24a-3).
Type 4) sandstone and/or siltstone beds with very thin mudstone stringers, and lignites (well 204/14-2, 204/19-1 and 204/19-4, 204/24-1, 204/24a-3 and 204/24a-5, 204/25a-2, 204/25a-3). The sandstone is described as moderate to well sorted, ranging between very fine to coarse grained, and contains in well 204/19-1, 204/24-1, and 204/24a-3 glauconitic detritus.

Wire-line log trend:
Large-scale (full package):
aggradational-retrogradational
Small-scale (up to 50 m):

Interpretation:
Similar complexity and lithology as Unit 4b. The sandstones contain glauconitic detritus indicating marine sandstones either deposited as xx or xx. The parallel reflectors and the sedimentology suggests a continuous transgression and deposition of an aggrating nature of the Estuarine fill.

Environment:
Estuarine facies association

The Moray Group

The Balder Formation, T50 (Fig. 3.5)

Summary describtion: paralic (low velocity lignite mudstone facies) through littoral and sublittoral (sandy facies) to outher shelf (high velocity mudstone facies) (Knox et al., 1997).

Characteristics by Knox et al. (1997)*:* grey, variable silty and carbonaceous mudstone with abundant layers of green-grey to grey-green tuffs. Low gamma ray. The formation is sometimes informally divided into two component parts: a lower and an upper unit. The upper part contains grey mudstone with lower tuff content, indicated by higher gamma ray defined in the northern FSC and much of the central FSC. In the southern FSC (quadrant 204 and 205) the Balder Formation is sand dominated and tuff rich mudstones are absent. Further south the tuff-mudstones reappear but the mudstone is thinly bedded with lignite reflecting low velocity mudstone. This is overlain by grey higher velocity mudstones included within the Balder Formation. All above makes the boundaries difficult to define.

Interpretation: delta top/coastal plain (highstand) (Ebdon et al., 1995)

Upper boundary: depending where the well is located, but top is defined by downward incoming of grey, carbonaceous mud with sporadic tuffs and on log is often somewhat arbitrary (Knox, (1997).

Lower boundary: a downward change from mudstone with abundant tuffs to darker grey mudstone with fewer tuffs. It is downward increase in gamma ray however sometimes arbitrary (Knox et al., 1997).

Reg correlation: equivalent of Balder Formation in the North Sea Basin (Knox et al., 1997).

The Hildassay Sandstone Member, equivalent to the Sele and Dornoch Formation and T45 (Fig. 3.5)

Summary describtion: sandstones possible capped by coal (Ebdon et al., 1997).

Characteristics by Knox et al. *(1997):* consists of predominantly mudstone and sandstone. In detail the sandstone facies consists of claystone, mudstone, siltstone and sandstone of highly variable lithology, with thin lignites (the sequence describtions are based on core from well 206/2-1 and 208/x-x, the sandstone is cemented with kaolinite with local tight cementation by calcite) there is no regular organization of facies, with small-scale upward-coarsening and upward-fining cycles both being present. The mudstone facoes consosts dominantly of mudstone and siltstone interbedded with fine-coarse grained sandstone. The wireline log signature shows upwards coarsening cycles. There arte no cores taken in this facies.

Interpretation: based on the above description the sequence is interpreted to represent mostly prograding shallow marine facies, but ranging from paralic 'delta top' facies in proximal setting to 'prodelta' facies in distal setting (Knox et al., 1997). The paleoenvironment is interpreted to represent delta top/coastal plain (Ebdon et al., 1997)

Upper boundary: sharp downward decrease in GR.

Lower boundary: downward change from sst-mudst.

Regional corr: passes distally into siltstone and mudstone.

The Colsay Sandstone Member (equivalent to the Forties and T40 (Fig. 3.5)

Characteristics by Knox, (1997): consists dominantly of mudstone and sandstone (facies 1a and 1b) and mudstone (facies 2). A bed of basaltic lava is present in well 205/9-1 (Knox et al., 1997). Facies 1a: consists of claystone, mudstone, siltstone and sandstone, of highly variable facies, with thin lignites. There is no regular organization of facies, with small-scale upward-coarsening and upward-fining cycles both being present. Facies 1b represents dominantly mudstone and siltstone, interbedded with fine-coarse grained sandstone. The log trend shows upward-coarsening cycles. Facies 2: contains largely mudstone. However, in the central FSC (well 214/28-1 and core data) a thick sandstone section (Shanmugam et al. 1995) represent local mounded sand body characterized by thinly bedded sandstones with serrated gamma ray log signature that lacks evidence of the upward-coarsening profile of the prograding facies. This sandstone dominating section is restricted to the area around 214/28-1, but equivalent mudstone dominate in well 208/21-1 and well 208/17-1 that include thin sandstone beds.

Interpretation: mostly prograding shallow marine facies, but ranging from paralic 'delta top' facies in proximal setting (facies 1a and 1b interpreted to represent the more distal 'progradational' sucession, but still in the delta top facies) to 'prodelta' facies (facies 2) in distal setting (Knox et al., 1997). The coarsening cycles (facies 1b) are largely restricted to the basal part of the succession, whereas in more distal sections e.g quadrant 206, facies 1b constitute the bulk of the succession. Furthermore, the T40 sandstone interval in the central FSC (Facies 2) is interpreted to represent a major lowstand fan (not observed on seismic) (Ebdon et al., 1995).

Upper boundary: a downward change from mudstone-sandandstone.

Lower boundary: adownward change from erratic signatures to uniform mudstone facies of the Lamba Formation (in distal section). In more proximal area the sequence is more difficult to detect, but basal beds are more sandy and the uppermost sediments of the Lamba Formation are more variable in lithology (Knox et al., 1997).

Extent: is present in central FSC, in basinal areas. In southern FSC the sequence is absent through non-deposition or erosion (Ebdon et al. 1995).

Regional corelation: passes distally into siltstone and mudstone (Knox et al., 1997).

REFERENCES

Ahorner, L. 1970. Seismo-tectonic relations between the graben zones of the upper and lower Rhine valley. *In*: Müller, J.H. Illies, St. (Eds). Graben problems, 155-166

Ahorner, L. 1975. Present-day stress field and seismotectonic block movements along major fault zones in central Europe. *Tectonophysics* **29**, 233-249

Ali, J.R. & Jolley, D.W. 1996. Chronostratigraphic framework for the Thanetian and lower Ypresian deposits of southern England. *In*: Knox, R.W.O'B., Corfield, R.M. & Dunay, R.E. (Eds). Correlation of the Early Paleogene in Northwest Europe. *Geological Society Special Publication*, **101**, 129-144

Ali, J.R. and Hailwood, E.A. 1998. Magnetostratigraphic (re)calibration of the Paleocene/Eocene boundary interval in Holes 550 and 549, Goban Spur, eastern North Atlantic. *Earth and Planetary Science Letters* **161**, 201-213

Allen, P.R. and Allen, J.R. 1990. Basin Analysis, principles and applications. Blackwell Science, UK. 451p.

Andersen, M.S. 1988. Late Cretaceous and early Tertiary extension and volcanism around the Faeroe Islands. *In*: Morton, A.C. & Parson, L.M. (eds). Opening of the NE Atlantic. *Geological Society Special Publication* **39**, 115-122

Andersen, M.S. and Boldreel, L.O. 1995. Tertiary compression structures in the Faroe-Rockall area. The tectonics, sedimentation and Palaeo-oceanography of the North Atlantic Region. *In*: R.A. Scrutton, M.S. Stoker, G.B. Shimmield and A.W. Tudhope (eds). *Geological Society Special Publication* **90**, 215-216

Andersen, M.S., Nielsen, T., Sørensen, B.A., Boldreel, O.L., & Kuijpers, A. 2000. Cenozoic sediment distribution and tectonic movements in the Faroe region. *Global and Planetary Change* **24**, 239-259

Anderson, D.L., Tanimoto, T. and Zhang, Y.S. 1992. Plate tectonics and hotspots: The third dimension. *Science* **256**, 1645-1651

Anderson, D.L. 1998. The edge effects of the mantle. *In*: Gurnis, M. et al., (eds). The core-mantle boundary region: American Geophysical Unit Geodynamics Series 28, 255-271

Artyushkov, E.V. 1973. Stresses in the lithosphere caused by crustal thickness inhomogeneities. *Journal of geophysical Research* **78**, 7675-7708

Ashcroft, W.A., Hurst, A. and Morgan, C. J. Reconciling gravity and seismic data in the Faeroe-Shetland Basin, West of Shetland. *In*: Fleet, A.J. and Boldy, S.A.R. (eds). Petroleum Geology of Northwest Europe: Proceedings of the 5th Conference. Geological Society, London, 595-600.

Aubry M.-P., Berggren W.A. ; Stott L. and Sinha A. 1996. The Upper Paleocene-Lower Eocene stratigraphic record and the Paleocene-Eocene boundary carbon isotope excursion: implications for geochronology. *In*: Knox R.W. O'B., Corfield, R.M. & Dunay, R.E. (Eds). Correlation of the early Paleogene in northwest Europe. *Geological Society Special Publication* **101**, 353-380

Bailey, N.J.L., Walker, P. and Sauer, M.J. Geochemistry and source rock potential of the West of Shetlands. Petroleum Geology of North West Europe. *In*: Brooks, J and Glennie, K. (eds). 711-721

Barton A.J. and White R.S. 1997. Volcanism on the Rockall continental margin. *Journal of the Geological Society, London* **154**, 531-536

Barton A.J. and White R.S. 1997. Crustal structure of Edoras Bank continental margin and mantle thermal anomalies beneath the North Atlantic. *Journal of Geophysical Research* **102**, 3109-3129

Beerling, D.J. and Jolley, D.W. 1998. Fossil plants record an atmospheric 12CO2 and temperature spike across the Palaeocene-Eocene transition in NW`Europe. *Journal of the Geological Society* **155**, 591-594

Bell, B.R. and Jolley, D.W. 1997. Application of palynological data to the chronology of the Palaeogene lava fields of the British Province: implications for magmatic stratigraphy. *Geological Society, London* **154**, 701-708

Berggren, W.A., Kent, D.V., Swisher, C.C. and Aubry, M.-P. 1995. A revised Cenozoic geochronology and chronostratigraphy. *In*: Berggren, W.A (Eds) Geochronology, time scales and global stratigraphic correlation. *Society for Sedimentary Geology Special Publication* **54**, 129-212

Berggren, W.A. and Aubry, M.P. 1996. A late Paleocene-early Eocene NW European and North Sea magnetobiochronological correlation network. *In*: Knox,

R.W.O'B., Corfield, R.M. and Dunay, R.E. (Eds). Correlation of the Early Paleogene in Northwest Europe. *Geological Society Special Publication* **101**, 309-352

Berggren, W.A., Kent, D.V., Swisher, C.C. and Aubry, M-P. 1995. Geochronology Time Scales and Global Stratigraphic Correlation. *Society for Sedimentary Geology Special Publication* **54**, 130pp

Berggren, W.A., Kent, D.V., Swisher, C.C. and Aubrey, M.P. 1995. A revised Cenozoic geochronology and chronostratigraphy. *In*: Berggren, W.A., Kent, D.V. and Hardenbol, J. (Eds). Geochronology, Time Scales and Stratigraphic Correlation: a Framework for an Historical Geology. *Society of Economic Paleontologists and Mineralogists*, Special Volume, **54**

Bertram, G.T. and Milton, N.J. 1988. Reconstructing basin evolution from sedimentary thickness; the importance of palaeobathymetric control, with reference to the North Sea. *Basin Research* **1**, 247-257

Bird, P. 1998. Testing hypotheses on plate-driving mechanisms with global lithosphere models including topography, thermal structure, and faults. *Journal of geophysical Research* **103**, 10,115-10,129

Blystad, P., Brekke, H., Færseth, R.B., Larsen, B.T., Skogseid, J. and Tørudbakken, B. 1995. Structural elements of the Norwegian continental shelf. Part II: the Norwegian Sea region. *Norwegian Petroleum Directorate Bulletin* **8**

Boldreel, L.O. and Andersen, M.S. 1993. Late Paleocene to Miocene Compression in the Faroe-Rockall area. *In*: Parker, J.R. (eds) Petroleum Geology of Northwest Europe: Proceedings of the 4th Conference. Geological Society, London, 1025-1034

Boldreel, L.O. and Andersen, M.S. 1994. Tertiary development of the Faeroe-Rockall Plateau based on reflection seismic data. *Bulletin of the geological Society Denmark* **41**, 162-180

Boldreel, L.O., Andersen, M.S. 1998. Tertiary compressional structures on the Faroe-Rockall Plateau in relation to northeast Atlantic ridge-push and Alpine foreland stresses. *Tectonophysics* **300**, 13-28

Bott, M.H.P., Sunderland, J., Smith, P. J., Casten, U. and Saxov, S. 1974. Evidence for continental crust beneath the Faeroe Islands. *Nature* **248**, 202-204

Bott M.H.P. 1982. The interior of the Earth: its structure, constitution and evolution. (2nd edition). 416pp

Bott M.H.P. and Kusznir N.J. 1984. The origin of tectonic stress in the lithosphere. *Tectonophysics* **105**, 1-13

Bott, M.H.P. and Smith, P.J. 1984. Crustal structure of the Faroe-Shetland Channel. *Geophysical Journal Royal Astronomical Society* **76**, 383-398

Bott, P.H.M. 1988. A new look at the causes and consequences of the Icelandic hot-spot. *In*: Morton, A.C. and Parson, L.M. (eds). Opening of the NE Atlantic. *Geological Society Special Publication* **39**, 15-23

Bott, P.H.M. 1991. Ridge push and associated plate interior stress in normal and hot spot regions. *Tectontphysics* **200**, 17-32

Bott, P.H.M. 1992. Passive margins and their subsidence. *Journal of the Geological Society, London* **149**, 805-812

Bott, P.H.M., 1993. Modelling the plate-driving mechanism. *Journal of the Geological Society, London* **150**, 941-951

Boulter, M.C. and Manum, S.B. 1989. The Brito-Arctic igneous province flora round the Paleocene/Eocene boundary. *In*: Eldholm O. (Eds). *Proceedings of the Ocean Drilling Program, Scientific results* **104**, 663-680

Brewer, J.A. and Smythe, D.K. 1984. MOIST and the continuity of crustal reflector geometry along the Caledonian- Appalachian orogen (UK). *Journal of the Geological Society, London* **141**, 105-120

Brodie, J. and White, N. 1994. Sedimentary basin inversion caused by igneous underplating: Northwest European continental shelf. *Geology* **22**, 147-150

Brodie, J. and White, N. 1995. The link between sedimentary basin inversion and igneous underplating. *In*: Buchanan, J,G. & Buchanan, P.G. (eds). Basin inversion. *Geological Society Special Publication* **88**, 21-38

Brooks, C.K. 1973. Tertiary of Greenland; A Volcanic and Plutonic Record of Continental Break-up. Arctic Geology Memoir. *American Association of Petroleum Geologists* **19**, 150-160

Bujak, J.P. & Mudge, D.C. 1994. A high-resolution North Sea Eocene dinocyst zonation. *Journal of the Geological Society* **151**, 449-462

Bujak, J.P. and Brinkhuis, H. 1998. Global warming and dinocyst changes across the Paleocene/Eocene epoch boundary. In, Late Paleocene-early Eocene climatic and biotic events in the marine and terrestrial records. Columbia University Press, New York, 277-295

Campbell, H.I. & Griffiths, W.R. 1990. Implications of mantle plume structure for the evolution of flood basalts. *Earth and Planatary Science Letters* **99**, 79-93

Campbell, H.I. 2001. Identification of ancient mantle plumes. *Geological Society of America, Sepecial Paper* **352**, 5-21

Cande, S.C., LaBrecque, J.L., Larson, R.L., Pittman, W.C., Golovchenko, X. and Haxby, W.F. 1989. Magnetic lineations of the world's ocean basins Pagination: 13 . 1 sheet. Tulsa, OK, American Association of Petroleum Geology, United States

Cande S.C. and Kent D.V. 1992. A new geomagnetic polarity time scale for the late Cretaceous and Cenozoic. *Journal of Geophysical Research* **97**,13,917-13,951

Cande, S.C. & Kent, D.V. 1995. Revised calibration of the geomagnetic polarity timescale for the Late Cretaceous and Cenozoic. *Journal of Geophysical Research* **100 (B4)**, 6093-6095.

Cartwright, J.A. 1994. Episodic basin-wide hydrofracturing of overpressured early Cenozoic mudrock sequences in the North Sea basin. *Marine and Petroleum Geology* **11**, 587-607

Cartwright, J.A. and Lonergan, L. 1996. Volumetric concentration during the compaction of mudrocks: A mechanism for the development of regional-scale polygonal fault systems. *Basin Research* **8**, 183-193

Casten, U. 1973. The Crust Beneath the Faeroe Islands. *Nature* **241**, 83-84

Casten, U. and Nielsen, P.H. 1975. Faeroe Islands; a microcontinental fragment? *Journal of Geophysics* **41**, 357-366

Celâl Şengör, M.A. 2001. Elevation as indicator of mantle-plume activity. *Geological Society of America Special Paper* **352**, 183-217

Chalmers, J.A., Larsen, L.M. & Pedersen, A.K. 1995. Widespread Palaeocene volcanism around the northern North Atlantic and Labrador Sea: evidence for a large, hot, early plume head. *Journal of the Geological Society* **152**, 965-969

Chambers, L.M. and Fitton, J.G. 2000. Geochemical transitions in the ancestral Iceland Plume; evidence from the Isle of Mull Tertiary volcano, Scotland. *Journal of the Geological Society, London* **157**, 261-263

Chapple, W.M. and Tullis, T.E. 1977. Evaluation of the forces that drive the plates. *Journal of Geophysical Research* **82**, 1967-1984

Clarke, D.B. and Upton, B.G.J. 1971. Tertiary basalts of Baffin island; field relations and tectonic setting. *Canadian Journal of Earth Sciences* **8**, 248-258

Clarke, D.B. and Pedersen, A.K. 1976. Tertiary volcanic province of West Greenland. *In*: Escher, A.and Watt, W.S. (Eds). Geology of Greenland. Grønlands Geologiske Undersøgelse, Copenhagen 364-385.

Clift, P.D. and Turner, J. 1994. Tectonic evolution of the NE Atlantic volcanic margins and the influence of the Icelandic hotspot. AGU 1994 fall meeting Eos, Transactions, American Geophysical Union 75, 607

Clift, P.D., Turner, J. and ODP Leg 152 Scientific Party. 1995. Dynamic support by the Iceland Plume and its effect on subsidence of the northern Atlantic margins. *Journal of the Geological Society* **152**, 935-941

Clift, P.D. 1999. The thermal of Paleocene magmatic underplating in the Faeroe-Shetland-Rockall region. *In*: Fleet, A.J. and Boldy, S.A.R. (eds). Petroleum Geology of Northwest Europe: Proceedings of the 5th Conference. Geological Society, London, 585-593

Cloetingh, S. 1992. Intraplate stresses; a tectonic cause for third-order cycles in apparent sea level? *In*: Wilgus, C.K., Hastings, B.S. Ross, C.A. Posamentier, H.W., Van Wagoner, J. and Kendall, C.G.St.C. (Eds). Sea-level changes; an integrated approach. *Society of Economic Paleontologists and Mineralogists, Special Publication* **42**, 19-29

Coffin, M.F. and Eldholm, O. 1992. Volcanism and continental break-up; a global compilation of large igneous provinces. *In*: Storey, B.C., Alabaster, T. and

Pankhurst, R.J. (Eds). Magmatism and the causes of continental break-up. *Geological Society Special Publications* **68**, 17-30

Cooper, M.M., Evans, C.A., Lynch, J.D., Neville, G. and Newley, T. 1999. The Foinaven Field: managing reservoir development uncertainty prior to start-up. *In*: Fleet, A.J. and Boldy, S.A.R. (eds). Petroleum Geology of Northwest Europe: Proceedings of the 5th Conference. Geological Society, London, 675-692

Courtney, R.C. and White, R.S. 1986. Anomalous heat flow and geoid across the Cape Verde Rise; evidence for dynamic support from a thermal plume in the mantle. *Geophysical Journal of the Royal Astronomical Society* **87**, 815-867

Cox, K.G. 1989. The role of mantle plumes in the development of continental drainage patterns. *Nature* **342**, 873-877

Dahlen, F.A. 1981. Isostasy and the ambient state of stress in the oceanic lithosphere. *Journal of Geophysical Research* **86B**, 7801-7807

Dam, G., Larsen, M., Nohr-Hansen, H. and Pulvertaft, T.C.R. 1999. Discussion on the erosional and uplift history of NE Atlantic passive margins: constraints on a passing plume. *Journal of the Geological Society* **156**, 653-656

Dam, G. and Sønderholm, M. 1994. Lowstand slope channels of the Itilli succession (Maastrichtian-Lower Paleocene), Nuussuaq, West Greenland. *Sedimentary Geology* **94**, 49-71

Dam, G. and Sønderholm, M. 1998. Sedimentological evolution of a fault-controlled Early Paleocene incised-valley system, Nuussuaq Basin, West Greenland. *In*: (eds). Relative Role of Eustacy, Climate and Tectonism in Continental Rocks. *Society for Sedimentary Geology Special Publication* **59**, 109-121

Dam, G., Larsen, M. and Sønderholm, M. 1998. Sedimentary response to mantle plumes: Implications from Paleocene onshore successions, West and East Greenland. *Geology* **26**, 207-210

Dalrymple, R.W., Boyd, R. and Zaitlin, B.A. History of research, types and internal organisation of incised-valley systems: introduction to the volume. *In*: Dalrymple, R.W., Boyd, R. and Zaitlin, B.A. (Eds). Incised-Valley systems: Origin and Sedimentary Sequences. *Society for Sedimentary Geology Special Publication* **51**, 3-10

Davies, R., Cloke, I., Cartwright, J., Robinson, A., and Ferrero, C. 2004. Post-breakup compression of a passive margin and its impact on hydrocarbon prospectivity: An example from the Tertiary of the Faeroe-Shetland Basin, United kingdom. *AAPG Bulletin* **88**, 1-20

Dawers, N. H., Berge, A. M., Häger, K.–O., Puigdefabregas, C. and Underhill, J. R. 1999. Controls on Late Jurassic, subtle sand distributiuon in the Tampen Spur area, Nprthern North Sea. *In*: Fleet, A.J. and Boldy, S.A.R. (eds). Petroleum Geology of Northwest Europe: Proceedings of the 5th Conference. Geological Society, London, 827-838

de Voogd, B.and Keen, C.E. 1987. Lithoprobe east; results from reflection profiling of the continental margin; Grand Banks region. *Geophysical Journal of the Royal Astronomical Society* **89**, 195-200

Dean, K., McLachlan, K. & Chambers, A. 1999. Rifting and the development of the Faroe-Shetland Basin. *In*: Fleet, A.J. and Boldy, S.A.R. (eds) Petroleum Geology of Northwest Europe: Proceedings of the 5th Conference. Geological Society, London, 533-544

Deegan, C.E. & Scull, B.J. 1977. A standard lithostratigraphic nomenclature for the central and northern North Sea. Institute of Geological Sciences Report 77/25

Dewey, F. J. & Windley, F. B. 1988. Palaeocene-Oligocene tectonics of NW Europe. *In*: Morton, A.C. & parson, L. M. (eds). Early Tertiary Volcanism and the Opening of the NE Atlantic, *Geological Society Special Publication* **39**, 25-31

Dewey J.F. 1988. Midplate seismicity exterior to former rift-basins. *Seismological Research Letters* **59**, 213-218

Dewey J.F. 1988. Extensional collapse of orogens. *Tectonics* **7**, 1123-1139

Donn, W.L. and Ninkovich, D. 1980. Rate of explosive volcanism in the North Atlantic Ocean inferred from deep sea cores. *Journal of Geophysical Research* **85**, 5455-5460

Doré, A.G. 1992. Synoptic palaeogeography of the Northeast Atlantic Seaway: late Permian to Cretaceous. *In*: Parnell, J. (eds). Basins on the Atlantic Seaboard: Petroleum Geology, Sedimentology and Basin Evolution. *Geological Society Special Publication* **62**, 421-446

Doré, A.G. and Lundin, E.R. 1996. Cenozoic compressional Structures on the NE Atlantic margin : nature, origin and potential significance for hydrocarbon exploration. *Petroleum Geoscience* **2**, 299-311

Doré, A.G., Lundin, E.R., Birkeland, OE, Eliassen, P.E. and Jensen L.N. 1997. The NE Atlantic Margin: implications of Late Mesozoic and Cenozoic events. *Petroleum Geoscience* **3**, 117-131

Doré, A.G., Lundin, E.R., Fichler, C. & Olesen, O. 1997. Patterns of basement structure and reactivation along the NE Atlantic margin. *Journal of the Geological Society, London* **154**, 85-92

Doré, A.G., Lundin, E.R., Jensen, L.N., Birkeland, OE., Eliassen, P.E. & Fichler, C. 1999. Principal tectonic events in the evolution of the northwest European Atlantic margin, 41-60. *In*: Fleet, A.J. and Boldy, S.A.R. (eds). Petroleum Geology of Northwest Europe: Proceedings of the 5th Conference. Geological Society, London, 41-60

Duindam, P. and Van Hoorn, B. 1987. Structural evolution of the west Shetland continental margin. *In*: Brooks, J. & Glennie, K.W. (Eds.): Petroleum Geology of Northwest Europe, 765-773

Duncan, R.A. and Richards, M.A. 1991. Hotspots, mantle plumes, flood basalts, and true polar wander. *Reviews of Geophysics* **29**, 31-50

Earle, M.M., Jankowski, E.J., Vann, I.R. 1985. Structural and Stratigraphic Evolution of the Faeroe-Shetland Channel and Northern Rockall Trough

Ebdon, C.C., Granger, P.J., Johnson, H.D., Shimmield, M.S. and Tudhope, G.B. 1995. Early Tertiary Evolution and Sequence Stratigraphy of the Faroe-Shetland Basin: implications for hydrocarbon prospectivity. Sedimentation and Palaeoceanography of the North Atlantic Region. *Geological Society Special Publications* **90**, 51-69

Egloff, J. and Johnson, G.L. 1975. Morphology and structure of the southern Labrador Sea. *Canadian Journal of Earth Sciences* **12**, 2111-2133

Eidvin, T., Jansen, E., Rundberg, Y., Brekke, H. and Grogan, P. 2000. The upper Cainozoic of the Norwegian continental shelf correlated with the deep sea record

of the Norwegian Sea and the North Atlantic. *Marine and Petroleum Geology* **17**, 579-600

Eldholm O., Sundvor E. and Myhre A. 1979. Continental margin off Lofoten-Vesteralen, northern Norway. Marine *Geophysical Researches* **4**, 3-35

Eldholm, O. & Sundvor, E. 1980. The continental margins of the Norwegian-Greenland Sea: recent results and outstanding problems. Phil. Trans. Royal Society, London **294A**, 77-86

Eldholm, O. and Grue, K. 1994. North Atlantic volcanic margins; dimensions and production rates. *Journal of Geophysical Research* **99B**, 2955-2968

Eldholm, O., Gladczenko, T.P., Skogseid, J. and Planke, S. 2000. Atlantic volcanic margins; a comparative study. *In*: Nottvedt, A. (Eds). Dynamics of the Norwegian margin. *Geological Society Special Publications* **167**, 411-428

Eldholm, O., Gladczenko, P.T., Skogseid, J and Planke, S. 2000. Atlantic volcanic margins: a comparative study. *In*: Nøttvedt, A. et al. (eds). Dynamics of the Norwegian Margin. *Geological Society Special Publication* **167**, 411-428

Eldholm, O., Tsikalas, F. and Faleide, I. J. 2002. Continental margin off Norway 62-75 ° N: Palaeogene tectono-magmatic segmentation and sedimentation. *In*: Jolley, D.W. and Bell, B.R. (eds). The North Atlantic Igneous Province: Stratigraphy, Tectonic, Volcanic and Magmatic Processes. *Geological Society Special Publication* **197**, 39-68

Ellis, D., Bell, B.R., Jolley, D.W. and O'Callaghan, M. 2002. The stratigraphy, environment of eruption and age of the Faroes Lava Group, NE Atlantic Ocean. *In*: Jolley, D.W.and Bell, B.R. (Eds.). The North Atlantic igneous province; stratigraphy, tectonic, volcanic and magmatic processes. *Geological Society Special Publications* **197**, 253-269

Ellison, R.A., Knox, R.W.O'B., Jolley, D.W. & King, C. 1994. A revision of the lithostratigraphical classification of the early Palaeogene strata in the London Basin and East Anglia. *Proceedings of the Geologists Association* **105**, 187-197

Ellison, R.A., Ali, J.R., Hine, N.M. and Jolley, D.W. 1996. Recognition of Chron C25n in the upper Paleocene Upnor Formation of the London Basin, UK. *In*: Knox, R.W.O'B., Corfield, R.M.and Dunay, R.E. (Eds). Correlation of the early

Paleogene in Northwest Europe. *Geological Society Special Publication* **101**, 185-193

England, P.C. and McKenzie, D.P. 1982. A thin viscous sheet model for continental deformation. *Geophysical Journal of Royal Astronomy Society* **70**, 295-322

Falvey, D.A. 1974. The development of continental margins in plate tectonic theory. *The APEA Journal* **14**, 95-106

Fitch, F.J., Heard, G.L. and Miller, J.A. 1988. Basaltic magmatism of Late Cretaceous and Palaeogene age recorded in wells NNE of the Shetlands. *In*: Morton, A.C.and Parson, L.M. (Eds). Early Tertiary volcanism and the opening of the NE Atlantic. *Geological Society Special Publication* **39**, 253-262

Fitton, G.J., Saunders, D.A., Norry, J.M., Hardarson, S.B. & Taylor, N.R. 1997. Thermal and chemical structure of the Iceland plume. *Earth and Planatary Letters* **153**, 197-208

Forsyth, D.W. and Uyeda, S. 1975. On the relative importance of the driving forces of plate motion. *The Geophysical Journal of the Royal Astronomical Society* **43**, 163-200

Gibb, F.G.F., and Kanaris-Sotiriou, R. 1988. The geochemistry and origin of the Faeroe-Shetland sill complex. *In*: Morton, A.C. and Parson, L.M. (eds). Opening of the NE Atlantic. *Geological Society Special Publication* **39**, 241-252

Gibson, T.G., Bybell, L.M., Owens, J.P. 1993. Latest Paleocene lithologic and biotic events in neritic deposits of southwestern New Jersey. *Paleoceanography* **8**, 495-514

Golke, M., and Coblentz, D. 1996. Origins of the Europeanregional stress field. *Tectonophysics* **266**, 11–24

Green, P.F., Duddy, I.R., Hegarty, K.A. and Bray, R.J. 1999. Early Tertiary flow along the UK Atlantic margin and adjacent areas. *In*: Fleet, A.J. and Boldy, R.A.S. (eds). Petroleum Geology of Northwest Europe: Proceedings of the 5th Conference. Geological Society, London, 349-357

Griffiths, W.R. & Campbell, H.I. 1990. Stirring and structure in mantle starting plumes. *Earth and Planatary Science Letters* **99**, 66-78

Gronlie, G., Chapman, M. and Talwani, M. 1979. Jan Mayen Ridge and Iceland Plateau: origin and evolution. *Norsk Polarinstitutt Skrifter* **170**, 25-47

Hald, N. and Waagstein, R. 1984. Lithology and chemistry of a 2-km sequence of lower Tertiary tholeiitic lavas drilled on Suduroy, Faeroe Islands (Lopra-1). The deep drilling project 1980-1981 in the Faeroe Islands. *Annales Societatis Scientiarum Faroensis, Supplementum* **9**, 15-38

Haq, U.B., Hardenbol, J. and Vail, R. P. 1987. Chronology of Fluctuating Sea Levels Since the Triassic. *Science* **235**, 1156-1166

Hazeldine, R.S., Ritchie, J.R. and Hitchen, K. 1987. Seismic and well evidence for the development of the Faroe-Shetland Basin.

Heilmann-Clausen, C. 1985. Dinoflagellate stratigraphy of the Uppermost Danian to Ypresian in the Viborg 1 borehole, Central Jylland, Denmark. *Danmarks Geologiske Undersøgelser* **7A**, 1-69

Hjelstuen, O.B., Eldholm, O. and Skogseid, J. 1999. Cenozoic evolution of the northern Vøring margin. *GSA Bulletin* **111**, 1792-1807

Hill, I.R. 1991. Starting plumes and continental break-up. *Earth and Planetary Science Letters* **104**, 398-416

Hinz, K. and Weber, J. 1975. Zum geologischen Aufbau des Norwegischen Kontinentalrandes und der Barents-See nach reflexionsseismischen Messungen. Translated: The geologic structure of the Norwegian continental margin and of the Barents Sea from seismic reflection surveys. Ergaenzungsband, 3-29

Hinz, K. and Schlueter, H.U. 1978. Der Nordatlantik; Ergebnisse geophysikalischer Untersuchungen der BGR an nordatlantischen Kontinentalraendern. Translated: The North Atlantic; results of geophysical investigations by the Federal Institute for Geosciences and Natural Resources on North Atlantic continental margins. *Erdoel-Erdgas-Zeitschrift* **94**, 271-280

Hinz, K., Eldholm, O., Block, M and Skogseid, J. 1993. Evolution of North Atlantic continental margins. In: Parker, J. R. (eds). Petroleum Geology of Northwest Europe: Proceedings of the 4th Conference. Geological Society, London, 901-913

Hitchen, K. and Ritchie, J.D. 1987. Geological Review of the West of Shetlans Area. *In*: Brooks, J. and Glennie, K (eds). Petroleum Geology of North West Europe. 737-749

Hjelstuen, B.O., Eldholm, O., Skogseid, J. 1997. Vøring Plateau diapir fields and their structural and depositional settings. *Marine Geology* **144**, 22-57

Hjelstuen, B.O., Eldholm, O., Skogseid, J. 1999. Cenozoic evolution of the northern Vøring margin. *GSA Bulletin* **111**, 1792-1807

Holbrook, W.S. and Keleman, P.B. 1993. Large igneous province on the US Atlantic margin and implications for magmatism during continental breakup. *Nature* **364**, 433-436

Holmes M.A. 1998. Alteration of uppermost lavas and volcaniclastics recovered during Leg 152 to the East Greenland margin. *Proceedings of the Ocean Drilling Program Scientific Results* **152**, 115-128

Hooker, J.J. The sequence of mammals in the Thanetian and Ypresian of the London and Belgium Basins. Location of the Palaeocene-Eocene boundary. *Newsletter of Stratigraphy* **25**, 75-90

Japsen, P. 1997. Regional Neogene exhumation of Britain and the western North Sea. *Journal of the Geological Society, London* **154**, 239-247

Japsen, P. and Chalmers, A.J. 2002. Neogene uplift and tectonics around the North Atlantic: overview. *Global and Planetary Change* **24**, 165-173

Jolley, D.W. 1996. The earliest Eocene sediments of eastern England: an ultra-high resolution palynological correlation. *In*: Knox, R.W.O'B., Corfield, R.M. and Dunay, R.E. (Eds). Correlation of the Early Paleogene in Northwest Europe. *Geological Society Special Publication* **101**, 219-254

Jolley, D.W. 1997. Palaeosurface palynofloras of the Skye lava field and the age of the British Tertiary volcanic province. *In*: Widdowson, M. (eds). Palaeosurfaces: Recognition, Reconstruction and Palaeoenvironmental Interpretation. *Geological Society Special Publication* **120**, 67-94

Jolley, D.W. 1998. Palynostratigraphy and depositional history of the Palaeocene Ormesby/Thanet depositional sequence set in southeastern England and its

correlation with continental West Europe and the Lista Formation, North Sea. *Review of Palaeobotany and Palynology* **99**, 265-315

Jolley, D.W. and Bell, B.R. 2002. Genesis and age of the Erlend Volcano, NE Atlantic margin. *In*: Jolley, D.W.and Bell, B.R. (Eds). The North Atlantic igneous province; stratigraphy, tectonic, volcanic and magmatic processes. *Geological Society Special Publications* **197**, 95-110

Jolley, D.W., Clarke, B. and Kelley, S. 2002. Paleogene time scale miscalibration: Evidence from the dating of the North Atlantic igneous province. *Geology* **30**, 7-10

Jones, R.W. and Milton, N.J. 1994. Sequence development during uplift: Palaeogene stratigraphy and relative sea-level history of the Outer Moray Firth, UK North Sea. *Marine and Petroleum Geology* **11**, 157-165

Joppen, M. and White, R.S. 1990. The structure and subsidence of Rockall Trough from two-ship seismic experiments. *Journal of Geophysical Research* **95B**, 19,821-19,837

Keen, C.E., Mudford, B., Stockmal, G.S., Welsink, H. and Quinlan, G. 1987. Deep crustal structure and evolution of the rifted margin northeast of Newfoundland: results from LITHOPROBE East. *Canadian Journal of Earth Sciences* **24**, 1537-1549

Keen, C.E. and De Voogd, B. 1988. The continent- ocean boundary at the rifted margin off eastern Canada: new results from deep seismic reflection studies. *Tectonics* **7**, 107-124

Keen, C.E., Peddy, C., De Voogd, B. and Matthews, D. 1989. Conjugate margins of Canada and Europe: results from deep reflection profiling. *Geology* **17**, 173-176

Keen, C.E., Kay, W.A. and Roest, W.R. 1990. Crustal anatomy of a transform continental margin. *Tectonophysics* **173**, 527-544

Kelly, D.C., Bralower, T.J., Zachos, J.C., Permoli S.I. and Thomas, E. Rapid diversification of planktonic foraminifera in the tropical Pacific (ODP Site 865) during the late Paleocene thermal maximum. *Geology* **24**, 423-426

Kennett J.P. and Stott L.D. 1991. Abrupt deep-sea warming, palaeoceanographic changes and benthic extinctions at the end of the Palaeocene. *Nature* **353**, 225-229

Kent, R. 1991. Lithospheric uplift in eastern Gondwana: evidence for a long-lived mantle plume system? *Geology* **9**, 19-23

Kent, R.W., Storey, M. & Saunders, D.A. 1992. Large igneous provinces: Sites of plume impact or plume incubation. *Geology* **20**, 891-894

Kent, R.W. 1995. Magnesian basalts from the Hebrides, Scotland: chemical composition and relationship to the Iceland plume. *Journal of the Geological Society* **152**, 979-983

Kimbell, S.G., Gatliff, W.R., Ritchie, D.J. Walker, D.S.A. and Williamson, P.J. 2004. Regional three-dimensional gravity modelling of the NE Atlantic margin. *Basin Research* **16**, 259-278

Kioerbøe, L. 1999. Stratigraphic relationships of the Lower Tertiary of the Faroe Basalt Plateau and the Faroe-Shetland Basin. *In*: Fleet, A.J. and Boldy, S.A.R. (eds). Petroleum Geology of Northwest Europe: Proceedings of the 5th Conference. Geological Society, London, 559-571.

Knox, R.W.O'B. 1983. Volcaniclastics in the Oldhaven Beds. *Proceedings of the Geologists Association* **94**, 245-250

Knox, R.W.O'B. and Morton, A.C. 1983. Stratigraphic distribution of Early Palaeocene pyroclastic sediments. *Proceedings of the Yorkshire Geological Society* **44**, 355pp

Knox R.W.O'B., and Morton A.C. 1988. Early Tertiary N Atlantic volcanism in sediments of the North Sea Basin. *In*: Morton, A.C. and Parson, L.M. (eds). Opening of the NE Atlantic. *Geological Society Special Publication* **39**, 407-419

Knox, R.W.O'B. and Holloway, S. 1992. Paleogene of the central and northern North Sea. *In*: Knox, R.W.O'B. and Cordey, W.G. Lithostratigraphic nomenclature of the UK North Sea. Nottingham: British Geological Survey

Knox, R.W.O'B. 1994. From regional stage to standard stage: implications for the historical Paleogene stratotypes of NW Europe. GFF **116**, 55-56

Knox, R.W.O'B. 1996. Tectonic controls on sequence development in the Palaeocene and earliest Eocene of southeast England: implications for North Sea stratigraphy. *In*: Hesselbo, S.P. and Parkinson, D.N. (eds). Sequence Stratigraphy in Briotish Geology. *Geological Society Special Publication* **103**, 209-230

Knox, R.W.O'B. 1996. Correlation of the early Paleogene in northwest Europe: an overview. *In*: Knox, R.W.O'B., Corfield, R.M. and Dunay, R.E. (eds). Correlation of the Early Paleogene on Northwest Europe. *Geological Society Special Publication* **101**, 1-11

Knox, R.W.O'B., Holloway, S., Kirby, G.A. and Baily, H.E. 1997. Stratigraphic nomenclature of the UK North West Margin. Early Paleogene lithostratigraphy and sequence stratigraphy. Nottingham: British Geological Survey.

Knutz, C.P. and Cartwright, J. 2003. Seismic stratigraphy of the West Shetland Drift: Implications for late Neogene paleocirculation in the Faeroe-Shetland gateway. *Paleooceanography* **18(4)**, 17,1-17,17

Kristoffersen, Y. 1978. Sea-floor spreading and the early opening of the North Atlantic. *Earth Planetary Science Letters* **38**, 273-290

Kusznir, N. J. and Park, R.G. 1987. The extensional strength of the continental lithosphere: its dependence on geothermal gradient, and crustal composition and thickness. *In*: Coward, M.P., Dewey, J.F. & Hancock, P.L. (eds). Continental Extensional Tectonics. *Geological Society Special Publication* **28**, 35-52.

Lake, S.D. and Karner, G.D. 1987. The structure and evolution of the Wessex Basin, southern England; an example of inversion tectonics. *Tectonophysics* **137**, 347-378

Lamers, E. and Carmichael, S.M.M. 1999. The Paleocene deepwater sandstone play West of Shetlands. *In*: Fleet, A.J. and Boldy, S.A.R. (eds). Petroleum Geology of Northwest Europe: Proceedings of the 5th Conference. Geological Society, London, 645-659

Larsen, H.C. 1984. Geology of East Greenland shelf. *In*: Spencer, A.M., Johnsen, S.O., Moerk, A., Nysaether, E., Songstad, P. and Spinnangr, A. Petroleum geology of the North European margin 329-339.

Larsen, H.C. 1988. A multiple and propagating rift model for the NE Atlantic. *In*: Morton, A.C. & Parson, L.M. (eds). Opening of the NE Atlantic. *Geological Society Special Publication* **39**, 157-158

Larsen, H.C. and Jakobsdóttir. 1988. Distribution, crustal properties and significance of seawards-dipping sub-basement reflectors off E Greenland. *In*: Morton, A.C.

and Parson, L.M. (eds). Opening of the NE Atlantic. *Geological Society Special Publication* **39**, 95-114

Larsen, H.C. 1990. The East Greenland shelf. The Arctic Ocean Region: Boulder, Colorado. *In*: A. Grantz, L. Johnson and J. F. Sweeney (ed), Geological Society of America. *The Geology of North America* **L**, 185-210

Larsen, H.C., Saunders, D.A, Clift, D.P., et al. 1994. Introduction: break-up of the southeast Greenland margin and the formation of Irminger basin: background and scientific objectives. *Proceedings of the Ocean Drilling Program, Scientific results* **152**, 5-16

Larsen, H.C. and Saunders, D.A. 1998. Tectonism and volcanism at the southeast Greenland rifted margin: A record of plume impact and later continental rupture. *Proceedings of the Ocean Drilling Program, Scientific results* **152**, 503-533

Larsen, L.M and Watt, S.W. 1985. Episodic volcanism during break-up of North Atlantic: evidence from the East Greenland plateau basalts. *Earth Planetary science Letters* **73**, 105-116

Larsen, L.M. Hamberg, L. Olavssen, S., Norgaard-Petersen, N. and Stemmerik, L. 1999. Basin Evolution in Southern East Greenland: An outcrop analog for Cretaceous-Paleogene Basins on the North Atlantic Volcanic Margins. *AAPG Bullitin* **83**, 1236-1261

Larsen, L.M., Waagstein, R., Pedersen, A.K. and Storey, M. 1999. Trans-Atlantic correlation of the palaeogenevolcanic successions in the Faeroe Islands and East Greenland. *Journal of the Geological Society, London* **156**, 1081-1095

Larsen, T.B., Yuen, D.A. and Storey, M. 1991. Ultrafast mantle plumes and implications for flood basalt volcanism in the Northern Atlantic Region. *Tectonophysics* **311**, 31-43

Larsen, T.B. & Yuen, D.A. 1997. Ultrafast upwelling bursting through the upper mantle. *Earth and Planetary Science Letters* **146**, 393-399

Larsen, T.B., Yuen, D.A. and Storey, M. 1999. Ultrafast mantle plumes and implications for flood basalt volcanism in the Northern Atlantic Region. *Tectonophysics* **311**, 31-43

Latin, D.M., Dixon, J.E. and Fitton, J.G. 1990. Rift-related magmatism in the North Sea basin. *In*: Blundell, D.J.and Gibbs, A.D (Eds). Tectonic evolution of the North Sea rifts. *International Lithosphere Program* **181**, 101-144

Latin, D.M., Dixon, J.E., Fitton, J.G. and White, N. 1990. Mesozoic magmatic activity in the North Sea basin; implications for stretching history. *In*: Hardman, R.F.P.and Brooks, J. (Eds). Proceedings of Tectonic events responsible for Britain's oil and gas reserves. *Geological Society Special Publications* **55**, 207-227

Latin, D. and Waters, F.G. 1991. Melt generation during rifting in the North Sea. Nature **351**, 559-562

Latin, D. and Waters, F.G. 1992. Basaltic magmatism in the North Sea and its relationship to lithospheric extension. *Tectonophysics* **208**, 77-90

Lawver, L.A. & Muller, R.D. 1994. Iceland hotspot track. Geology, 22, 311-314

Lister, C.R.B. 1975. Gravitational drive on oceanic plates caused by thermal contraction. *Nature* **257**, 663-665

Lott, G.K., Knox, R.W.O., Harland, R. and Hughes, M.J. 1983. The stratigraphy of Palaeogene sediments in a cored borehole of the coast of North-East Yorkshire, Pagination: 8. Report - Natural Environment Research Council, Institute of Geological Sciences (BGS, UK), 83-9

Lowell, D.J. 1995. Mechanics of basin inversion from worldwide examples. *In*: Buchanan, J,G. and Buchanan, P.G. (eds). Basin inversion. *Geological Society Special Publication* **88**, 39-57

Lu, G. and Keller, G. 1993. The Palaeocene-Eocene transition in the Antarctic Indian Ocean: Inference from planktonic foraminifera. *Marine Micropaleontology* **21**, 101-142

Lund, J. 1983. Biostratigraphy of coal interbedded in the basalts on the Faeroe Islands. *The American Association of Stratigraphic Palynologists, Palynology* **7**, 241-242

Lundin, E. and Doré, G.A. 1997. A tectonic model for the Norwegian passive margin with implications for the NE Atlantic: Early Cretaceous to break-up. *Journal of the Geological Society, London* **154**, 545-550

Lundin, E. and Doré, G.A. 2002. Mid-Cenozoic post-breakup deformation in the passive margins bordering the Norwegian-Greenland Sea. *Marine and petroleum Geology* **19**, 79-93

McKenzie, D. 1978. Some remarks on the development of sedimentary basins. *Earth and Planetary Science Letters* **40**, 25-32

McKenzie, D. 1984. A possible mechanism for epeirogenic uplift. *Nature* **307**, 616-618

McKenzie, D. and Bickle, M.J. 1988. The volume and composition of melt generated by extension of the lithosphere. *Journal of Petrology* **29**, 625-679

Mcleod, A.E., Dawers, N.H., Underhill, J.R. 2000. The propagation and linkage of normal faults: insights from the Strathspey-Brent-Stratford fault array, northern North Sea. *Basin Research* **12**, 263-284

Megson, J.B. 1987. The evolution of the Rockall Trough and implications for the Faeroe Shetland Trough. *In*: Brooks, J. and Glennie, K.W. (Eds). Petroleum geology of north west Europe. 653-665

Meijer, P. and Wortel, M.J.R. 1992. The dynamics of motion of the South American Plate. *Journal of Geophysical Research* **97**, 11915-11931

Menzies, M., Baker, J. & Chazot, G. 2001. Cenozoic plume evolution and flood basalts in Yemen: A key to understanding older examples. *Geological Society of America, Special Paper* **352**, 23-36

Milton, N.J., Bertram, G.T. and Vann, I.R. 1990. Early Palaeogene tectonics and sedimentation in the Central North Sea. *In*: Hardman, R.F.P. & Brooks, J. (Eds). Tectonic Events Responsible for Britain's Oil and Gas Reserves. *Geological Society Special Publication* **55**, 339-351

Mitchell, S.M., Beamish, G.W.J., Wood, M.Wmalacek, S.J., Armentrout, J.A., Damuth, J.E. and Olson, H.C. 1993. Paleogene sequence stratigraphic framework of the Faeroe basin. In: Parker, J. R. (eds). Petroleum Geology of Northwest Europe: Proceedings of the 4th Conference. Geological Society, London, 1011-1023

Molnar, P. and Atwater, T. 1978. Interarc spreading Cordilleran tectonics as alternates related to the age of subducted oceanic lithosphere. *Earth Planetary Science Letters* **41**, 330-340

Morgan, W.J. 1971. Convection plumes in the lower mantle, *Nature* **230**, 42-43.

Morgan, W.J. 1972. Plate motions and deep mantle convection. *Geological Society American Memoir* **132**, 7-22

Morgan, W.J. 1981. Hotspot tracks and the early rifting of the Atlantic. *In*: Papers presented to the Conference on the Processes of Continental Rifting, Lunar Planetary Institute, Houston, 1-4

Morton, A.C. & Knox R.W.O'B. 1990. Geochemistry of late Palaeocene and early Eocene tephras from the North Sea Basin. *Journal of the Geological Society, London* **147**, 425-437

Mosar, J. 2000. Depth of the extensional faulting on the Mid-Norway Atlantic passive margin. *Norges Geologiske undersøgelse Bulletin* **437**

Mosar, J., Lewis, G. and Torsvik, H.T. 2002. North Atlantic sea-floor spreading rates: implications for the Tertiary development of inversion structures of the Norwegian-Greenland Sea. *Journal of Geological Society, London* **159**, 503-515

Mudge, D.C. and Rashid, B. 1987. The Geology of the Faeroe Basin area. *In*: Brooks, J. and Glennie, K.W. (Eds). Petroleum Geology of Northwest Europe, 751-763

Mudge, D.C. and Copestake, P. 1992a. A revised Lower Palaeogene lithostratigraphy for the Outer Moray Firth. *Marine and Petroleum Geology* **9**, 53-69

Mudge, D.C. and Copestake, P. 1992b. Lower Palaeogene stratigraphy of the Northern north Sea. *Marine and Petroleum Geology* **9**, 287-301

Mudge, D.C. and Bujak, J.P. 1994. Eocene stratigraphy of the North Sea. *Marine and Petroleum Geology* **11**, 166-181

Mudge, D.C. and Bujak, J.P. 1996a. Palaeocene biostratigraphy and sequence stratigraphy of the UK central North Sea. *Marine and Petroleum Geology* **13**, 295-312

Mudge, D.C. and Bujak, J.P. 1996b. An integrated stratigraphy for the Palaeocene and Eocene of the North Sea. *In*: Knox, R.W.O'B., Corfield, R.M. and Dunay,

R.E. (Eds). Correlation of the Early Paleogene in Northwest Europe. *Geological Society Special Publication* **101**, 91-113

Mudge, D.C. and Bujak, J.P. 2001. Biostratigraphic evidence for evolving palaeoenvironments in the Lower Paleogene of the Faeroe-Shetland Basin. *Marine and Petroleum Geology* **18**, 577-590

Mussett, E.A., Dagley, P and Skelhorn, R.R. 1988. Time and duration of activity around the British Tertiary Igenous Province. *In*: Morton, A.C. and Parson, L.M. (eds). Early tertiary Volcanism and the Opening of the NE Atlantic. *Geological Society Special Publications* **39**, 337-348

Mutter, J.C. and Zehnder, C.M. 1988. Deep crustal structure and magmatic processes: the inception of seafloor spreading in the Norwegian-Greenland Sea. *In*: Morton, A. C. and Parson, L. M. (eds). Opening of the NE Atlantic. *Geological Society Special Publication* **39**, 35-48

Nadin, P.A. and Kusznir, N.J. 1995. Palaeocene uplift and Eocene subsidence in the northen North Sea Basin from 2D forward and reverse stratigraphic modeling. *Journal of the Geological Society* **152**, 833-848

Nadin, P.A., Kusznir, N.J. and Toth, J. 1995. Transient regional uplift in the Early Tertiary of the northern North Sea and the development of the Iceland Plume. *Journal of the Geological Society* **152**, 953-958

Nadin, A.P., Kusznir, J.N., Cheadle, J.M. 1997. Early Tertiary plume uplift of the North Sea and Faeroe-Shetland Basins. *Earth and Planatary Science Letters* **148**, 109-127

Naylor, P.H., Bell, R.B., Jolley, W.D., Durnall, P. and Fredstad, R. 1999. Paleogene magmatism in the Faroe-Shetland Basin: influences on uplift history and sedimentation. *In*: Fleet, A.J. and Boldy, S.A.R. (eds). Petroleum Geology of Northwest Europe: Proceedings of the 5th Conference. Geological Society, London, 545-558

Neal, J. E. 1996. A summary of Paleogene sequence stratigraphy in northwest Europe and the North Sea. *In*: Knox. R.W.O'B., Corfield, R.M. and Dunay, R.E. (eds). Correlation of the Early Paleogene in Northwest Europe. *Geological Society Special Publication* **101**, 15-42

Noe-Nygaard, A. and Rasmussen, J. 1968. Petrology of a 3,000 metre sequence of basaltic lavas in the Faeroe islands. *Lithos* **1**, 286-304

Norris, D.R. and Röhl, U. 1999. Carbon cycling and chronology of climate warming during the Palaeocene/Eocene transition. *Nature* **401**, 775-778

O'Connor, J.M., Stoffers, P., Wiltrans, J. R., Shannon, P.M., Morrissey, S.T. 2000 Evidence from episodic seamount volcanism for pulsing of the Iceland plume in the past 70 Myr. *Nature* **408**, 954-958

Parker, J.R. 1975. Lower Tertiary sand development in the Central North Sea. *In*: Woodland, A.W. (eds). Petroleum Geology and the Continental Shelf of Northwest Europe. Applied Science, Barking, 447-453

Petersen, T and Skogseid, J. 1989. Vøring Plateau volcanic margin: extension, melting and rifting. *In*: Eldholm, O., Thiede, J., Taylor, E., et al., *Scientific results of the Ocean Drilling Program* **104**, 985-991

Plint, A.G. 1982. Eocene sedimentation and tectonics in the Hampshire basin. *Journal of the Geological Society, London* **139**, 249-254

Price, S., Brodie, J., Whitham, A and Kent, R. 1997. Mid-Tertiary rifting and magmatism in the Traill Ø region, East Greenland. *Journal of the Geological Society, London* **54**, 419-434

Rainbird, H.R. and Ernst, E.R. 2001. The sedimentary record of mantle-plume uplift. *Geological Society of America, special paper* **352**, 227-245

Rasmussen, J. and Noe-Nygaard, A. 1970. Geology of the Faroe Islands. Danmarks Geologiske Undersogelse 1. Serie, 25

Rasmussen, J. 1990. The Origin of the Faroe Islands. Danmarks Geologiske Undersogelse, Copenhagen

Rea, D.K., Zachos, J.C., Owen, R.M. and Gingerich, P.D. Global changes at the Paleocene-Eocene boundary: climatic and evolutionary consequences of tectonic events, Palaeogeogr. *Palaeoclimatology Palaeoecology* **79**, 117-128

Ridd, M.F. 1983. Aspects of the Tertiary geology of the Faroe-Shetland Channel. *In*: Bott, M.H.P., Saxov, S., Talwani, M. and Thiede, J. (Eds). Structure and Development of the Greenland-Scotland Ridge. Plenum press, New York, 133-158

Riisager, P., Riisager, J., Abrahamsen, N. and Waagstein, R. 2002. New Paleomagnetic pole and magnetostratigrahy of Faroe Islands flood volcanics, North Atlantic igneous province. *Earth and Planetary Science Letters* **201**, 261-276

Ritchards, M.A., Duncan, R.A and Courtillot, V.E. 1989. Flood basalts and hot-spot tracks: plume heads and tails. *Science* **246**, 103-107

Ritchie, J. D. and Hitchen, K. 1996. Early Paleogene offshore igneous activity to the northwest of the UK and its relationship to the North Atlantic Igneous Province. *In*: Knox. R.W.O'B., Corfield, R.M. and Dunay, R.E. (eds). Correlation of the Early Paleogene in Northwest Europe. *Geological Society Special Publication* **101**, 63-78

Ritchie, D.J. Gatliff, W.R. and Richards, C.P. 1999. Early Tertiary magmatism in the offshore NW UK margin and surrounds. *In*: Fleet, A.J. and Boldy, S.A.R. (eds). Petroleum Geology of Northwest Europe: Proceedings of the 5th Conference. Geological Society, London, 573-584

Ritchie, D. J., Johnson, H. and Kimbell, S. G. 2003. The nature and age of Cenozoic contractional deformation within the NE Faroe-Shetland Basin. *Marine and Petroleum Geology* **20**, 399-409

Roberts, D.G. 1975. Marine geology of the Rockall Plateau and Trough. *Transcript of the Royal Society, London* **A278**, 447-509

Roberts, D.G., Morton, A.C. and Backman, J. 1984. Late Paleocene-Eocene Volcanic Events in the northern Atlantic ocean. *In*: Roberts, D.G., Schnitker, D. et al. *Proceedings of the Ocean Drilling Program, Initial Reports* **81**, 913-923

Roberts, D.G. 1989. Basin inversion around the British Isles. Inversion Tectonics. *In*: M.A. Cooper and D.G. Williams (eds). *Geological Society, London, Special Publication* **44**, 131-150

Roberts, D.G., Backman, J., Morton, A.C., Murray, J. and Keene, J.B. 1994. Evolution of volcanic rifted margins: Synthesis of Leg 81 Results on the West Margin of Rockall Plateau. *Proceedings of the Ocean Drilling Program Initial Reports* **81**, 883-911.

Roberts, A.M., Alundin, E.R. and Kusznir, N.J. 1997. Subsidence of the Vøring Basin and the influence of the Atlantic continental margin. *Journal of Geological Society of London* **154**, 551-557

Roberts, D.G., Thompson, M., Mitchener, B., Hossack, J., Carmicheal, S., Bjoernseth, H-M. 1999. Palaeozoic to Tertiary rift and basin dynamics: mid-Norway to the Bay of Biscay – a new context for hydrocarbon prospectivity in the deep water frontier. *In*: Fleet, A.J. and Boldy, S.A.R. (eds). Petroleum Geology of Northwest Europe: Proceedings of the 5th Conference. Geological Society, London, 7-40

Roest, R.W. and Srivastava, P.S. 1991. Kinematics of the plate boundaries between Eurasia, Iberia, and Africa in the North Atlantic from the Late Cretaceous to the present. *Geology* **19**, 613-616

Roest, W.R. and Srivastava, S.P. Sea-floor spreading in the Labrador Sea: a new reconstruction. *Geology* **17**, 1000-1003

Rohrman, M. and Van Der Beek, P. 1996. Cenozoic postrift domal uplift of North Atlantic margins: An asthenospheric diapirism model. *Geology* **24**, 901-904

Rolle, F. 1985. Late Cretaceous-Tertiary sediments offshore central West Greenland: lithostratigraphy, sedimentary evolution, and petroleum potential: Canadian. *Journal of Earth Sciences* **22**, 1001-1019

Rumph, B. Reaves, C.M., Orange, V.G. and Robinson, D.L. 1993. Structuring and transfer zones in the Faeroe Basin in a regional tectonic context. *In*: Parker, J.R. (eds). Petroleum Geology og Northwest Europe. Preceedings of the 4th Conference. Geological Society, London, 999-1010

Röhl, U, Bralower, J.T., Norris, D.R. and Wefer, G. 2000. New chronology for the late Paleocene thermal maximum and its environmental implications. *Geology* **28**, 927-930

Sabadini, R. and Yuen, D.A. 1989. Plate motion and dragging of the upper mantle: lateral variations of lithosphere thickness and their implications for intraplate deformation. *Annales Geophysicae* **10**, Supplement I, C83

Saunders, D.A., Storey, M., Kent, W. R. and Norry, J.M. 1992. Consequences of plume-lithosphere interactions. *In*: Storey, B.A., Alabaster, Y. and Pankhurst, R.

J. (eds). Magmatism and the causes of Continental break-up. *Geological Society Special Publication* **68**, 41-60

Saunders, D.A., Fitton, G. J., Kerr, C.A., Norry, J.M. and Kent, W.R. 1997. The North Atlantic Igneous Province. *In*: Large Igneous Provinces: Continental, Oceanic, and Planetary Flood Volcanism. *Geophysical Monograph* **100,** 45-93

Saunders, D.A., Larsen, C.H. and Fitton, G. J. 1998. Magmatic development of the southeast Greenland margin and evolution of the Iceland plume: Geochemical constraints from leg 152. *Proceedings of the Ocean Scientific Results* **152**, 479-501

Schilling, J.-G and Noe-Nygaard. 1974. Faeroe-Iceland plume: rare earth evidence. *Earth Planetary Science Letters* **24**, 1-14

Sheridan, R.E. 1974. Atlantic continental margin of North America. *In*: C.A. Burk and Drake C.L. (eds). The Geology of Continental margins. Springer-verlag, New York, 391-408

Sleep, N.H. 1990. Hotspots and mantle plumes: some phenomenology. *Journal of Geophysical Research* **95**, 6715-6736

Skar, T., van Balen, R. and Cloetingh, S. 2000. The effect of intraplate compression on differential movements on the mid-Norwegian margin. European Geophysical Society, Nice 2000, abstract.

Skogseid, J. & Eldholm, O. 1988. Early Cainozoic evolution of the Norwegian volcanic passive margin and the formation of marginal highs. *In*: Morton, A.C. and Parson, L. M. (eds). Opening of the NE Atlantic. *Geological Society Special Publication* **39**, 49-56

Skogseid, J. and Eldholm, O. 1989. Vøring Plateau continental margin: seismic interpretation, stratigraphy and vertical movements. *In*: Eldholm, O., Thiede, J., Taylor, E. et al. (eds). *Proceedings of the Ocean Drilling Program, Scientific Results* **104**, 993-1030

Skogseid, J., Pedersen, T., Eldholm, O and Larsen, B. T. 1992. Tectonism and magmatism during NE Atlantic continental break-up: the Vøring margin. *In*: Storey, B.C., Alabaster, T and Pankhurst, R.J. (eds). Magmatism and the causes of

continental break-up. *Geological Society, London, Special Publications* **68**, 305-320

Skogseid, J. 1994. Dimensions of the Late Cretaceous-paleocene Northeast Atlantic rift derived from Cenozoic subsidence. *Tectonophysics* **240**, 225-247

Skogseid, J., Planke, S., Faleide, I. J., Pedersen, T., Eldholm, O. and Neverdal, F. 2000. NE Atlantic continental rifting and volcanic margin formation. *In*: Nøttvedt, A. et al. (eds). Dynamics of the Norwegian Margin. *Geological. Society Special Publication* **167**, 295-326

Smallwood, R. J. 2002. Tertiary inversion in the Faroe-Shetland Channel and the development of major erosional scarps.

Smallwood, R. J. & Gill, E. C. 2002. The rise and fall of the Faroe-Shetland Basin: evidence from seismic mapping of the Balder Formation. *Journal of the Geological Society, London* **159**, 627-630

Smythe, D.K. 1983. Faeroe-Shetland Escarpment and continental margin of the Faroes. *In*: Bott, M.H.P., Saxov, S., Talwani, M. and Theide, J. (eds). Structure and Development of the Greenland-Scotland Ridge: new Methods and Concepts. Plenum Press, New York, 109-119

Spencer, M.A., Birkeland, OE., Knag, G.OE. and Fredsted, R. 1999. Petroleum systems of the Atlantic margin of northwest Europe. In: Fleet, J.A and Boldy, R.A.S. (eds). Petroleum Geology of Northwest Europe: Proceedings of the 5th Conference. Geological Society, London, 231-246

Srivastava, S.P. 1978. Evolution of the Labrador Sea and its bearing on the early evolution of the north Atlantic. *Journal of the Royal Astronomy Society* **52**, 313-357

Srivastava, S.P. and Tapscott, C.R. 1986. Plate kinematics of the North Atlantic. *In*: Vogt, P.R. and Tucholke, B.E (eds). The Western North Atlantic Region. Geological Society of America, Boulder, CO

Stoker M.S. 1994. A record of late Cenozoic stratigraphy, sedimentation and climate change from the Hebrides Slope, NE Atlantic Ocean. *Journal of Geological Society* **151**, 235-249

Stoker, M.S. 1994. The influence of glacigenic sedimentation on slope-apron development on the continental margin off northwest Britain. *In*: Scrutton, R.A. (Eds). The tectonics, sedimentation and palaeoceanography of the North Atlantic region. *Geological Society, Special Publication* **90**, 159-177

Stoker, S.M., Morton, C.A., Evans, D., Hughes, J.M., Harland, R. and Graham, K.D. 1988. Early tertiary basalts and tuffaceous sandstones from the Hebrides Shelf and Wyville-Thomson Ridge, NE Atlantic. *In*: Morton, A.C. and Parson, L.M. (eds). Early tertiary Volcanism and the Opening of the NE Atlantic. *Geological Society Special Publication* **39**, 271-282

Stoker, M.S., Hitchen, K. and Graham, C.C. 1993. The geology of the Hebrides and West Shetland shelves, and adjacent deep-water areas. British Geological Survey United Kingdom Offshore Regional Report. HMSO, London.

Stoker, M.S.1997. Mid-late Cenozoic sedimentation on the continental margin off NW Britain. *Journal of Geological Society* **154**, 509-515

Stoker, M.S. 1999. Stratigraphic nomenclature of the UK North West margin: 3. Mid- to Late Cenozoic Stratigraphy. British geological Survey, Edinburgh.

Stoker, M.S. 2002. Late Neogene development of the UK Atlantic Margin: *In*: Doré, A.G., Cartwright, J., Stoker, M.S., Turner, J.P. and White, N. (eds). Exhumation of the North Atlantic Margin: Timing, Mechanisms and Implications for Petroleum Exploration. *Geological Society, London, Special Publications* **196**, 313-330

Storey, M., Duncan, R.A., Pedersen, A.K., Larsen, L.M. & Larsen, H.C. 1998. 40Ar/39Ar geochronology of the West Greenland Tertiary volcanic province. *Earth and Planetary Science Letters* **160**, 569-586

Storey, C.B., Leat, T.P. and Ferris, K.J. 2001. The location of mantle-plume centers during the initial stages of Gondwana breakup. *Geological Society of America Special Paper* **352**, 71-79

Stuevold, M.L., Skogseid, J. and Eldholm, O. 1992. Post-Cretaceous uplift events on the Vøring continental margin. *Geology* 919-922

Stott, L.D., Sinha, A., Thiry, M., Aubry, M-P. & Berggren, W.A. 1996. Global d13C changes across the Paleocene-Eocene boundary: criteria for terrestrial-marine

correlations. *In*: Knox, R.W.O'B., Corfield, R.M. and Dunay, R.E. (Eds). Correlation of the Early Paleogene in Northwest Europe. *Geological Society Special Publication* **101**, 381-399

Summerfield, M.A. 1991. Global Geomorphology: An introduction to the study of landforms. Longman Scientific & Technical. New York.

Tackley, P.J., Stevenson, D.J., Glatzmaier, G.A. and Schubert, G. 1993. Effects of an endothermic phase transition at 650 km depth in a spherical model of convection in the Earth's mantle. *Nature* **361**, 699-704

Talwani, M. and Eldholm, O.1977. Evolution of the Norwegian-Greenland Sea. *Geological Society of America Bullitin* **88**, 969-999

Thiede J. 1983. History of the north polar seas during the past 5 million years. Palaeoclimatic research and models. Proc. workshop, Brussels, 178-180

Thiede, J. and Eldholm, O. 1983. Speculations about the paleodepth of the Greenland-Scotland Ridge during late Mesozoic and Cenozoic times. *In*: Bott, Martin H.P., Saxov, S., Talwani, M. and Thiede, J. (Eds). Structure and development of the Greenland-Scotland Ridge; new methods and concepts, NATO Conference Series. IV. *Marine Sciences* **8**, 445-456

Thomas, J. E. 1996. The occurrence of the dinoflagellate cyst Apectodinium (Costa and Downie, 1976) Lentin and Williams (1977) in the moray and Montrose Groups (Danian and Thanetian) of the UK central North Sea. *In*: Knox, R.W. O'B., Corfield, R. M. and Dunay, R.E. (eds) Correlation of the Early Paleogene in Northwest Europe. *Geological Society Special Publication* **101**

Thomas, E. and Shackelton, N. J. 1996. The Paleocene-Eocene benthic foraminiferal extinction and stable isotope anomalies. *In*: Knox, R.W.O'B., Corfield, R.M. and Dunay, R.E. (eds). Correlation of the Early Paleogene in Northwest Europe. *Geological Society Special Publication* **101**, 404-441

Thompson, R.N. and Gibson, S.A. 1991. Subcontinental mantle plumes, hotspots and pre-existing thinspots. *Journal of Geological Society, London* **148**, 973-977

Tucholke, B. and Fry, V. 1985. Basement Structure and Sediment Distribution in Northwest Atlantic Ocean. *The American Association of Petroleum Geologists Bulletin* **69**, 2077-2097

Turcotte, D.L. and Schubert, G. 1982. Geodynamics: Applications of Continuum Physics to Geological Problems. John Wiley, New York.

Turner, J.D and Scrutton, R.A. 1993. Subsidence patterns in western margin basins: evidence from the Faeroe-Shetland basin. *In*: Parker, J.R. (eds). Petroleum Geology of Northwest Europe: Proceedings of the 4th Conference. Geological Society, London, 975-983

Underhill, J.R. and Partington, M.A.1993. Jurassic thermal doming and deflation in the North Sea; implications of the sequence stratigraphic evidence. *In*: Parker, J.R. (Eds). Petroleum geology of Northwest Europe; Proceedings of the 4th conference. Geological Society of London, 337-345

Underhill, J.R. 2001. Controls on the Genesis and Prospectivity of Paleogene Palaeogeomorphic Traps, East Shetland Platform, UK North Sea. *Marine and Petroleum Geology* **18**, 259-281

Vågnes, E. Gabrielsen, H.R. & Haremo, P. 1998. Late Cretaceous-Cenozoic intraplate contractional deformation at the Norwegian continental shelf: timing, magnitude and regional implications. *Tectonophysics* **300**, 29-46

Vail, P.R., Mitchum R.M., and Thompson, S. 1977, Seismic stratigraphy and global changes of sea level, part 3: relative changes of sea level from coastal onlap. *In*: Payton, C.W. (eds). Seismic Stratigraphy Applications to Hydrocarbon Exploration: Tulsa. *American Association of Petroleum Geologists Memoir* **26**, 63-97

Vail, P.R. and Hardenbol, J. 1979. Sea-level changes during Tertiary. *Oceanus* **22**, 71-79

Vail, P.R., Bowman, S.A., Eisner, P.N. and Perez-Cruz, G. 1991. The stratigraphic signatures of tectonics, eustasy, and sedimentation: an overview. *In*: A. Seilacher and G. Eisner (eds). Cycles and Events in Stratigraphy, II. Springer-Verlag, Tübingen.

Van Wagoner, J.C., Mitchum, R.M., Campion, K.M., and Rahmanian, V.D., 1990. Siliciclastic sequence stratigraphy in well logs, cores and outcrops: concepts for high resolution correlation of time and facies: Tulsa. *American Association of Petroleum Geologists Methods in Exploration* **7**, 55 p

Vogt, P.R., Johnson, G.L. and Krisjansson, L. 1980. Morphology and magnetic anomalies north of Iceland. *Journal of Geophysics* **47**, 67-80

Waagstein, R. 1988. Structure, composition and age of the Faeroe basalt plateau. *In*: Morton, A.C. and Parson, L.M. (eds). Opening of the NE Atlantic. *Geological Society Special Publication* **39**, 225-238

Waagstein, R. 1995. Early Tertiary volcanism in the Faroe region and the initiation of the North Atlantic mantle plume. International Lithosphere Programme, August-September, Torshavn, Faroe Islands

Waagstein, R. and Heilmann-Clausen, C. 1995. Petrography and biostratigraphy of Paleogene colcaniclastic sediments dredged from the Faeroes Shelf. *In*: Scrutton, R.A., Stoker, M.S., Shimmield, G.B. & Tudhope, A.W. (Eds). The tectonics, sedimentation and palaeoceanography of the North Atlantic region. *Geological Society Special Publication* **90**, 179-197

Watts, A.B. 1982. Tectonic subsidence, flexure and global changes in sea level. *Nature* **297**, 469-474

Watts, A.B., Karner, G.D. and Steckler, M.S. 1982. Lithospheric flexure and the evolution of sedimentary basins. *Phil. Trans. R. Soc. London* **A305**, 249-281

Vink, G.E. 1984. A hotspot model for Iceland and the Voering Plateau. *Journal of Geophysical Research* **89B**, 9949-9959

White, R.S. 1988. A hot-spot model for early Tertiary volcanism in the N. Atlantic. *In*: Morton, A.C. and Parson, L.M. (eds). Opening of the NE Atlantic. *Geological Society Special Publication* **39**, 3-13

White, S.R. 1992. Crustal structure and magmatism of North Atlantic continental margins. *Journal of the Geological Society, London* **149**, 841-854.

White, S.R. 1992. Magmatism during and after continental break-up. *Geological Society, London Special Publication* **68**, 1-16

White, N. and Lovell, B. 1997. Measuring the pulse of a plume with the sedimentary record. *Nature* **387**, 888-891

White, N and McKenzie, D.P. 1988. Formation of the steer's head geometry of sedimentary basins by differential stretching of the crust and mantle. *Geology* **16**, 250-253

White, S.R., Spence, G.D., Fowler, S.R., Mckenzie, M.D., Westerbrook, G.K. and Bowen, A.N. 1987. Magmatism at rifted continental margins. *Nature* **330**, 439-444

White, S. R. & Mckenzie, M. D. 1989. Magmatism at Rift Zones: The Generation of Volcanic Continental Margins and Flood basalts. *Journal of Geophysical Research* **94**, 7685-7729

White, S.R, McKenzie, M.D. and O'Nions, K.R. 1992. Oceanic crustal thickness from seismic measurements and rare earth element inversions. *Journal of Geophysical Research* **97**, 19683-19715

White, S.R. and Mckenzie, M. D. 1995. Mantle plumes and flood basalts. *Journal of Geophysical Research* **100**, 17, 543-17, 585

White. S.R., Brown, W.J, Smallwood, R.J. 1995. The temperature of the Iceland plume and origin of outward-propagating V-shaped ridges. *Journal of Geological Society, London* **152**, 1039-1045

Williams, E.G. and Gostin, A.V. 2000. Mantle plume uplift in the sedimentary record: origin of kilometre-deep canyons within late Neoproterozoic successions, South Australia. *Journal of the geological Society, London* **157**, 759-768

Williams, G.D., Powell, C.M., and Cooper, M.A. 1989. Geometry and kinematics of inversion tectonics. *In*: Cooper, M.A. and Williams, G.D. (eds). Inversion Tectonics. *Geological Society, London, Special Publication* **44**, 3-15

Wilson, M. 1993. Plate-moving mechanisms: constraints and controversies. *Journal of Geological Society, London* **150**, 923-926

Vogt, P.R. and Avery, O.E. 1974. Detailed magnetic surveys in the north-east Atlantic and Labrador Sea. *Journal of Geophysical Research* **79**, 363-389

Vågnes, E., Gabrielsen, R.H. and Haremo, P. 1998. Late Cretaceous-Cenozoic intraplate contractional deformation at the Norwegian continental shelf: timing, magnitude and regional implications. *Tectonophysics* **300**, 29-46

Zachos, J.C., Lohmann, K.C., Walker, J.C.G. and Wise, S.W. 1993. Abrupt climate change and transient climates during the Paleogene: a marine perspective. *Journal of Geology* **101**, 191-213

Zachos, J.C., Flower, P. B. & Paul, H. 1997. Orbitally placed climate oscillations across the Oligocene/Miocene boundary. *Nature* **388**, 567-570

Zaitlin, B.A., Dalrymple, R.W. and Boyd, R. 1994. The Stratigraphic Organization of Incised –Valley systems associated with relative sea-level change. *In*: Dalrymple, R. W., Boyd, R. & Zaitlin, B. A. (Eds). Incised-Valley systems: Origin and Sedimentary Sequences. *SEPM Special Publication* **51**, 45-60

Ziegler, P.A. 1982. Geological Atlas of Western and Central Europe. Elsevier, Amsterdam.

Ziegler, P.A. 1987. Late Cretaceous and Cenozoic intra-plate compressional deformations in the Alpine foreland – a geodynamic model. *Tectonophysics* **137**, 389-420

Ziegler, P.A. 1988. Evolution of the Arctic-North Atlantic and the Western Tethys. *Memoir of the American Association of Petroleum Geologists* **43**

Ziegler, P.A. 1989. Geodynamic model for Alpine intra-plate compressional deformation in Western and Central Europe. *In*: Cooper, M.A. and Williams, G. D. (eds). Inversion Tectonics. *Geological Society Special Publication* **44**, 63-85

Ziegler, P.A. 1990. Geological Atlas of western and central Europe. Shell International Petroleum Maatschappij B.V. The Hauge.

Ziegler, P.A. 1993. Plate-moving mechanisms: their relative importance. *Journal of the Geological Society, London* **150**, 927-940

Ziegler, P.A., Cloetingh, S. and Van Wees, J-D. 1995. Dynamics of intra-plate compressional deformation: the Alpine foreland and other examples. *Tectonophysics* **252**, 7-59

Ziegler, P.A., Van Wees, J-D. and Cloetingh, S. 1998. Mechanical controls on collision-related compressional intraplate deformation. *Tectonophysics* **300**, 103-129

Zoback, M.L. 1992. First- and second-order patterns of stress in the lithosphere: The World Stress Map Project. *Journal of Geophysical Research* **97**

Zonenshain, L.P., Kusmin, M.I. and Natapov, L.M.. 1990. Geology of the USSR: A plate-tectonic synthesis. *Geodynamic Series* **21**, 242pp